# USE OF LANDSAT TM AND ETM+ TO DESCRIBE INTRA-SEASON CHANGE IN VEGETATION, WITH CONSIDERATION FOR WILDLIFE MANAGEMENT

by

Roberta J. Lay

B.A., University of Northern British Columbia, 2002

THESIS SUBMITTED IN PARTIAL FULFILLMENT OF

THE REQUIREMENTS FOR THE DEGREE OF

MASTER OF NATURAL RESOURCES AND ENVIRONMENTAL STUDIES

THE UNIVERSITY OF NORTHERN BRITISH COLUMBIA

April 2005

© Roberta J. Lay, 2005

## ABSTRACT

Many studies have used seasonal differences in multi-temporal Normalized Difference Vegetation Index (NDVI) values to help explain movements of large mammal species such as barren-ground caribou (*Rangifer tarandus greenlandicus*). These studies, however, have typically relied upon coarse-resolution NDVI information (i.e., 250-1000m). The Thematic Mapper (TM) and Enhanced Thematic Mapper Plus (ETM+) onboard the Landsat satellites capture 30-m multi-spectral data, but because of the limited satellite overpass schedule, these data are less frequently available and consequently more likely to be contaminated by clouds. I assessed the success of several models containing multiple terrain inputs and vegetation information (derived by maximum likelihood classification of TM data with overall accuracy 77%) to predict NDVI in clouded areas and to map uniform NDVI surfaces. Using these data, I employed change detection techniques to derive the phenological differences of vegetation between images from four months during the growing season of 2001 and related these to seasonal changes for 11 vegetation types in the Greater Besa-Prophet Area of the Muskwa-Kechika Management area in northern British Columbia.

## TABLE OF CONTENTS

ABSTRACT ..... ii

TABLE OF CONTENTS ..... iii

LIST OF TABLES ..... vi

LIST OF FIGURES ..... xi

ACKNOWLEDGEMENTS ..... xiv

CHAPTER ONE – THESIS INTRODUCTION AND STUDY RATIONALE ..... 1

1.1 Context ..... 1
1.2 Study Rationale ..... 8
1.3 Introduction to Methodologies and Primary Concepts ..... 10
*Supervised classification ..... 10*
*Normalized Difference Vegetation Index (NDVI) ..... 11*
1.4 Thesis Organization ..... 12
1.5 Literature Cited ..... 13

CHAPTER TWO – CLASSIFICATION OF POTENTIAL LARGE MAMMAL HABITAT IN A MOUNTAIN LANDSCAPE USING LANDSAT TM DATA ..... 15

2.1 Introduction ..... 15
2.2 Methods ..... 16
*Study Area ..... 16*
*Data Input ..... 17*
*Field Data Collection ..... 17*
*Spectral Signature Development ..... 21*
*Post-classification Filtration ..... 24*
*Post-classification modelling ..... 25*
*Accuracy Assessment ..... 25*
2.3 Results ..... 28
*Overall Accuracy ..... 28*
*Per-class Accuracies ..... 34*
2.4 Discussion ..... 36
*Accuracy ..... 36*
*Interpretation of Results ..... 39*
*Considerations for Wildlife Management / Use of the Data ..... 42*
*Conclusions ..... 44*
2.5 Literature Cited ..... 45

CHAPTER THREE – CONSIDERATIONS FOR THE PRODUCTION OF AN INTRA-SEASON PHENOLOGY DATASET USING LANDSAT TM AND ETM+: RELATIONSHIPS AMONG NDVI, VEGETATION AND TOPOGRAPHY IN A MOUNTAIN LANDSCAPE IN NORTHERN BRITISH COLUMBIA ..... 49

3.1 Introduction ..... 49
3.2 Methods ..... 56
*Study Area* ..... *56*
*Data Preparation* ..... *56*
*Regression Analysis to Predict NDVI* ..... *59*
3.3 Results ..... 65
*Initial cross-sensor radiometric comparison* ..... *65*
*NDVI models* ..... *66*
*Mapping* ..... *69*
3.4 Discussion ..... 73
*Radiometric Distortion/Normalization* ..... *73*
*Model Performance* ..... *76*
*Conclusions* ..... *79*
3.5 Literature Cited ..... 81

CHAPTER FOUR – INTRA-SEASON CHANGE IN VEGETATION IN A NORTHERN MOUNTAIN ECOSYSTEM USING LANDSAT TM AND ETM+ ..... 85

4.1 Introduction ..... 85
*Change Detection* ..... *87*
*Scale* ..... *89*
4.2 Methods ..... 91
*Study Area and Data Inputs* ..... *91*
*Change Detection* ..... *92*
4.3 Results ..... 97
*Vegetation Profiles* ..... *97*
*Image Differencing* ..... *99*
*Standardized Principal Component Analysis* ..... *110*
4.4 Discussion ..... 115
*Synopsis of results* ..... *115*
*Confounding Factors and Sources of Error* ..... *119*
*Conclusions and Considerations* ..... *122*
4.5 Literature Cited ..... 124

CHAPTER FIVE – USE OF LANDSAT TM AND ETM+ TO DESCRIBE INTRA-SEASON CHANGE IN VEGETATION WITH CONSIDERATION FOR WILDLIFE MANAGEMENT. ..... 129

5.1 Data assumptions and limitations ..... 129
*Topography and Decreasing Solar Angle* ..... *129*
*Atmosphere* ..... *132*
*Classification and Geometric Correction Errors, and Model Performance* ..... *132*

*Ground-truth Information* ..... *134*
5.2 Use of the data ..... 134
5.3 Literature Cited ..... 137

APPENDIX A: Post-classification modelling 'rules' developed for the maximum likelihood classification of the Greater Besa-Prophet Area in northern British Columbia. ..... 138

APPENDIX B: Distribution and coordinates of all locations used to train and assess the accuracy of the maximum likelihood classification developed for the Greater Besa-Prophet Area in northern British Columbia. ..... 140

APPENDIX C: Detailed descriptions of classes in the final maximum likelihood vegetation classification developed for the Greater Besa-Prophet Area in northern British Columbia ..... 146

APPENDIX D: Confusion matrices and accuracy statistics of the maximum likelihood classifications developed for the Greater Besa-Prophet Area in northern British Columbia. ..... 161

APPENDIX E: Original coefficients of models developed for all multiple linear regression models used to predict NDVI values in the Greater Besa-Prophet Area in northern British Columbia, 2001-2003. ..... 174

APPENDIX F: Coefficients of multiple linear regression models using 'transition zone' class to predict NDVI values in the Greater Besa-Prophet Area in northern British Columbia, 2001-2003 ..... 189

APPENDIX G: Per-class minimum (min), maximum (max), mean, standard deviation (s) and range for NDVI and NDVI derived from multiple linear regression (MNDVI) in the Greater Besa-Prophet Area in northern British Columbia, 2001 ..... 195

APPENDIX H: Tables of loadings for standardized principal component analysis of the Greater Besa-Prophet Area in northern British Columbia, 2001 .... 201

## LIST OF TABLES

Table 2.1. The 29-class vegetation classification scheme developed for the Greater Besa-Prophet Area in northern British Columbia. ..... 20

Table 2.2. Brief descriptions of the 15-class scheme used to classify the landscape of the Greater Besa-Prophet area in northern British Columbia. ..... 30

Table 2.3. Overall accuracy and KAPPA statistic ($\kappa$) of each classification iteration that used the 15-class scheme (see Table 2.2) developed for the Greater Besa-Prophet Area in northern British Columbia. ..... 32

Table 2.4. Accuracy of the 15-class vegetation classification scheme developed for the Greater Besa-Prophet Area in northern British Columbia before and after post-classification modeling. ..... 33

Table 3.1. Landsat Thematic Mappper (TM) and Enhanced Thematic Mapper (ETM+) images that were collected for the Greater Besa-Prophet Area in northern British Columbia, 2001-2003. Solar azimuth and elevation were calculated using the approximate centre of the Greater Besa-Prophet Area and the date and time the image was collected. ..... 58

Table 3.2. 15-class vegetation scheme used as input information in the multiple regression analyses to predict the Normalized Difference Vegetation Index (NDVI) in the Greater Besa-Prophet Area of northern British Columbia. ..... 63

Table 3.3. Minimum (Min) and Maximum (Max) monthly Normalized Vegetation Index (NDVI) values across vegetation types in the Greater Besa-Prophet Area and Landsat Thematic Mapper (TM) and Enhanced Thematic Mapper (ETM+) Path and Row compared to the validated adjusted $r^2$ (Val. Adj. $r^2$) of top-performing predictive models 2001-2003. Models are coded by inputs: vegetation (V), slope (S), aspect (A), elevation (E) and angle of incidence (I)..... 67

Table 3.4. Validated adjusted $r^2$ (Val. Adj. $r^2$) of top-performing models that included vegetation before (15-class input) and after 'transition zone' class (16-class input) was included in the modelling procedures for the Greater Besa-Prophet Area in northern British Columbia. ..... 68

Table 3.5. Per-class minimum (min), maximum (max), mean, standard deviation (s) and range for the Normalized Difference Vegetation Index (NDVI) and NDVI derived from multiple linear regression (MNDVI) analysis for August 2001 in the Greater Besa-Prophet Area in northern British Columbia. ..... 70

Table 3.6. Landscape and per-class image-to-image correlation (r) for the Normalized Difference Vegetation Index (NDVI) and NDVI derived from multiple linear regression analysis (MNDVI) of the Greater Besa-Prophet Area in northern British Columbia. ..... 72

Table 4.1. Brief descriptions of the 15-class scheme used to classify the landscape of the Greater Besa-Prophet area in northern British Columbia. ..... 94

Table 4.2. Normalized Difference Vegetation Index (NDVI) and NDVI derived from multiple linear regression analysis (MNDVI) values and standard error ($\sigma$) by vegetation type among months of the 2001 growing season in northern British Columbia. Values marked with a common letter indicate no significant difference within vegetation types between months, determined by Tukey's Honest Significant Difference (HSD)..... 98

Table 4.3. Loadings in each component of near-monthly NDVI derived from multiple linear regression analysis (MNDVI) in the Greater Besa-Prophet Area of northern British Columbia, 2001. ..... 112

Table A1. Post-classification modelling 'rules' developed for the 15 classes of the Greater Besa-Prophet Area in northern British Columbia. ..... 139

Table B1. Coordinates of all locations used to train 15-class maximum likelihood classification developed for the Greater Besa-Prophet Area in northern British Columbia. Spatial reference: UTM Zone 10N, NAD83. ..... 142

Table B2. Coordinates of all locations used to assess the accuracy of the 15-class maximum likelihood classification developed for the Greater Besa-Prophet Area in northern British Columbia. Spatial reference: UTM Zone 10N, NAD83. ..... 144

Table D1. Confusion matrix of the 15-class maximum likelihood classification of the Greater Besa-Prophet Area in northern British Columbia. Inputs: TM bands 5, 4, 3, DEM, slope, angle of incidence. No filtration or modelling. ..... 162

Table D2. Accuracy Statistics of the 15-class maximum likelihood classification of the Greater Besa-Prophet Area in northern British Columbia. Inputs: TM bands 5, 4, 3, DEM, slope, angle of incidence. No filtration or modelling. ..... 163

Table D3. Confusion matrix of the 15-class maximum likelihood classification of the Greater Besa-Prophet Area in northern British Columbia. Inputs: TM bands 5, 4, 3, DEM, slope, angle of incidence, and NDVI. No filtration or modelling. ..... 164

Table D4. Accuracy Statistics of the 15-class maximum likelihood classification of the Greater Besa-Prophet Area in northern British Columbia. Inputs: TM bands 5, 4, 3, DEM, slope, angle of incidence, and NDVI. No filtration or modelling ..... 165

Table D5. Confusion matrix and of 15-class maximum likelihood classification of the Greater Besa-Prophet Area in northern British Columbia. Inputs: TM bands 5, 4, 3, DEM, slope, angle of incidence, and second principal component from the 6-band TM principal component analysis. No filtration or modelling..... 166

Table D6. Accuracy Statistics of the 15-class maximum likelihood classification of the Greater Besa-Prophet Area in northern British Columbia. Inputs: TM bands 5, 4, 3, DEM, slope, angle of incidence, and second principal component from the 6-band TM principal component analysis. No filtration or modelling. ..... 167

Table D7. Confusion matrix and of 15-class maximum likelihood classification of the Greater Besa-Prophet Area in northern British Columbia. Inputs: TM bands 5, 4, 3, DEM, slope, angle of incidence, and third principal component from the 6-band TM principal component analysis. No filtration or modelling. ..... 168

Table D8. Accuracy Statistics of the 15-class maximum likelihood classification of the Greater Besa-Prophet Area in northern British Columbia. TM bands 5, 4, 3, DEM, slope, angle of incidence, and third principal component from the 6-band TM principal component analysis. No filtration or modelling. ..... 169

Table D9. Confusion matrix of the 15-class maximum likelihood classification of the Greater Besa-Prophet Area in northern British Columbia. Inputs: TM bands 5, 4, 3, DEM, slope, angle of incidence, and Tasseled Cap 'greenness' component. No filtration or modelling. ..... 170

Table D10. Accuracy Statistics of the 15-class maximum likelihood classification of the Greater Besa-Prophet Area in northern British Columbia. TM bands 5, 4, 3, DEM, slope, angle of incidence, and Tasseled Cap 'greenness' component. No filtration or modelling. ..... 171

Table D11. Confusion matrix of the 15-class maximum likelihood classification of the Greater Besa-Prophet Area in northern British Columbia after post-classification modelling and filtration. Inputs: TM bands 5, 4, 3, DEM, slope, angle of incidence, and Tasseled Cap 'greenness' component. ..... 172

Table D12. Accuracy Statistics of the 15-class maximum likelihood classification of the Greater Besa-Prophet Area in northern British Columbia after post-classification modelling and filtration. Inputs: Inputs: TM bands 5, 4, 3, DEM, slope, angle of incidence, and Tasseled Cap 'greenness' component. ... 173

Table E1. Original $\beta$ coefficients and standard error ($\sigma$) for top five multiple linear regression models used to predict NDVI values for 04 Jun 2001 in the Greater Besa-Prophet Area in northern British Columbia. Models are listed by adjusted $r^2$ ..... 175

Table E2. Original $\beta$ coefficients and standard error ($\sigma$) for top five multiple linear regression models used to predict NDVI values for 22 Jul 2001 in the Greater Besa-Prophet Area in northern British Columbia. ..... 176

Table E3. Original $\beta$ coefficients and standard error ($\sigma$) for top five multiple linear regression models used to predict NDVI values for 14 Aug 2001 in the Greater Besa-Prophet Area in northern British Columbia. ..... 177

Table E4. Original $\beta$ coefficients and standard error ($\sigma$) for top five multiple linear regression models used to predict NDVI values for 15 Aug 2001 (Path 49 row 20) in the Greater Besa-Prophet Area in northern British Columbia. ..... 178

Table E5. Original $\beta$ coefficients and standard error ($\sigma$) for top five multiple linear regression models used to predict NDVI values for 16 Aug 2001 (Path 51 Row 20) in the Greater Besa-Prophet Area in northern British Columbia. ..... 179

Table E6. Original $\beta$ coefficients and standard error ($\sigma$) for top five multiple linear regression models used to predict NDVI values for 16 September 01 in the Greater Besa-Prophet Area in northern British Columbia. ..... 180

Table E7. Original $\beta$ coefficients and standard error ($\sigma$) for top five multiple linear regression models used to predict NDVI values for 01 October 01 in the Greater Besa-Prophet Area in northern British Columbia. ..... 181

Table E8. Original $\beta$ coefficients and standard error ($\sigma$) for top five multiple linear regression models used to predict NDVI values for 31 May 2002 in the Greater Besa-Prophet Area in northern British Columbia. ..... 182

Table E9. Original $\beta$ coefficients and standard error ($\sigma$) for top five multiple linear regression models used to predict NDVI values for 15 Jun 2002 in the Greater Besa-Prophet Area in northern British Columbia. ..... 183

Table E10. Original $\beta$ coefficients and standard error ($\sigma$) for top five multiple linear regression models used to predict NDVI values for 24 Jun 2002 in the Greater Besa-Prophet Area in northern British Columbia. ..... 184

Table E11. Original $\beta$ coefficients and standard error ($\sigma$) for top five multiple linear regression models used to predict NDVI values for 09 Aug 2002 in the Greater Besa-Prophet Area in northern British Columbia. ..... 185

Table E12. Original $\beta$ coefficients and standard error ($\sigma$) for top five multiple linear regression models used to predict NDVI values for 09 May 2003 in the Greater Besa-Prophet Area in northern British Columbia. ..... 186

Table E13. Original $\beta$ coefficients and standard error ($\sigma$) for top five multiple linear regression models used to predict NDVI values for 25 Jun 2003 in the Greater Besa-Prophet Area in northern British Columbia. ..... 187

Table E14. Original $\beta$ coefficients and standard error ($\sigma$) for top five multiple linear regression models used to predict NDVI values for 29 Jul 2003 in the Greater Besa-Prophet Area in northern British Columbia. ..... 188

Table F1. $\beta$ coefficients standard error ($\sigma$) for multiple linear regression models that included a transition zone class used to predict NDVI values for 04 Jun 2001 in the Greater Besa-Prophet Area in northern British Columbia. ..... 190

Table F2. $\beta$ coefficients and standard error ($\sigma$) for multiple linear regression models that included a transition zone class used to predict NDVI values for 22 Jul 2001 in the Greater Besa-Prophet Area in northern British Columbia. ..... 191

Table F3. $\beta$ coefficients and standard error ($\sigma$) for multiple linear regression models that included a transition zone class used to predict NDVI values for 15 Aug 2001 in the Greater Besa-Prophet Area in northern British Columbia. ..... 192

Table F4. $\beta$ coefficients and standard error ($\sigma$) for multiple linear regression models that included a transition zone class used to predict NDVI values for 16-September-01 in the Greater Besa-Prophet Area in northern British Columbia..... 193

Table F5. $\beta$ coefficients and standard error ($\sigma$) for multiple linear regression models that included a transition zone class used to predict NDVI values for 01 October 2001 in the Greater Besa-Prophet Area in northern British Columbia..... 194

Table G1. Per-class minimum (min), maximum (max), mean, standard deviation (s) and range for NDVI and NDVI derived from multiple linear regression (MNDVI) analysis for June 2001 in the Greater Besa-Prophet Area in northern British Columbia. ..... 196

Table G2. Per-class minimum (min), maximum (max), mean, standard deviation (s) and range for NDVI and NDVI derived from multiple linear regression (MNDVI) analysis for July 2001 in the Greater Besa-Prophet Area in northern British Columbia. ..... 197

Table G3. Per-class minimum (min), maximum (max), mean, standard deviation (s) and range for NDVI and NDVI derived from multiple linear regression (MNDVI) analysis for August 2001 in the Greater Besa-Prophet Area in northern British Columbia. ..... 198

Table G4. Per-class minimum (min), maximum (max), mean, standard deviation (s) and range for NDVI and NDVI derived from multiple linear regression (MNDVI) analysis for September 2001 in the Greater Besa-Prophet Area in northern British Columbia. ..... 199

Table G4. Per-class minimum (min), maximum (max), mean, standard deviation (s) and range for NDVI and NDVI derived from multiple linear regression (MNDVI) analysis for October 2001 in the Greater Besa-Prophet Area in northern British Columbia. ..... 200

Table H1. Tables of loadings for all NDVI and MNDVI standardized principal component analysis of the Greater Besa-Prophet Area in northern British Columbia. ..... 201

## LIST OF FIGURES

Figure 1.1. The Muskwa-Kechika Management Area (MKMA) and Greater Besa-Prophet Area (GBPA) research area are located in northern British Columbia. ..... 3

Figure 1.2. The Greater Besa-Prophet Area and its three subunits in northern British Columbia..... 4

Figure 2.1. Final classification of the Greater Besa-Prophet Area (overall accuracy 77.33%) in northern British Columbia overlain on shaded relief derived from British Columbia Terrain and Resource Information Management (TRIM) digital elevation model. ..... 35

Figure 3.1. The Greater Besa-Prophet study and its associated subunits in northern British Columbia, within Landsat Thematic Mapper (TM) and Enhanced Thematic Mapper (ETM+) world referencing system (WRS) path 50 row 20 and on the boundary of the overlap between paths 51 and 49. ..... 57

Figure 3.2. Normalized Difference Vegetation Index (NDVI) imagery for the Greater Besa-Prophet Area in 2001, derived from Landsat Thematic Mapper (TM) and Enhanced Thematic Mapper (ETM+) at-satellite spectral radiances. Black areas indicate non-vegetated and clouded or missing areas masked from all analyses. ..... 60

Figure 3.3. Normalized Difference Vegetation Index (NDVI) imagery for the Greater Besa-Prophet Area in 2002 and 2003, derived from Thematic Mapper (TM) and Enhanced Thematic Mapper (ETM+) at-satellite spectral radiances. Black areas indicate non-vegetated and clouded or missing areas masked from all analyses. ..... 61

Figure 3.4 Continuous modelled Normalized Difference Vegetation Index (NDVI) images derived from the top-performing multiple linear regression models in 2001 for the Greater Besa-Prophet Area. ..... 71

Figure 4.1. Time-series profiles of monthly Normalized Difference Vegetation Index (NDVI) and NDVI derived from multiple linear regression analysis (MNDVI) for three characteristic vegetation types (*Dryas*-dominated Alpine, Burned / Disturbed areas and Spruce) in the Greater Besa-Prophet Area, British Columbia, June-September, 2001. ..... 100

Figure 4.2. Normalized Difference Vegetation Index (NDVI) difference images for July-June, August-July, September-August and September – June, 2001 in the Greater Besa-Prophet Area of northern British Columbia. Areas of black indicate areas of cloud, cloud shadow, and non-vegetated areas. ..... 103

Figure 4.3. Frequency of NDVI derived from multiple linear regression analysis (MNDVI) change values and within-class ranges of change for the July-June,

2001 difference images of the Greater Besa-Prophet Area in northern British Columbia. ..... 106

Figure 4.4. Frequency of NDVI derived from multiple linear regression analysis (MNDVI) change values and within-class ranges of change for the August-July, 2001 difference images of the Greater Besa-Prophet Area in northern British Columbia. ..... 107

Figure 4.5. Frequency of NDVI derived from multiple linear regression analysis (MNDVI) change values and within-class ranges of change for the September-August, 2001 difference images of the Greater Besa-Prophet Area northern British Columbia..... 108

Figure 4.6. MNDVI difference images for July-June, August-July, and September-August, 2001 in the Greater Besa-Prophet Area of northern British Columbia. ..... 109

Figure 4.7. Standardized principal component (SPCA) images of near-monthly NDVI derived from multiple linear regression analysis (MNDVI) in the Greater Besa-Prophet Area of northern British Columbia, 2001. Images are displayed with a linear contrast stretch and dichromatic colour palette to maximize contrast between extreme values of the data. ..... 111

Figure B1. Distribution of all locations used to train and assess the accuracy of the final 15-class maximum likelihood classification developed for the Greater Besa-Prophet Area in northern British Columbia. ..... 141

Figure C1. The Sedge Wetland class of the 15-class maximum likelihood classification developed for the Greater Besa-Prophet Area in northern British Columbia. ..... 147

Figure C2. The Shrub class of the 15-class maximum likelihood classification developed for the Greater Besa-Prophet Area in northern British Columbia. ..... 148

Figure C3. The Low-productivity Spruce of the 15-class maximum likelihood classification developed for the Greater Besa-Prophet Area in northern British Columbia. ..... 149

Figure C4. The Gravel Bar class of the 15-class maximum likelihood classification developed for the Greater Besa-Prophet Area in northern British Columbia. ..... 150

Figure C5. The Rock class of the 15-class maximum likelihood classification developed for the Greater Besa-Prophet Area in northern British Columbia. ..... 151

Figure C6. The Rock/Crustose Lichen class of the 15-class maximum likelihood classification developed for the Greater Besa-Prophet Area in northern British Columbia ..... 152

Figure C7. The Water and Snow classes of the 15-class maximum likelihood classification developed for the Greater Besa-Prophet Area in northern British Columbia. ..... 153

Figure C8. The Pine class of the 15-class maximum likelihood classification developed for the Greater Besa-Prophet Area in northern British Columbia ..... 154

Figure C9. The Sub-alpine Spruce Transition zone class of the 15-class maximum likelihood classification developed for the Greater Besa-Prophet Area in northern British Columbia. ..... 155

Figure C10. The Spruce class of the 15-class maximum likelihood classification developed for the Greater Besa-Prophet Area in northern British Columbia. ..... 156

Figure C11. The Riparian Spruce class of the 15-class maximum likelihood classification developed for the Greater Besa-Prophet Area in northern British Columbia. ..... 157

Figure C12. The *Dryas*-dominated Alpine class of the 15-class maximum likelihood classification developed for the Greater Besa-Prophet Area in northern British Columbia. ..... 158

Figure C13. The Moist Alpine class of the 15-class maximum likelihood classification developed for the Greater Besa-Prophet Area in northern British Columbia. ..... 159

Figure C14. The Burned/Disturbed Area class of the 15-class maximum likelihood classification developed for the Greater Besa-Prophet Area in northern British Columbia. ..... 160

## ACKNOWLEDGEMENTS

The following research was made possible with a grant from the Muskwa-Kechika Management Area Trust Fund and the generous contribution of satellite imagery by Rod Backmeyer, British Columbia Ministry of Water, Land and Air Protection.

The organization and relevance of my project and this thesis would not have been the same without the guidance, patience and scrutiny of my supervisory committee, Roger Wheate, Kathy Parker and Darwyn Coxson. I am indebted to Roger for having the patience and confidence in me to let me think independently, even when it meant he had to ride in the back of the helicopter. He will be a friend always. To Kathy, I owe thanks for her wisdom, organizational skills, and her unique perspective that always seemed to spur a new stampede of ideas.

Many of the skills and abilities I needed to complete this project are attributable to two people. Scott Emmons taught me heaps about PCI, EASI and UNIX, but more importantly taught me that there is probably always a creative, and maybe convoluted, solution to every problem and that finding it can be fun. Thanks Scott, for never putting a lid on my tens of gigabytes of data storage and giving me everything I ever asked for- especially your time. Dave Gustine taught me more than perhaps even I can ever appreciate. There is no adequate way to express the extent of his contribution to my graduate project and my life. From stats, to fixing Ira, to driving for ice cream in your pajamas, thanks Spants, for everything.

I am indebted to so many others for their help, support and friendship. Todd Rinaldi, who (in typical fashion) showed up late, was a comfort and a positive distraction as soon as he arrived. He has permanently altered my outlook on life and for that, I am eternally grateful. Both Dave and Todd also fed me a lot. The 'ungulates', Jeremy Ayotte, the aforementioned Dave Gustine, Brian Milakovic and Andrew Walker, always had more faith in me than I did, and Kathy always managed to make me feel like an important part of their team. I will be grateful for the time I spent with them always. Janet Marsh was a great companion in the field and she taught me everything I know about plants. Everyone should have a portable Janet. Nancy Alexander was responsible for the original conception of the project and secured funding. She was also always willing to take care of Indy, spoiling her in the manner to which she has become accustomed, which was greatly appreciated. Neal Mavin was a great pilot, but I am more grateful to him for his interest in my research and his willingness to help; it made fieldwork a lot easier. Mike Gillingham provided software and hardware and was always eager to solve any puzzle that I presented. The Williams family provided accommodations for fieldwork, and Melissa was an excellent field assistant. Thanks to Tim Phaneuf for coffee and hockey. You made my days bright. Special thanks to Jennifer Crosby and Mel Wiebe who were always there for me, especially when I was tired of boys.

To my parents, thank you for making me shovel the driveway and pile rocks, and for teaching me that no matter how much you cry, the work still needs to get done; that lesson has proved invaluable. Thank you also for your unending support and for your unwavering assertion that I can do anything I set my mind to.

Finally, I must thank my two most unassuming and loyal friends, Indiana and Josephine Brown, who helped keep everything in perspective.

# CHAPTER ONE – THESIS INTRODUCTION AND STUDY RATIONALE

## 1.1 CONTEXT

The Muskwa-Kechika Management Area (MKMA) is a 6.3 million hectare wilderness area in northern British Columbia. It was founded to facilitate resource exploration while protecting wildlife diversity and habitat (Muskwa-Kechika Management Area 2001). Conservation and management strategies of the MKMA are spatially distributed; it is comprised of 15 protected areas surrounded by special management and wildland zones that allow different levels of resource extraction and or disturbance (Muskwa-Kechika Management Area 2001). The Besa-Prophet Pre-Tenure Planning Area is a portion of the MKMA that permits exploration and extraction of oil and gas resources and has been identified as having high natural gas potential. Although there is essentially no industrial activity in the area at present, increased applications for petroleum exploration may result in significant landscape alteration.

The Besa-Prophet area has some of the highest habitat ratings in British Columbia for several species of ungulates (BC Ministry of Sustainable Resource Management 2002). Landscape disturbance could influence the existing movement patterns of these and other large mammals or change available habitat resources of multiple species. If resource extraction and environmental stewardship are to co-exist upon the landscape of the Besa-Prophet, baseline seasonal vegetation information must be used to identify habitat types and monitor their change over time. With this

information, resource use by mammal species could be monitored seasonally to help determine the most effective modes of industrial access into the area to minimize landscape alteration and changes to critical seasonal habitats.

The Greater Besa-Prophet Area (GBPA) is the 740,887-ha research area that frames the Besa-Prophet Pre-tenure Planning Area (Figure 1.1). Boundaries were determined based on known migration of large mammals. The GBPA is located between 57°10’ N - 57° 50' N latitude and 122° 50’ - 124° 30’ longitude and straddles the border of the Northern Canadian Rocky Mountains and Muskwa Plateau ecoregions of the Boreal Cordillera and Taiga Plain ecozones (Ecological Stratification Working Group 1995). The area has been segmented into four units within the British Columbia Ministry of Forests Biogeoclimatic Ecosystem Classification (BEC) (Demarchi 1996): Western Muskwa Ranges, Eastern Muskwa Ranges, Muskwa Foothills, and Sikanni Chief Upland. For the purpose of describing the vegetation in the current research, the Eastern and Western Muskwa Ranges were combined because of their similarity (Figure 1.2). The three resulting units are further stratified by three biogeoclimatic zones, which represent finer scale attributes: Boreal White and Black Spruce (BWBS), Spruce Willow Birch (SWB), and Alpine Tundra (AT).

The Sikanni Chief Upland in the easternmost portion of the study area is mostly included in the Muskwa Plateau ecoregion of the Taiga Plane ecozone and is comprised primarily of the BEC BWBS. Temperatures remain below 0°C for 5-7

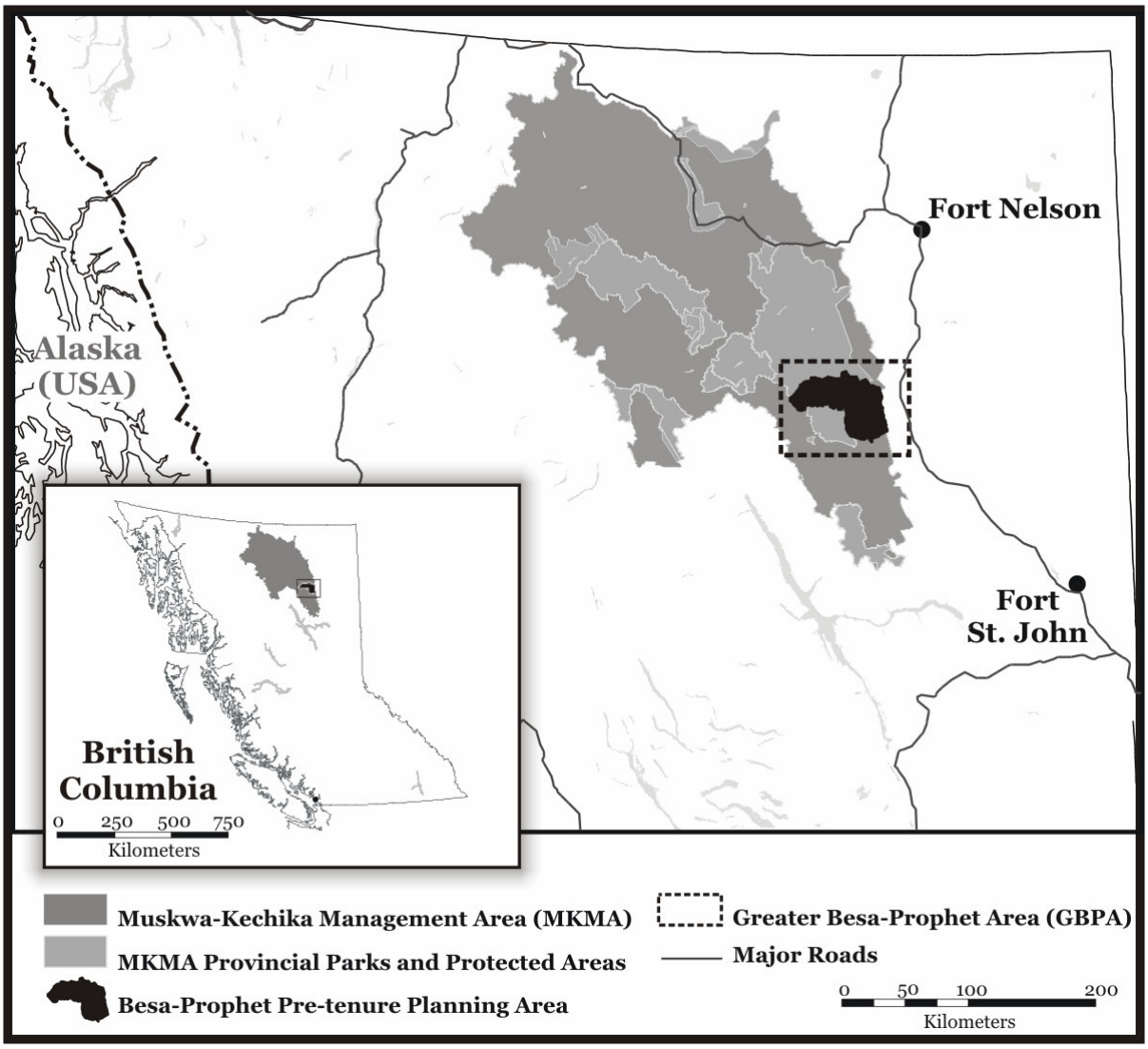


Figure 1.1. The Muskwa-Kechika Management Area (MKMA) and Greater Besa-Prophet Area (GBPA) research area are located in northern British Columbia.

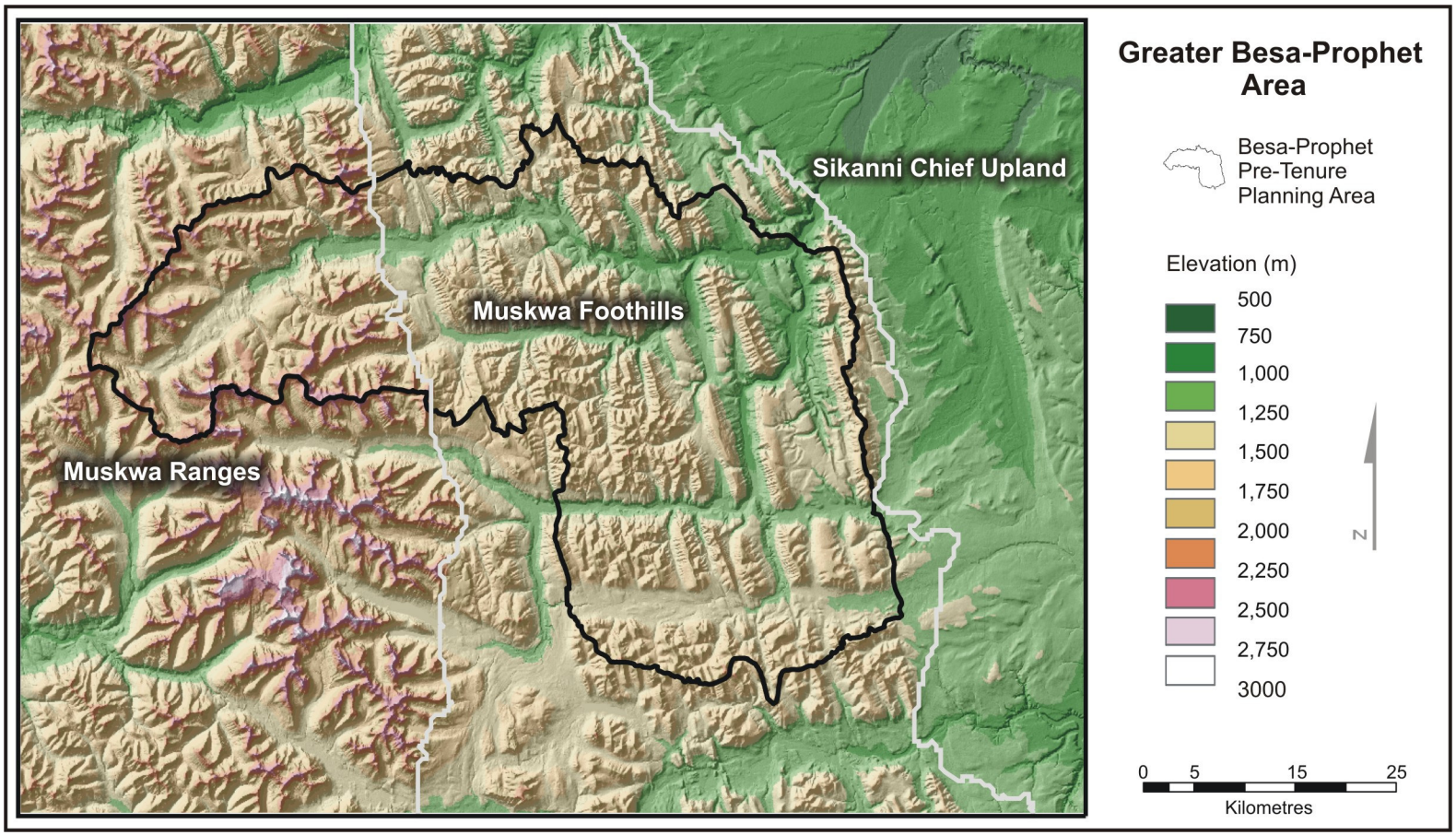


Figure 1.2. The Greater Besa-Prophet Area and its three subunits in northern British Columbia.

months of the year, and above 10°C for fewer than 4 months of the year (DeLong et al. 1991). Mean summer temperature is 12°C and mean winter temperature is -15°C (Ecological Stratification Working Group 1995). Precipitation averages between 330 and 570mm annually, with 35-55% falling as snow (DeLong et al.1991). The area is flat or gently rolling, with an elevation range from 600-1300m. Vegetation cover is principally white spruce (*Picea glauca*) or hybrid spruce (*P. glauca x engelmannii*) and black spruce (*P. mariana*) with an understory dominated by willow (*Salix sp.*) shrubs, sedges (*Carex aquatilis*) and moss species. Mixed lodgepole pine (*Pinus contorta*) stands are also present on morainal or lacustrine soils (DeLong et al. 1991). Open areas have sedge and willow shrubs (< 2m) and contain standing water for many months of the year.

The Muskwa Foothills and Muskwa Ranges subunits of the study area fall within the Northern Canadian Rocky Mountain Ecoregion of the Boreal Cordillera ecozone. The landscape of these subunits has been modified by extensive glaciation and erosion, creating high peaks, extensive plateaus, and wide valleys. Vegetation, precipitation and average temperature are all subject to vertical and aspect zonation. Discontinuous permafrost and rock outcrops are found throughout the area (Ecological Stratification Working Group 1995).

The Muskwa Foothills are characterized by repeated east-west drainages with elevations ranging from 1100m to 2100m. Areas below 1700-1800m are included in the BEC SWB zone. The SWB zone is the montane to sub-alpine zone that occurs

at higher elevations than the BWBS zone. The temperature averages above 10°C for only 1-3 months of the year and mean annual precipitation is 460-2000mm (Pojar and Stewart 1991a). Thirty-five to 60% of all precipitation falls as snow that is usually absent in valleys by June. Snow may persist through the summer at higher elevations, although snow does not begin to accumulate across the GBPA until October (Sims 1999). Valleys are lined with white spruce or sub-alpine fir (*Abies lasiocarpa*) to the tree line (approximately 1400-1600m). Lodgepole pine is found on well-drained, mid-elevation benches and disturbed areas of the Muskwa Foothills, but is not common. Understory species of spruce and pine areas vary with drainage. Undisturbed, open slopes and meadows primarily consist of willow shrubs less than 2m in height. Bog birch (*Betula glandulosa*) and shrubby cinquefoil (*Potentilla fruticosa*) are found in drier areas.

South-facing slopes of the Muskwa Foothills have been repeatedly burned and these areas are dominated by fuzzy-spiked wildrye (*Elymus innovatus*). Fireweed (*Epilobium angustifolium*), alpine sweet-vetch (*Hedysarum alpinum*), tall bluebells (*Mertensia paniculata*), and tall Jacob's ladder species (*Polemonium caeruleum*) are also commonly found in burned areas. With age, burns usually include aspen (*Populus tremuloides*) and balsam poplar (*P. balsamifera sp. balsamifera*) in the shrub layer (<2m) and these may develop into mature trees if left undisturbed. Understory species of treed burns are similar to those found in burns that are more recent.

The lowest elevations within the Muskwa Foothills subunit are along river valleys, and have vegetation similar to the Sikanni Chief Upland. Rivers are lined with sedge fens and carex marshes. White and black spruce are frequent in these riparian areas, although density of trees is low, and height is significantly lower than those trees found at higher elevations and greater slope. Pine/bog birch/ lichen areas can be found on rapidly drained deposits along valleys (Pojar and Stewart 1991a), but are less common than the spruce/willow/*Carex* associations.

Shrubs usually dominate the sub-alpine. Species composition is similar to those at lower elevations, although bog birch and shrubby cinquefoil are more common. Areas above 1800m and windswept ridges in the Muskwa Foothills fall within the BEC AT zone. Temperatures remain below 0°C for 7-11 months, mean annual precipitation is 700-3000mm, and 70-80% of all precipitation falls as snow (Pojar and Stewart 1991b). The distribution of species varies depending on aspect and slope. Generally, southerly or well-drained aspects are dominated by Altai fescue (*Festuca altaica*), dwarf shrubs such as white mountain-avens (*Dryas octopetala*), and various lichen species such as furled paperdoll (*Flavocetraria cucullata*), grey reindeer (*Cladina rangiferina*), rockworm (*Thamnolia vermicularis*), and baby finger (*Dactylina arctica*). Most northerly aspects and late snowmelt areas are dominated by moss species such as step moss (*Hylocomium splendens*) or red-stemmed feathermoss (*Pleurozium schreberi*), and may also include sedges (*Carex sp.*), net-veined willow (*Salix reticulata*) and four-angled mountain heather (*Cassiope tetragona*). Wind-swept, higher elevation areas in the Muskwa Foothills and rock outcrops are mostly limited to lichen cover, particularly roctripe lichens (*Umbilicaria sp.*), although other

vegetation species such as moss campion (*Silene acaulis*) and louseworts (*Pedicularis sp.*) do occur infrequently.

The Muskwa Ranges are the most westerly portion of the study area subset, consisting of U-shaped valleys, steep slopes and peaks as high as 3000m. At elevations below 2100m, mountain vegetation species are typical of those in the Muskwa Foothills subunit. Above 2100m, vegetation is mostly limited to lichens that form colonies among rocks such as those found in windswept areas of the foothills subunit. Vegetation is uncommon above 2500m. Avalanche events are most common on the north and south facing slopes of the Muskwa Ranges. Vegetation regeneration is similar to that of burned areas elsewhere in the study area or is primarily dominated by shrubs (particularly on north-facing slopes).

Large mammals found in the study area include the following: caribou (*Rangifer tarandus caribou*), elk (*Cervus elaphus*), moose (*Alces alces*), Stone's sheep (*Ovis dalli stonei*), white-tailed (*Odocoileus viginianus*) and mule deer (*O. hemionus*), mountain goats (*Oreamnos americanus*), wolves (*Canis lupus*), grizzly (*Ursus arctos*) and black bears (*U. americanus*) and wolverines (*Gulo gulo*) (Sims 1999, D. Gustine, pers. comm.).

## 1.2 STUDY RATIONALE

Habitat information that may be related to the seasonal requirements of ungulates can be extracted from raw data using arithmetic, geometric, algebraic and other

transformations (Billingsley et al. 1983). Analysis of spatial information in this way is the only practical means of monitoring ecosystems consistently and in a timely fashion as data are captured repeatedly over the same area (Roughgarden et al. 1991, Wickland 1991). Several authors have attempted to use remotely-sensed data to improve analyses of seasonal resource use by large mammals. However, there is little research involving the application of these methods in a mountain environment using a multi-temporal dataset comprised of moderate resolution imagery such as Landsat Thematic Mapper (TM) and Enhanced Thematic Mapper (ETM+) data.

My research used the Landsat TM and ETM+ to describe changes in vegetation through the growing season. I assumed that vegetation type, distribution and seasonal differences are related to the habitat needs of large mammals found in the GBPA, and that these species may respond to seasonal changes in vegetation. The primary objective of this thesis, however, was to investigate concepts and methodologies related to remote sensing research, not mammal behaviour. The data and information created from the research are being employed in three related wildlife habitat research projects within the GBPA. For a more complete discussion of the behavioural responses of mammals to terrestrial conditions of the Besa-Prophet, please refer to works by D. Gustine, A. Walker and B. Milakovic.

## 1.3 INTRODUCTION TO METHODOLOGIES AND PRIMARY CONCEPTS

The Landsat program began with the launch of the space-borne Landsat 1 Multi-Spectral Scanner in 1972. The TM sensor onboard Landsat 4 and 5 (launched in 1982 and 1984 respectively) included six bands of 30-m resolution data captured in the visible and reflective infrared portions of the spectrum and one 120-m thermal infrared band. The ETM+ sensor onboard Landsat 7 is the most recently-launched Landsat scanner. ETM+ data consist of six bands of 30-m resolution visible, near and mid infrared, a 15-m resolution panchromatic band, and two 60-m thermal infrared bands. Both sensors repeatedly captured imagery for the same area at separate 16-day intervals until the ETM+ sensor malfunctioned in early 2003. Potentially (with cloud-free conditions), seasonal imagery could be compiled at approximately eight-day intervals through the growing season.

I have used several statistical, arithmetic and qualitative methods for the purposes of describing change in the GBPA with TM and ETM+ data. The procedures are dependent primarily upon two inputs: a supervised image classification and the Normalized Difference Vegetation Index (NDVI).

### *Supervised classification*

A supervised image classification associates satellite-derived imagery with terrain variables and other landscape information such as field-collected vegetation information to assign pixels to a pre-defined scheme. A (Gaussian) maximum likelihood classifier computes the statistical probability of each pixel in the dataset

belonging to one of the classes in the stratified scheme (Gorte 2002, Lillesand and Keifer 1994, Haralick and Fu 1983). Probability is determined with the development of 'training sets' – representations of the spectral response patterns of landscape classes that have been determined by spatially relating *a priori* attribute information to input imagery (Lillesand and Keifer 1994). This signature is not a consistent, predictable spectral value, but rather a probability distribution of the relative frequency of a range of signatures (Haralick and Fu 1983).

***Normalized Difference Vegetation Index (NDVI)***

Healthy green vegetation absorbs 80%-90% of the energy in the visible red wavelengths (630-690 nm) and reflects 40%-50% of the near infra-red (NIR) (760-900 nm) (Jensen 1996, Knipling 1970). This reflectance/absorption separation at approximately 700 to 740 nm is known as the 'red edge' (Horler et al. 1983) and is the fundamental principle underlying many techniques that are used to extract vegetation information from satellite data. The mathematical exploitation of satellite bands to derive this information (usually in the red and NIR wavelengths) is a vegetation index – a quantitative measure of the vigour of vegetation (Bannari et al. 1995). The most commonly applied index is the Normalized Difference Vegetation index (NDVI). The NDVI is given as:

$$NDVI = \left( \frac{TM_4 - TM_3}{TM_4 + TM_3} \right)$$

*Equation 1.1*

where TM4 is the near infrared (band 4, TM/ETM+), and TM3 is the visible red (band 3, TM/ETM+). These data have been found to be related to net primary productivity, biomass, leaf area index, crown closure and other vegetation characteristics (Purevdorj et al. 1998, Baret and Guyot 1991, Tucker and Sellers 1986).

## 1.4 THESIS ORGANIZATION

This thesis has been organized into three separate research chapters in addition to this introduction and a final conclusion. The chapters are written as three independent pieces of research, although the chapters are interrelated. In Chapter 2, the procedures used to develop a vegetation classification for the Greater Besa-Prophet Area are described. Chapter 3 explains common pre-processing methods applied to remotely-sensed data, and their applicability to this study. It also describes methods used to investigate the relationships between NDVI and several independent variables in the GBPA. Chapter four uses data created in the previous chapters to describe relative changes in vegetation over the growing season in the GBPA.

Much of the research presented in each chapter was the result of a collaborative effort with other GBPA researchers. Any mention of 'we' found in each chapter makes reference to these collaborators. At the beginning of some chapters, is a list of potential co-authors should the works be submitted for publication.

## 1.5 LITERATURE CITED


Bannari, A., Morin, D., and Bonn, F. (1995). A Review of Vegetation Indices. *Remote Sensing Reviews*, 13: 95-120.

Baret, F. and Guyot, G. (1991) Potentials and Limits of Vegetation Indices for LAI and APAR Assessment. *Remote Sensing of Environment*, 35: 161-173.

Billingsley, F.C. (1983). Data Processing and Reprocessing, in R.N. Colwell (Ed.), *Manual of Remote Sensing*, 2nd Edition, Vol. 1, (pp. 719-722). Falls Church, Virginia, USA: Sheridan Press.

British Columbia Ministry of Sustainable Resource Management (2002). Besa-Prophet Pre-Tenure Plan – Phase 1. British Columbia Ministry of Sustainable Resource Management, Victoria BC 120pp.

DeLong, C., Annas, R.M., and Stewart, A.C. (1991). Boreal White and Black Spruce Zone. In Meidinger, D. and Pojar, J., eds. *Ecosystems of British Columbia. Ministry of Forests*, Victoria BC. 330pp.

Demarchi, D.A. (1996). An Introduction to the Ecoregions of British Columbia. Ministry of Environment Lands and Parks, Victoria BC. 47pp.

Ecological Stratification Working Group. (1995). A National Ecological Framework for Canada. Agriculture and Agri-Food Canada, Research Branch, Centre for Land and Biological Resources Research and Environment Canada, State of the Environment Directorate, Ecozone Analysis Branch, Ottawa/Hull.

Gorte, B. (2002). Supervised Image Classification. In Stein, A., Van Der Meer, F., and Gorte, B. (Eds.) *Spatial Statistics for Remote Sensing* (pp. 153-162). Dordrecht: Kluwer Academic Publishers.

Haralick, R.M., and Fu, K. (1983). Pattern Recognition and Classification. in R.N. Colwell (Ed.), Manual of Remote Sensing, 2nd Edition, Vol. 1, (pp. 719-722). Falls Church, Virginia, USA: Sheridan Press.

Horler, H.H.N., Dockray, M., and Barber, J. (1983). The red edge of plant leaf reflectance. *International Journal of Remote Sensing,* 4: 273-288.

Jensen, J.R., (1996). Introductory Digital Image Processing. A Remote Sensing Perspective 2nd ed. Upper Saddle River: Prentice Hall, Inc.

Knipling, E.B. (1970) Physical and Physiological Basis for the Reflectance of Visible and Near-infrared Radiation From Vegetation. *Remote Sensing of Environment,* 1 (3): 155-159.

Lillesand, T.M., and Kiefer, R.W. (1994). *Remote Sensing and Image Interpretation.* New York: Wiley.

Muskwa-Kechika Management Area (2001). Backgrounders. http://www.muskwa-kechika.com/who/background.html

Pojar, J., and Stewart, A.C. (1991a). Spruce - Willow – Birch Zone. In Meidinger, D. and Pojar, J., eds. Ecosystems of British Columbia. BC Ministry of Forests, Victoria BC. 330pp.

Pojar, J., and Stewart, A.C. (1991b). Alpine Tundra Zone. In Meidinger, D. and Pojar, J., eds. Ecosystems of British Columbia. BC Ministry of Forests, Victoria BC. 330pp.

Purevdorj T.S, Tateishi, R., Ishiyamas, T., and Honda, Y. (1998) Relationships Between Percent Vegetation Cover and Vegetation Indices. *International Journal of Remote Sensing,* 19 (18): 3519-3535.

Roughgarden, J. Running, S.W., and Matson, P.A. (1991) What Does Remote Sensing Do For Ecology? *Ecology,* 72 (6): 1918-1922.

Sims, R.A. and Associates (1999). Terrestrial Ecosystem Mapping (TEM) with Wildlife Habitat Interpretations of Besa-Prophet Area. Part 1: TEM Report. Prepared for BC Environment Lands and Parks, Oil and Gas Division, Fort St. John, BC. 169pp.

Tucker, C. J. and Sellers, P.J. (1986) Satellite Remote Sensing of Primary Productivity. *International Journal of Remote Sensing,* 7: 1395-1416.

Wickland, D.E. (1991) Mission to Planet Earth: The Ecological Perspective. *Ecology,* 72 (6): 1923-1933.

# CHAPTER TWO – CLASSIFICATION OF POTENTIAL LARGE MAMMAL HABITAT IN A MOUNTAIN LANDSCAPE USING LANDSAT TM DATA

## 2.1 INTRODUCTION

Management of wildlife species is dependent on knowledge of critical seasonal habitat requirements and their distribution within the area that animals can use. To determine the distribution of potential habitat, the landscape can be segmented into units, delineated by the boundaries of components relevant to the species such as thermal cover, hiding cover and forage (Leckenby et al. 1985). These data, however, are rarely available and costly to create using traditional mapping techniques.

Several authors have used classification of satellite imagery to delineate potential large mammal habitats (Johnson et al. 2003, Franklin et al. 2002, Huber and Casler 1990, Leckenby et al. 1985, Laperriere et al. 1980). These may be used as inputs to statistical models such as habitat suitability indices and resource selection functions (Johnson et al. 2004, Apps et al. 2004, Miranda and Porter 2003, Boyce et al. 2003, Nielsen et al. 2003, Jepsen et al. 2002, McLoughlin et al. 2002, Osborne 2001, Rettie and Messier 2000, Arthur et al. 1996). Resource selection functions quantify habitat use relative to its availability, which can be related to the fitness of the individual (Rettie and Messier 2000, Manly et al. 1993).

Using satellite imagery for habitat mapping may partially reduce the human bias and error introduced with traditional techniques such as air photo interpretation and may be a more cost-effective alternative to traditional mapping techniques. Leckenby et al. (1985) found that habitat information from remote sensing data was more consistent and precise than data derived from other sources. In mountainous terrain, however, topographic variation hinders classification efforts by altering the typical reflectance of vegetation types that is received by the orbiting sensor (from differential illumination), or by complicating the distribution of vegetation across the landscape (Wilson and Franklin 1992). As a result, the accurate characterization of vegetation in mountainous terrain with satellite imagery can be extremely challenging and accuracy may be lower than classification in other areas.

The goal of this project was to create a vegetation classification for multi-species wildlife habitat studies that included the most specific information about vegetation communities as possible. The primary objective was to determine the level of detail that could be extracted about the vegetation communities of a mountainous area using a satellite image classification.

## 2.2 METHODS

### *Study Area*

This study occurred in the Greater Besa-Prophet Area (GBPA) in northern British Columbia. A detailed description of the study area can be found in Chapter 1.

### *Data Input*

A cloud-free Landsat 5 TM scene (path 50, row 20, August 15, 2001) was used as input for the supervised classification. The image was orthocorrected with a satellite orbital model (PCI OrthoEngine® v8.2, Richmond Hill, ON, Canada) using the British Columbia Terrain and Resource Inventory Management (TRIM) hydrologic and transportation layers and digital elevation model. The image was resampled to 25-m resolution to match the resolution of the digital elevation model using bilinear interpolation and subset to match the extents of the GBPA.

### *Field Data Collection*

The vegetation classification scheme was not pre-determined prior to the beginning of the project. Fieldwork was conducted on four occasions (June 2001, October 2001, June 2002 and August 2002) to collect data for development of spectral signatures. Because the GBPA is a rugged and remote wilderness area with no road access, plot locations were accessed by helicopter. Locations that were not suitable for access by air (e.g., forested areas, steep slopes, etc.) were accessed on foot. A preferential sampling scheme was adopted, i.e., plot sites were chosen for their variability of percent cover, leading and understory species type and aspect in order to be representative of variable reflectance values for their class, but were not the result of a random or stratified sampling scheme. This information was determined on-site, not with prior mapping schemes or legends, and was undertaken so that plot locations fell in areas most appropriate for signature development and were reasonably accessible to survey. Therefore, sampling criteria included the

following: 1) locations fell as close as possible to the centre of a homogenous vegetation region (at least 2500m$^2$, or four resampled Landsat TM or ETM+ pixels), 2) plot sites were accessible, and 3) vegetation types were not pre-determined before sampling to minimize bias in data collection.

Vegetation sampling occurred in a circular area within a 10-m minimum radius of the plot location. At each plot location, dominant species type and percent cover were recorded for species occurring in four layers: tree (woody vegetation >2m), shrub (woody vegetation <2m), herb (non-woody vascular plants <2m and dwarf shrubs), and moss/lichen. Secondary species were also recorded. Each layer was then assigned a percentage of total vegetation at the plot, and each plot was photographed. There were 146 full plots sampled on the landscape in this manner.

All locations were displayed on 1-m resolution digital orthophotography to ensure that the recorded vegetation type was contiguous over a radius of 50m and suitable for use in the classification process. Those locations falling on vegetation boundaries, those that did not achieve a contiguous area greater than 2500m$^2$, and those with questionable spatial accuracy were not used. Vegetation types that were spectrally distinct but with limited characteristics that would make them visually discernable at the resolution of aerial photography (i.e., texture or tone) such as alpine areas, were checked for positional accuracy only based on site descriptions collected while in the field.

The detailed information of the leading species and understory combinations of these full plots was used to develop a vegetation classification that differentiated homogeneous vegetation types by grouping them in a hierarchical scheme. First, plot data were separated into three groups, based on their spatial distribution: alpine (vegetation in the herb or moss/lichen layer at elevations >1600m), sub-alpine (areas above tree line, not including alpine areas) and montane (areas within or below tree line or exhibiting similar vegetation). Plots were then separated into broad groups based on the percent cover of the leading species types in each sampled layer (tree, shrub, herb, and moss/lichen). Leading species, aspect, and understory types further divided these groups. This grouped, hierarchical scheme allowed vegetation classes (representing vegetation types) to be collapsed into more general or broad classes if the data available were insufficient to differentiate vegetation types. Vegetation types in riparian areas (those areas with the water table at or near the surface for most months of the year) were isolated from the scheme as unique classes (i.e., these areas were distinct from areas sharing leading species types). Points for classes that were not field-truthed (e.g., snow/glaciers and water) or non-vegetated and under sampled (e.g., gravel bars and rocks) were selected by interpretation of orthophotography. These points were selected only in well-known areas of the study area. Table 2.1 lists the 29 classes defined in this manner.

Table 2.1. The 29-class vegetation classification scheme developed for the Greater Besa-Prophet Area in northern British Columbia.

**MONTANE**

***Treed***

1. Balsam Poplar / Aspen
2. Deciduous / Coniferous Mix
3. Pine: Dry understory
4. Pine: Shrub / Moss understory
5. Pine / Spruce Mix
6. Spruce
7. Low-productivity Spruce

***Forbs / Shrub***

8. Recent Burn: Grass / Shrub
9. Mixed Deciduous Shrubs
10. Deciduous Shrub: Willow
11. Fescue
12. Avalanche Track

***Riparian***

13. Sedge Wetland
14. Riparian Spruce

**ALPINE**

15. Alpine Grass
16. Mountain-Avens / Lichen
17. Mountain-Avens / Fescue
18. Mountain-Avens / Lupine / Rock
29. Moist Alpine

**SUB-ALPINE**

20. Krumholtz
21. Sub-alpine Shrub: Bog Birch
22. Sub-alpine Shrub: Willow
23. Sub-alpine Shrub: Bog Birch /Willow /Cinquefoil
24. Treeline: Spruce to Sub-alpine Shrub transition

**NON-VEGETATED**

25. Gravel Bar
26. Rock Outcrop / Talus / Bedrock
27. Rock / Crustose Lichen
28. Water
29. Snow / Glacier

There were three primary phases of the classification process used to associate the 29-class scheme with actual landscape features and vegetation types using satellite data: 1) development of spectral signatures, and statistical association of signatures, plot information, and terrain variables using a maximum likelihood classifier, 2) post-classification filtering, 3) post-classification modelling. Each phase included several iterations of the methods to determine the most successful strategy for applying the classification scheme to the landscape. The accuracy of each classification was assessed with each variation of input or method in each phase, and the output with the highest accuracy was used for subsequent phases.

### *Spectral Signature Development*

Classification Inputs

The selection of inputs to be used in a supervised classification influences the accuracy of the classification because of the differences in the reflectance of cover types in different wavelengths (Liu et al. 1997) and the distribution of these types on the landscape (e.g., slope, aspect and elevation). We selected Landsat TM bands and their derivatives as inputs to the maximum likelihood scheme and performed the classification for each input combination using the same training areas. These imagery-based derivatives were selected based on low correlation with band and terrain inputs to reduce dimensionality (number of inputs to process) and redundancy. We assumed these inputs could improve classification accuracy because they have been found to be correlated with ground vegetation (NDVI and Tasseled Cap 'Greenness') or provided data with reduced topographic effect. Input

image layers included TM band 5 (mid-infrared), TM band 4 (near infrared) and TM band 3 (red). Derivatives included the Normalized Difference Vegetation Index (NDVI), tasseled cap 'greenness' component, and components 2 and 3 from the TM six-band (excluding thermal) principal component analysis.

The primary determinant of the distribution of features at the landscape level in a mountain environment is topography (Bian and Walsh 1993). This includes such elements as topographic position, slope, and aspect (Hills and Pierpoint 1960). Hence, vegetation cover characteristics are partly allied with the topographic characteristics of the landscape upon which they are located. Elevation controls altitudinal zonality, slope determines drainage characteristics, and aspect controls flow direction, solar radiation, evaporation, snow retention and some soil properties (Florinsky and Kuyakova 1996). For these reasons, elevation, slope and angle of incidence (representing the angle of the surface to the sun at the time the image was captured) were used as inputs to the classification in order to predict more efficiently a class for each pixel using the pre-defined scheme.

Training Areas

The number of training areas and pixels per training area were dependent upon the spatial characteristics of the cover type (i.e., estimated contiguous area at the training location determined by ground knowledge of the site), and frequency on the landscape, although each class had at least five independent training areas. Orthophotography (1-m resolution) was used to aid in the selection of the most

appropriate pixels for each training area. The number of pixels used as training pixels at each site was determined using the 'seed' procedure in PCI Imageworks. The seeding procedure 'grows' irregular regions of training areas based upon the digital numbers of the input bands (PCI Geomatica v9.1, Richmond Hill, ON, Canada). Seeded areas were trimmed if they did not agree with the area that could be reasonably discerned with visual interpretation of the orthophotography, or that did not agree with field observations regarding the site. For those classes that could not be identified in the orthophotography (i.e., classes such as the alpine classes that had little easily-identifiable texture or tone), training pixels were limited to the pixel upon which the plot fell and its nearest adjacent pixels. Training adjacent pixels in this manner should have partially accounted for any GPS error that could have occurred during data collection.

Signature separability is measured as the statistical difference between pairs of spectral signatures. To maximize signature separability and create signatures that best represented each vegetation class, separability among classes was assessed using Bhattacharya distance (PCI Geomatica v9.1, Richmond Hill, ON, Canada) after each plot was added as training data. This ensured that the best combination of training plots and pixels was used for each vegetation class. A maximum likelihood classification was performed using each combination of input bands to determine the most efficient combination of inputs and to determine the quality of the training areas. For each iteration of the classification, a confusion matrix was generated that listed output classification of all training areas. A confusion matrix uses cross-tabulation of the classification output against verified reference data to quantify the

misclassification of features (Congalton and Green 1993, Congalton 1999). The overall accuracy of the classification is the ratio of the sum of the correctly classified (reference) data of all classes to the total number of all points in the matrix (Skidmore 2002, Congalton and Green 1993). In the training stage, the confusion matrix is generated from the classified data and the training areas used to develop the classification. This provides a relative indication of classification accuracy before an independent assessment using reference data. This procedure helped to identify training areas that were consistently misclassified.

We assumed that misclassified training areas were not representative of the spectral characteristics of the class as it was defined (statistically) by the other training areas, and misclassified training areas were often removed from the set of training areas. Training areas were edited in this fashion until separability among classes was maximized and overall accuracy of the classification of the training areas was >95%. The output of the maximum likelihood classification with the highest training area accuracy was considered to be the final classification and was selected for further accuracy assessment and analysis.

***Post-classification Filtration***

A modal filter was applied using a 3 x 3 moving window to the output classification to remove anomalous pixels from homogenous areas. Any single pixels remaining were merged into the class of contiguous neighbours. This procedure ensured that the variation in the classification was not significantly higher than in the original input imagery (Colby and Keating 1998).

### *Post-classification modelling*

This step investigated the improvement of the classification by empirically defining terrain-based 'rules' for the spatial distribution of each class on the landscape. Although terrain variables (slope, aspect, elevation and angle of incidence) were used in the classification, these inputs did not sufficiently limit the delineation of classes that were spectrally similar but spatially distinct (i.e., although the Moist Alpine class was found on northerly slopes, the classifier did not limit the class to these areas). Rules were developed to better associate vegetation types with vegetation classes using observations and data gathered during field research. These rules primarily relied upon associations of slope, aspect and elevation as the primary determinants of class membership. Rules developed for each class can be found in Appendix A (Table A1).

### *Accuracy Assessment*

A final sampling trip (June 2003) was conducted in order to collect independent data to access the accuracy of the classification. Ninety-six accuracy assessment plots were visited. At these plot locations, leading species and understory combinations were recorded in considerably less detail than full plots. Two hundred and twenty-five observations also were made from helicopter, and these were used in a similar fashion to the accuracy assessment points, but only where the class type was easily determined by air, and the vegetation was homogeneous for at least 1ha. Full plot data not used as training areas were also used as accuracy assessment points.

Concurrent research in the GBPA involved the collection of vegetation information at a level of detail similar to that of the full plots of this study. Fifty vegetation plots were made available from these projects (D. Gustine, A. Walker, unpublished data). In the interest of consistency, however, these data were used only as accuracy assessment points when necessary to augment sample size. All data used as accuracy assessment points were subject to the same quality assurance procedures as data used for training areas. Locations and distribution of all points used for classification and accuracy assessment are found in Appendix B (Fig. B1, Table B1 and Table B2).

Congalton and Green (1993) suggested that accuracy should be assessed using a minimum sample of 50 independent accuracy assessment points per class and that schemes with a large number of classes (i.e., >12) should have 75-100 independent accuracy assessment points per class to ensure statistically valid results. Points used for accuracy assessment were determined based on the uniformity of the plot (determined by percent cover of leading species and relevant understory species), informed knowledge of the area on the ground, and contiguous area of the vegetation type on the ground. Points used for accuracy assessment in classes having points of equal quality were chosen using a random number generator. The number of points used to assess the accuracy of each classification iteration varied depending upon the number of classes in the hierarchical scheme (Table 2.1), although sample sizes were consistent across classes for each scheme.

Currently, the most widely accepted methods to measure the accuracy of a classification are the generation of a confusion matrix (such as that used to assess the accuracy of the training areas) and computation of a metric such as the KAPPA ($\kappa$) coefficient (Foody 2002, Skidmore 2002, Congalton and Green 1993). The confusion matrix developed to assess the accuracy of each classification iteration used the independent (not used for training) data collected in the field. The major diagonal of the matrix characterizes accuracy versus the errors of omission and commission that are the off-diagonal elements in the matrix (Foody 2002, Skidmore 2002, Congalton 1999). This accuracy was reported as overall accuracy (correctly classified sample/total number of sample units for all classes), average overall accuracy, and producer's and user's accuracy (for each class). The producer's accuracy is computed by dividing the total number of correct sample units in an individual class by the total number of reference units (Congalton and Green 1993, Congalton 1999). User's accuracy is computed by dividing the total number of correctly classified pixels in an individual class by the total number of sample pixels classified as that class (Congalton and Green 1993, Congalton 1999). The confusion matrix, because of its ability to account for errors of omission and commission in each class, provides a more accurate measurement of accuracy than a simple analysis of the percent of points correctly allocated. The $\kappa$ statistic incorporates the effect of chance occurrence in the classification and was computed for the classification overall and for each class.

A commonly recommended target for the overall accuracy is 85% (Foody 2002, Congalton 1999, Anderson et al. 1979) and this target was set for the overall classification and within classes. If the accuracy of the final classification was determined to be unacceptably low, classes in the hierarchical scheme were collapsed into more general classes in order to increase the overall accuracy of the classification. A new set of accuracy assessment points was assembled for each classification iteration.

## 2.3 RESULTS

### *Overall Accuracy*

None of the outputs that used the 29-class scheme achieved an overall accuracy greater than 50%. Classes most often confused were those of similar vegetation type (e.g., shrub) but of different species composition (e.g., mixed deciduous shrubs and deciduous shrub: willow), or classes with the same leading species but different secondary species (e.g., *Dryas*/lichen and *Dryas*/fescue). Low-accuracy classes were collapsed into more general classes, and this resulted in a new scheme of 15 classes. Table 2.2 provides a general description of each class in this scheme, and Table 2.3 summarizes variation in accuracy of the 15-class scheme by derivative input. For a more detailed description, and the distribution of classes on the landscape, see Appendix C (Figs. C1-C14). Confusion matrices and all accuracy statistics for each 15-class vegetation classification are located in Appendix D (Tables D1-D12).

The base classification (without derivatives) achieved an overall accuracy of 70.00% (n=150 with 10 samples per class) (Table 2.3). Accuracy was improved with the addition of the Tasseled Cap 'greenness' (TCG) component (72.67%), or the third principal component (PC3) (72.00%), but did not improve with the addition of the 2nd principal component (PC2) (70.00%). Accuracy decreased with the addition of the NDVI (69.33%). Classification accuracy did not increase with the combination of more than one imagery derivative.

Application of the 3 x 3 modal filter, and post-classification modelling rules (see Appendix A) improved the overall accuracy of the best classification (base & TCG) (Table D11) by 5.33% to a final accuracy of 77.33% (Table 2.3). The producer's accuracy and user's accuracies of many classes increased (Table D12), although some individual producer's and user's accuracy decreased. The overall increase in accuracy and the increase in the accuracy of many classes with low accuracy, however, were considered to be of greater interest than the decrease in accuracy for some classes. Table 2.4 shows the 15-class scheme and the accuracy of each class in the base

Table 2.2. Brief descriptions of the 15-class scheme used to classify the landscape of the Greater Besa-Prophet area in northern British Columbia.

| CLASS | DESCRIPTION |
|---|---|
| **MONTANE** | |
| ***Treed*** | |
| Pine | Lodgepole pine (*Pinus contorta)* found on well-drained, mid-elevation benches and some disturbed areas. Class includes mature and growing stands. |
| Spruce | Mature white spruce (*Picea glauca)* or sub-alpine fir (*Abies lasiocarpa*) found on well-drained soils. Often associated with shrub (i.e., willow (*Salix sp.*)/ soopolallie *(Sheperdia canadensis*) or grass understory. |
| Low-productivity Spruce | White spruce primarily found on north-facing slopes. Low density and reduced height and diameter compared to mature spruce of other classes. Understory is primarily moss (e.g., *Pleurozium schreberi*). |
| ***Forbs / Shrub*** | |
| Mixed Deciduous Shrubs | Shrubs <2m. Variable % cover of willow, bog birch (*Betula glandulosa)*, or shrubby cinquefoil *(Potentilla fruiticosa)*. Includes sub-alpine shrubs. |
| ***Riparian*** | |
| Sedge Wetland | Dominated by sedge (*Carex aquatilis*). Some moss species or willow depending on duration of seasonal standing water. |
| Riparian Spruce | White spruce or black spruce (*P. mariana*) associated with sedge or willow. Found in riparian areas and poorly drained stands in the Eastern Lowland area. |
| ***Other*** | |
| Burns / Disturbed | Burns and disturbed areas. Recent disturbances are primarily dominated by fuzzy spiked wildrye (*Elymus innovatus*). With age these areas develop Aspen (*Populus tremuloides*) and Balsam Poplar (*P. balsamifera*) shrubs (<2m) and trees (>2m). May be associated with stands of Pine. |

Table 2.2. Continued.

| CLASS | DESCRIPTION |
|---|---|
| **SUB-ALPINE** | |
| Sub-alpine Spruce Transition | Transition from mature spruce or fir to sub-alpine shrubs at treeline. Includes krummholz. |
| **ALPINE** | |
| *Dryas*-dominated Alpine | Mountain avens (*Dryas octopetala)* and fescue (*Festuca altaica*) dominated alpine. Moderate to steep southerly slopes. |
| Moist Alpine | Poorly drained and northerly alpine slopes. Primarily dominated by moss with net-veined willow (*Salix reticulata*). Class also includes sites dominated by four-angled mountain heather (*Cassiope tetragona).* |
| **NON-VEGETATED** | |
| Gravel Bar | Gravel bars of current stream courses. Class also includes dry streambeds. Usually non-vegetated, although Drummond's mountain avens (*Dryas drummondii)* may occur. |
| Rock Outcrop / Talus /Bedrock | Outcrops of talus and high-elevation, non-vegetated bedrock. |
| Rock / Crustose Lichen | Large frost-broken boulders with significant cover of crustose lichen such as *Melanelia hepatizon.* |
| Water | Permanent water bodies. |
| Snow / Glacier | Permanent snowfields and glaciers. |

Table 2.3. Overall accuracy and KAPPA statistic ($\kappa$) of each classification iteration that used the 15-class scheme (see Table 2.2) developed for the Greater Besa-Prophet Area in northern British Columbia.

| Input | Overall Accuracy | Overall $\kappa$ |
|---|---|---|
| 5,4,3, DEM, Slope, Angle of Incidence (Base) | 70.00% | 0.68 |
| Base and Principal Component 2 | 70.00% | 0.679 |
| Base & NDVI | 69.33% | 0.67 |
| Base & Principal Component 3 | 72.00% | 0.7 |
| Base & Tasseled Cap 'Greenness' (TCG) | 72.67% | 0.71 |
| Base, TCG & all modelling and filtration | 77.33% | 0.76 |

Table 2.4. Accuracy of the 15-class vegetation classification scheme developed for the Greater Besa-Prophet Area in northern British Columbia before and after post-classification modeling.

| CLASS | BASE CLASSIFICATION *Overall Accuracy 69.33% κ 0.7* | | | POST-MODELLING AND FILTRATION *Overall Accuracy 77.33% κ 0.757* | | |
|---|---|---|---|---|---|---|
| | *producer* | *user* | *κ* | *producer* | *user* | *κ* |
| **MONTANE** | | | | | | |
| ***Treed*** | | | | | | |
| Pine | 50.00% | 55.56% | 0.5238 | 60.00% | 60.00% | 0.64 |
| Spruce | 50.00% | 50.00% | 0.4643 | 60.00% | 66.67% | 0.64 |
| Low-productivity Spruce | 50.00% | 83.33% | 0.8214 | 70.00% | 87.50% | 0.87 |
| ***Forbs / Shrub*** | | | | | | |
| Mixed Deciduous Shrubs | 70.00% | 50.00% | 0.4643 | 80.00% | 53.33% | 0.50 |
| ***Riparian*** | | | | | | |
| Sedge Wetland | 50.00% | 55.56% | 0.5238 | 70.00% | 77.78% | 0.76 |
| Riparian Spruce | 90.00% | 56.25% | 0.5312 | 90.00% | 69.23% | 0.62 |
| ***Other*** | | | | | | |
| Burned / Disturbed | 80.00% | 88.89% | 0.881 | 80.00% | 88.89% | 0.88 |
| **SUB-ALPINE** | | | | | | |
| Sub-alpine Spruce Transition | 70.00% | 87.50% | 0.8661 | 80.00% | 100.00% | 1.00 |
| **ALPINE** | | | | | | |
| *Dryas*-dominated Alpine | 70.00% | 50.00% | 0.4643 | 60.00% | 75.00% | 0.73 |
| Moist Alpine | 40.00% | 80.00% | 0.7857 | 60.00% | 75.00% | 0.73 |
| **NON-VEGETATED** | | | | | | |
| Gravel Bar | 80.00% | 88.89% | 0.881 | 90.00% | 90.00% | 0.89 |
| Rock | 90.00% | 64.29% | 0.6173 | 100.00% | 62.50% | 0.62 |
| Rock / Crustose Lichen | 70.00% | 87.50% | 0.8661 | 70.00% | 87.50% | 0.87 |
| Water | 90.00% | 100.00% | 1.00 | 90.00% | 100.00% | 1.00 |
| Snow / Glacier | 100.00% | 100.00% | 1.00 | 100.00% | 100.00% | 1.00 |

classification and with all post-classification modelling and filtration. Figure 2.1 shows the final classification with all filtration and modelling applied.

### *Per-class Accuracies*

Base Classification

In the base classification, eight classes had user's or producer's accuracies lower than 60% (Table D2): Sedge Wetland, Shrub, Low-productivity Spruce, Pine, Spruce, Riparian Spruce, *Dryas*-dominated Alpine, and Moist Alpine. The coniferous classes were primarily confused with other coniferous classes. High producer's accuracy and low user's accuracy in the Low-productivity Spruce class indicate it was over-represented on the landscape, while low producer's accuracy and high user's accuracy indicate that the Riparian Spruce class was under-represented on the landscape compared to its actual distribution on the ground. The Alpine classes had similar patterns of omission/commission and were primarily confused with one another. High producer's accuracy and low user's accuracy in Moist Alpine areas and the reverse in the *Dryas*-dominated Alpine areas suggest that the *Dryas*-dominated Alpine class was over-represented on the landscape, erroneously reducing the assignment of Moist Alpine. *Dryas*-dominated Alpine areas were also confused with the Rock and Rock / Crustose Lichen classes. Sedge wetland was primarily confused with Shrub, whereas some Shrub areas were classified as Riparian Spruce and *Dryas*-dominated Alpine.

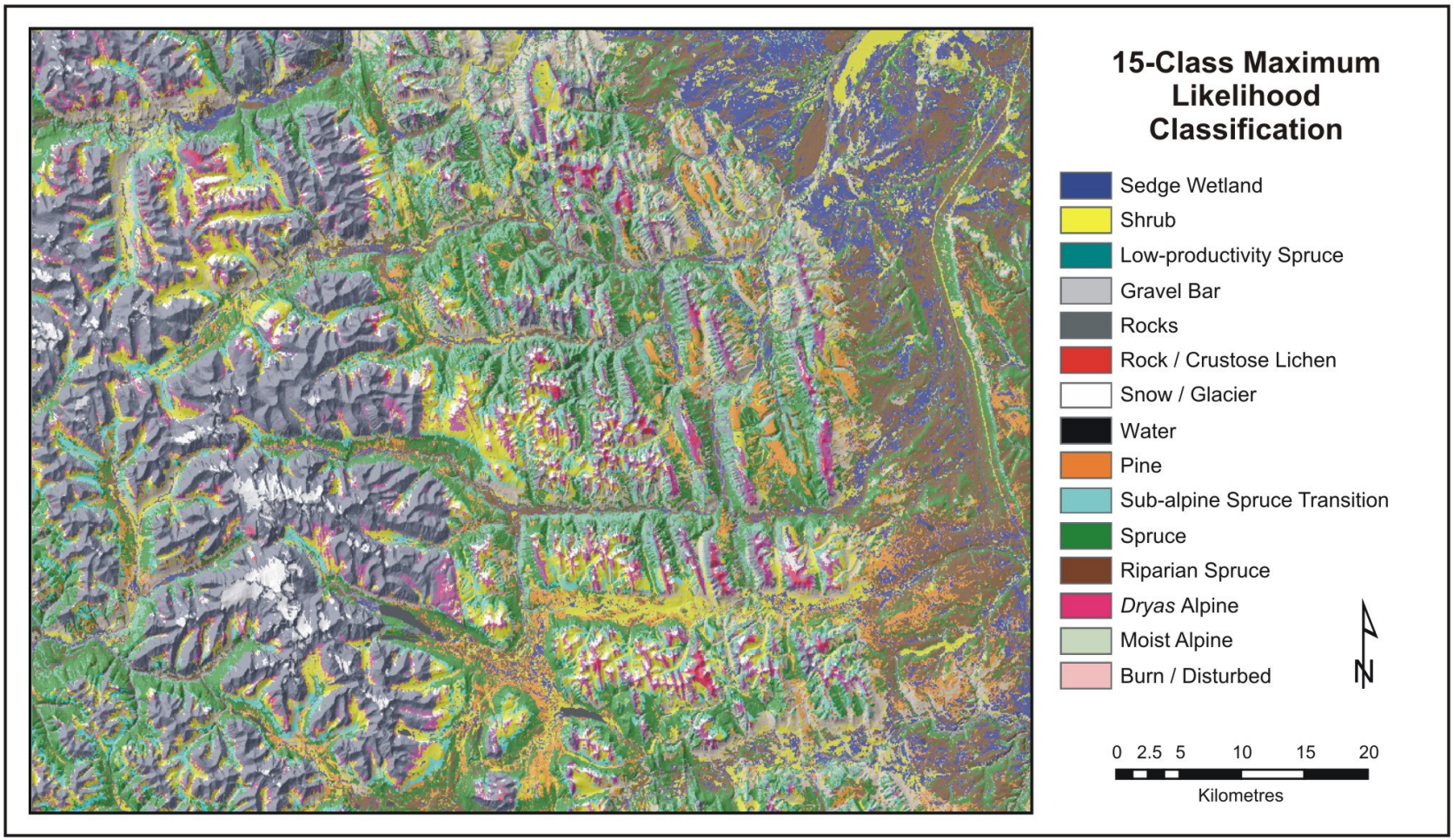


Figure 2.1. Final classification of the Greater Besa-Prophet Area (overall accuracy 77.33%) in northern British Columbia overlain on shaded relief derived from British Columbia Terrain and Resource Information Management (TRIM) digital elevation model.

Final Classification

In the final classification, both user's and producer's accuracy increased from the base classification for all of the eight classes mentioned above (Table D12) except the alpine classes and the rock class. Confusion between Moist Alpine and *Dryas*-dominated Alpine decreased, but increased between Moist Alpine and Shrub. User's accuracy decreased in the *Dryas*-dominated Alpine but producer's accuracy increased. The opposite was true for Moist Alpine.

## 2.4 DISCUSSION

### *Accuracy*

The accuracy target of 85% for the Maximum Likelihood classification of the GBPA, as recommended by Foody (2002), Congalton (1999), and Anderson et al. (1979), was not achieved. Nor has this accuracy been achieved in many other studies. For instance, Tobler et al. (2003) used a maximum likelihood classifier to distinguish 15 land cover types in the coastal savannah of Tanzania and achieved an overall accuracy of 77% ($\kappa$=0.75). The 8-class maximum likelihood classification created by Cingolani et al. (2004) for a mountain rangeland in central Argentina achieved an overall accuracy of 78% ($\kappa$=0.74). Overall accuracy achieved by Yool (1995) was 78% for six classes in rugged terrain. Colby and Keating (1998) achieved a higher accuracy (81.1% overall) for a five-class scheme in a mountain area in Costa Rica, but used a non-Lambertian topographic normalization algorithm prior to the classification. Pedroni (2003) manipulated class probabilities prior to maximum

likelihood classification to increase accuracy of a 33-class scheme from 68.7% to 89.0% in a complex landscape in central Costa Rica.

Classification accuracy in this study improved when the third principal component and the Tasseled Cap 'Greenness' component were added to the classification. The general patterns of increase in overall accuracy suggest that TCG and PC3 added relevant information to aid in distinguishing between vegetation types. This information may have included indications of vegetation health. These inputs may have helped reduce the influence of confounding variables such as topography or inconsistent atmospheric characteristics. Although the NDVI has been found by several authors to be related to the same variables as TCG, such as biomass, net primary productivity, biomass, leaf area index, crown closure and other vegetation characteristics (Purevdorj et al. 1998, Baret and Guyot 1991, Tucker and Sellers 1986, Crist and Cicone 1984), it did not increase the classification accuracy.

Filtering the classification using a modal filter to remove single pixels from homogenous areas also increased accuracy. Similar to collapsing the number of classes in the scheme (from 29 to 15), accuracy would likely increase with further spatial generalization of the classification. Because this generalization may have removed pixels from transition zones between classes (e.g., edges of burned areas that border coniferous stands) or mixed classes not labeled in the scheme (e.g., a mixed pine and spruce stand), this was the greatest generalization that we were willing to apply. Further generalization may have increased classification accuracy, but erroneously reduced the spatial distribution and specificity of the classes.

We were satisfied that the classification accuracy of 77.33% in this study was sufficient for the classification to represent the vegetation of the GBPA, particularly as this study had a greater number of classes than many of the above studies. Accuracy might have been increased if the original TM imagery had been corrected for topographic effects (such as Colby and Keating 1998), or if a more complex classification system was used such as the neural networks employed by Yool (1995) or the manipulation of probabilities used by Pedroni (2003).

The total sample size for classifying habitats in the GBPA was determined by assessing 10 sample points per class. These samples were selected because they represented 'pure' vegetation types as defined in the classification scheme. The large sample size of 75-100 points per class recommended by Congalton and Green (1993) was logistically unachievable in the GBPA. Homogeneous communities of vegetation are rare in the study area, and are primarily defined by aspect, drainage and elevation (see Chapter 1). To achieve the statistically valid sample recommended by Congalton and Green (1993), 1125-1500 independent samples would have had to have been collected. The landscape of the GBPA is a surface of continuously changing classification types and locating this number of 'pure' areas is unlikely, particularly areas that are contiguous for at least 2500$m^2$. Furthermore, the cost of fieldwork would have precluded collecting this amount of data.

***Interpretation of Results***

Confusion that was the result of low separability among similar classes reduced the overall accuracy achieved. The following is a synopsis of the major confusion among classes and possible explanations for each.

Coniferous Areas

The four coniferous classes (Spruce, Riparian Spruce, Low-productivity Spruce and Pine) were poorly separated in the base classification. In the 29-class scheme, the Pine class was separated into two types: dry and shrub/moss understories, but these were collapsed together in the 15-class scheme. As a result, understories of the Pine, Spruce, and Riparian Spruce classes were highly variable and potentially quite similar. The conglomeration of all stem densities of species in the coniferous classes may have exacerbated this lack of separability. For instance, open pine stands with dry or shrub understories may have had spectral signatures more similar to open spruce stands with similar understories than closed Pine stands with moss understories. Similarly, higher than average stem density and crown closure in Low-productivity Spruce areas may have caused them to be classified as Spruce. Some confusion among coniferous types was removed using post-classification modelling (Table A1), but these models were only appropriate for classes with distinct or specific associations with the available terrain variables (slope, aspect and elevation). For instance, Riparian Spruce was separated from the Spruce and Low-productivity Spruce by limiting Riparian Spruce areas to areas of negligible slope. This increased the user's accuracy of Riparian Spruce from 56.25% to 69.23% and

reduced the number of Spruce and Low-productivity Spruce classes that were erroneously classified as Riparian Spruce. Similarly, Low-productivity Spruce was limited to northerly slopes, reducing its confusion with other Spruce areas.

The Pine class could not be modeled in such a manner, but did increase user's and producer's accuracy in the final classification. It is likely that this increase in accuracy was the result of the application of the 3 x 3 modal filter. Many pine areas are found in or adjacent to disturbed areas and consequently are often found within other types, particularly Spruce. The 3 x 3 filter may have removed pixels in transition zones from Pine to Spruce stands and increased the accuracy of the class.

Alpine Areas

*Dryas*-dominated Alpine areas and Moist Alpine areas were distinguished from one another by assigning them to southerly and northerly slopes respectively. This did not, however, alter the confusion between *Dryas*-dominated Alpine areas and Rock and Gravel bar types, nor did it reduce confusion between Moist Alpine and Shrub. These secondary confusions are likely the result of the existence of transition zones between 'pure' classes. For instance, percent cover of shrubs in the sub-alpine zone declines with increasing elevation, until the area becomes 'true' alpine (dwarf shrubs only). Consequently, there is a zone of transition from shrub to alpine, which likely explains the confusion between Moist Alpine and Shrub. The additional confusion in the final classification suggests the 3 x 3 filter may have amalgamated a Moist Alpine area that was near or in a transition zone into a Shrub area. The confusion among

*Dryas*-dominated Alpine, Rock and Rock / Crustose Lichen also is likely due to transition, as percent cover of *Dryas* and other dwarf shrubs in the alpine declines with increasing elevation making intermediate areas difficult to classify. Transition zones also made selecting 'representative' areas for training difficult (i.e., plots that may have been located in transition zones were classified into a single class).

Most confusion among classes can be explained by similarity of spectral signatures (e.g., Burned / Disturbed Areas and Shrub) or by the transition of one 'pure' class or vegetation type to another in similar areas (e.g., Sedge Wetland, Shrub and Riparian Spruce). Topography (particularly shadowing on northerly slopes) did not appear to reduce significantly the accuracy of the classification although aspect was the primary feature of the Low-productivity Spruce and Moist Alpine classes. Also, the majority of the most extreme terrain shadows typically appear at higher elevations where vegetation is less likely, and hence confusion was not represented in the confusion matrices of the classifications. Visual inspection of the classification suggested that some of the more obvious terrain shadows in potentially vegetated areas were incorrectly classified as Rock, but this was not represented in the confusion matrix. It is likely, however, that these areas (generally on steep north-facing slopes) were not sampled because they were relatively inaccessible on foot and by air. This may have biased the confusion matrix toward a higher user's accuracy for the Rock class than was actually present in the classification, and reduced the confusion among other classes (i.e., shadowed areas were classified as rock rather than vegetated and so no confusion was evident in the matrix between vegetated classes).

### *Considerations for Wildlife Management / Use of the Data*

Level of Detail / Number of Classes

The supervised classification was an efficient method to characterize the vegetation of the Greater-Besa Prophet Area. These data provide information that should contain significantly less bias and potential for human error than some traditional mapping techniques because they are based upon the statistical differences in the reflectance and distribution of vegetation types, rather than a visual delineation of boundaries. Furthermore, these data are accompanied by an estimate of their accuracy that is not usually a consistent feature of other mapping efforts. In areas where there has been no existing mapping effort, classification of satellite imagery is a low-cost method to create vegetation information at the landscape level.

The goal of this project was to create a vegetation classification for multi-species wildlife habitat studies that included the most specific information about vegetation communities as possible. The 15-class scheme was the best balance of accuracy and level of detail for the GBPA using the data collected during field research. Consideration should be given to differences in accuracy among classes, however, and inferences may need to be limited where classes were not well distinguished from one another (e.g. Pine and Spruce). Furthermore, a statistically sound analysis of resource use by large mammals such as a resource selection function may require amalgamation of habitats depending on the use and availability of those habitats by the species and the statistical similarity of the classification inputs within

the habitat models (Johnson et al. 2003, Miranda and Porter 2003). The hierarchical scheme of the classification devised for the GBPA has allowed classes to be easily amalgamated into higher order classes if per-class accuracy is a concern, or if classes are not relevant to the species of concern. Similar to the amalgamation from 29 to 15 classes, it is likely that the accuracy of the classification would increase if classes were further amalgamated.

Scale

Rettie and Messier (2000) asserted that although animal behaviour may be interpreted differently based on the scale of observation, not all scales are equally important, and the scale of selection by animals is hierarchical based on limiting factors. For instance, they suggested that predator avoidance by woodland caribou (*Rangifer tarandus*) was the primary limiting factor to individual fitness and that the most effective method of predation avoidance by caribou was to avoid habitats of species sharing the same predators. This coarse scale of selection was stronger than selection of finer scale attributes such as forage availability (Rettie and Messier 2000). McLoughlin et al. (2002) suggested that a similar hierarchical pattern of selection existed for grizzly bears (*Ursus arctos*) in the central Canadian arctic. Coarse-scale habitat selection by bears in the arctic was primarily based on food availability, where the interacting factors of intra-specific predation influenced selection at finer scales (McLoughlin et al. 2002). The primary limiting factor for both species determined selection at coarse scales.

Mapping for analyses of hierarchical habitat selection such as those cited above must be of sufficient quality to offer information at multiple scales in order to capture both coarse and fine scale selection if possible. The classification of the GBPA used 25-m resolution imagery to create the vegetation classification. This resolution was reduced with the application of the 3 x 3 filter, making the minimum mapping unit 0.56ha. These data do not provide information at a finer resolution and stand characteristics cannot be assumed below this scale. The data do, however, provide data appropriate for analysis of landscape-level (coarse-scale) habitat selection.

### *Conclusions*

Classification of the vegetation of the GBPA was successful at a moderate level of detail. Although not all classes of interest could be distinguished, the classification data should be a useful resource to those interested in the management of wildlife species in the area. Further research could test methods other than the Maximum Likelihood classifier to determine if greater accuracy could be achieved. Additionally, validity of the results could be improved with a larger sample size. Although the specific vegetation types of the 15-class scheme are relevant to the GBPA only, the results per derivative should be appropriate in other areas, as should the level of detail in the scheme and the scale of the final output.

## 2.5 LITERATURE CITED


Anderson, J.R. Hardy, E.E., Roach, J.T., and Witmer, R.E. (1979). A land use and land cover classification system for use with remote sensor data. Washington, DC: Government Printing Office (US Geological Survey, Professional Paper 964).

Apps, C.D., McClellan, B.N., Woods, J.G. and Proctor, M.F. (2004). Estimating grizzly bear distribution and abundance relative to habitat and human influence. *Journal of Wildlife Management,* 68(1):138-152.

Arthur, S.M., Manly, B.F.J, McDonald, L.L., and Garner, G.W. (1996). Assessing habitat selection when availability changes. *Ecology,* 77(1): 215-227.

Baret, F. and Guyot, G. (1991) Potentials and Limits of Vegetation Indices for LAI and APAR Assessment. *Remote Sensing of Environment*, 35: 161-173.

Bian, L. and Walsh, S.J. (1993). Scale dependencies of vegetation and topography in a mountainous environment of Montana. *Professional Geographer,* 45 (1): 1-11.

Boyce, M.S., Mao, J.S., Merrill, E.H., Fortin, D., Turner, M.G., Fyxell, J. and Turchin, P. (2003). Scale and heterogeneity in habitat selection by elk in Yellowstone National Park. *Ecoscience,* 10 (4): 421-431.

Crist, E.P., and Cicone, R.C. (1984). A physically-based transformation of Thematic Mapper Data - the TM Tasseled Cap. *IEEE Transactions on Geoscience and Remote Sensing,* DE22 (3): 256-263.

Cingolani, A.M., Renison, D., Zak, M.R., Cabido, M.R. (2004). Mapping vegetation in a heterogeneous mountain rangeland using Landsat data: an alternative method to define and classify land-cover units. *Remote Sensing of Environment,* 92: 84-97.

Colby, J.D. and Keating, P.L. (1998). Land cover classification in the tropical highlands: the influence of anisotropic reflectance. *International Journal of Remote Sensing,* 19(8): 1479-1500.

Congalton, R.G. (1999). A review of assessing the accuracy of classifications of remotely sensed data. *Remote Sensing of Environment,* 37: 35-46.

Congalton, R.G., and Green, K. (1993). A practical look at the sources of confusion in error matrix generation. *Photogrammetric Engineering and Remote Sensing,* 59: 641-644.

Demarchi, D.A. (1996). An Introduction to the Ecoregions of British Columbia. Ministry of Environment Lands and Parks, Victoria BC. 47pp.

Florinsky, I.V., and Kuryakova, G.A. (1996). Influence of topography on some vegetation cover properties. *Catena,* 27: 123-141.

Foody, G.M. (2002). Status of land cover classification accuracy assessment. *Remote Sensing of Environment,* 80: 185-201.

Franklin, S.E., Peddle, D.R., Dechka, J.A., and Stenhouse, G.B. (2002). Evidential reasoning with Landsat TM, DEM and GIS data for landcover classification in support of grizzly bear habitat mapping. *International Journal of Remote Sensing,* 23 (21): 4633-4652.

Hills, G.A., and G. Pierpoint, (1960). Forest Site Evaluation in Ontario. Ontario Department of Lands and Forests, Technical Series, Research Report No. 42. - Toronto, Ontario.

Huber, T.P., and Casler, K.E. (1990). Initial analysis of Landsat TM data for elk habitat mapping. *International Journal of Remote Sensing,* 11 (5): 907-912.

Jepsen, J.U., Eide, N.E., Prestrud, P. and Jacobsen, L.B. (2002). The importance of prey distribution in habitat use by arctic foxes (Alopex *lagopus*). *Canadian Journal of Zoology,* 80: 418-429.

Johnson, C.J., Alexander, N.D., Wheate, R.D., and Parker, K.L. (2003). Characterizing woodland caribou habitat in sub-boreal and boreal forests. *Forest Ecology and Management,* 180: 241-248.

Johnson, C.J., Seip, D.R., and Boyce, M.S. (2004). A quantitative approach to conservation planning: using resource selection functions to map the distribution of mountain caribou at multiple scales. *Journal of Applied Ecology,* 41: 238-25.

Laperriere A.J., Dent P.C., Gassaway W.C. and Nodler F.A. (1980). Use of LANDSAT data for moose habitat analyses in Alaska. *Journal of Wildlife Management* 44: 881-887.

Leckenby, D.A., Isaacson, D.L., and Thomas, S.R. (1985). Landsat application to elk habitat management in northeast Oregon. *Wildlife Society Bulletin,* 13: 130-134.

Liu, J., Chen, M. Cihlar, J. and Park, W.M. (1997). A process-based boreal ecosystem productivity simulator using remote sensing inputs. *Remote Sensing of Environment,* 62: 158-175.

Manly, B.F.J., McDonald, L.L. and Thomas, D.L. (1993). *Resource selection by animals: statistical design and analysis for field studies.* London: Chapman and Hall.

McLoughlin, P.D., Case, R.L., Gau, R.J., Cluff, H.D., Mulders, R. and Messier, F. (2002). Hierarchical habitat selection by barren ground grizzly bears in the central Canadian Arctic. *Oecologia,* 132: 102-108.

Miranda, B.R. and Porter, W.F. (2003). Statewide habitat assessment for white-tailed deer in Arkansas using satellite imagery. *Wildlife Society Bulletin,* 31(3): 715-726.

Nielsen, S.E., Boyce, M.S., Stenhouse, G.B., and Munro, R.H.M. (2003). Development and testing of phenologically driven grizzly bear habitat models. *Ecoscience,* 10 (1): 1-10.

Osborne, P.E., Alonso, J.C., and Bryant, R.G. (2001). Modelling landscape-scale habitat use using GIS and remote sensing: a case study with great bustards. *Journal of Applied Ecology,* 38: 458-471.

Pedroni, L. (2003). Improved classification of Landsat TM data using modified prior probabilities in large and complex landscapes. *International Journal of Remote Sensing,* 24(1): 91-113.

Purevdorj T.S, Tateishi, R., Ishiyamas, T., and Honda, Y. (1998) Relationships Between Percent Vegetation Cover and Vegetation Indices. *International Journal of Remote Sensing,* 19 (18): 3519-3535.

Rettie, W.J. and Messier, F. (2000). Hierarchical habitat selection by woodland caribou: its relationship to limiting factors. *Ecography,* 23: 466-478.

Skidmore, A.K. (2002). Accuracy assessment of spatial information. In Stein, A. van Der Meer, F. and Gorte, B. (eds.) Spatial *statistics for remote sensing.* pp 197-208.

Tobler, M.W., Cochard, R. and Edwards, P.J. (2003). The impact of cattle ranching on large-scale vegetation patterns in a coastal savanna in Tanzania. *Journal of Applied Ecology,* 40: 430-444.

Tucker, C. J. and Sellers, P.J. (1986) Satellite Remote Sensing of Primary Productivity. *International Journal of Remote Sensing,* 7: 1395-1416.

Wilson, B.A., and Franklin, S.E. (1992). Characterization of alpine vegetation cover using satellite remote sensing in the Front Ranges, St. Elias Mountains, Yukon Territory. *Global Ecology and Biogeography Letters,* 2: 90-95.

Yool, S.R. (1995). Land cover classification in rugged areas using simulated moderate resolution remote sensor data and an artificial neural network. *International Journal of Remote Sensing,* 19(1):85-96.

# CHAPTER THREE – CONSIDERATIONS FOR THE PRODUCTION OF AN INTRA-SEASON PHENOLOGY DATASET USING LANDSAT TM AND ETM+: RELATIONSHIPS AMONG NDVI, VEGETATION AND TOPOGRAPHY IN A MOUNTAIN LANDSCAPE IN NORTHERN BRITISH COLUMBIA[1]

## 3.1 INTRODUCTION

The ability to monitor ecosystems consistently and efficiently over time is critical to identify correctly changes to terrestrial landscapes. A significant component of remote sensing research has investigated the changes in vegetation over time. The radiance recorded by an orbiting sensor, however, is influenced by temporal differences in target reflectance (e.g., phenological state), atmospheric characteristics and solar illumination angle at the time of capture (Du et al. 2002, Myneni et al. 1998, Holben and Justice 1981). Aerosols and gases present in the atmosphere absorb and scatter radiation and this pollutes the reflectance of terrestrial features that is recorded by the orbiting sensor (Myneni and Asrar 1994). These impairments may be seasonally dependent and may be amplified in areas of rugged terrain such as mountain ranges. Consequently, the digital data of one scene may not be directly comparable to others.

The effect of many radiometric differences can be avoided or reduced in inter-year studies by using images that are near 'anniversary date' (i.e., as close to the same day of capture as possible in each year), but an increasing amount of research has considered the use of intra-year change detection, particularly changes in vegetation

[1] Chapter may be submitted for publication with the following authorship: R.J. Lay, D.D. Gustine and R.D. Wheate

phenology over one or more growing seasons using vegetation indices such as the Normalized Difference Vegetation Index (NDVI). Most of these studies have used low spatial resolution Advanced Very High Resolution Radiometer (AVHRR) (1.1km) or Moderate-resolution Imaging Spectroradiometer (MODIS) (250m) data (e.g., Hoare and Frost 2004, Suzuki et al. 2003, Oindo 2002, Groten and Ocatre 2002, Xin et al. 2002, Lee et al. 2002, Chen et al. 2000, Borak et al. 2000, Duchemin et al. 1999, Schwartz and Reed 1999, Lobo et al 1997, Nemani and Running 1997, Markon et al. 1995). The high temporal resolution of these data has allowed techniques to be developed that reduce the differences among multi-temporal imagery. Data 'compositing' removes pixels contaminated by differences in atmosphere and clouds. Individual images are merged with others within a predetermined time period, and individual pixels are selected that are of the highest radiometric quality.

Imagery from medium resolution sensors such as the Landsat Thematic Mapper (TM) and Enhanced Thematic Mapper (ETM+) are not collected at a sufficient rate for this procedure to be mimicked. Clouded areas and their shadows completely mask the reflectance information in all bands, removing them from use. All other pixels may be contaminated by atmospheric interference and differential illumination. More specifically, for Landsat data the multiplicative effect of absorption is negligible because TM bands were selected to avoid absorption effects, but scattering (an additive effect) may be considerable (Song et al. 2001). For instance, increased aerosols decrease the contrast between the near infrared NIR and red reflectance values captured by an orbiting sensor (Myneni and Asrar 1994). The NDVI, which is

based on this contrast, is significantly lower at the top of the atmosphere than it is at the top of the canopy (Myneni and Asrar 1994). The NDVI equation (Eq. 3.1) might be altered to reflect this effect (Eq. 3.2):

*Equation 3.1*

$$NDVI = \left( \frac{TM_4 - TM_3}{TM_4 + TM_3} \right)$$

*Equation 3.2*

$$NDVI = \left( \frac{(TM_4 - TM_3) - (A_4 - A_3)}{(TM_4 + TM_3) - (A_4 + A_3)} \right)$$

where TM4 and TM3 are both Landsat TM or ETM+ bands 4 and 3, and A4 and A3 are the atmospheric influence for each band respectively (Song et al. 2001).

Topography also may have a profound impact on medium-resolution, remotely-sensed data. In areas of significant topography, a non-vertical sun angle differentially illuminates inclined surfaces on different aspects (Shepherd and Dymond 2003, Holben and Justice 1981) based on sun-sensor-surface geometry, and the geometric and radiometric properties of the land cover (Burgess et al. 1995). There are both direct and indirect influences of topography on remotely-sensed data. Indirect effects include those effects that are the result of physical features of the topography: the shading of slopes not directly illuminated by the sun, or the illumination of shaded slopes by the irradiance of adjacent slopes (Burgess et al. 1995). Furthermore, seasonal differences in sun angle and sun-sensor-surface

geometry change the magnitude of the influence of the atmosphere. NIR radiance decreases with increased atmospheric absorption as the solar zenith angle is increased. Greater solar zenith angles result in increased atmospheric scattering in the red wavelengths, artificially deflating NDVI values (Myneni and Asrar 1994, Eastman and Fulk 1993, Middleton 1991). In northern latitudes, as the angle of the sun becomes very low (i.e. later in the season), this differential illumination can be extreme. Direct effects are the result of dissimilar depths of atmosphere that cause the radiance of terrestrial surfaces to be diffused differentially such as elevational differences. Regardless of the homogeneity of the vegetation type and/or density within a cover type, the variation in radiance values captured by an orbiting sensor is greatly increased if the cover type is located on different slopes and aspects. This effect is easily identifiable in Landsat imagery as a visual appearance of relief (Holben and Justice 1981). The seasonal decrease in solar angles in northern latitudes exacerbates differences on opposing aspects, and reduces the congruence between multi-temporal images.

Despite the above limitations, the spatial resolution of Landsat and other medium-resolution data makes them a useful resource for change detection at finer scales than can be detected with AVHRR or MODIS data. Landsat data capture a large spatial area in each scene compared to higher spatial resolution sensors such as Ikonos or Quickbird at a relatively low cost, making multi-temporal datasets relatively inexpensive to obtain (Pedroni 2003). Several methods have been developed to 'correct' the radiometric distortion in scenes to enable comparison of multi-date imagery. The most efficient methods use data collected about the characteristics at

the precise time the image was captured; however, these data are rarely available, particularly for historical datasets. Many authors have proposed methods of normalizing data for radiometric effects without sensor or atmospheric information using a reference image (Hall et al. 1991). These methods are collectively known as relative radiometric normalization (RRN) techniques (Du et al. 2002, Yuan and Elvidge 1996). Although there has been considerable research that has investigated various RRN methods, the chosen algorithm is determined by input imagery, terrain characteristics, ancillary information about the capture date, and objectives of the research using the imagery (McGovern et al. 2002). Some of the algorithms most commonly used to normalize multiple satellite images to a common radiometric reference image and remove the influence of the atmosphere include dark area subtraction, histogram matching and linear regression.

Dark area subtraction assumes that features having minimal reflectance should have the same digital numbers regardless of image date. These features are the darkest features of the image, often deep lakes (Yuan and Elvidge 1996). Correction factors are determined by the shifts in reflectance values for pixels of these dark features (McGovern et al. 2002).

Histogram matching is useful for comparing images with slightly different sun angles or atmospheric effects. It is a non-linear method of matching the shape of the histograms of the subject image to the histogram of a reference image so that the distributions of digital numbers are as similar as possible (Yang and Lo 2000, Chavez and MacKinnon 1994). Histogram matching is inappropriate for quantitative

analysis, however, unless the surface features in the scene have experienced minimal or no change.

Linear regression transforms rely on the assumption that the difference in reflectance of ground features captured by space-borne sensors at two different dates can be expressed as a linear function (Du et al. 2002, Yang and Lo 2000, Caselles and Lopez Garcia 1989). This explains atmospheric and calibration differences as linearly related so that a linear equation can be used to perform the normalization. Linear transforms are dependent on the selection of Pseudo Invariant Features (PIFs) (Du et al. 2002). Commonly used PIFs include large, non-vegetated surfaces such as sand, airports, wide roads, industrial areas and other cultural features, deep dark lakes, gravel, etc. There are several methods of selecting PIFs. Schott et al. (1988) isolated anthropomorphic features from imagery that were considered to be invariant. Per-band means and standard deviations were determined for the overall imagery using coefficients based on the shifts and scaling required to match the PIFs. Yuan and Elvidge (1996) developed a no-change regression normalization technique that relied on the analysis of the scattergram between the subject and reference image. Pixels of no-change are found within a threshold about the regression line, and these pixels are used to fit all input bands (Yang and Lo, 2000). PIFs should meet the following criteria: 1) be approximately the same elevation as the elevation of primary interest within the scene, 2) contain little or no vegetation, as vegetation changes with environmental differences (stress, disturbance etc.) and phenology, 3) be located on flat terrain so that changes in sun angle have consistent effect on the reflectance of features, and 4) include a range of

brightness values, representing those found in the scene, in order for regression models to perform adequately. If the preceding criteria are satisfied, it is assumed that: 1) effects are independent of one another and total effect is the linear sum of each effect, 2) reflectance properties of the PIF features are invariant over the change-detection time period, 3) linear effects that are to be corrected for are spatially homogenous for all PIFs, and 4) consistently changed PIFs are not the majority of targets in the scene (Du et al. 2002, Heo and FitzHugh 2000, Eckhardt et al. 1990, Schott et. al 1988).

The above RRN methods were developed to enable direct comparisons of multiple images of different dates. Using these methods, intra-season phenology studies should be able to apply methods developed for lower-resolution data such as AVHRR and MODIS to moderate resolution data such as Landsat TM and ETM+. The above methods do not, however, remove cloud and cloud shadows from imagery. This can significantly reduce the availability of continuous imagery across one's area of interest. These methods also do not remove topographic error from the data. The goal of this project was to create a set or sets of single-year TM and ETM+ data for the purpose of examining the change in vegetation phenology over the growing season in a mountain environment, similar to those generated using AVHRR and MODIS. There were two primary objectives: to determine the relationships among NDVI, vegetation type and topography and if those relationships varied seasonally; and to attempt to replace areas obscured by clouds to create a uniform intra-seasonal vegetation dataset.

## 3.2 METHODS

### *Study Area*

This study was conducted in the Greater Besa-Prophet Area (GBPA) in northern British Columbia. It falls within Landsat TM and ETM+ path 50, row 20; however, path overlap at this latitude makes partial images of the study area available from paths 51 and 49 (Figure 3.1). A detailed description of the study area can be found in Chapter 1.

### *Data Preparation*

Seven ETM+ and seven TM images were collected for three years (2001-2003) (Table 3.1). Orthocorrection was processed with a satellite orbital model in PCI OrthoEngine® v8.2 (Richmond Hill, ON, Canada), using British Columbia Terrain and Resource Inventory Management (TRIM) hydrologic and transportation coverages, and Digital Elevation Model (DEM). Root mean square (RMS) error was better than 0.5 pixels for all images, and each image was resampled to 25m using bilinear interpolation in order to match the resolution of the DEM. All but one image (15 Aug 2001) contained some cloud contamination, and any image from an adjacent-path (path 51 or path 49) image was missing data from some parts of the study area.

All TM images were converted to at-satellite spectral radiances using calibration procedures specified by the U.S. Geological Survey (Chander and Markham 2003). ETM+ datasets were converted with scene-specific data. Thirty-two bit radiance

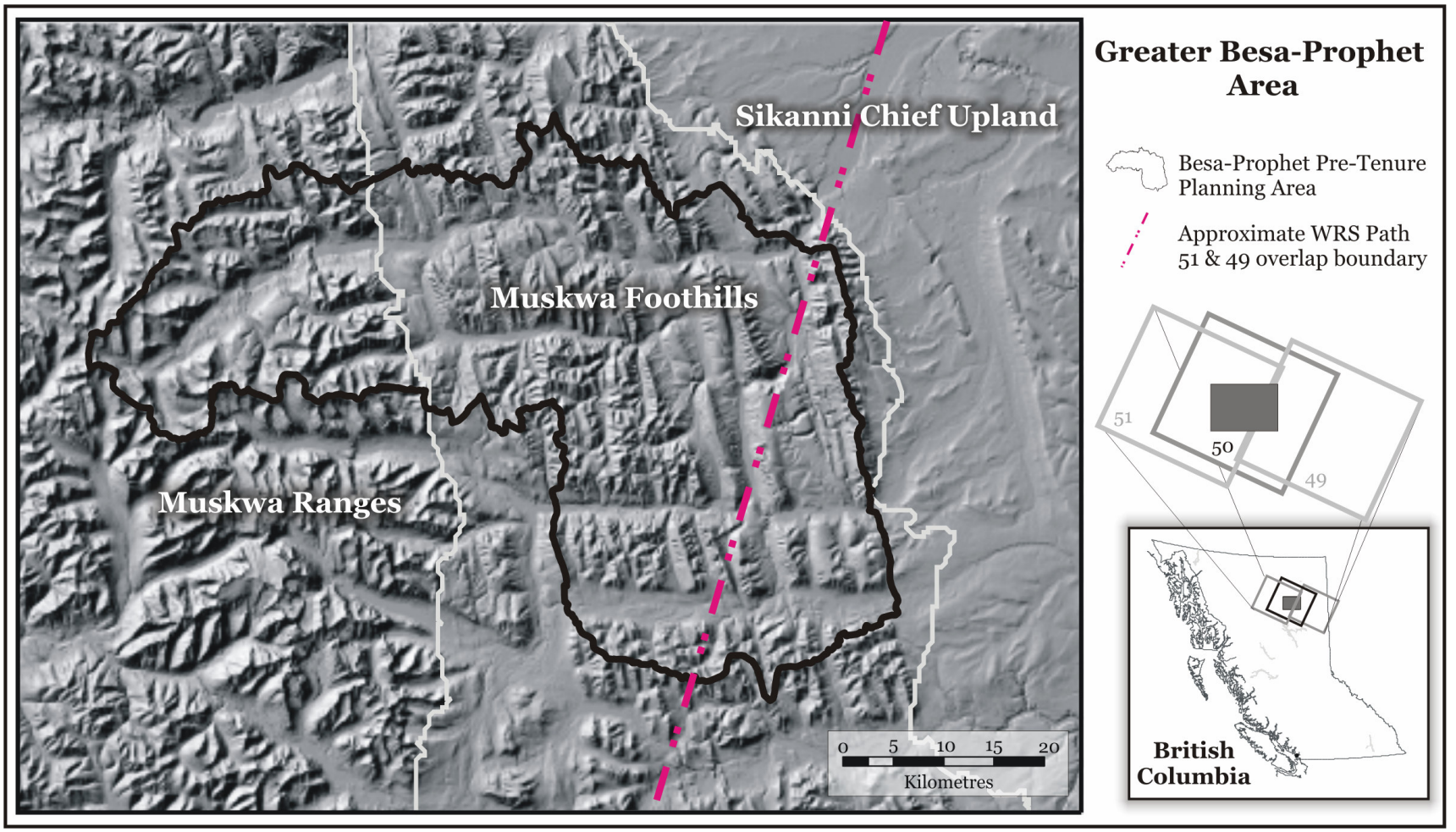


Figure 3.1. The Greater Besa-Prophet study and its associated subunits in northern British Columbia, within Landsat Thematic Mapper (TM) and Enhanced Thematic Mapper (ETM+) world referencing system (WRS) path 50 row 20 and on the boundary of the overlap between paths 51 and 49.

Table 3.1. Landsat Thematic Mappper (TM) and Enhanced Thematic Mapper (ETM+) images that were collected for the Greater Besa-Prophet Area in northern British Columbia, 2001-2003. Solar azimuth and elevation were calculated using the approximate centre of the Greater Besa-Prophet Area and the date and time the image was collected.

| Date | Sensor | Path/Row | Solar Azimuth | Solar Elevation |
|---|---|---|---|---|
| 04 Jun 2001 | ETM+ | 50/20 | 114.48 | 40.81 |
| 22 Jul 2001 | ETM+ | 50/20 | 114 | 37.84 |
| 14 Aug 2001 | ETM+ | 51/20 | 122.01 | 34.64 |
| 15 Aug 2001 | TM | 50/20 | 122.24 | 34.39 |
| 16 Aug 2001 | ETM+ | 49/20 | 122.47 | 34.14 |
| 16 Sep 2001 | TM | 50/20 | 126.75 | 23.58 |
| 01 Oct 2001 | ETM+ | 51/20 | 130.63 | 18.84 |
| 31 May 2002 | ETM+ | 49/20 | 119 | 42.23 |
| 15 Jun 2002 | TM | 50/20 | 117.29 | 43.07 |
| 24 Jun 2002 | TM | 49/20 | 116.71 | 42.91 |
| 09 Aug 2002 | TM | 51/20 | 120.86 | 35.93 |
| 09 May 2003 | ETM+ | 50/20 | 122.28 | 38.39 |
| 25 Jun 2003 | TM | 51/20 | 116.68 | 42.87 |
| 29 Jul 2003 | TM | 49/20 | 118.79 | 38.4 |

values for bands 3 and 4 of all image datasets were used to calculate the NDVI for each image. Radiometric normalization without an accurate measure to quantify the quality of outputs was deemed inappropriate for the GBPA, and consequently none were applied to the data. Figures 3.2 and 3.3 show the NDVI images generated for each image, for each year.

Linear regression was used to determine the relationship between multi-sensor images in order to assess the ability of the radiance conversion to account for sensor calibration. The three August 2001 images were captured over three days and should have experienced negligible change in surface reflectance. Areas of missing data were masked from the analysis, and bands 3 and 4 (as inputs to NDVI) of the three images were compared. Pixels that deviated from the regression line were isolated on the image.

***Regression Analysis to Predict NDVI***

Clouded areas and areas of cloud shadows were masked from each image by manual interpretation of TM/ETM+ band 1, a mid-infrared (ETM+/TM band 5) to green (ETM+/TM band 2) ratio and the thermal bands of each image (ETM+/TM band 6 (60m) and 6 respectively). Areas of data that were missing from adjacent-path images (path-missing) were added to these masks, to remove them from the analysis (Figures 3.2 and 3.3).

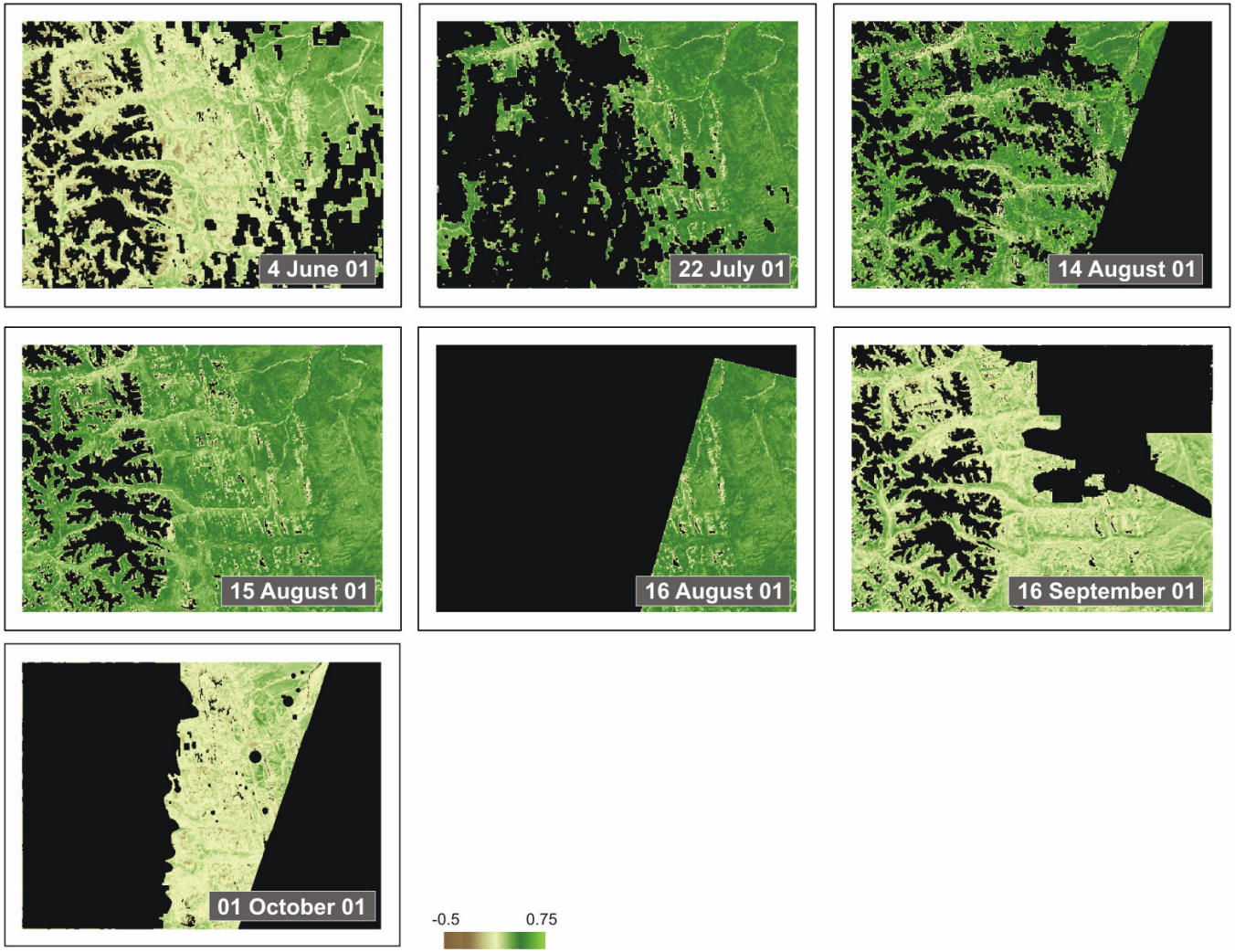


Figure 3.2. Normalized Difference Vegetation Index (NDVI) imagery for the Greater Besa-Prophet Area in 2001, derived from Landsat Thematic Mapper (TM) and Enhanced Thematic Mapper (ETM+) at-satellite spectral radiances. Black areas indicate non-vegetated and clouded or missing areas masked from all analyses.

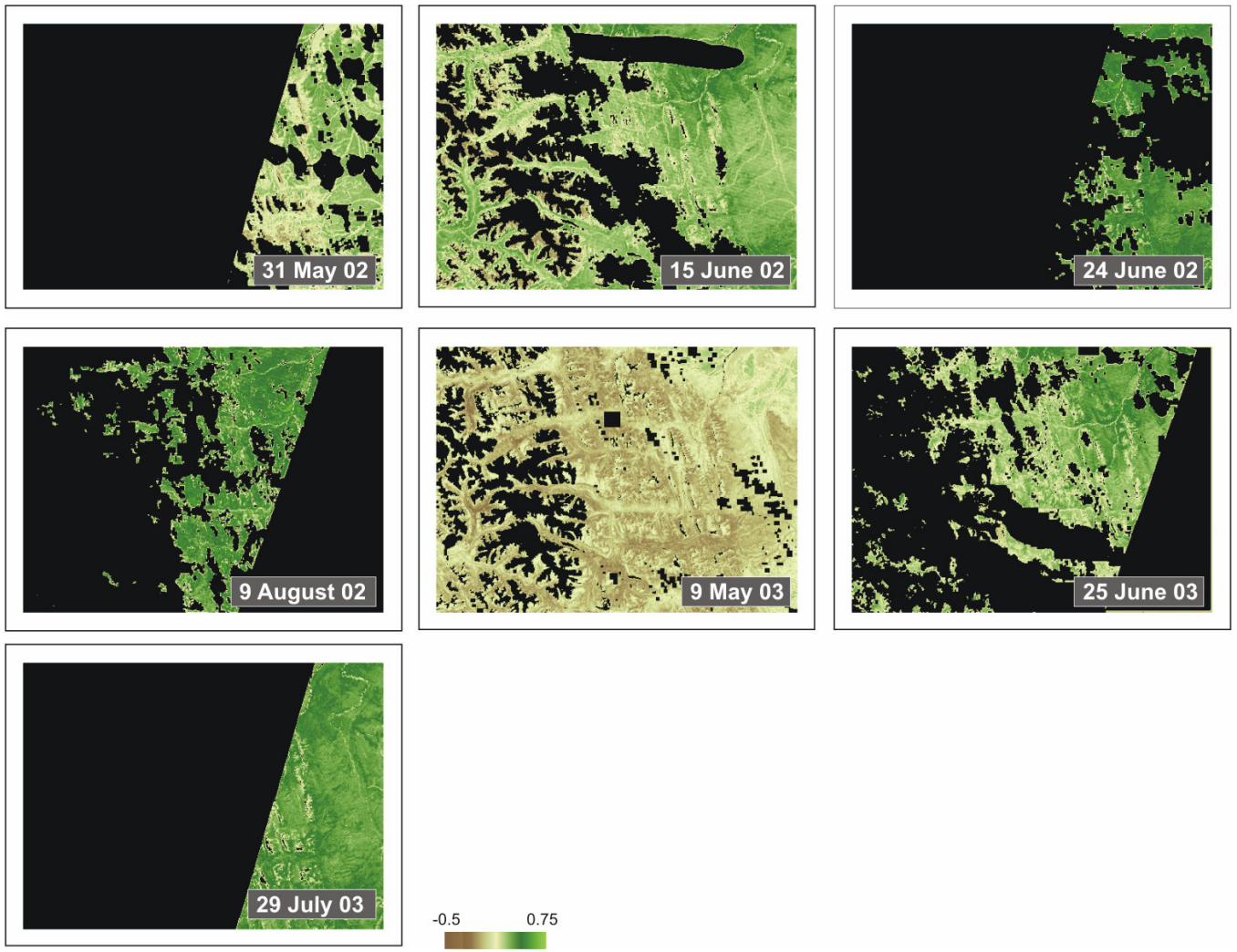


Figure 3.3. Normalized Difference Vegetation Index (NDVI) imagery for the Greater Besa-Prophet Area in 2002 and 2003, derived from Thematic Mapper (TM) and Enhanced Thematic Mapper (ETM+) at-satellite spectral radiances. Black areas indicate non-vegetated and clouded or missing areas masked from all analyses.

The remaining number of pixels varied by image and ranged from 206,200 (24 June 2002) to 11,854,192 (15 Aug 2001) pixels. To predict NDVI for areas of missing data, we used multiple linear regression to examine the relationships among NDVI (dependent variable) and several independent variables: vegetation, angle of incidence, slope (°), aspect, and elevation (km). Vegetation type was derived from a supervised, 15-class maximum likelihood classification of the 15 Aug 2001 image that had an overall accuracy of 77.33% (Table 3.2).

The 1:20,000 TRIM DEM was used as elevation input, and to generate slope, aspect and angle of incidence layers. Angle of incidence was calculated using solar elevation and azimuth data (Table 3.1) for the approximate scene centre of each image, relative to its date and time of capture. Aspect was categorized by cardinal direction to remove conflicts between 360° and 0°. Vegetation type and aspect were incorporated into the regression analysis using deviation coding (Menard 2002). All model inputs were evaluated for colinearity and multicolinearity and were discarded if tolerance scores were <0.20 (Menard 2002).

A random sample was generated using 0.01% of the smallest dataset (n=2,062 pixels). This sample was deemed sufficient to 'capture' all categories of each categorical variable while still addressing concerns for independence of data points. We used an ecologically plausible model set in the regression analysis in order to attempt to explain NDVI distribution across the landscape. Top-performing models (within 0.05 of the $r^2$ of the best model) were validated using a new independent

Table 3.2. 15-class vegetation scheme used as input information in the multiple regression analyses to predict the Normalized Difference Vegetation Index (NDVI) in the Greater Besa-Prophet Area of northern British Columbia.

| CLASS | DESCRIPTION |
|---|---|
| **MONTANE** | |
| ***Treed*** | |
| Pine | Lodgepole pine (*Pinus contorta)* found on well-drained, mid-elevation benches and some disturbed areas. Class includes mature and growing stands. |
| Spruce | Mature white spruce (*Picea glauca)* or sub-alpine fir (*Abies lasiocarpa*) found on well-drained soils. Often associated with shrub (i.e., willow (*Salix sp.*)/ soopolallie *(Sheperdia canadensis*) or grass understory. |
| Low-productivity Spruce | White spruce primarily found on north-facing slopes. Low density and reduced height and diameter compared to mature spruce of other classes. Understory is primarily moss (e.g., *Pleurozium schreberi*). |
| ***Forbs / Shrub*** | |
| Mixed Deciduous Shrubs | Shrubs <2m. Variable % cover of willow, bog birch (*Betula glandulosa)*, or shrubby cinquefoil *(Potentilla fruiticosa)*. Includes sub-alpine shrubs. |
| ***Riparian*** | |
| Sedge Wetland | Dominated by sedge (*Carex aquatilis*). Some moss species or willow depending on duration of seasonal standing water. |
| Riparian Spruce | White spruce or black spruce (*P. mariana*) associated with sedge or willow. Found in riparian areas and poorly drained stands in the Eastern Lowland area. |
| ***Other*** | |
| Burns / Disturbed | Burns and disturbed areas. Recent disturbances are primarily dominated by fuzzy spiked wildrye (*Elymus innovatus*). With age these areas develop Aspen (*Populus tremuloides*) and Balsam Poplar (*P. balsamifera*) shrubs (<2m) and trees (>2m). May be associated with stands of Pine. |

Table 3.2 Cont'd

| CLASS | DESCRIPTION |
|---|---|
| **SUB-ALPINE** | |
| Sub-alpine Spruce Transition | Transition from mature spruce or fir to sub-alpine shrubs at treeline. Includes krummholz. |
| **ALPINE** | |
| *Dryas*-dominated Alpine | Mountain avens (*Dryas octopetala)* and fescue (*Festuca altaica*) dominated alpine. Moderate to steep southerly slopes. |
| Moist Alpine | Poorly drained and northerly alpine slopes. Primarily dominated by moss with net-veined willow (*Salix reticulata*). Class also includes sites dominated by four-angled mountain heather (*Cassiope tetragona).* |
| **NON-VEGETATED** | |
| Gravel Bar | Gravel bars of current stream courses. Class also includes dry streambeds. Usually non-vegetated, although Drummond's mountain avens (*Dryas drummondii)* may occur. |
| Rock Outcrop / Talus /Bedrock | Outcrops of talus and high-elevation, non-vegetated bedrock. |
| Rock / Crustose Lichen | Large frost-broken boulders with significant cover of crustose lichen such as *Melanelia hepatizon.* |
| Water | Permanent water bodies. |
| Snow / Glacier | Permanent snowfields and glaciers. |

random subset (n=2,062) of data from each image. The best models were considered to be those with the highest adjusted $r^2$ values, unless two models explained within 0.1% of the same variation. In this case, the model with the fewest parameters was selected as the final model for each image date.

The coefficients of the final models were used to predict NDVI values for missing data. Coefficients of the final models were used as weighting factors and added to the intercept for each image date. New raster layers were generated for the entire landscape. These new continuous surfaces were regressed against original NDVI on a pixel-to-pixel basis to determine overall correlation.

## 3.3 RESULTS

### *Initial cross-sensor radiometric comparison*

Both the 16 August and the 14 August image were highly correlated with the cloud-free 15 August (TM) image (band 3: r=0.90 and r=0.89, band 4: r=0.91 and r=0.90 respectively). In band 3, differences for both comparisons of images were mostly attributed to slightly lower values of non-vegetated surfaces in shadowed areas on the ETM+ imagery. Band 4 differences were found in areas of water features and glacial ice. These areas of major difference were deemed to be of little interest to the current investigation. NDVI images generated from the ETM+ data had similarly high correlations with the TM data (August 16: r=0.96, August 14: r=0.88).

***NDVI models***

Statistics for the top-performing model for each input image relative to the minimum and maximum NDVI value (all vegetation types) and Landsat TM/ETM+ WRS path and row are listed in Table 3.3. Coefficients of each model can be found in Appendix E.

Modelled data consistently underestimated NDVI values in non-vegetated types (Rocks and Rock / Crustose Lichen) that bordered vegetated areas, reducing the overall relationship between original and modelled NDVI. A transition zone 'class' was created for these pixels. The original data were subtracted from modelled data. Areas in the two rock classes that had differences greater than the median difference (0.078) were assigned a new value in the classification. This transition zone was added as a new class in the multiple regression analyses and overall adjusted $r^2$ values increased in many models. Table 3.4 shows the performance of the top models before and after the transition zone class was included in the modelling procedure. Appendix F lists the coefficients for all models that used the new transition zone class and lists the validated adjusted $r^2$ for each model.
No other vegetation type had differences of this magnitude between values of the original NDVI and the modelled data, and no other adjustments of this manner were made. Data from 2002 and 2003 were not modelled with the transition zone class because of the overall poor performance of models for these years (see Table 3.3 & Appendix E). Within vegetated classes, minimum NDVI values were consistently less than model estimates for each image. The variation and range for the NDVI data were greater and had consistently higher maximum values per vegetation class

Table 3.3. Minimum (Min) and Maximum (Max) monthly Normalized Vegetation Index (NDVI) values across vegetation types in the Greater Besa-Prophet Area and Landsat Thematic Mapper (TM) and Enhanced Thematic Mapper (ETM+) Path and Row compared to the validated adjusted $r^2$ (Val. Adj. $r^2$) of top-performing predictive models 2001-2003. Models are coded by inputs: vegetation (V), slope (S), aspect (A), elevation (E) and angle of incidence (I).

| Date | Min | Max | WRS Path/Row | Top Model | Val. Adj. $r^2$ |
|---|---|---|---|---|---|
| 04 Jun 2001 | -0.41 | 0.58 | 50/20 | VSAE | 0.639 |
| 22 Jul 2001 | -0.45 | 0.72 | 50/20 | VAE | 0.674 |
| 15 Aug 2001 | -0.38 | 0.74 | 50/20 | VE | 0.845 |
| 16 Sep 2001 | -0.46 | 0.57 | 50/20 | VAE | 0.774 |
| 01 Oct 2001 | -0.30 | 0.46 | 50/20 | VSAE | 0.520 |
| 31 May 2002 | -0.45 | 0.43 | 49/20 | VSAE | 0.597 |
| 15 Jun 2002 | -0.44 | 0.61 | 50/20 | VSAE | 0.548 |
| 24 Jun 2002 | -0.32 | 0.61 | 49/20 | VSAE | 0.778 |
| 09 Aug 2002 | -0.24 | 0.72 | 51/20 | VSAE | 0.635 |
| 09 May 2003 | -0.47 | 0.34 | 50/20 | VSAE | 0.236 |
| 25 Jun 2003 | -0.61 | 0.72 | 51/20 | VSA | 0.178 |
| 29 Jul 2003 | -0.45 | 0.68 | 49/20 | VA | 0.508 |

Table 3.4. Validated adjusted $r^2$ (Val. Adj. $r^2$) of top-performing models that included vegetation before (15-class input) and after 'transition zone' class (16-class input) was included in the modelling procedures for the Greater Besa-Prophet Area in northern British Columbia.

| Date | Val. Adj. $r^2$ (original) | Val. Adj. $r^2$ (with transition zone) |
|---|---|---|
| 04 Jun 2001 | 0.606 | 0.606 |
| 22 Jul 2001 | 0.674 | 0.677 |
| 15 Aug 2001 | 0.845 | 0.865 |
| 16 Sep 2001 | 0.774 | 0.815 |
| 01 Oct 2001 | 0.520 | 0.50 |

than the models predicted. Table 3.5 shows these differences for the most successful model (15 August 2001). Appendix G lists results for all 2001 images.

For each month, vegetation type explained approximately 50% or more of the variation in NDVI across the landscape, except for three images (October 01, May 03, and June 03). When NDVI values were highest, vegetation type explained more than 60-80% of the variation. Images missing large amounts of data from the Muskwa Ranges (i.e., path 49, row 20 images or images with significant cloud cover in the west) consistently had lower adjusted $r^2$ values for top models than images that included this area, even though average NDVI values for images excluding the Sikanni Chief Upland generally had lower mean NDVI. The two autumnal images (September and October 2001) had higher adjusted $r^2$ values than all other images with similar overall mean NDVI. Models for 2001 imagery consistently performed better than models in 2002 and 2003, although 2001 had more full-scene images.

### *Mapping*

The mapped, modelled data that were compared to original NDVI are shown in Figure 3.4. When all non-vegetated surfaces were masked from the image-to-image regression analysis, correlation (r) values were considerably lower than when all pixels were included (Table 3.6). Values were lower still when image-to-image regression was calculated individually for each vegetation classes.

Table 3.5. Per-class minimum (min), maximum (max), mean, standard deviation (s) and range for the Normalized Difference Vegetation Index (NDVI) and NDVI derived from multiple linear regression (MNDVI) analysis for August 2001 in the Greater Besa-Prophet Area in northern British Columbia.

| Vegetation Class | NDVI MIN | MNDVI MIN | NDVI MAX | MNDVI MAX | NDVI MEAN | MNDVI MEAN | NDVI RANGE | MNDVI RANGE | NDVI s | MNDVI s |
|---|---|---|---|---|---|---|---|---|---|---|
| **Sedge Wetland** | -0.376 | 0.323 | 0.567 | 0.406 | 0.387 | 0.388 | 0.944 | 0.083 | 0.070 | 0.010 |
| **Shrub** | -0.305 | -0.195 | 0.738 | 0.509 | 0.444 | 0.442 | 1.043 | 0.704 | 0.074 | 0.034 |
| **Low-Productivity Spruce** | -0.158 | 0.273 | 0.532 | 0.333 | 0.312 | 0.301 | 0.690 | 0.060 | 0.054 | 0.010 |
| **Pine** | -0.183 | 0.328 | 0.565 | 0.389 | 0.360 | 0.359 | 0.748 | 0.061 | 0.054 | 0.007 |
| **Sub-alpine Spruce Transition** | 0.070 | 0.404 | 0.617 | 0.430 | 0.419 | 0.417 | 0.547 | 0.026 | 0.051 | 0.003 |
| **Spruce** | -0.138 | 0.289 | 0.560 | 0.358 | 0.318 | 0.322 | 0.698 | 0.069 | 0.059 | 0.012 |
| **Riparian Spruce** | -0.236 | 0.283 | 0.537 | 0.343 | 0.324 | 0.321 | 0.772 | 0.060 | 0.047 | 0.009 |
| **Dryas Alpine** | -0.102 | 0.299 | 0.613 | 0.350 | 0.319 | 0.325 | 0.715 | 0.051 | 0.088 | 0.007 |
| **Moist Alpine** | -0.050 | 0.300 | 0.546 | 0.340 | 0.299 | 0.322 | 0.597 | 0.041 | 0.083 | 0.005 |
| **Burned / Disturbed** | 0.058 | 0.440 | 0.715 | 0.512 | 0.472 | 0.475 | 0.657 | 0.072 | 0.066 | 0.012 |
| **Sedge Wetland** | -0.376 | 0.323 | 0.567 | 0.406 | 0.387 | 0.388 | 0.944 | 0.083 | 0.070 | 0.010 |

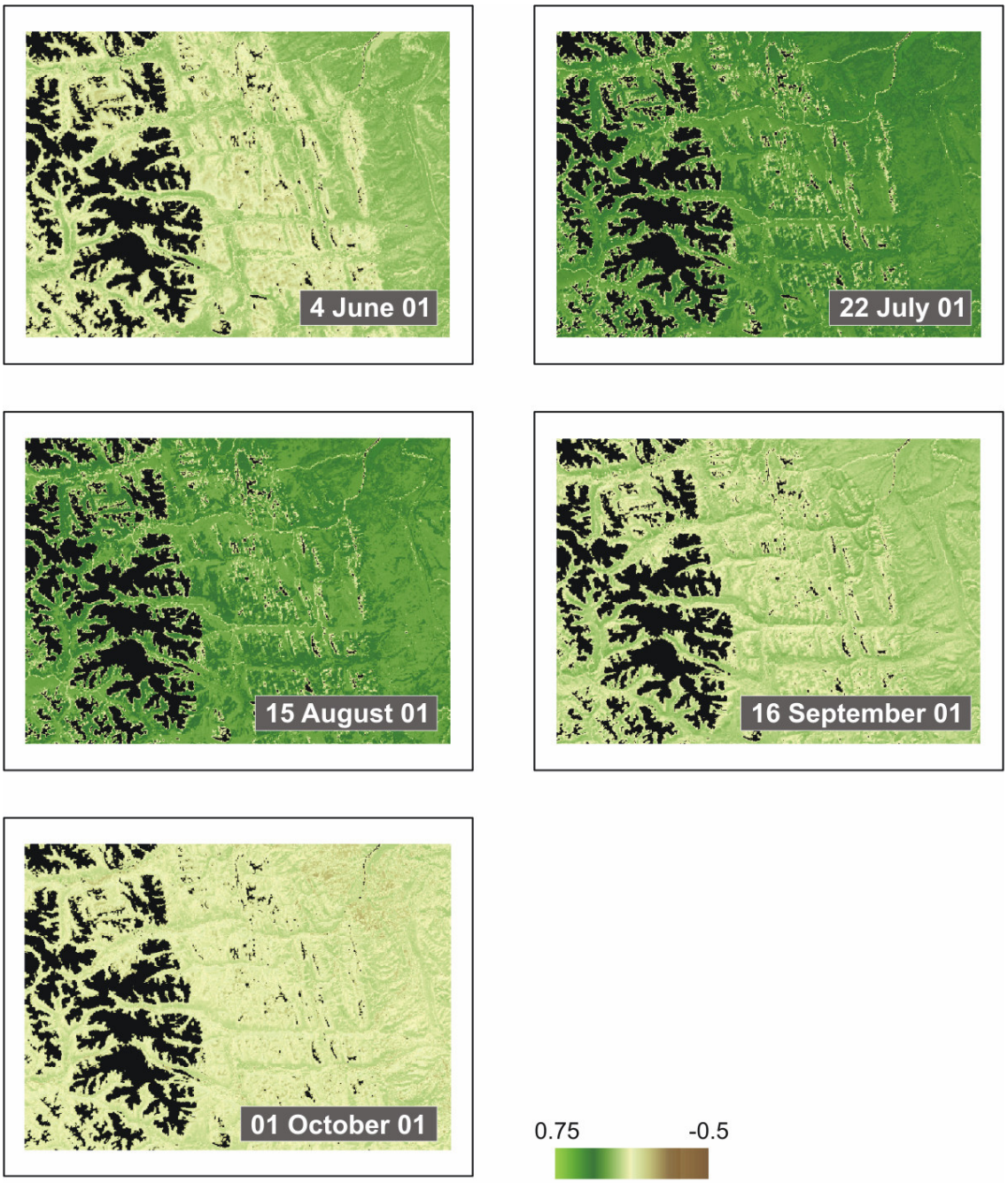


Figure 3.4 Continuous modelled Normalized Difference Vegetation Index (NDVI) images derived from the top-performing multiple linear regression models in 2001 for the Greater Besa-Prophet Area.

Table 3.6. Landscape and per-class image-to-image correlation (r) for the Normalized Difference Vegetation Index (NDVI) and NDVI derived from multiple linear regression analysis (MNDVI) of the Greater Besa-Prophet Area in northern British Columbia.

| | r (image-to-image) | | | | |
|---|---|---|---|---|---|
| **Vegetation Class** | **June** | **July** | **August** | **September** | **October** |
| **Landscape (all classes)** | 0.71 | 0.75 | 0.94 | 0.85 | 0.46 |
| **Landscape (vegetated classes only)** | 0.59 | 0.36 | 0.70 | 0.42 | 0.09 |
| | | | | | |
| **Sedge Wetland** | 0.40 | 0.42 | 0.28 | 0.01 | 0.06 |
| **Shrub** | 0.51 | 0.34 | -0.06 | 0.05 | 0.21 |
| **Low-Productivity Spruce** | 0.29 | 0.23 | 0.22 | 0.49 | 0.32 |
| **Pine** | 0.10 | 0.43 | 0.53 | 0.36 | 0.001 |
| **Sub-alpine Spruce Transition** | 0.25 | 0.10 | 0.04 | 0.53 | 0.12 |
| **Spruce** | 0.20 | 0.31 | 0.01 | 0.34 | 0.23 |
| **Riparian Spruce** | 0.25 | 0.36 | 0.11 | -0.06 | 0.05 |
| **Dryas Alpine** | 0.11 | 0.22 | 0.16 | 0.20 | 0.04 |
| **Moist Alpine** | 0.16 | 0.16 | 0.17 | 0.15 | 0.09 |
| **Burned / Disturbed** | 0.29 | 0.24 | -0.07 | 0.10 | 0.05 |

## 3.4 DISCUSSION

### *Radiometric Distortion/Normalization*

Our objective to create a set or sets of seasonal NDVI data suitable for phenology studies made statistical adjustments/histogram matching inappropriate because these adjustments may have removed differences in imagery related to phenology rather than to radiometric distortion. Basic statistical differences among images are critical to the intended analysis of vegetation change. Additionally, the topographic characteristics and landscape features of the GBPA violate many of the inherent requirements of dark object subtraction and linear regression normalization with PIFs.

Radiometric normalization methods were determined to be inappropriate to the objectives of this study and for application in the GBPA. In most studies, multi-temporal imagery is either near-anniversary date, or radiometric normalization is used to remove seasonal and other differences (Kauffman and Seto 2001). Even though the histogram characteristics (mean, standard deviation and dynamic range, etc.) of each input image may be slightly skewed by the various influences as described previously, matching these values to a common reference image would remove changes of interest to the study. In addition, there is approximately 2400-m difference in elevation in the study area. Consequently, atmospheric differences are not likely to be uniform across the study area, even on days with low aerosol counts.

The criteria for the selection of PIFs also were not satisfied in the study area for numerous reasons. First, the two-lane Alaska Highway is the only non-vegetated cultural feature visible on the image. Its width is insufficient to isolate it from the wide-cut areas on each side of the road that are dominated by shrubs. Second, rock outcrops, which might be assumed to be non-vegetated, are often grouped or confused with rock outcrops having small amounts of intermittent lichen or other alpine vegetation. Bare rock areas without intermittent vegetation are only consistently found above 2200-2500m. Atmospheric characteristics at this elevation would not represent the rest of the GBPA. Additionally, these bare rock areas are generally found on steep slopes; average slope for these areas is 36°. Slopes can be as steep as 81° and would have more extreme irradiance relative to the rest of the image, therefore making the spectral response of these areas atypical for the rest of the study area. Third, there are few gravel bars wide enough to exhibit a response that is not mixed with that of sedges and/or water. Changing water levels seasonally exacerbates these mixtures. Additionally, many gravel bars have at least some amount of Drummond's Mountain Avens (*Dryas* drummondii) or encroaching shrubs (e.g., Willow (*Salix* sp.)). Fourth, large lakes are infrequent in the GBPA. Those lakes that are found in the study area do not exhibit consistent spectral reflectance, as glacial runoff and consequent changes in sediment loadings change the characteristics of these lakes on an almost daily basis. In spring (May, June) many lakes are frozen, dramatically changing their spectral characteristics. Fifth, transform coefficients are determined from a limited subset (PIFs) of the overall image and extrapolation of the slope of the derived transform from the PIFs to the overall image could result in significant error (McGovern et al. 2002). Finally, linear

transformation based on the techniques developed by Yuan and Elvidge (1996) assumes that a large portion of the scene has not changed between image dates (McGovern et al. 2002).

*Solar illumination angle and topographic considerations*

Middleton (1991) found a significant linear relationship between the NDVI with solar illumination angle for various prairie grass species, but also found that the response depended on the site-specific canopy attributes such as leaf area index. There were four vegetation index responses to changes in solar zenith angle (SZA) for grassland species; therefore, a general correction model would be inappropriate to account for change in SZA over the growing season. Extensive knowledge of the canopy characteristics at the time of image capture would be necessary to 'correct' the sun angle effect (Middleton 1991). Solar correction models that assume Lambertian surface reflectance may only be valid for a limited range of incident angles (Colby and Keating 1998). Normalization of imagery for topographic effects also has considerable limitations for similar reasons (Civco 1989).

There may be instances in which the majority of radiometric effects can be avoided. For instance, transformations of band reflectances are closely correlated with biophysical qualities and less susceptible to external variables (e.g. solar zenith angle) than the 'raw' data collected by the sensor (Wiegand et al. 1991). Ratio-based transformations, such as the NDVI, should reduce a large proportion of topographic effect (Holben and Justice 1981).

### *Model Performance*

Model inputs explained much of the variation in NDVI values across the landscape. The relationship between NDVI and the independent variables used in the models was not as predictive within vegetation types. NDVI variation within classes was more likely explained by micro-site differences in biomass, density, composition of species at the pixel level, mixed pixels (due to transition zones between classes and post-classification filtering), and localized differences in atmosphere and/or irradiance. This suggested that the modelling procedure was most appropriate among classes, rather than within them, i.e. analysis was most appropriate for groups of pixels representing relative NDVI rather than individual pixels.

The performance of the models is most likely related to two factors and their interactions: 1) spatial distribution of input data available to draw the random sample (i.e., NDVI data not obscured by clouds) and 2) seasonal differences in NDVI values (related to image date).

#### Spatial Distribution

There are two possible reasons why models that included data from the Muskwa Ranges performed better than those that were missing these data. First, although topographic variables did not always improve model performance, topographic variation reflected in the supervised classification (terrain variables were included in the classification), and the distribution of vegetation types by slope/aspect (relative to

environmental gradients of plant growth) may have aided the prediction of NDVI for these areas. It may also be possible, however, that the increased percentage of non-vegetated and rock classes (particularly in the Muskwa Ranges) may have inflated overall $r^2$ values for these areas because the low variation for the Rock class was predictable. The drop in $r^2$ values for the landscape when non-vegetated classes were removed would suggest that this was at least partially the case.

Seasonal NDVI values

Bian and Walsh (1993) used multiple regression to assess the relationship between topographic variables and information from a vegetation index at several scales. They found that elevation explained the most variation within vegetation index values, while slope and aspect explained very little. In the current investigation, vegetation type replaced elevation as the primary predictor of NDVI, and this relationship varied by month. It is likely that the phenological state of the vegetation changed the amount of variation in NDVI and consequently changed its relationship to vegetation type.

In spring and late summer/autumn, there was not enough variation in vegetation to predict NDVI adequately. Plant characteristics often related to NDVI (i.e., biomass or photosynthetic activity) may not have been significant enough to make them unique by vegetation species in spring, or may have declined beyond that point in autumn. Model performance was highest for summer NDVI images (July and August), when we assumed that vegetation was at maximum photosynthetic activity,

and NDVI values were the highest. Summer months also required fewer inputs to help explain variation in NDVI values across the image, (i.e., terrain inputs increased $r^2$ values in June and September, but were insignificant in the July/August models).

Terrain variables increased model performance in months with relatively low NDVI. This differential performance was true despite solar angle. Terrain variables increased model performance in June of each year (highest sun angle) and in September and October of 2001 (lowest sun angles). Autumnal images did have higher $r^2$ values, however, indicating that the low sun angle could have amplified differences of slope/aspect, making them easier to predict than months with high sun and less terrain effect. The ratio-based NDVI did not, therefore, sufficiently reduce the topographic effect of low sun angle in late summer/fall in the GBPA. This effect was obvious as a visual representation of relief in the September and October modelled images.

Addition of 'transition zone' class

Adding the 'transition zone' class as input to the models increased adjusted $r^2$ of July, August and September models, but did not increase performance in June and decreased adjusted $r^2$ in October. The transition zone may have been made up of pixels coded as non-vegetated in the supervised classification, but because of their vegetative component had NDVI values higher than 'true' non-vegetated areas. These areas might have included areas in transition zones from vegetated areas to non-vegetated areas (Rock), but may also have included areas of shadow that were

incorrectly coded as rocks in the classification. Removing these areas from Rock and Rock / Crustose Lichen classes increased our ability to predict (low) NDVI values in Rock and Rock / Crustose Lichen and explain the overall variation in NDVI on the landscape.

### *Conclusions*

Unlike many pre-processing procedures in image processing, radiometric normalization of imagery may not be able to rely on standardized approaches (McGovern et al. 2002). Furthermore, radiometric pre-processing beyond dark area subtraction may not always produce significantly improved imagery (Collins and Woodcock 1996). We were not satisfied that radiometric normalization techniques could be applied to the data from our study area with a reasonable estimate of the possible addition of uncontrolled or unidentifiable error. We assumed that the NDVI was a useful descriptor of the relative characteristics of vegetation despite atmospheric effects and other impairments to radiometric quality (Holben et al. 1990, Kaufman 1984), and that topographic effect not eliminated by ratioing should be identifiable during interpretation (within analysis).

In this research, the number of variables used to predict NDVI values was small, and vegetation type (determined using the supervised classification results) was the primary predictor of NDVI values on the landscape. For this reason, the variation in NDVI values on the landscape was significantly reduced and the pixel groups were primarily delineated by the vegetation classes. The reduction in variation within

classes explained the low correlation between NDVI and modelled data within vegetation classes. Heterogeneity within classes, however, may have been at least partially related to spatially explicit, differential atmospheric and/or topographic effects that could confound or confuse the results of change analysis. If the modelled data can be considered as a relative indicator of vegetation 'greenness', they are valid to describe changes in vegetation phenology using methods developed for lower spatial resolution data. These data, however, are only suitable for analysis at the minimum mapping unit of the classification (0.56ha), not the original resolution of the data (0.063ha).

The modelling procedures explained some of the primary determinates of the variation in NDVI across the GBPA, although NDVI could not be predicted for some images particularly in fall and early spring, with a reasonable degree of certainty. If careful attention is paid to the potential radiometric confusion that may influence change detection techniques such as the effect of lower sun angles in September and October, then the selected methods and their results or derivatives could be scrutinized for anomalous effects.

The results presented here suggest some of the possible limitations of using Landsat TM or ETM+ to create an intra-season, medium-resolution dataset suitable for phenology studies similar to others developed for lower-resolution data. These results also show that data derived from models developed to predict areas under clouds help to explain the characteristics of NDVI and may be useful as a relative indicator of seasonal vegetation phenology.

## 3.5 LITERATURE CITED


Bian, L., Walsh, S. (1993) Scale dependencies of vegetation and topography in a mountainous environment in Montana. *Professional Geographer,* 45: 1-11.

Borak, J.S., Lambin, E.F., and Strahler, A.H. (2000). The use of temporal metrics for land cover change detection at coarse spatial scales. *International Journal of Remote Sensing,* 21 (6&7): 1415-1432.

Burgess, D. W., Lewis, P., and Muller, J.-P. A. L. (1995) Topographic effects in AVHRR NDVI data. *Remote Sensing of Environment,* 54: 223-232.

Casselles, V., and Lopez Garcia, M.J. (1989). An alternative approach to estimate atmospheric correction in multi-temporal studies. *International Journal of Remote Sensing,* 10 (6): 1127-1134.

Chander, G. and Markham, B. (2003) Revised Landsat-5 TM radiometric calibration procedures and postcalibration dynamic ranges. IEEE Transactions on Geosciences and Remote Sensing. 41 (11): 2674-2677.

Chavez, P.S. Jr., and MacKinnon, D.J. (1994) Automatic detection of vegetation changes in the Southwestern United States using remotely sensed images. *Photogrammetric Engineering and Remote Sensing,* 60 (5): 571-583.

Chen, X., Zhongjun, T., Schwartz, M.D., and Xu, C. (2000) Determining the growing season of land vegetation on the basis of plant phenology and satellite data in Northern China. *International Journal of Biometeorology,* 44: 97-101.

Civco, D.L. (1989) Topographic normalization of Landsat Thematic Mapper digital imagery. *Photogrammetric Engineering and Remote Sensing,* 55: 1303-1309.

Colby, J.D. and Keating, P.L. (1998). Land cover classification in the tropical highlands: the influence of anisotropic reflectance. *International Journal of Remote Sensing,* 19(8): 1479-1500.

Collins, J.B., and Woodcock, C.E. (1996). An assessment of several linear change detection techniques for mapping forest mortality using Multi-temporal Landsat TM data. *Remote Sensing of Environment,* 56 (1): 66-77.

Du, Y., Teillet, P.M., and Cihlar, J. (2002). Radiometric normalization of multi-temporal high-resolution satellite images with quality control for land cover change detection. *Remote Sensing of Environment,* 82: 123-134.

Duchemin, B., Goubier, J. and Courrier, G. (1999) Monitoring phenological key stages and cycle duration of temperate deciduous forest ecosystems with NOAA/AVHRR data. *Remote Sensing of Environment,* 67: 51-67.

Eastman, J.R., and Fulk, M. (1993) Long sequence time series evaluation using standardized principal components. *Photogrammetric Engineering and Remote Sensing,* 59 (6): 991-996.

Eckhardt, D.W., Verdin, J.P., and Lyford, G.R. (1990) Automated update of an irrigated lands GIS using SPOT HRV Imagery. *Photogrammetric Engineering and Remote Sensing,* 56 (11): 1515-1522.

Groten, S.M.E., and Ocatre, R. (2002) Monitoring the length of the growing season with NOAA. *International Journal of Remote Sensing,* 23: 2797-2815.

Hall, F.G., Strebel, D.E., Nickeson, J.E., and Goetz, S.J. (1991) Radiometric rectification: toward a common radiometric response among multisensor images. *Remote Sensing of Environment,* 35: 11-27.

Heo, J., and FitzHugh, T.W. (2000) A standardized radiometric normalization method for change detection using remotely sensed imagery. *Photogrammetric Engineering and Remote Sensing,* 66 (2): 173-181.

Hoare, D. and Frost, P. (2004) Phenological description of natural vegetation in southern Africa using remotely-sensed vegetation data. *Applied Vegetation Science*, 7:19-28.

Holben, B., and Justice, C. (1981) An examination of the use of spectral band ratioing to reduce the topographic effect on remotely sensed data. *International Journal of Remote Sensing,* 2: 115-133.

Holben, B., Kaufman, Y.J. and Kendall, J.D. (1990) NOAA-11 AVHRR visible and near-IR in-flight calibration. *International Journal of Remote Sensing,* 11 (8): 1511-1519.

Kaufman, Y.J. (1984) Atmospheric effects on remote sensing of surface reflectances. *SPIE Remote Sensing,* 475: 20-33.

Kaufmann, R.K., and Seto, K.C. (2001) Change detection, accuracy, and bias in a sequential analysis of Landsat imagery in the Pearl River Delta, China: econometric techniques. *Agriculture, Ecosystems and Environment,* 85: 95-105.

Lee, R., Yu, F., Price, K.P., Ellis, J., and Shi, P. (2002) Evaluating vegetation phenological patterns in Inner Mongolia using NDVI time-series analysis. *International Journal of Remote Sensing,* 23 (12): 2505-2512.

Lobo, A., Ibanez Marti, J.J., and Gimenez-Cassina, C.C. (1997) Regional scale hierarchical classification of temporal series of AVHRR vegetation index. *International Journal of Remote Sensing,* 18 (15): 3167-3193.

Markon, C.J., Fleming, M.D., and Binnian, E.F. (1995) Characteristics of vegetation phenology over the Alaskan landscape using AVHRR time-series data. *Polar Record,* 31 (177): 179-190.

McGovern, E.A. Holden, N.M., Ward, S.M., and Collins, J.F. (2002) The radiometric normalization of multi-temporal Thematic Mapper imagery of the midlands of Ireland - a case study. *International Journal of Remote Sensing,* 4: 751-766.

Menard, S. (2002). Applied logistic regression analysis. Second edition. Thousand Oaks California: Sage Publications.

Middleton, E.M. (1991) Solar zenith angle effects on vegetation indices in tallgrass prairie. *Remote Sensing of Environment,* 38: 45-62.

Myneni, R.B., and Asrar, G. (1994) Atmospheric effects and spectral vegetation indices. *Remote Sensing of Environment,* 47: 390-402.

Myneni, R.B., Tucker, C.J., Asrar, G. and Kelling, C.D. (1998) Interannual variations in satellite-sensed vegetation data from 1981-1991. *Journal of Geophysical Research,* D6: 6145-6160.

Nemani, R. and Running, S.W. (1997) Land cover characterization using multi-temporal red, near-IR, and thermal-IR data from NOAA/AVHRR. *Ecological Applications,* 7: 79-90.

Oindo, B.O. (2002) Predicting mammal species richness and abundance using multi-temporal NDVI. *Photogrammetric Engineering and Remote Sensing,* 68 (2): 623-629.

Pedroni, L. (2003). Improved classification of Landsat TM data using modified prior probabilities in large and complex landscapes. *International Journal of Remote Sensing,* 24(1): 91-113.

Peet, R.K. (2000) Forests and Meadows of the Rocky Mountains. In Barbour, M.G. and Billings, W.D. (Eds.) North American Terrestrial Vegetation 2nd Ed. (pp 5-122). New York: Cambridge University Press.

Schott, J.R., Salvaggio, C., and Volchok, W.J. (1988) Radiometric scene normalization using pseudoinvariant features. *Remote Sensing of Environment,* 26: 42370.

Schwartz, M.D., and Reed, B.C. (1999) Surface phenology and satellite sensor-derived onset of greenness: an initial comparison. *International Journal of Remote Sensing,* 17: 3451-3457.

Shepherd, J.D. and Dymond, J.R. (2003) Correcting satellite imagery for the variance of reflectance and illumination with topography. *International Journal of Remote Sensing,* 24 (17): 3503-3514.

Song, C., Woodcock, C.E., Seto, K.C., Lenny, M.P., and Macomber, S.A. (2001) Classification and change detection using Landsat TM data: when and how to correct atmospheric effects? *Remote Sensing of Environment,* 75: 230-244.

Suzuki, R., Nomaki, T., and Yasunari, T. (2003) West-east contrast of phenology and climate in northern Asia revealed using a remotely sensed vegetation index. *International Journal of Biometeorology,* 47: 126-138.

Wiegand, C.L., Richardson, A.J., Escobar, D.E., and Gerbermann, A.H. (1991) Vegetation indices in crop assessments. *Remote Sensing of Environment,* 35 105-119.

Xin, J., Zhenrong, Y., van Leeuwen, and L., Driessen, P.M. (2002) Mapping crop key phenological stages in the North China Plain using NOAA time series images. *International Journal of Applied Earth Observation and Geoinfomation,* 4: 109-117.

Yang, X., and Lo, C.P. (2000) Relative radiometric normalization performance for change detection from multi-date satellite images. *Photogrammetric Engineering and Remote Sensing,* 66 (8): 967-980.

Yuan, D., and Elvidge, C.D. (1996) Comparison of relative radiometric normalization techniques. *ISPRS Journal of Photogrammetry and Remote Sensing,* 51: 117-126.

# CHAPTER FOUR – INTRA-SEASON CHANGE IN VEGETATION IN A NORTHERN MOUNTAIN ECOSYSTEM USING LANDSAT TM AND ETM+[2]

## 4.1 INTRODUCTION

Determining the relationships among landscape features and the use of resources by mammals requires spatial information that is collected at a scale that is as relevant to as many scales of the habitat requirements of the species being studied as possible. Numerous GIS and remote sensing methods have been developed that can provide data related to landscape pattern and composition. These methods include the manipulation of digital reflectance of terrestrial surfaces by satellite remote sensing using arithmetic, geometric, algebraic and other transformations (Billingsley 1983). Much research has contended that classification of vegetation from remotely-sensed data may be a low-cost alternative to traditional techniques for mapping habitat or developing habitat suitability indices (HSI) for mammals (Apps 2004, Johnson et al. 2003, Franklin et al. 2002, Huber and Casler 1990) or for determining habitats that mammals may preferentially select using resource selection functions (RSF) (Johnson et al. 2004, Boyce et al. 2003, Nielsen et al. 2002, Jepsen et al. 2002, McLoughlin et al. 2002, Osborne et al. 2001, Rettie and Messier 2000, Arthur et al. 1996). Seasonal differences in habitat characteristics such as food availability may also be derived for these analyses by identifying relative changes in vegetation with intra-season, multi-temporal imagery.

[2] Chapter may be submitted for publication with the following authorship: R.J. Lay, R.D. Wheate and D.D. Gustine.

Several authors have used satellite-derived estimates of vegetation 'greenness' such as the Normalized Difference Vegetation Index (NDVI) or Tasseled Cap 'Greenness' component to estimate the timing of phenological changes (Hoare and Frost 2004, Suzuki et al. 2003, Hall-Beyer 2003, Oindo 2002, Groten and Ocatre 2002, Xin et al. 2002, Griffith et al. 2002, Lee et al. 2002, Chen et al. 2000, Duchemin et al. 1999, Schwartz and Reed 1999, Markon et al. 1995). These indices take advantage of the contrast between high absorption in the visible wavelengths and high reflectance of the near-infrared wavelengths by green vegetation (Bannari et al. 1995, Crist and Cicone 1984) and have been found to be related to net primary productivity, biomass, leaf area index, crown closure and other vegetation characteristics (Purevdorj et al. 1998, Bannari et al. 1995, Cihlar et al. 1991, Baret and Guyot 1991, Tucker and Sellers 1986, Crist and Cicone 1984). A positive change in 'greenness' values over an intra-season, multi-temporal image sequence likely corresponds to changes in vegetation phenology such as growth of new tissue or increased above-ground biomass (Groten and Ocatre 2002), and may be related to forage quality as new plant tissue is highly digestible (Cameron and Whitten 1980). Griffith et al. (2002) found that this change was related to movement of caribou (*Rangifer tarandus greenlandicus*) in northern Alaska.

These studies employed various techniques to derive the change between images of different dates and relate this to phenological changes in vegetation. There is no consensus within remote sensing research literature as to which change detection procedure performs best because the success of change detection methods

depends on the landscape characteristics of the study area, the type of change being analysed and the temporal resolution of the data (Kaufmann and Seto 2001).

### *Change Detection*

The following describes some commonly applied change detection techniques, particularly those related to change in seasonal phenology of vegetation.

#### Phenological Modelling

Zhang et al. (2003) used logistic models to fit the change of reflectances of multi-temporal imagery, and used the rate of change in the fitted logistic models to identify the dates of changes from one phenological phase to another. These phases included green-up (the commencement of photosynthetic activity), maturity (maximum plant leaf area), senescence (the rapid decrease of photosynthetic activity and leaf area), and dormancy (physiological activity near zero).

#### Vegetation Profiles

The creation of a vegetation profile is a simple method to describe the change in 'greenness' values within season or between years. A vegetation profile summarizes NDVI values at pre-determined temporal intervals in sequence by computing summary statistics (e.g., min, max, mean, median, and mode) under a mask of vegetation types. Markon et al. (1995) estimated onset, peak and duration of vegetation 'greenness' by calculating maximum NDVI values for particular time periods during the growing season. The dates when these values exceeded a pre-determined threshold (onset), or did not continue to increase (peak) were recorded. The number of days between onset and the date that NDVI fell below a threshold

value was determined to be the duration of 'greenness'. Eastman and Fulk (1993) used a time-series profile of monthly mean NDVI values to help partially explain the outputs of standardized principal component analysis (SPCA).

Image Differencing

Subtraction of geometrically registered images of different dates produces an output image that is the change (difference) between these pairs. Output data are usually normally distributed (Mas 1999, Jensen 1996); pixels that do not change are distributed about the mean, whereas changed pixels are found at the tails of the distribution (Borak et al. 2000, Price et al. 1992). Thresholds of change can be developed to determine 'change' and 'no change' pixels in the output histogram using standard deviations from the mean or by empirical examination (Khorram 1999).

Standardized Principal Component Analysis

Principal component analysis (PCA) can be used to remove redundancy in correlated data by rotating data axes in multi-dimensional space so that they are uncorrelated and to create new images that explain progressively less of the variance among the original inputs (Eastman and Fulk 1993, Eklundh and Singh 1993, Richards 1984, Byrne et al. 1980). Standardized PCA (SPCA) eigenvectors are computed using a correlation matrix so that each band has zero mean and unit variance and has equal weight in the new images (Anyamba and Eastman 1996, Eastman and Fulk 1993, Eklundh and Singh 1993, Fung and LeDrew 1987).

Many authors have used principal component analysis to detect changes present in multi-temporal data (Hall-Beyer 2003, Li and Kafatos 2000, Anyamba and Eastman 1996, Hirosawa et al. 1996, Eastman and Fulk 1993, Richards 1984, Byrne et al. 1980). In time series data, principal component analysis is used to isolate patterns of temporal change, since areas of a constant value are highly correlated, and regions of change have low correlation (Li and Kafatos 2000, Anyamba and Eastman 1996, Richards 1984, Byrne et al. 1980). The temporal coefficients (loadings) are used to show correlation between output components and the original data (Anyamba and Eastman 1996, Li and Kafatos 2000). Several authors have compared climate patterns with the output of SPCA to determine the relationships between them (Li and Kafatos 2000, Anyamba and Eastman 1996). Standardization in this manner may minimize the differences caused by sun angle or atmospheric differences (Fung and LeDrew 1987). Mas (1999) found that SPCA removed variability in multi-temporal imagery that was the result of sensor and atmospheric differences remaining after radiometric normalization had been applied.

***Scale***

Many of the studies that have attempted to detect changes in seasonal vegetation phenology have used low spatial resolution data such as AVHRR (1km) or MODIS (250m) (e.g., Suzuki et al. 2003, Hall-Beyer 2003, Oindo 2002, Groten and Ocatre 2002, Xin et al. 2002, Lee et al. 2002, Chen et al. 2000, Borak et al. 2000, Duchemin et al. 1999, Schwartz and Reed 1999, Nemani and Running 1997, Lobo et al. 1997,

Markon et al. 1995). In complex terrain and heterogeneous landscapes such as mountainous areas, these low-resolution data are insufficient to describe change in vegetation communities. For instance, in the boreal Rocky Mountains, vegetation growth is primarily related to several environmental gradients such as elevation, moisture (particularly related to aspect), and soil type (Peet 2000, Hills and Pierpoint 1960). These gradients may be further differentiated by disturbance events and differences in stand age (Peet 2000). In rugged terrain, data with low spatial resolution such as Advanced Very High Resolution Radiometer (AVHRR) and Moderate-resolution Imaging Spectroradiometer (MODIS) would not capture much of the variation in vegetation that is the result of these interacting environmental conditions because these would be at a sub-pixel scale (Hall-Beyer 2000). Some information about coarse-scale habitat selection by animals may be derived from these low-resolution data, but the heterogeneity of a mountain landscape would confound most assessment of habitat use. Fine-scale habitat information in mountainous areas is not discernable. It is unlikely that low-resolution vegetation information would improve any analysis of resource selection for most species.

The 30-m resolution Thematic Mapper (TM) and Enhanced Thematic Mapper (ETM+) onboard the Landsat satellites (5 and 7 respectively) repeatedly captured imagery until the ETM+ sensor malfunctioned in April 2003. The sun-synchronous orbit of Landsat allows for consistent illumination and time of day (subject to illumination differences with time of year) for each scene. Because both sensors' orbits allowed them to repeat data capture for each scene (path and row) at separate 16-day intervals, datasets consisting of seasonal, community-level imagery could

potentially have been compiled at approximately eight-day intervals. Landsat TM and ETM+ data may also be more suited to vegetation analyses than AVHRR data because the TM and ETM+ bands were organized to exploit the differential reflectance of vegetation (Jensen 1996) while the AVHRR, for instance, was not specifically designed for such applications (Zhang et al. 2003).

Our goal was to produce information about the change in vegetation phenology using Landsat TM and ETM+ data that would be appropriate for use in habitat suitability models or resource selection functions for large mammals. The primary objective was to determine if change detection methods that have been developed using low-resolution satellites in uniform terrain could be applied to 30-m resolution Landsat TM and ETM+ imagery in a mountain environment.

## 4.2 METHODS

### *Study Area and Data Inputs*

This study was conducted in the Greater Besa-Prophet Area (GBPA) in northern British Columbia. For a detailed description of the study area, see Chapter 1.

Two datasets were prepared for change detection analyses: 1) TM and ETM+ NDVI derived from at-satellite spectral radiances, and 2) data derived from multiple linear regression techniques used to estimate NDVI values for areas of missing data (MNDVI) (see Chapter 3). No radiometric normalization was applied to these data; for a complete description of pre-processing and modelling techniques, see Chapter

3. Both datasets were used in the change analyses in order to assess the consistency of results between NDVI and MNDVI. Each dataset included data captured 4 June, 22 July, 15 August, and 16 September 2001. October 2001 data were omitted from the analysis because of the limited spatial distribution of cloud-free data, reduced range of values (consistent near-zero or negative values indicated vegetation had senesced), low model performance (see Chapter 3), presence of new snow, and extreme shadowing that was the result of low sun angle for the capture date. Data for 2002 and 2003 were not analysed because of the low temporal resolution of the collected imagery, large areas of path-missing and clouded areas, and the inability to compensate for these problems with a reasonable degree of certainty using multiple regression (see Chapter 3).

***Change Detection***

The temporal resolution of the input data collected for the GBPA was not sufficient to analyse phenological changes using the rate of change in fitted models. Instead, three other change detection methods were employed in order to detect characteristics of plant phenology in the study area: vegetation profiling, image differencing and SPCA. For all analyses, MNDVI images were analysed using the entire modelled landscape, and using the cloud-masks for consistent comparison with the NDVI dataset. Areas of the GBPA that remained negative for the entire season and areas in generally non-vegetated classes such as gravel bars were not included in the analysis of change in NDVI values; any change in these areas was assumed to be anomalous and/or the result of mixed pixels within classes.

Vegetation Profiles

Vegetation profiles were generated for each vegetated class of a 15-class maximum likelihood classification (Table 4.1) (see Chapter 2). A random sample of 2,062 pixels was selected from each (MNDVI and NDVI) dataset to avoid autocorrelation of sample data. Pixel locations were kept consistent for each month's sample to assure control of slope, aspect and elevation within analyses. Analysis of variance (ANOVA) was used to determine whether there was a significant effect ($\alpha$=0.05) of month on the NDVI values of each vegetation type. All post-hoc analyses for multiple comparisons were performed with Tukey's Honest Significant Difference (HSD). Although input data were not normally distributed, sample sizes were equal; therefore, p-values were likely only mildly distorted (Ott 1993). Peak 'greenness' (maturity) was determined as the month when the mean NDVI value was the highest.

Image Differencing

Images earlier in the season were subtracted from those of later months in pairs to assess the change in vegetation phenology. Each difference image was tested for normality using the Shapiro-Wilk W test (Statistica 6.1, StatSoft Inc., Tulsa OK, USA). Data from each vegetation class were assessed individually for normality in

Table 4.1. Brief descriptions of the 15-class scheme used to classify the landscape of the Greater Besa-Prophet area in northern British Columbia.

| CLASS | DESCRIPTION |
|---|---|
| **MONTANE** | |
| ***Treed*** | |
| Pine | Lodgepole pine (*Pinus contorta)* found on well-drained, mid-elevation benches and some disturbed areas. Class includes mature and growing stands. |
| Spruce | Mature white spruce (*Picea glauca)* or sub-alpine fir (*Abies lasiocarpa*) found on well-drained soils. Often associated with shrub (i.e., willow (*Salix sp.*)/ soopolallie *(Sheperdia canadensis*) or grass understory. |
| Low-productivity Spruce | White spruce primarily found on north-facing slopes. Low density and reduced height and diameter compared to mature spruce of other classes. Understory is primarily moss (e.g., *Pleurozium schreberi*). |
| ***Forbs / Shrub*** | |
| Mixed Deciduous Shrubs | Shrubs <2m. Variable % cover of willow, bog birch (*Betula glandulosa)*, or shrubby cinquefoil *(Potentilla fruiticosa)*. Includes sub-alpine shrubs. |
| ***Riparian*** | |
| Sedge Wetland | Dominated by sedge (*Carex aquatilis*). Some moss species or willow depending on duration of seasonal standing water. |
| Riparian Spruce | White spruce or black spruce (*P. mariana*) associated with sedge or willow. Found in riparian areas and poorly drained stands in the Eastern Lowland area. |
| ***Other*** | |
| Burns / Disturbed | Burns and disturbed areas. Recent disturbances are primarily dominated by fuzzy spiked wildrye (*Elymus innovatus*). With age these areas develop Aspen (*Populus tremuloides*) and Balsam Poplar (*P. balsamifera*) shrubs (<2m) and trees (>2m). May be associated with stands of Pine. |

Table 4.1 Cont'd

| CLASS | DESCRIPTION |
|---|---|
| **SUB-ALPINE** | |
| Sub-alpine Spruce Transition | Transition from mature spruce or fir to sub-alpine shrubs at treeline. Includes krummholz. |
| **ALPINE** | |
| *Dryas*-dominated Alpine | Mountain avens (*Dryas octopetala)* and fescue (*Festuca altaica*) dominated alpine. Moderate to steep southerly slopes. |
| Moist Alpine | Poorly drained and northerly alpine slopes. Primarily dominated by moss with net-veined willow (*Salix reticulata*). Class also includes sites dominated by four-angled mountain heather (*Cassiope tetragona).* |
| **NON-VEGETATED** | |
| Gravel Bar | Gravel bars of current stream courses. Class also includes dry streambeds. Usually non-vegetated, although Drummond's mountain avens (*Dryas drummondii)* may occur. |
| Rock Outcrop / Talus /Bedrock | Outcrops of talus and high-elevation, non-vegetated bedrock. |
| Rock / Crustose Lichen | Large frost-broken boulders with significant cover of crustose lichen such as *Melanelia hepatizon.* |
| Water | Permanent water bodies. |
| Snow / Glacier | Permanent snowfields and glaciers. |

each difference image to determine if change thresholds could be applied at the class level. If so, changes were isolated across classes (i.e., landscape changes) and within vegetation classes. Magnitude of change was differentiated using standard deviations from the mean. Pixels with values less than one standard deviation from the mean were considered constant (no change).

To supplement discussion of the onset and duration of photosynthetic activity, June NDVI and MNDVI data were subtracted from the September images of each dataset respectively. Positive values indicated NDVI values that were higher in September than in June, while negative values were the reverse.

Standardized Principal Component Analysis

Standardized PCA (SPCA) was used to assess the change in seasonal NDVI values of the GBPA using the PCA procedure of the IDRISI Kilimanjaro software system (Clark Labs, Clark University, Worcester MA, USA). MNDVI and NDVI values were each used in independent analyses in order to assess the agreement between them. Although analysis was conducted on the entire GBPA image subset, it was limited to vegetated areas only to ensure that anomalous change in non-vegetated surfaces did not influence analysis of vegetation change. Non-vegetated areas were assigned a value of zero for all inputs. This ensured that these regions were represented in the first component, removing them from consequent change components (Eastman and Fulk 1993). Areas of cloud or missing data (for all months of NDVI data) were removed in the same manner and a dataset was created

from MNDVI with the same areas removed to determine whether limited spatial distribution of data influenced the results of SPCA. All methods were repeated for each of the three subunits of the GBPA (see Chapter 1) by excluding all areas outside each subunit in a similar manner. Component images were enhanced with a linear contrast stretch and patterns were identified with a qualitative examination of the distribution of relatively high, moderate and low values.

The first component image in SPCA (PC1) explains most of the variance and consequently demonstrates common patterns of variation (Hall-Beyer 2003, Anyamba and Eastman 1996). A strong positive loading for an input image to a component suggests a latent spatial pattern in the input image that is similar to that shown in the component, while a strong negative loading indicates a pattern that is the inverse of the evident pattern (Eastman and Fulk 1993). In multi-temporal datasets, components derived after PC1 describe residual temporal patterns (Anyamba and Eastman 1996). Component two (PC2) is orthogonal to PC1 and explains the variability in the data that was uncorrelated with that explained in component one and is the first change image (Hall-Beyer 2003, Eastman and Fulk 1993).

## 4.3 RESULTS

### *Vegetation Profiles*

The vegetation profiles were the only change detection method employed that directly described change in vegetation by type (Table 4.2). There was a significant

Table 4.2. Normalized Difference Vegetation Index (NDVI) and NDVI derived from multiple linear regression analysis (MNDVI) values and standard error ($\sigma$) by vegetation type among months of the 2001 growing season in northern British Columbia. Values marked with a common letter indicate no significant difference within vegetation types between months, determined by Tukey's Honest Significant Difference (HSD).

| Vegetation Type | June | July | August | September | $\sigma$ (all months) |
|---|---|---|---|---|---|
| **MNDVI** | | | | | |
| Sedge Wetland | 0.279 | 0.419 | 0.387 | 0.231 | 0.002 |
| Shrub | 0.110 | 0.460 | 0.449 | 0.225 | 0.002 |
| Low-Productivity Spruce | 0.215 | 0.353 | 0.301 | 0.155 | 0.003 |
| Pine | 0.268 | 0.387 | 0.359 | 0.255 | 0.002 |
| Sub-alpine Spruce | 0.123 | 0.442 | 0.417 | 0.261 | 0.002 |
| Spruce | 0.226 | 0.346 | 0.323 | 0.213 | 0.001 |
| Riparian Spruce | 0.259 | 0.359 | 0.321 | 0.219 | 0.001 |
| Dryas Alpine | 0.049 | 0.331[a] | 0.326[a] | 0.166 | 0.002 |
| Moist Alpine | 0.005 | 0.291 | 0.322 | 0.132 | 0.002 |
| Burned / Disturbed | 0.176 | 0.478[b] | 0.475[b] | 0.273 | 0.002 |
| **NDVI** | | | | | |
| Sedge Wetland | 0.172 | 0.351[a] | 0.350[a] | 0.210 | 0.009 |
| Shrub | 0.082 | 0.464 | 0.444 | 0.216 | 0.004 |
| Low-Productivity Spruce | 0.211 | 0.346 | 0.309 | 0.154 | 0.005 |
| Pine | 0.245 | 0.384[b] | 0.367[b] | 0.254 | 0.006 |
| Sub-alpine Spruce | 0.130 | 0.443[c] | 0.418[c] | 0.244 | 0.003 |
| Spruce | 0.223 | 0.327 | 0.306 | 0.194 | 0.009 |
| Riparian Spruce | 0.254 | 0.342 | 0.316 | 0.220 | 0.003 |
| Dryas Alpine | 0.061 | 0.309[d] | 0.311[d] | 0.157 | 0.010 |
| Moist Alpine | 0.014 | 0.302[e] | 0.293[e] | 0.109 | 0.012 |
| Burned / Disturbed | 0.145 | 0.461[f] | 0.453[f] | 0.268 | 0.002 |

effect of month on NDVI and MNDVI values for each vegetation type: (MNDVI $F > 1144_{(3, 136)}$, NDVI $F > 101_{(3, 216)}$), although between-month differences were not always consistent between NDVI and MNDVI datasets (Table 4.2). All vegetation types significantly increased in NDVI and MNDVI between June and July, but the identified changes in NDVI values between July and August were different for NDVI and MNDVI data. NDVI values decreased in all vegetation types, although many did not decrease significantly. The MNDVI data showed more significant decreases within classes than the NDVI dataset and a continued increase in the Moist Alpine class from July to August. All values decreased significantly from August to September in both datasets. There were no marginal significant differences; therefore, we were satisfied that potential distortion from non-normality was not present. Figure 4.1 shows the changes in NDVI and MNDVI values for three characteristic vegetation types in 2001.

***Image Differencing***

Three images for each dataset were created from the subtraction of the original monthly data: spring (July-June), summer (August-July) and autumnal (September-August). These images mimic the results of the profiles, but display the changes spatially.

NDVI

The distribution of the landscape outputs derived from NDVI data was not normally distributed; each image had a large number of outliers that were infrequent on the

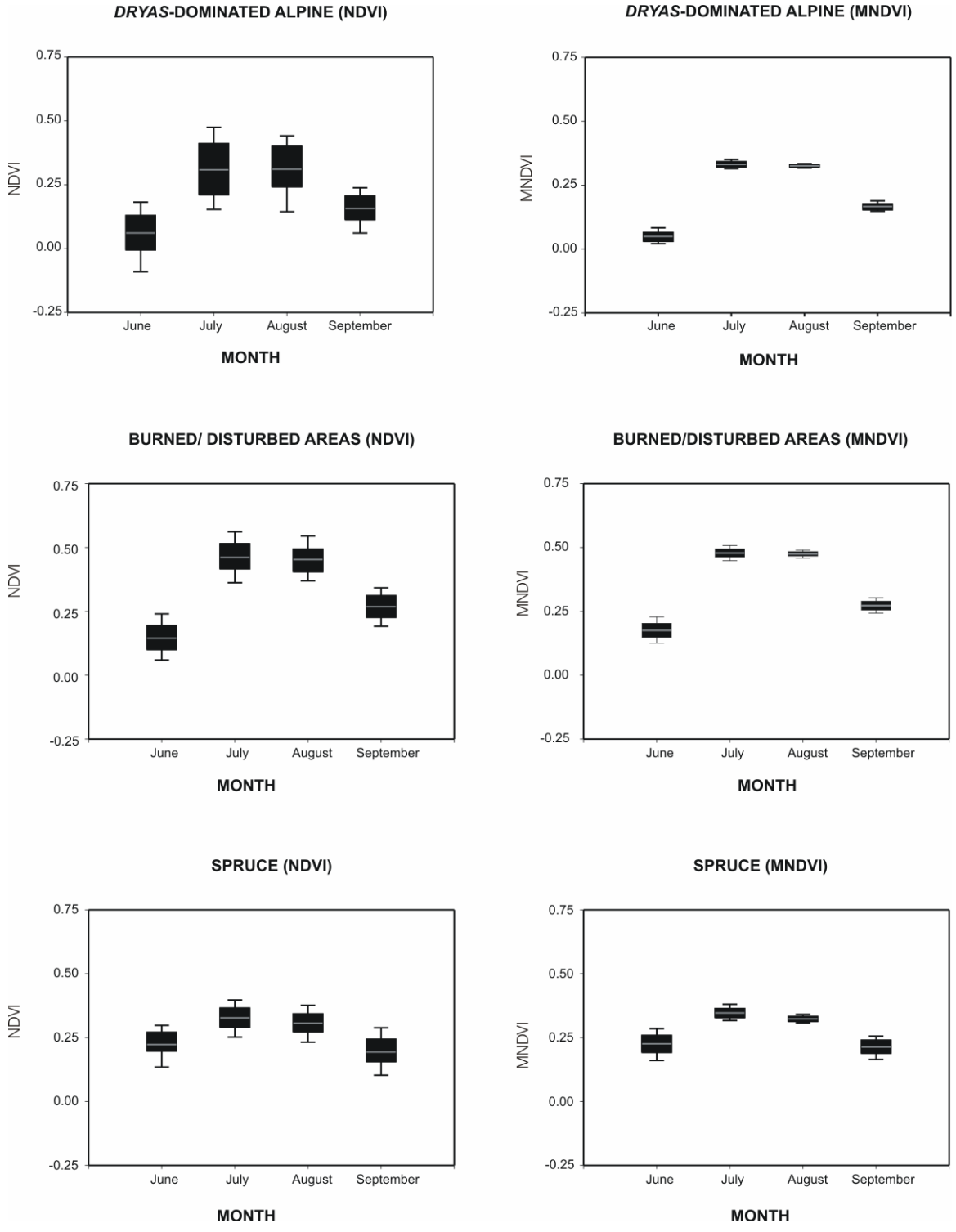


Figure 4.1. Time-series profiles of monthly Normalized Difference Vegetation Index (NDVI) and NDVI derived from multiple linear regression analysis (MNDVI) for three characteristic vegetation types (*Dryas*-dominated Alpine, Burned / Disturbed areas and Spruce) in the Greater Besa-Prophet Area, British Columbia, June-September, 2001.

landscape but skewed the distribution of each change image. These outliers were likely the result of changes in water levels in riparian areas, the influence of June snow in the spring image and the presence of increased terrain shadow in September, or pixels contaminated by cloud or haze that were not sufficiently masked, although the cause of other outliers was unidentifiable. Some extreme change values could have been the result of poor geometric registration of some pixels, but these areas were not obvious on the image. Many outliers were removed in the summer image by assigning a value of zero to negative NDVI values in each input image, which removed artificially inflated change values (NDVI values below zero are considered to be meaningless). Only the summer difference image became normal with this transformation; the spring and autumnal images were positively and negatively skewed, respectively.

Each vegetation type was assessed individually for normality in each difference image to determine if change thresholds could be applied at the class level. In the spring image, none of the coniferous classes were normally distributed. Outliers were trimmed from the data to determine if these data would become normal. Removal thresholds were derived empirically, but usually fell about the 5th and 95th percentile for each class. Pine and Low-productivity Spruce areas became normal with outliers removed, but Spruce and Riparian Spruce data could not be trimmed in this way. In the summer change image, only the Sub-alpine Spruce Transition class was normally distributed, but all other classes were normalized with the trimming of outliers. In the autumnal difference image, a similar pattern to the spring image was found: none of the coniferous classes but Pine were normally distributed and these

could not be trimmed to become normally distributed. All other (non-coniferous) classes except the Sub-alpine Spruce Transition class were normally distributed. All analysis of the monthly change in NDVI by class used the trimmed, normally distributed NDVI data for each class whenever possible. Where a normal distribution was not achieved, change was considered to be too highly variable to describe without error. The spatial distribution of change values in the NDVI dataset was usually without readily identifiable pattern. Most spatial associations were related to the distribution of change values across the landscape rather than within vegetation types.

*NDVI Image Differencing: Per-class Patterns*

The only classes that demonstrated an obvious spatial pattern when thresholds were applied were the Burned / Disturbed and Shrub classes in the spring change image. Shrub and Burned / Disturbed areas with change greater than one standard deviation from the mean were generally located higher than 1600m, and Shrubs with change greater than two standard deviations from the mean were almost exclusively found above this elevation. Figure 4.2 shows the difference images for each pair of dates.

*NDVI Image Differencing: Landscape Patterns*

There was a significant amount of data missing from each NDVI image because of clouds and cloud shadow making spatial patterns difficult to identify. The changes identified with image differencing, however, were more obvious across the

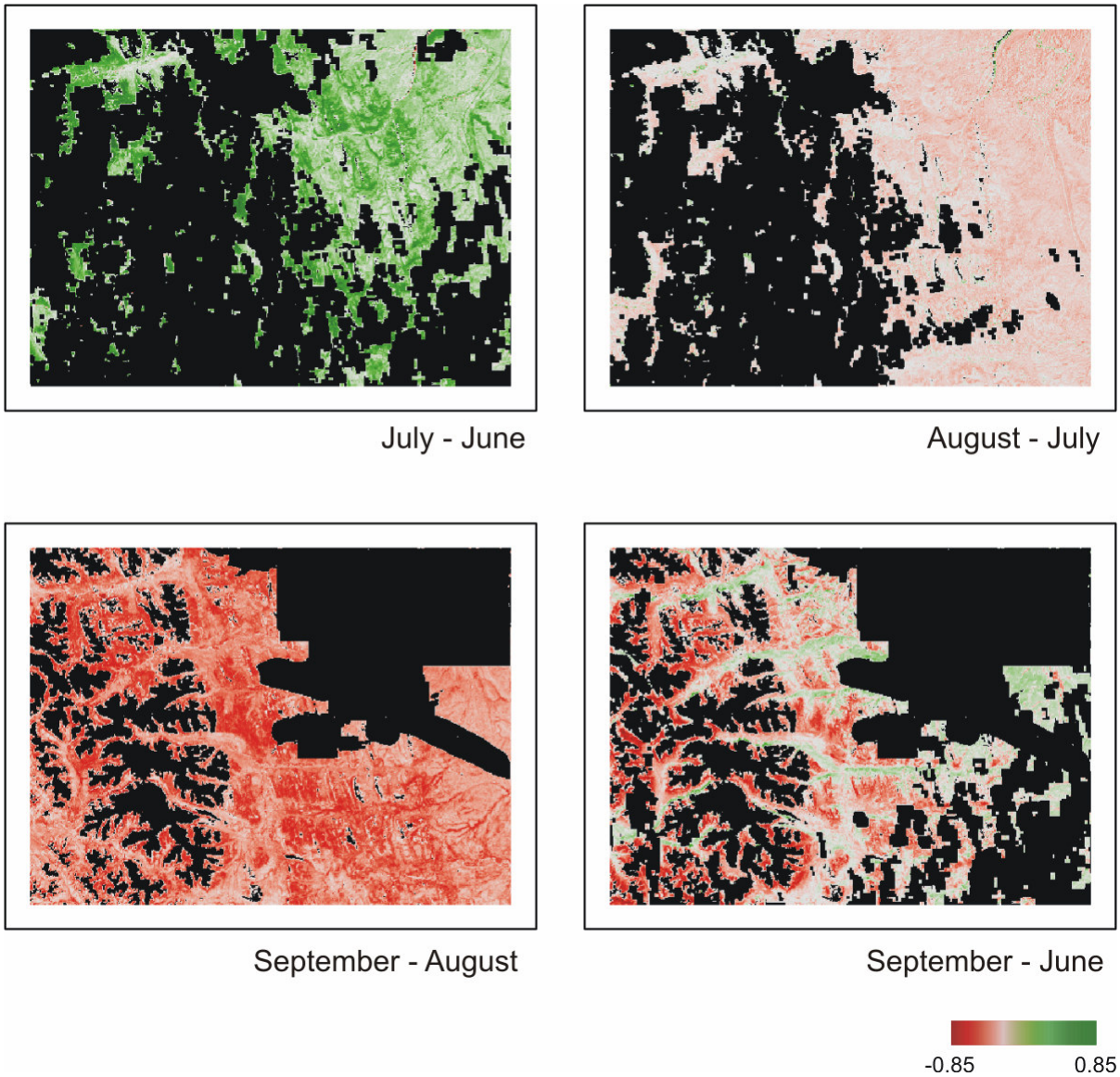


Figure 4.2. Normalized Difference Vegetation Index (NDVI) difference images for July-June, August-July, September-August and September – June, 2001 in the Greater Besa-Prophet Area of northern British Columbia. Areas of black indicate areas of cloud, cloud shadow, and non-vegetated areas.

landscape than within classes. In the spring image, most areas had positive change values and the highest positive values were related to elevation, although much of the Sikanni Chief Upland remained relatively constant (little positive or negative change). Areas of decrease were primarily pixels classified as Sedge-dominated Wetlands, while most of the constant areas in the Sikanni Chief Upland and throughout the Muskwa Foothills area were found in coniferous areas.

The continued increase in NDVI value for some Burned / Disturbed areas in the summer image was the most obvious pattern on the landscape for these months. There were also high values in some Sedge-dominated Wetland areas in the northwest corner of the study area. Negative change from August to September was obvious in the alpine and sub-alpine areas of the study area in the autumnal image. Most Burned / Disturbed areas decreased but retained high NDVI values in September and consequently showed the least change on the landscape.

The September-June difference images provided a considerable amount of information regarding the duration of vegetation activity. In the NDVI dataset, the coniferous areas in the Sikanni Chief Upland area, the Low-productivity Spruce class, some areas of Riparian Spruce and north-facing coniferous classes were negative, indicating these areas had higher NDVI values in June than in September. Other classes found on north-facing slopes such as Moist Alpine and Shrub areas were not consistently negative. Alpine and sub-alpine areas had the highest positive values, and much of the non-coniferous area below 1600m had values at or near zero, indicating that the vegetation was more productive in September than June.

Modelled Normalized Difference Vegetation Index (MNDVI)

Landscape and within-class differences in the MNDVI dataset were multi-modal or heavily skewed (Figures 4.3, 4.4, and 4.5). All change from June to July was positive, although there were two distinct groups of change evident in the MNDVI frequency histogram (Figure 4.3) Classes with higher change were the alpine classes, Burned / Disturbed areas, Moist Alpine, Sub-alpine Spruce Transition zone, and Shrub areas. All coniferous classes and the Sedge-dominated Wetlands increased, but considerably less than other classes. There was the least change between months in all classes between July and August in the MNDVI dataset, although there was a very small peak of positive values, representing Moist Alpine areas (Figure 4.4). This positive peak was not evident in the NDVI dataset.

All change in MNDVI data was negative from August to September, and there was no pattern evident in the output histogram (Figure 4.5). Coniferous areas had the least MNDVI change, while Shrub and Burned / Disturbed areas had the greatest difference, although each class was highly variable. The MNDVI dataset showed similar patterns to the NDVI dataset in the September-June difference image. Sub-alpine and alpine areas had the highest positive values, while many coniferous areas (particularly the Low-productivity Spruce class) had the lowest negative values. Not all coniferous areas were negative, however, and some coniferous areas (primarily spruce) on northerly slopes were positive or near zero. Figure 4.6 shows the output of the MNDVI differencing across the study area.

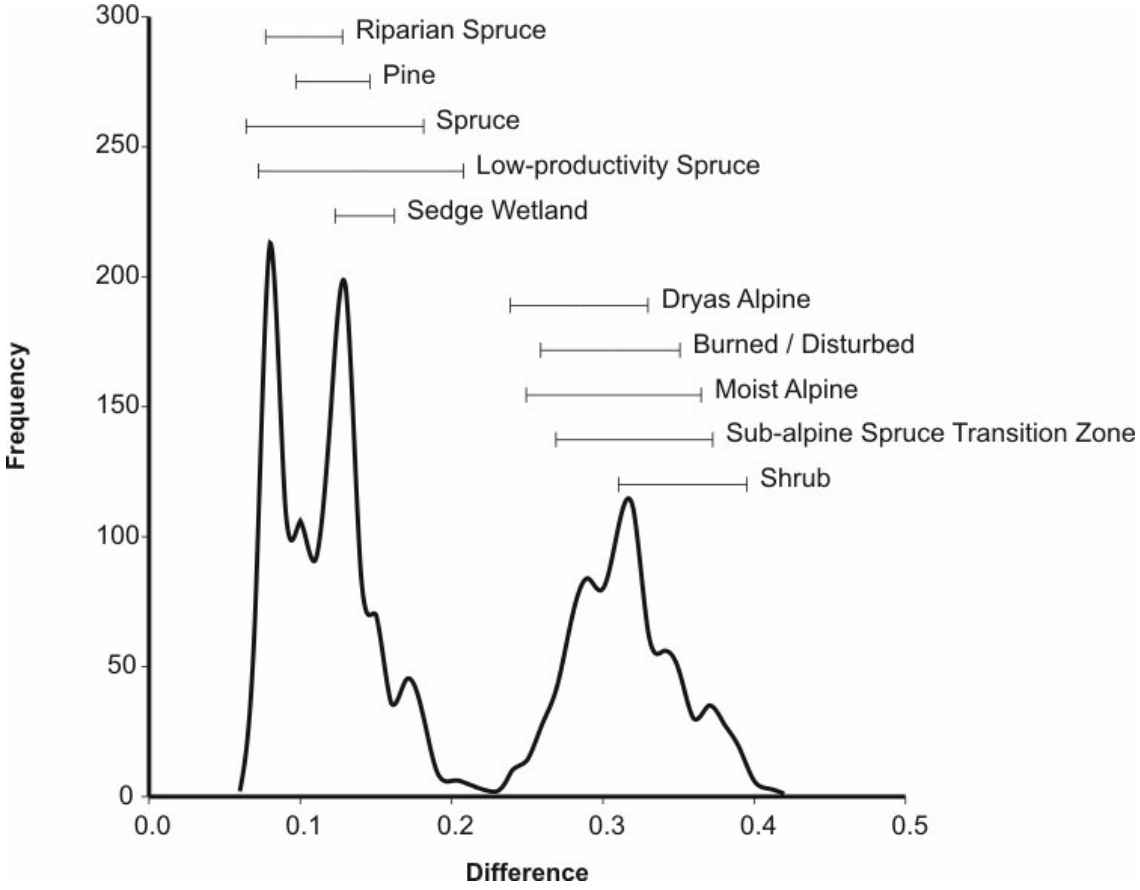


Figure 4.3. Frequency of NDVI derived from multiple linear regression analysis (MNDVI) change values and within-class ranges of change for the July-June, 2001 difference images of the Greater Besa-Prophet Area in northern British Columbia.

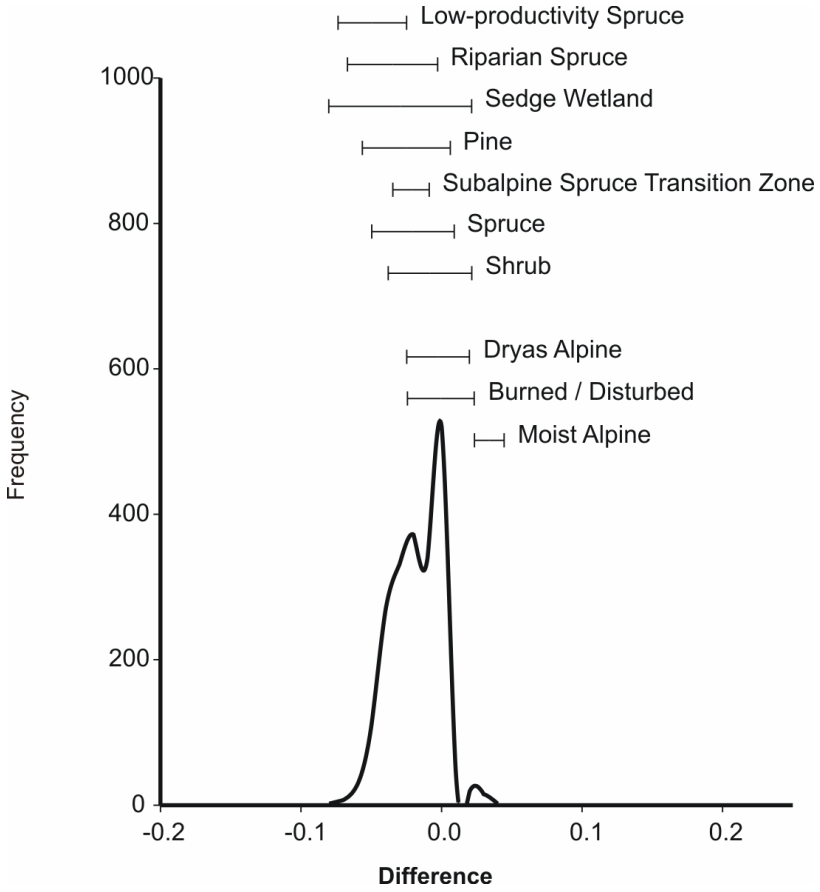


Figure 4.4. Frequency of NDVI derived from multiple linear regression analysis (MNDVI) change values and within-class ranges of change for the August-July, 2001 difference images of the Greater Besa-Prophet Area in northern British Columbia.

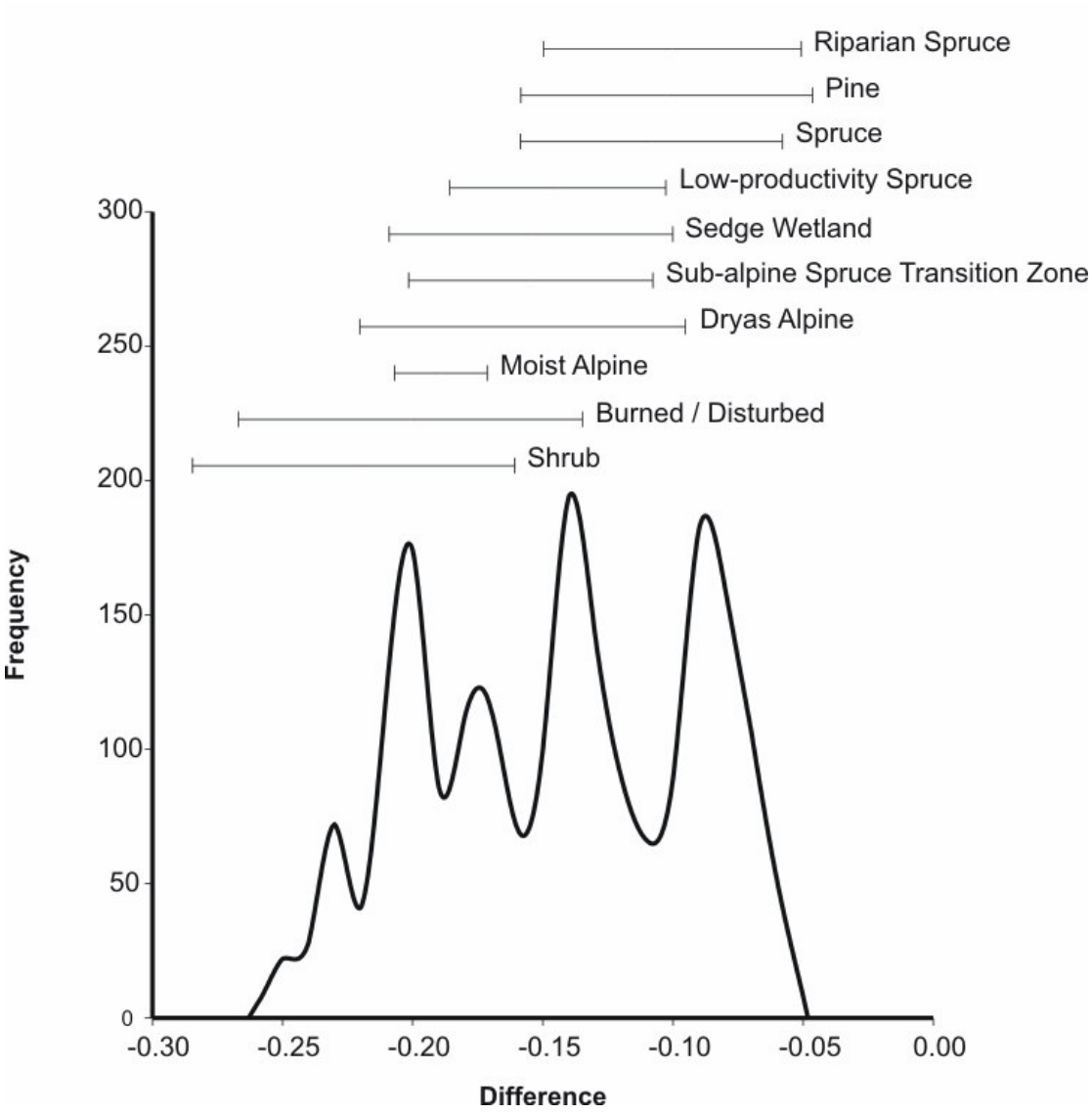


Figure 4.5. Frequency of NDVI derived from multiple linear regression analysis (MNDVI) change values and within-class ranges of change for the September-August, 2001 difference images of the Greater Besa-Prophet Area northern British Columbia.

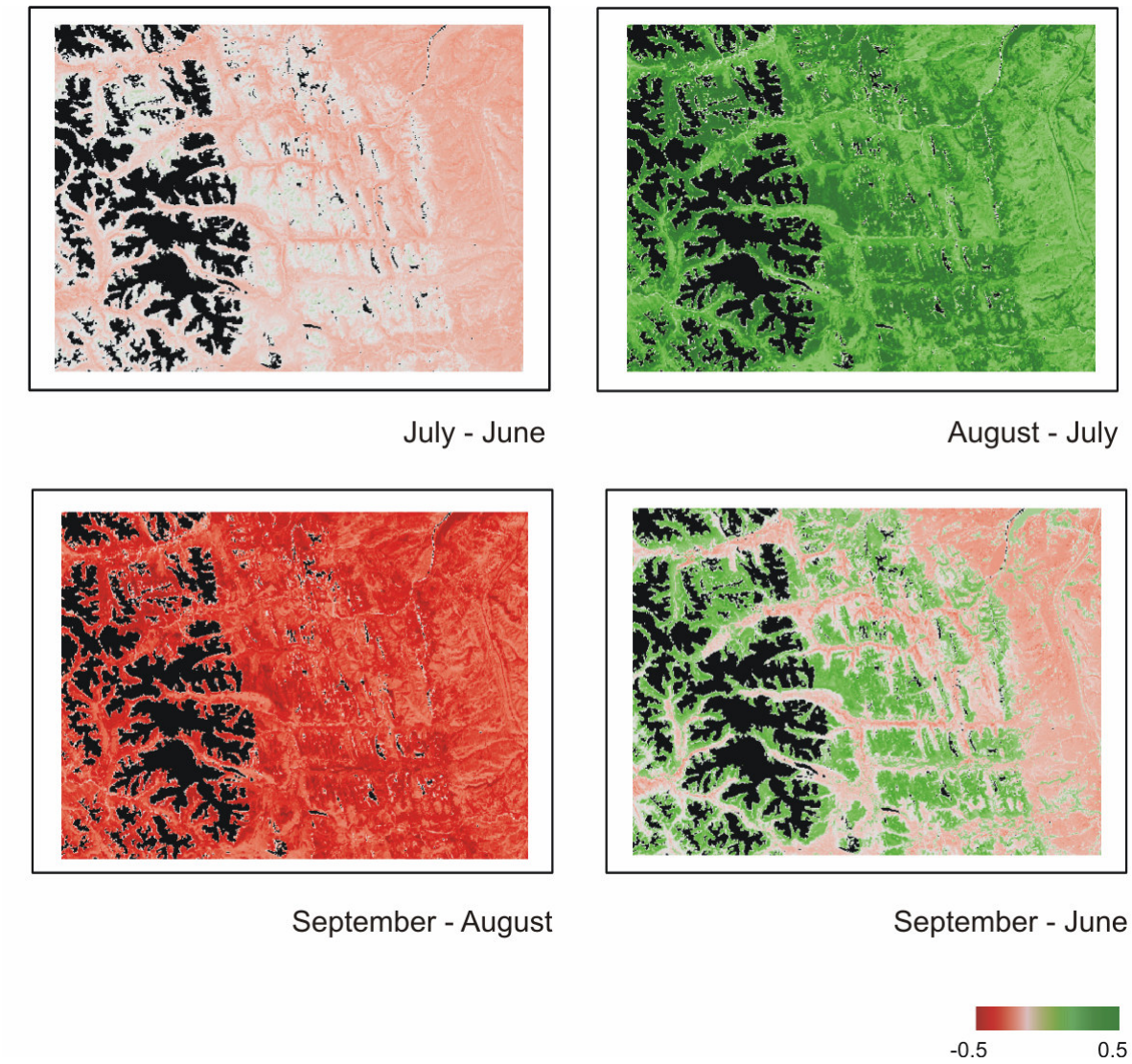


Figure 4.6. Difference images of NDVI derived from multiple linear regression analysis (MNDVI) for July-June, August-July, and September-August, 2001 in the Greater Besa-Prophet Area of northern British Columbia.

### *Standardized Principal Component Analysis*

Component images (Figure 4.7) and loadings (Table 4.3) were used to analyse outputs of all variations of the standardized principal component analysis (i.e., NDVI, MNDVI, MNDVI with masks, and regional SPCA of each subunit). All variations of the analysis identified very similar patterns of change across the landscape for June – September 2001. Although there were some differences between NDVI and MNDVI data, the relative order of the loadings of images in each component was the same for components 1-3, and similar for component 4. Most interpretation of the loadings and component images (Figure 4.7 and Table 4.3) was based on the MNDVI SPCA because these data had a continuous surface of values that was not broken by clouds. Components for radiance-masked MNDVI data were very similar to the landscape MNDVI, although there was less variation overall. Differences among each subunit of the GBPA (Sikanni Chief Upland, Muskwa Foothills and Muskwa Ranges) were nominal and did not merit discussion. Tables of loadings for all SPCA iterations can be found in Appendix H.

Component 1

PC1 explained 99.44% of the variation in MNDVI values for the four months analysed in 2001. Loading values were high and consistent for each input month, indicating that this component likely represented the spatial variability of the characteristic values (Eastman and Fulk 1993) that included topographic influence. On the landscape, the highest values for this component were found in Burned / Disturbed and Shrub areas. The lowest values were found in

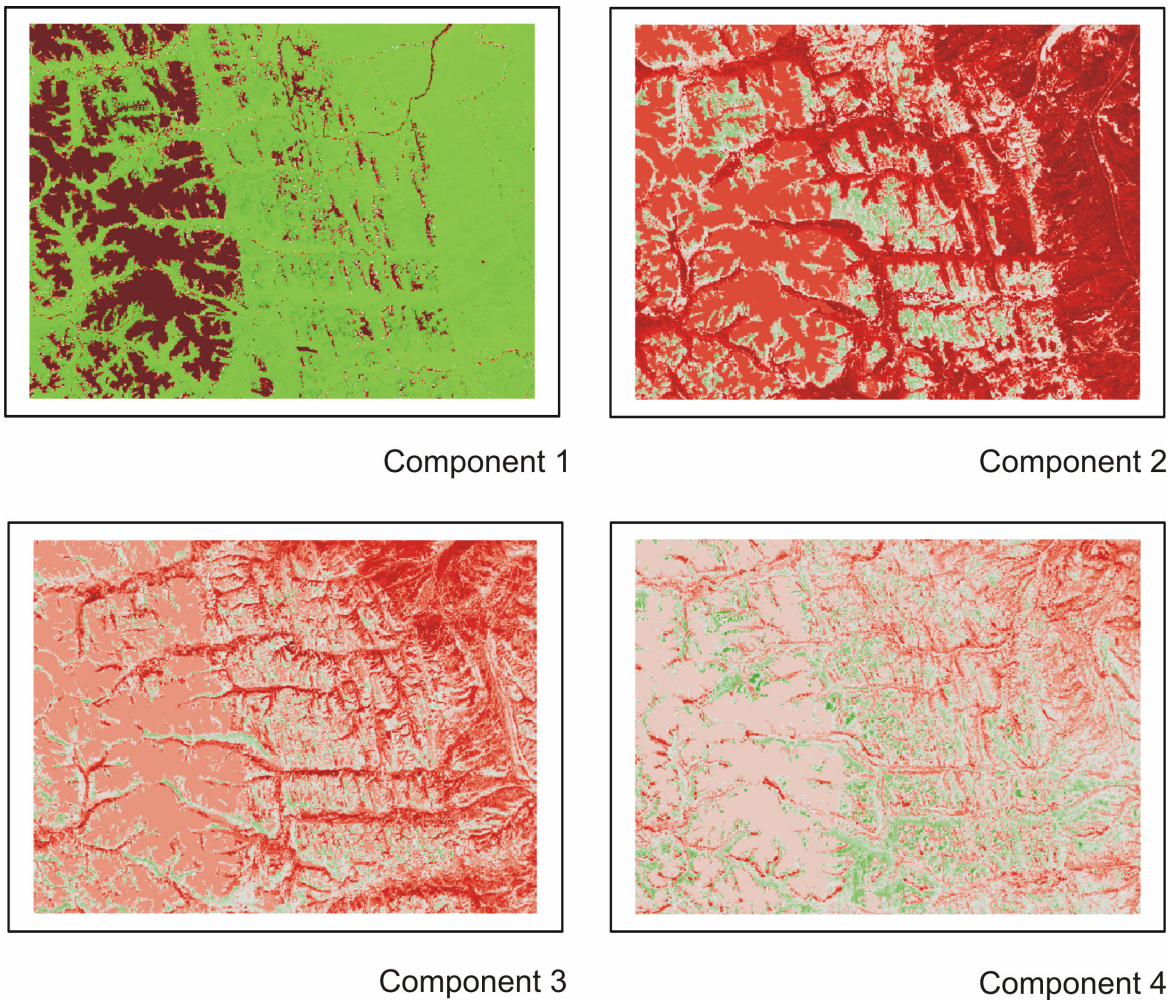


Figure 4.7. Standardized principal component (SPCA) images of near-monthly NDVI derived from multiple linear regression analysis (MNDVI) in the Greater Besa-Prophet Area of northern British Columbia, 2001. Images are displayed with a linear contrast stretch and dichromatic colour palette to maximize contrast between extreme values of the data.

Table 4.3. Loadings in each component of near-monthly NDVI derived from multiple linear regression analysis (MNDVI) in the Greater Besa-Prophet Area of northern British Columbia, 2001. Total % variation is the amount of variation in the dataset explained by each principal component over the four-month period (June – September).

| Image | Component 1 | Component 2 | Component 3 | Component 4 |
|---|---|---|---|---|
| **NDVI - with cloud masks** | | | | |
| Total % variation | **99.65** | **0.28** | **0.06** | **0.02** |
| June | 0.996 | -0.086 | -0.013 | 0.003 |
| July | 0.999 | 0.042 | -0.023 | -0.016 |
| August | 0.999 | 0.044 | -0.003 | 0.020 |
| September | 0.999 | -0.001 | 0.039 | -0.007 |
| **MNDVI - with NDVI cloud mask** | | | | |
| Total % variation | **99.84** | **0.15** | **0.01** | **0** |
| June | 0.998 | -0.063 | -0.005 | 0.001 |
| July | 0.999 | 0.025 | -0.007 | -0.005 |
| August | 0.999 | 0.037 | -0.004 | 0.005 |
| September | 0.999 | 0.001 | 0.017 | -0.001 |
| **MNDVI - no mask** | | | | |
| Total % variation | **99.44** | **0.52** | **0.03** | **0.01** |
| June | 0.993 | -0.118 | -0.010 | 0.002 |
| July | 0.999 | 0.047 | -0.014 | -0.010 |
| August | 0.998 | 0.069 | -0.008 | 0.010 |
| September | 0.999 | 0.001 | 0.032 | -0.001 |

the alpine classes, and the Moist Alpine class had slightly lower values than those of the *Dryas*-dominated Alpine areas. The influence of topography was obvious in this component image.

Component 2

PC2 explained only 0.52% of the variation in the MNDVI dataset. The loadings of this component suggested that it represents the difference between June and the summer images (July and August). As the MNDVI loading was slightly higher for August than July, this indicated that there was more variability explained by August, and the high positive values in the component image were more correlated with August than July in the MNDVI dataset.

The highest positive values in the MNDVI component two were found in shrub areas of the sub-alpine, followed by (from highest to lowest) Moist Alpine areas, the Sub-alpine Spruce Transition zone, *Dryas*-dominated Alpine areas and Burned / Disturbed areas (higher values increased with elevation), and low-elevation shrubs. The lowest negative values were found in Riparian Spruce classes, particularly in the Sikanni Chief Upland. Low-productivity Spruce and areas of Spruce on north and east-facing slopes had negative values closest to zero.

Component 3

The third principal component of the MNDVI dataset explained 0.03% of the variance in the dataset. The loadings for this component suggested that there was a positive relationship in September, with the other months contributing very little. Spatial patterns were more difficult to interpret, although positive values appeared to be

associated with the Sub-alpine Spruce Transition zone and Moist Alpine classes. High values were also associated with the coniferous classes, particularly Spruce and Pine on south and west-facing slopes. The lowest values were found in the Low-productivity Spruce class, followed by Shrubs with negligible aspect and Sedge-dominated Wetlands (particularly in the Sikanni Chief Upland).

Component 4

The fourth component of the MNDVI data explained the remaining 0.01% of the variance in the dataset. The loadings suggested that this component represented the difference between July and August. Although spatial patterns were difficult to interpret, the highest values were found in Moist Alpine areas, and the lowest values were found in the Sub-alpine Spruce Transition zone. Also obvious in this component were the influences of slope and aspect that were included in the June and September models, but not in July and August (see Chapter 3).

NDVI

Although the ranking of images in component two was similar for the NDVI dataset, August contributed less in the NDVI dataset than in the MNDVI dataset. Additionally, component two in the NDVI dataset explained only 0.28% of the variation in the dataset overall. There was more variation remaining in the fourth component in the NDVI dataset, although the contrast between July and August and to a lesser extent June and September was still evident.

## 4.4 DISCUSSION

The results for all change analyses were very similar for both the MNDVI and NDVI datasets. Inconsistencies were obvious: the number of significant differences between July and August in the vegetation profiles, the multi-modal MNDVI difference histograms, and the amount of variation remaining in higher components of the SPCA. Almost all differences could be attributed to the difference in variation between the MNDVI and NDVI datasets within each vegetation class. Because variation in NDVI on the landscape was explained with only a small number of inputs in the regression analysis, there were a limited number of potential output values in the MNDVI dataset and the variation was significantly reduced (see Chapter 3). The ratio of signal to noise that may confound change results using input datasets without radiometric correction (i.e., the NDVI dataset), however, may also be maximized in the MNDVI dataset for this reason. For the benefit of describing change in vegetation for the entire landscape, and providing general statements about the relative change in vegetative phenology with minimal radiometric distortion, the following synopsis of the change in vegetation phenology in the Greater Besa-Prophet area uses the MNDVI data wherever possible. Where the MNDVI and NDVI datasets did not agree, however, these differences are discussed.

### *Synopsis of results*

To interpret correctly the change in phenology of vegetation during the growing season of 2001 using Landsat TM and ETM+, all change detection methods must be considered together.

Spring

Although NDVI thresholds have been published that relate AVHRR NDVI values to the state of vegetation phenology in specific biomes, thresholds derived from finer resolution data such as TM and ETM+ might be more dependent on smaller-scale interactions of vegetation type, latitude, topography, and climatic variables because of the higher resolution of the data and the consequent increased variation among pixels. Therefore, thresholds are likely to be more scene-dependent than those developed for lower-resolution data. Additionally, it would not be appropriate to apply pre-determined thresholds to the MNDVI data, since these data were consistently higher and are considered relative, although they were highly correlated with original NDVI values (see Chapter 3). We did not have an image early enough in the season to provide a baseline of the lowest NDVI values, a precise estimate of the highest values from which to determine a threshold or the temporal resolution to identify when that threshold was surpassed. These temporal limitations and the lack of empirical data to support the selection of an onset threshold made estimates of the onset and duration of vegetation 'greenness' inappropriate.

Although it was not possible to determine the onset of photosynthetic activity and/or the significant accumulation of photosynthetic tissue for vegetation types in the GBPA, all types but the Moist Alpine class had some positive NDVI values by 4 June 2001. Classes were not uniformly positive; rather, all classes had some negative values in June. This indicated that onset of photosynthetic activity was not only

different among classes, but spatially dynamic within classes as well. All change detection methods also indicated that most vegetation classes experienced the major increase in values across the landscape after 4 June. The differences between June and September indicated that onset and duration of 'greenness' and/or rate of greenup was different among classes. Although some north-facing classes may have been affected by terrain shadow (i.e., coniferous classes on north-facing slopes), not all vegetation on north-facing slopes had negative values. It is likely that the influence of differential illumination was dependent on vegetation type, probably related to biomass and productivity differences between types.

Summer

There was little difference in vegetation 'greenness' between July and August for all classes, indicating that vegetation had reached peak by 22 July. As the exception, the Moist Alpine class followed a similar pattern to the other classes, but did not reach peak until August. There was more variability explained by August in principal component two than July, although the component was primarily the difference between June and the summer images (July and August).

Autumn

Changes between August and September 2001 were most difficult to interpret. Because all change from June to August was positive, it is obvious that vegetation in all classes was 'greening up' (e.g., accumulating biomass, increasing photosynthetic activity, etc). Conversely, all change from August to September in the MNDVI

dataset was negative, indicating that vegetation was nearing dormancy, reducing photosynthetic biomass.

Differences Among Vegetation Types

Coniferous areas and wetland classes had consistently lower values and lower amounts of change than other vegetation types. These classes remained constant or declined from June through the rest of the season. Decreases in Riparian areas may have been the result of increasing water levels due to seasonal melting of high-elevation snow packs through the summer and seasonal differences in rainfall. North and east-facing Spruce and Low-productivity Spruce areas experienced the least amount of change. Coniferous vegetation did not experience as much change as deciduous vegetation, although areas on south and west-facing slopes (that were more likely to have significant cover of vascular plants in the understory) experienced more change compared to similar areas on north and east-facing slopes. Areas in the sub-alpine and alpine regions (>1600m) showed higher positive change from June to July than other areas, and were the only areas that continued to increase from July to August on the landscape, although mean changes were not significantly higher.

All of the above analyses were limited to general comments about trends observed using each change detection method. In this way, we hoped to remove confounding factors from our understanding of change in vegetation across the GBPA landscape

and within vegetation types. As a result, some spatially-unique changes in vegetation that were not anomalous may not have not been identified.

### *Confounding Factors and Sources of Error*

NDVI Saturation

Because the NDVI asymptotically approaches saturation at high biomass densities (Mutanga and Skidmore 2004), its use as a direct measure of leaf area index or biomass is constrained. It was beyond the scope of this project, however, to measure directly these variables, or to differentiate between individual vegetation communities of the same vegetation class. Additionally, saturation might only be relevant for those areas with high biomass densities such as Burned / Disturbed areas and the Shrubs. In both datasets, Burned / Disturbed areas decreased between July and August, although not significantly, indicating that they remained relatively constant between the two months. This consistency could be related to saturation, but the temporal frequency of image dates would have had to be significantly increased to identify accurately a more precise 'peak' of NDVI values and to determine if characteristic NDVI was artificially asymptotic. At-canopy measurements would also be necessary to determine if NDVI saturation had occurred, or if vegetation had reached peak biomass. Many other vegetation types with relatively lower NDVI for the entire season also did not decrease significantly between these months, however, and, therefore, it is likely that the peak of vegetation growth in most areas fell between the 4 June and 22 July images.

Temporal Interval / Number of Inputs

The most significant limiting factor in this study was the number of input images used to assess the changes in seasonal phenology in the GBPA. The low temporal resolution of the data reduced our ability to estimate a precise 'peak' of vegetation biomass or photosynthetic activity, and it removed our ability to estimate a 'rate' of green-up or duration of growing season for 2001. Given the relative similarities between the changes in the NDVI and MNDVI datasets, the MNDVI dataset was believed to be a successful surrogate to clouded NDVI images. Consequently, more images could have been purchased to increase the temporal resolution of the data (i.e., clouded imagery originally deemed 'unsuitable' may have been successfully modelled to create cloud-free MNDVI data). Increasing the number of images may also have allowed us to detect anomalies in the rate of change from onset to peak 'greenness', particularly with SPCA. Anomalies, such as those related to weather events (i.e., summer snowfalls common in the GBPA) and their impacts may have been identified. This information could help to improve analysis of animal movements.

Topography / Decreasing Solar Angle

The behaviour of NDVI and MNDVI values for some classes did not suggest a systematic influence of decreasing solar illumination angle for spring and summer. For instance, the Moist Alpine class was found exclusively on northerly aspects (<90° and >270°) and was primarily in rugged terrain that may have been most susceptible to differential illumination. The general changes detected for this class

did not indicate contamination by differential illumination; the NDVI dataset indicated an increase in 'greenness' from June to July and no significant difference between July and August, despite the steady decrease in solar illumination angle for these months. Several other classes showed a similar pattern.

The autumnal difference image, however, included more contamination by differential illumination in September, and this must be considered when using the data. It is possible that the elevated loading for September in component three could have been indicative of differential illumination of slopes. This influence was most significant for areas of low relative NDVI, that is, in areas of high NDVI, the change in seasonal phenology was likely more significant than the differential illumination. This may also explain why some generally north-facing vegetation types had lower NDVI or MNDVI values in September while some retained higher values: the seasonal phenological characteristics of the plant (photosynthetic activity, biomass, etc.) overpowered the result of differential illumination for these types. Additionally, it was difficult to separate real differences that were the result of aspect from illumination differences (i.e., north-facing slopes generally have less productive vegetation communities than south-facing slopes), and it was also difficult to determine which strong negative values were the result of real changes in vegetation and which were anomalous. For instance, the low values of Sedge-dominated Wetlands were not likely the result of changing sun angle as these areas commonly have negligible slope. It is more likely that the low values of Sedge-dominated Wetlands reflected the decrease in NDVI or senescence of sedges in the Sikanni Chief Upland. Additional research should investigate whether a threshold of

NDVI value could be determined above which productivity and biomass offset illumination differences. For use of data from this study, the combined unknowns of the magnitude of topographic contamination of autumnal imagery and the difficult conceptualization of the relationship between plant death or dormancy and negative change values must be considered in analyses.

### *Conclusions and Considerations*

This research used Landsat TM and ETM+ to examine the major changes in plant phenology over one growing season. Many unknowns in this research could have been solved by collecting information about the change in phenology with ground measurements. These data could have been collected at the highest temporal resolution deemed necessary or feasible (i.e., samples could have been collected as often as logistically possible). The above results could then have been compared to the ground data. For instance, onset, rate, peak, and duration of vegetation growth could have been determined from ground data. Using these data, the near-monthly imagery could have been compared to the ground data to determine their relationship. This would validate all above results. Further research should also examine inter-year differences and their relationship to succession of plant communities (particularly in disturbed areas) and weather-related events including winter snow depth, date of snow melt and weather anomalies such as summer snowfalls. Additionally, more effort should be made to assess impairments to the radiometric quality of the original data that are the result of atmosphere, topographic variation, and differential illumination.

Despite the above limitations, this research has demonstrated that a significant amount of information can be derived from consecutive intra-season Landsat TM and ETM+ datasets about the relative changes in seasonal phenology. Although this information does not quantify changes in leaf area index or biomass, or their precise timing, it does provide information about the state of community-level vegetation in spring, summer and autumn. If these seasons can be related to some of the critical seasonal habitat requirements of large mammals (i.e., food availability), then these data may help to partially explain animal movements. The benefits of the spatial resolution of the data may outweigh the specific temporal limitations for wildlife studies.

## 4.5 LITERATURE CITED


Anyamba, A. and Eastman, J.R. (1996). Interannual variability of NDVI over Africa and its relation to El Niño/Southern Oscillation. *International Journal of Remote Sensing,* 17 (13): 253-2548.

Apps, C.D., NcLellan, B.N., Woods, J.G. and Proctor, M.F. (2004). Estimating grizzly bear distribution and abundance relative to habitat and human influence. *Journal of Wildlife Management,* 68(1):138-152.

Arthur, S.M., Manly, B.F.J, McDonald, L.L., and Garner, G.W. (1996). Assessing habitat selection when availability changes. *Ecology,* 77(1): 215-227.

Bannari, A., Morin, D., and Bonn, F. (1995). A review of vegetation indices. *Remote Sensing Reviews,* 13: 95-120.

Baret, F. and Guyot, G. (1991). Potentials and Limits of Vegetation Indices for LAI and APAR Assessment. *Remote Sensing of Environment,* 35: 161-173.

Billingsley, F.C. (1983). Data Processing and Reprocessing, in R.N. Colwell (Ed.). Manual of Remote Sensing, 2nd Edition, Vol. 1, (pp. 719-722). Falls Church, Virginia, USA: Sheridan Press.

Borak, J.S., Lambin, E.F., and Strahler, A.H. (2000). The use of temporal metrics for land cover change detection at coarse spatial scales. *International Journal of Remote Sensing,* 21: 1415-1432.

Boyce, M.S., Mao, J.S., Merrill, E.H., Fortin, D., Turner, M.G., Fyxell, J. and Turchin, P. (2003). Scale and heterogeneity in habitat selection by elk in Yellowstone National Park. *Ecoscience,* 10 (4): 421-431.

Byrne, G.F., Crapper, P.F., and Mayo, K.K. (1980). Monitoring land cover change by principal component analysis of multi-temporal Landsat data. *Remote Sensing of Environment,* 10 (3): 175-184.

Cameron, R.D., and Whitten, K.R. (1980). Nutrient dynamics of caribou forage on Alaska's Arctic Slope. In Reimers, E., Gaare, E., and Skjenneberg, S. (Eds.). Proceedings of the Second International Reindeer/Caribou Symposium, Roros, Norway, 1979.

Chen, X., Zhongjun, T., Schwartz, M.D., and Xu, C. (2000). Determining the growing season of land vegetation on the basis of plant phenology and satellite data in Northern China. *International Journal of Biometeorology,* 44: 97-101.

Cihlar, J., St.-Laurent, L., and Dyer, J.A. (1991). Relation between the normalized difference vegetation index and ecological variables. *Remote Sensing of Environment,* 35: 279-298.

Crist, E.P., and Cicone, R.C. (1984). A physically-based transformation of Thematic Mapper Data - the TM Tasseled Cap. *IEEE Transactions on Geoscience and Remote Sensing,* DE22 (3): 256-263.

Duchemin, B., Goubier, J. and Courrier, G. (1999). Monitoring phenological key stages and cycle duration of temperate deciduous forest ecosystems with NOAA/AVHRR data. *Remote Sensing of Environment,* 67: 68-82.

Eastman, J.R., and Fulk, M. (1993). Long sequence time series evaluation using standardized principal components. *Photogrammetric Engineering and Remote Sensing,* 59 (6): 991-996.

Eklundh, L; Singh, A. 1993. A comparative analysis of standardized and unstandardized principal components analysis in remote sensing. Int. J. Remote Sensing. 14(7): 1359-1370.

Franklin, S.E., Peddle, D.R., Dechka, J.A., and Stenhouse, G.B. (2002). Evidential reasoning with Landsat TM, DEM and GIS data for landcover classification in support of grizzly bear habitat mapping. *International Journal of Remote Sensing,* 23 (21): 4633-4652.

Fung, T., and E. LeDrew (1987). Application of principal components analysis to change detection. *Photogrammetric Engineering and Remote Sensing,* 53 (12): 1649-1658.

Griffith, B., Douglas, C., Walsh, N.E., Young, D., McCabe, T.R., Russell, D.E., White, G., Cameron, R.D., and Whitten, K.R. (2002). The Porcupine caribou herd. In Douglas, D.C., Reynolds, P.E., and Rhode, E.B. (Eds.) Arctic Refuge coastal plain terrestrial wildlife research summaries. U.S. Geological Survey, Biological Science Report USGS/BRD/BSR-2002-0001.

Groten, S.M.E., and Ocatre, R. (2002). Monitoring the length of the growing season with NOAA. *International Journal of Remote Sensing,* 23: 2797-2815.

Hall-Beyer, M. (2000). Principal components of NDVI time series as a technique to map Ecoregions: case study in Alberta, Canada. *Proceedings of the 22nd Annual Canadian Remote Sensing Symposium,* August 21-25, 2000).

Hall-Beyer, M. (2003). Comparison of single-year and Multiyear NDVI time series principal components in cold temperate biomes. *IEEE Transactions on Geoscience and Remote Sensing,* 41 (11): 2568-2574.

Hills, G.A., and G. Pierpoint, (1960). Forest Site Evaluation in Ontario. Ontario Department of Lands and Forests, Technical Series, Research Report No. 42. - Toronto, Ontario.

Hirosawa, Y., Marsh, S.E. and Kliman, D.H. (1996). Application of standardized principal component analysis to land-cover characterization using multi-temporal AVHRR Data. *Remote Sensing of Environment,* 58: 267-281.

Hoare, D. and Frost, P. (2004) Phenological description of natural vegetation in southern Africa using remotely-sensed vegetation data. *Applied Vegetation Science*, 7:19-28.

Huber, T.P., and Casler, K.E. (1990). Initial analysis of Landsat TM data for elk habitat mapping. *International Journal of Remote Sensing,* 11: 907-912.

Khorram, Siamak (ed.) (1999). Accuracy Assessment of Remote Sensing-derived change detection. Bethesda: American Society for Photogrammetry and Remote Sensing.

Jensen, J.R., (1996). Introductory Digital Image Processing: A Remote Sensing Perspective 2nd ed. Upper Saddle River: Prentice Hall, Inc.

Jepsen, J.U., Eide, N.E., Prestrud, P. and Jacobsen, L.B. (2002). The importance of prey distribution in habitat use by arctic foxes (Alopex *lagopus*). *Canadian Journal of Zoology,* 80: 418-429.

Johnson, C.J., Alexander, N.D., Wheate, R.D., and Parker, K.L. (2003). Characterizing woodland caribou habitat in sub-boreal and boreal forests. *Forest Ecology and Management,* 180: 241-248.

Johnson, C.J., Seip, D.R., and Boyce, M.S. (2004). A quantitative approach to conservation planning: using resource selection functions to map the distribution of mountain caribou at multiple scales. *Journal of Applied Ecology,* 41: 238-25.

Kaufmann, R.K., and Seto, K.C. (2001). Change detection, accuracy, and bias in a sequential analysis of Landsat imagery in the Pearl River Delta, China: econometric techniques. *Agriculture, Ecosystems and Environment,* 85: 95-105.

Lee, R. Yu, F., and Price, P. (2002). Evaluating vegetation phenological patterns in Inner Mongolia using NDVI time-series analysis. *International Journal of Remote Sensing,* 23 (12): 2505-2512.

Li, Z. and Kafatos, M. (2000). Interannual variability of vegetation in the United States and its relation to El Niño/Southern Oscillation. *Remote Sensing of Environment,* 71: 239-247.

Lobo, A., Ibanez Marti, J.J., and Gimenez-Cassina, C.C. (1997). Regional scale hierarchical classification of temporal series of AVHRR vegetation index. *International Journal of Remote Sensing,* 18 (15): 3167-3193.

Markon, C.J., Fleming, M.D., and Binnian, E.F. (1995). Characteristics of vegetation phenology over the Alaskan landscape using AVHRR time-series data. *Polar Record,* 31 (177): 179-190.

Mas, J.F. (1999). Monitoring land-cover changes: a comparison of change detection techniques. *International Journal of Remote Sensing,* 20 (1): 139-152.

McLoughlin, P.D., Case, R.L., Gau, R.J., Cluff, H.D., Mulders, R. and Messier, F. (2002). Hierarchical habitat selection by barren-ground grizzly bears in the central Canadian Arctic. *Oecologia,* 132: 102-108.

Mutanga, O., and Skidmore, A.K. (2004). Narrow band vegetation indices overcome the saturation problem in biomass estimation. *International Journal of Remote Sensing,* 25 (19): 3999-4014.

Nemani, R. and Running, S.W. (1997). Land cover characterization using multi-temporal red, near-IR, and thermal-IR data from NOAA/AVHRR. *Ecological Applications,* 7: 79-90.

Nielsen, S.E., Boyce, M.S., Stenhouse, G.B., and Munro, R.H.M. (2003). Development and testing of phenologically driven grizzly bear habitat models. *Ecoscience,* 10 (1): 2001.

Oindo, B.O. (2002). Predicting mammal species richness and abundance using multi-temporal NDVI. *Photogrammetric Engineering and Remote Sensing,* 68 (2): 623-629.

Osborne, P.E., Alonso, J.C., and Bryant, R.G. (2001). Modelling landscape-scale habitat use using GIS and remote sensing: a case study with great bustards. *Journal of Applied Ecology,* 38: 458-471.

Ott, R.L. (1993). An introduction to statistical methods and data analysis. 4th ed. Belmont: Wadsworth Inc.

Peet, R.K. (2000) Forests and Meadows of the Rocky Mountains. In Barbour, M.G. and Billings, W.D. (Eds.) North American Terrestrial Vegetation 2nd Ed. (pp 5-122). New York: Cambridge University Press

Price, K.P., Pyke, D.A. and Mendes, L. (1992). Shrub dieback in a semiarid ecosystem: the integration of remote sensing and GIS for detecting vegetation change. *Photogrammetric Engineering and Remote Sensing,* 58 (4): 455-463.

Purevdorj T.S, Tateishi, R., Ishiyamas, T., and Honda, Y. (1998). Relationships Between Percent Vegetation Cover and Vegetation Indices. *International Journal of Remote Sensing,* 19 (18): 3519-3535.

Rettie, W.J. and Messier, F. (2000). Hierarchical habitat selection by woodland caribou: its relationship to limiting factors. *Ecography,* 23: 466-478.

Richards, J.A. (1984). Thematic mapping from multi-temporal image data using the principal components transformation *Remote Sensing of Environment,* 16: 35-46.

Schwartz, M.D. and Reed, B.C. (1999). Surface phenology and satellite sensor-derived onset of greenness: an initial comparison. *International Journal of Remote Sensing,* 20: 3451-3457.

Suzuki, R., Nomaki, T. and Yasunari, T. (2003). West-east contrast of phenology and climate in northern Asia revealed using a remotely sensed vegetation index *International Journal of Biometeorology,* 47 (3): 126-138.

Tucker, C. J. and Sellers, P.J. (1986). Satellite remote sensing of primary productivity. *International Journal of Remote Sensing,* 7: 1395-1416.

Xin, J., Zhenrong, Y., van Leeuwen, L., Driessen, P.M. (2002). Mapping crop key phenological stages in the North China Plain using NOAA time series images *International Journal of Applied Earth Observation and Geoinfomation,* 4: 109-117.

Zhang, X., Friedl, M.A., Schaaf, C.B., Strahler, A.H., Hodges, J.C.F., Gao, F., Reed, B.C., and Huete, A. (2003). Monitoring vegetation phenology using MODIS. *Remote Sensing of Environment,* 84: 471-475.

# CHAPTER FIVE – USE OF LANDSAT TM AND ETM+ TO DESCRIBE INTRA-SEASON CHANGE IN VEGETATION WITH CONSIDERATION FOR WILDLIFE MANAGEMENT.

In this thesis, I have endeavored to characterize the vegetation of the Greater Besa-Prophet Area (GBPA) in northern British Columbia and to describe the distribution of gross changes in seasonal phenology using Landsat TM and ETM+. It was my overall objective to generate data that could be used in concurrent wildlife studies in the GBPA (using techniques developed for lower-spatial-resolution satellite data such as MODIS and AVHRR. The methods in this study provided a considerable amount of information about the distribution of the vegetation in the GBPA and the change in vegetation over one growing season, but users of the data must consider its creation, assumptions and limitations in order to interpret results and draw conclusions appropriately.

## 5.1 DATA ASSUMPTIONS AND LIMITATIONS

The following sections describe some of the most significant considerations of the data and information developed by the methods in this thesis by relating results and discussion from the previous three research chapters.

### *Topography and Decreasing Solar Angle*

Vegetation type (as defined in the 15-class supervised classification) was the best predictor of NDVI values for all months in the GBPA for 2001 (see Chapter 3). Although terrain variables increased the performance of some models, vegetation

type explained at least 52% (June, 2001) and as much as 86% (August, 2001) of the variation in NDVI values. Seasonal changes in NDVI and MNDVI are likely the result of variables related to vegetation change (i.e., phenology) and not extraneous factors related to terrain (i.e., elevation or differential illumination of slopes/aspects), but only at a relative scale (see Chapter 4). For instance, the vegetation profiles describe the mean differences among vegetation types in the GBPA. Image differencing described changes in each vegetation type relative to all others. Standardized principal component analysis identified sources of temporal variation and their distribution on the landscape. Each method identified gross changes on the landscape, but did not quantify change at the pixel level.

Topographic variation is inherent in vegetation distribution because vegetation type and its characteristics (i.e., density, productivity, leaf area etc.) are directly related to topographic position (Hills and Pierpoint 1960). Terrain variables were included in the classification scheme for this reason. Although the classification of vegetation types (Chapter 2) and the prediction of NDVI values in spring and autumn (Chapter 3) may have been aided by adding terrain variables, these may have also introduced or exacerbated topographic error. For instance, the derivatives added to the classification were included partly because they may have had less topographic variation than 'raw' TM bands. The final classification contained terrain-related errors, however, particularly shadowed areas (i.e., north-facing slopes) that were classified as rocks, even when they may have been at least partially vegetated. Additionally, although the Low-productivity Spruce class was found primarily on north-facing slopes, there is no way of checking whether the Spruce class was

erroneously classified as Low-productivity Spruce primarily because of its aspect (i.e., Spruce in shadow could have similar spectral characteristics to Low-productivity Spruce) without further investigation. Adding incidence to the classification might have negated the correction effects of derivatives despite increasing overall classification accuracy.

A similar circumstance occurred in the modelling procedures in Chapter 3. Topographic variables were used to predict NDVI in June, September and October 2001, because these helped to explain the variation in NDVI across the landscape. North-facing slopes were assigned lower values in the NDVI models because these areas had lower values in the original NDVI. South-facing slopes were assigned relatively higher values, but there was no way we could separate real differences of vegetation on north-facing slopes from terrain effect. In August, aspect was not a feature of the final models. Consequently, values differ on the basis of elevation and vegetation type only. In future studies similar to this research, it is important to realize that there may be a trade-off between increasing model success by adding terrain, and eliminating terrain from the model, which lowers overall correlation between original and modelled NDVI but increases the likelihood that the data is less contaminated. In the current study, overall adjusted $r^2$ for September using elevation and vegetation only (Table F4) was 0.787. The coefficients for aspect in the final (mapped) model (overall adjusted $r^2$=0.82) showed the greatest influence in north- and south-facing slopes. The increase in adjusted $r^2$ for the final September model may indicate that this model explained the variation in NDVI values more successfully than other models, but this variation may have been erroneous. Careful

consideration should be paid to correlation between terrain inputs and modeled data layers if these data are incorporated into resource selection functions. The ratio-based NDVI was not free of topography and this may have had several impacts (as discussed above) on interpretation of models. Further research should investigate the differences in results from models for September without the aspect variable.

### *Atmosphere*

Atmospheric differences among remotely-sensed imagery are considered a systematic error across the landscape within individual scenes. No atmospheric correction was applied to the input data because atmospheric interference was assumed inconsistent across the landscape and because several characteristics of the terrain of the study area and the nature of the study made common correction techniques inappropriate (see Chapter 3). This study provided general descriptive information regarding the relative seasonal change of several vegetation types, but not precise estimates of biomass, leaf area index, or productivity. Therefore, atmospheric influences are likely negligible.

### *Classification and Geometric Correction Errors, and Model Performance*

Pixels that were misclassified in the original vegetation classification and pixels not perfectly overlaying each other might have influenced the results of the change in vegetation greenness, particularly relative to NDVI. In the NDVI dataset, change was analysed per vegetation type. Erroneous pixels potentially could have quite different NDVI values, therefore changing the distribution of the NDVI data for the

vegetation type. These outliers should have been accounted for in the difference images with trimming. In the MNDVI dataset, vegetation class was a key indicator of vegetation 'greenness' (see Chapter 3) and the boundaries of each vegetation class determined the relative value assigned to each pixel; therefore, mis-classified pixels no longer contained 'greenness' values for their correct class, but rather for their assigned class. This may be advantageous statistically, as outliers would have been removed, but the MNDVI dataset was therefore reliant on the accuracy of the classification to delineate the boundaries of vegetation types for which MNDVI values were predicted. Because the change detection methods used the MNDVI data to provide spatially uniform information about the characteristics of vegetation throughout the growing season, these methods were dependent on the performance of the models. A good example of the magnitude of this dependency is the September-June subtraction used to estimate duration of greenness.

June models had the lowest model performance of 2001 (image to image $r^2$=0.608). This was less of a concern for the June to July comparison because the patterns of change were the same (all vegetation types in both datasets significantly increased) and there was a great amount of change between June and July. June and September values were more similar; therefore poorly modeled MNDVI values for June could have changed the relationship of June to September for some classes. Additionally, model performance was higher for September than June, although models may have been influenced by predictable differential illumination of slopes. Estimates of the duration of greenness, therefore, must consider these two limitations, which are entirely the result of the performance of each model.

### *Ground-truth Information*

Much of the above discussion may have been qualified with ground-truth data about the change in vegetation phenology in the GBPA – particularly on differing aspects. Ground-truthing may have helped to better separate phenology from systematic error. Furthermore, if the temporal resolution of the data could be increased with more favorable cloud cover conditions, or with a reconsideration of the usefulness of partial imagery given the relative success of the modelling techniques (see Chapter 3), ground research should be conducted to assess the accuracy of the changes identified using image profiles, image differencing, and standardized principal component analysis (Chapter 4). Ground research could provide information regarding the relationship between changes observed in Chapter 4 and change in vegetation on the ground, which would enable a more precise analysis of the change in NDVI and MNDVI.

## 5.2 USE OF THE DATA

The analyses of the change in vegetation phenology in the Greater Besa-Prophet Area were deliberately general and broad. Analysis at a finer scale would be inappropriate, considering potential impairments to radiometric quality, particularly in the NDVI dataset. The MNDVI dataset, however, provided information about the relative change in the phenology of vegetation in the GBPA. These data represented a ranking of pixels based on vegetation type and topographic position rather than a quantitative measurement of photosynthetic activity, productivity, leaf

area index or biomass. The MNDVI dataset, therefore, may be the most appropriate to be used in studies considering the relationship of phenology and the use of resources by various large mammal species. As inputs to resource selection functions, the MNDVI datasets make use of the difference in 'greenness' among vegetation communities while excluding some extraneous variation that could confound results of the selection functions. They do not, however, provide information for patches smaller than the minimum mapping unit of the supervised vegetation classification (0.6 ha). With some variations in data preparation methods and ground truthing, additional research could provide geographic information at a finer spatial scale.

Each of the change detection methods used in Chapter 4 suggests that each change detection method was adequate to describe changes in vegetation over the growing season, although only the difference images and principal component analysis provide information spatially. Because of the similarity of results between NDVI and MNDVI, the MNDVI data provide adequate information about the relative changes in vegetation in the GBPA and may not be as susceptible to outliers as the NDVI (Chapter 4). It is my suggestion therefore, that MNDVI be used in all subsequent use of the data (i.e., for wildlife management). Additionally, although data are similar, PC2 may be a more appropriate layer to define spatially spring green-up than the July-June difference image, because topographic variation may have been explained in PC1 and therefore reduced in PC2. To assess consistency among months, however, the difference images are adequate. MNDVI data should be used with the understanding that they are spatially delineated by the boundaries of the

original 15-class classification, and that the minimum mapping unit is therefore not equal to the original pixel size. If the above concerns regarding the use of the data are understood and incorporated, the methods used in this study are relevant for application in other areas. Although the nature of the results may change (e.g., variation explained by each principal component), this research suggests that methods developed for low-resolution sensors such as the AVHRR and MODIS are applicable to Landsat, and are useful in mountainous terrain despite some limitations.

## 5.3 LITERATURE CITED

Hills, G.A., and Pierpoint, G. (1960). Forest Site Evaluation in Ontario. Ontario Department of Lands and Forests, Technical Series, Research Report No. 42. - Toronto, Ontario.

**APPENDIX A: Post-classification modelling 'rules' developed for the maximum likelihood classification of the Greater Besa-Prophet Area in northern British Columbia.**

Table A1. Post-classification modelling 'rules' used to define the final 15 vegetation classes of the Greater Besa-Prophet Area in northern British Columbia.

| **Class** | **Model** |
|---|---|
| Riparian Spruce | & Slope > 10 = Spruce |
| Dryas-dominated Alpine | & ((Aspect >270) or (Aspect <90)) = Moist Alpine* |
| Moist Alpine | & ((Aspect <271) or (Aspect >89)) = Dryas-dominated Alpine* |
| Water | & Elevation >2500m = Snow/Glacier |
| Low-productivity Spruce | & ((Aspect <271) or (Aspect >89)) = Spruce |
| Sedge Wetland | & Slope > 10 = Shrub |
| All Vegetated Classes | & Elevation > 2500m = Rock |

* Applied in stages to avoid reversal of model logic

**APPENDIX B: Distribution and coordinates of all locations used to train and assess the accuracy of the maximum likelihood classification developed for the Greater Besa-Prophet Area in northern British Columbia.**

Figure B1. Distribution of all locations used to train and assess the accuracy of the final 15-class maximum likelihood classification developed for the Greater Besa-Prophet Area in northern British Columbia.

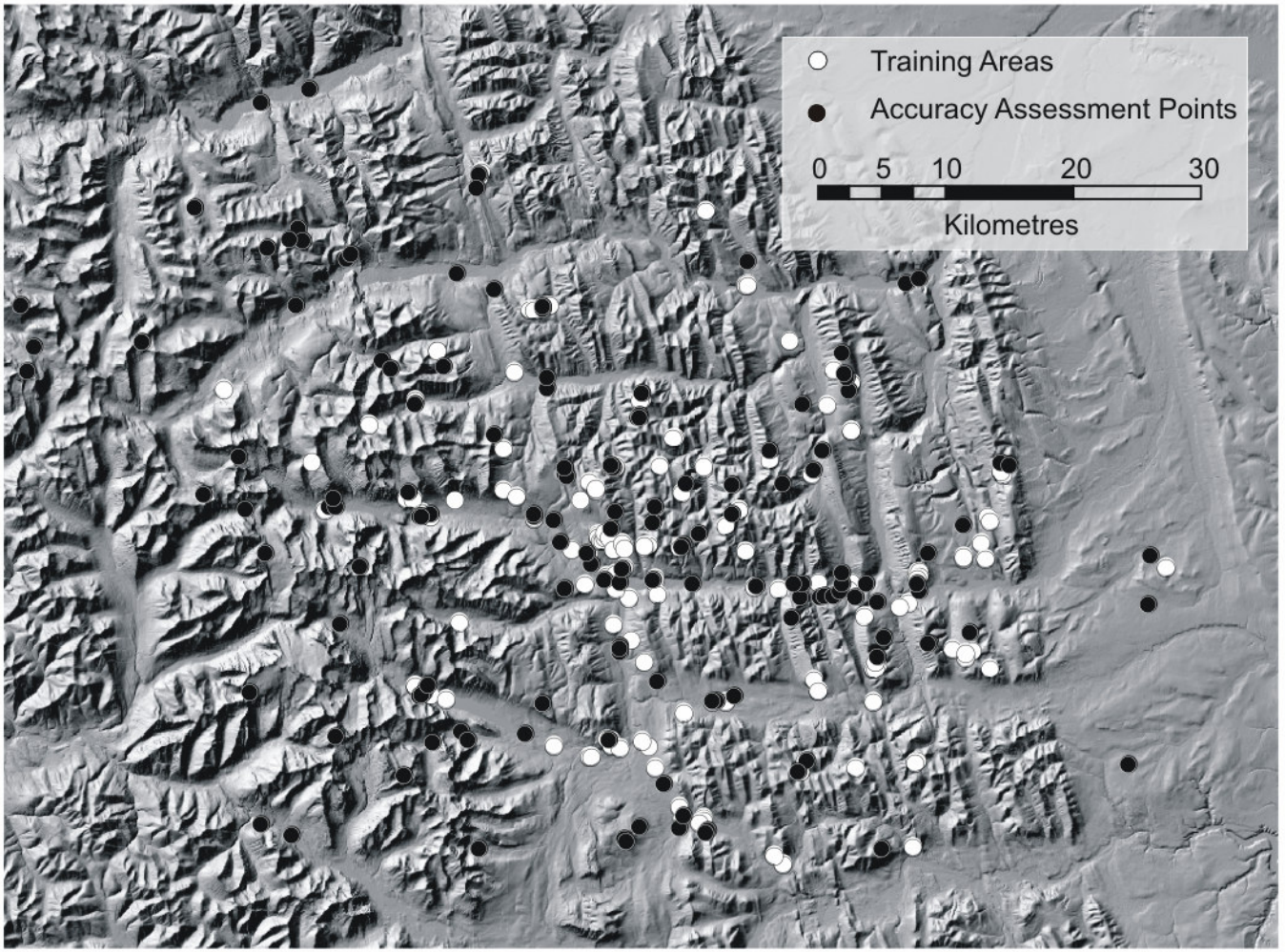

Table B1. Coordinates of all locations used to train 15-class maximum likelihood classification developed for the Greater Besa-Prophet Area in northern British Columbia. Spatial reference: UTM Zone 10N, NAD83.

| CLASS | EASTING | NORTHING |
|---|---|---|
| 1 | 459525 | 6353963 |
| 1 | 441849 | 6372183 |
| 1 | 441925 | 6372265 |
| 1 | 455460 | 6374036 |
| 1 | 455457 | 6374287 |
| 2 | 426304 | 6381986 |
| 2 | 460163 | 6366764 |
| 2 | 455700 | 6370440 |
| 2 | 455692 | 6370350 |
| 2 | 456155 | 6370668 |
| 2 | 437662 | 6379211 |
| 2 | 444739 | 6363778 |
| 2 | 455162 | 6353177 |
| 2 | 466687 | 6372486 |
| 2 | 454202 | 6373276 |
| 2 | 472927 | 6358262 |
| 2 | 484314 | 6368660 |
| 2 | 477262 | 6357408 |
| 2 | 484410 | 6360951 |
| 2 | 432170 | 6394620 |
| 2 | 462178 | 6348377 |
| 2 | 483495 | 6361607 |
| 2 | 446475 | 6399025 |
| 2 | 450575 | 6388275 |
| 2 | 449020 | 6383400 |
| 2 | 464680 | 6357430 |
| 2 | 480755 | 6367380 |
| 2 | 462114 | 6373821 |
| 2 | 463950 | 6375950 |
| 2 | 457318 | 6353785 |
| 2 | 472518 | 6359147 |
| 2 | 457098 | 6366381 |
| 2 | 475418 | 6366854 |
| 2 | 460462 | 6375979 |
| 2 | 484425 | 6361322 |
| 2 | 456567 | 6370368 |
| 2 | 457632 | 6369472 |
| 2 | 457112 | 6366248 |
| 3 | 457000 | 6367475 |
| 3 | 471587 | 6366427 |
| 3 | 469835 | 6366325 |
| 3 | 467964 | 6366373 |
| 3 | 475253 | 6366210 |
| 4 | 460333 | 6366006 |
| 4 | 474818 | 6367505 |
| 4 | 441887 | 6372157 |
| 4 | 441320 | 6358760 |
| 4 | 434256 | 6372476 |
| 4 | 473576 | 6380800 |
| 4 | 467341 | 6390297 |
| 5 | 467292 | 6390124 |
| 5 | 459549 | 6369764 |
| 5 | 477261 | 6360016 |
| 5 | 477526 | 6360173 |
| 5 | 477238 | 6360010 |
| 5 | 477455 | 6360063 |
| 5 | 469052 | 6376532 |
| 5 | 459353 | 6369594 |
| 5 | 465620 | 6371286 |
| 5 | 433141 | 6376191 |
| 5 | 476556 | 6364165 |
| 5 | 458059 | 6365552 |
| 5 | 457074 | 6375878 |
| 6 | 479305 | 6364847 |
| 6 | 456988 | 6375765 |
| 6 | 475743 | 6352344 |
| 6 | 486368 | 6360103 |
| 6 | 462040 | 6369620 |
| 6 | 461610 | 6378220 |
| 6 | 461576 | 6378170 |
| 7 | 477407 | 6360578 |
| 7 | 463865 | 6348317 |
| 7 | 463887 | 6348199 |
| 7 | 443812 | 6357687 |
| 7 | 463652 | 6347964 |
| 9 | 465571 | 6357559 |
| 9 | 454930 | 6353177 |
| 9 | 484260 | 6368870 |

Table B1. Continued

| CLASS | EASTING | NORTHING |
|---|---|---|
| 9 | 475485 | 6378690 |
| 9 | 456700 | 6354345 |
| 9 | 456679 | 6354000 |
| 9 | 461978 | 6349238 |
| 9 | 470214 | 6344640 |
| 9 | 449280 | 6373515 |
| 9 | 485647 | 6369853 |
| 9 | 474019 | 6383576 |
| 9 | 475398 | 6382476 |
| 9 | 475507 | 6378776 |
| 9 | 459041 | 6354388 |
| 9 | 486064 | 6368724 |
| 9 | 486196 | 6371917 |
| 9 | 486275 | 6371564 |
| 10 | 487469 | 6375230 |
| 10 | 446300 | 6398535 |
| 10 | 456290 | 6354477 |
| 10 | 456913 | 6369438 |
| 10 | 456910 | 6369445 |
| 10 | 487215 | 6375535 |
| 10 | 457571 | 6369890 |
| 10 | 440648 | 6373318 |
| 11 | 441200 | 6373324 |
| 11 | 467192 | 6390045 |
| 11 | 451825 | 6388615 |
| 11 | 463944 | 6375800 |
| 11 | 469368 | 6345347 |
| 11 | 452249 | 6353966 |
| 11 | 456798 | 6363436 |
| 11 | 458276 | 6362375 |
| 11 | 459268 | 6360504 |
| 11 | 462450 | 6356610 |
| 11 | 500152 | 6367919 |
| 11 | 479922 | 6365195 |
| 11 | 459241 | 6369750 |
| 11 | 470697 | 6385766 |
| 12 | 454570 | 6366708 |
| 12 | 460078 | 6367070 |
| 12 | 450704 | 6371850 |
| 12 | 441295 | 6358660 |
| 12 | 442450 | 6358020 |
| 12 | 442441 | 6372041 |
| 12 | 456273 | 6367295 |
| 13 | 472936 | 6358415 |
| 13 | 455609 | 6370520 |
| 13 | 454913 | 6374700 |
| 13 | 485037 | 6361489 |
| 13 | 450210 | 6388220 |
| 13 | 480710 | 6367760 |
| 13 | 480735 | 6367620 |
| 13 | 464130 | 6395945 |
| 14 | 448153 | 6377388 |
| 14 | 455822 | 6370115 |
| 14 | 455905 | 6370152 |
| 14 | 456109 | 6370382 |
| 14 | 471847 | 6352811 |
| 14 | 466674 | 6372506 |
| 14 | 480613 | 6352751 |
| 14 | 443120 | 6385000 |
| 14 | 471535 | 6351945 |
| 14 | 459038 | 6381056 |
| 14 | 467232 | 6369206 |
| 14 | 458851 | 6381132 |
| 15 | 480503 | 6352731 |
| 15 | 454966 | 6369052 |
| 15 | 457623 | 6367957 |
| 15 | 480670 | 6367110 |
| 15 | 472811 | 6366742 |
| 15 | 453622 | 6369361 |
| 15 | 444407 | 6373260 |
| 15 | 480286 | 6346076 |
| 15 | 472364 | 6375283 |
| 15 | 444479 | 6373269 |

Table B2. Coordinates of all locations used to assess the accuracy of the 15-class maximum likelihood classification developed for the Greater Besa-Prophet Area in northern British Columbia. Spatial reference: UTM Zone 10N, NAD83.

| CLASS | EASTING | NORTHING |
|---|---|---|
| 1 | 462070 | 6347486 |
| 1 | 465030 | 6357540 |
| 1 | 457345 | 6361876 |
| 1 | 484782 | 6362753 |
| 1 | 480740 | 6366195 |
| 1 | 463021 | 6366669 |
| 1 | 456200 | 6367050 |
| 1 | 455161 | 6368200 |
| 1 | 442528 | 6372116 |
| 1 | 453011 | 6375201 |
| 2 | 457685 | 6346673 |
| 2 | 451283 | 6357270 |
| 2 | 464570 | 6357440 |
| 2 | 466300 | 6357800 |
| 2 | 441990 | 6358120 |
| 2 | 457359 | 6361277 |
| 2 | 463627 | 6370520 |
| 2 | 440740 | 6373930 |
| 2 | 453156 | 6375000 |
| 2 | 432179 | 6394512 |
| 3 | 473138 | 6365603 |
| 3 | 471452 | 6365624 |
| 3 | 475816 | 6365635 |
| 3 | 473416 | 6365768 |
| 3 | 474077 | 6365834 |
| 3 | 474576 | 6366158 |
| 3 | 471745 | 6366564 |
| 3 | 474757 | 6366606 |
| 3 | 470984 | 6366608 |
| 3 | 451640 | 6381942 |
| 4 | 442226 | 6358600 |
| 4 | 435395 | 6363471 |
| 4 | 441697 | 6372016 |
| 4 | 434663 | 6372664 |
| 4 | 435206 | 6372731 |
| 4 | 441321 | 6380826 |
| 4 | 479767 | 6390337 |
| 4 | 480896 | 6390617 |
| 4 | 467433 | 6392023 |
| 4 | 433027 | 6405511 |

| CLASS | EASTING | NORTHING |
|---|---|---|
| 5 | 428069 | 6372510 |
| 5 | 487214 | 6376122 |
| 5 | 447610 | 6378360 |
| 5 | 458798 | 6379826 |
| 5 | 459078 | 6381731 |
| 5 | 435918 | 6392210 |
| 5 | 436342 | 6392547 |
| 5 | 432456 | 6393637 |
| 5 | 431422 | 6393700 |
| 5 | 446330 | 6398680 |
| 6 | 477569 | 6360931 |
| 6 | 481587 | 6362047 |
| 6 | 481688 | 6362063 |
| 6 | 462315 | 6369668 |
| 6 | 466170 | 6372229 |
| 6 | 470147 | 6374504 |
| 6 | 462613 | 6374662 |
| 6 | 469123 | 6377183 |
| 6 | 474843 | 6384689 |
| 6 | 429704 | 6393025 |
| 7 | 440403 | 6351665 |
| 7 | 435162 | 6354762 |
| 7 | 428362 | 6358162 |
| 7 | 436916 | 6368087 |
| 7 | 429670 | 6369031 |
| 7 | 424693 | 6373706 |
| 7 | 427468 | 6376643 |
| 7 | 410962 | 6383362 |
| 7 | 419962 | 6385687 |
| 7 | 410412 | 6388562 |
| 8 | 431622 | 6347030 |
| 8 | 429231 | 6347890 |
| 8 | 442631 | 6354206 |
| 8 | 449862 | 6354937 |
| 8 | 444931 | 6355018 |
| 8 | 498740 | 6365078 |
| 8 | 468056 | 6366537 |
| 8 | 411462 | 6385212 |
| 8 | 429217 | 6404482 |
| 8 | 446289 | 6346007 |

Table B2. Continued.

| VALUE | EASTING | NORTHING |
|---|---|---|
| 9 | 462299 | 6348561 |
| 9 | 497213 | 6352536 |
| 9 | 477606 | 6365198 |
| 9 | 481590 | 6369087 |
| 9 | 484220 | 6371311 |
| 9 | 452265 | 6371638 |
| 9 | 471615 | 6380800 |
| 9 | 475270 | 6381901 |
| 9 | 475079 | 6382845 |
| 9 | 474956 | 6383284 |
| 10 | 477853 | 6345897 |
| 10 | 457834 | 6346481 |
| 10 | 458910 | 6347703 |
| 10 | 456480 | 6354315 |
| 10 | 470804 | 6364019 |
| 10 | 453000 | 6366252 |
| 10 | 456680 | 6370919 |
| 10 | 487952 | 6375976 |
| 10 | 451306 | 6388132 |
| 10 | 451330 | 6388395 |
| 11 | 460832 | 6350968 |
| 11 | 445409 | 6354444 |
| 11 | 460349 | 6358978 |
| 11 | 478132 | 6362539 |
| 11 | 498895 | 6368895 |
| 11 | 452721 | 6369879 |
| 11 | 434931 | 6373345 |
| 11 | 473269 | 6377255 |
| 11 | 447573 | 6389820 |
| 11 | 446150 | 6397740 |
| 12 | 464224 | 6347382 |
| 12 | 457455 | 6361666 |
| 12 | 457313 | 6366746 |
| 12 | 459925 | 6366950 |
| 12 | 474786 | 6367556 |
| 12 | 450575 | 6371925 |
| 12 | 441900 | 6372050 |
| 12 | 450600 | 6372150 |
| 12 | 472614 | 6375562 |
| 12 | 444574 | 6391040 |
| 13 | 471959 | 6352784 |
| 13 | 481536 | 6361958 |
| 13 | 466165 | 6374334 |
| 13 | 453066 | 6375714 |
| 13 | 456700 | 6375715 |
| 13 | 456793 | 6375750 |
| 13 | 458898 | 6379897 |
| 13 | 443609 | 6383720 |
| 13 | 438750 | 6384202 |
| 13 | 423989 | 6396066 |
| 14 | 471369 | 6351892 |
| 14 | 462155 | 6369590 |
| 14 | 459866 | 6371516 |
| 14 | 457010 | 6372280 |
| 14 | 460135 | 6372691 |
| 14 | 466133 | 6374362 |
| 14 | 456677 | 6375916 |
| 14 | 458825 | 6379769 |
| 14 | 459168 | 6381672 |
| 14 | 439436 | 6383620 |
| 15 | 464048 | 6347091 |
| 15 | 441740 | 6357890 |
| 15 | 441805 | 6358015 |
| 15 | 442370 | 6358790 |
| 15 | 476626 | 6366584 |
| 15 | 480640 | 6366690 |
| 15 | 457525 | 6367840 |
| 15 | 454825 | 6369050 |
| 15 | 451730 | 6382910 |
| 15 | 432060 | 6388571 |

# APPENDIX C: Detailed descriptions of classes in the final maximum likelihood vegetation classification developed for the Greater Besa-Prophet Area in northern British Columbia

## SEDGE WETLAND 1

**General Description:**

The Sedge Wetland class is characterized by large open areas that have negligible slope and aspect and standing water for most months of the year. These areas are dominated by (*Carex aquatilis),* although willow (*Salix sp.*) shrubs can be found intermittently through some sites, particularly in transition areas to drier areas.

**Distribution:**

Sedge Wetlands are frequently found alternating with gravel bars along many rivers and creeks of the study area and surrounding lakes. They are also found in poorly drained areas of low elevation in the Sikanni Chief Upland.

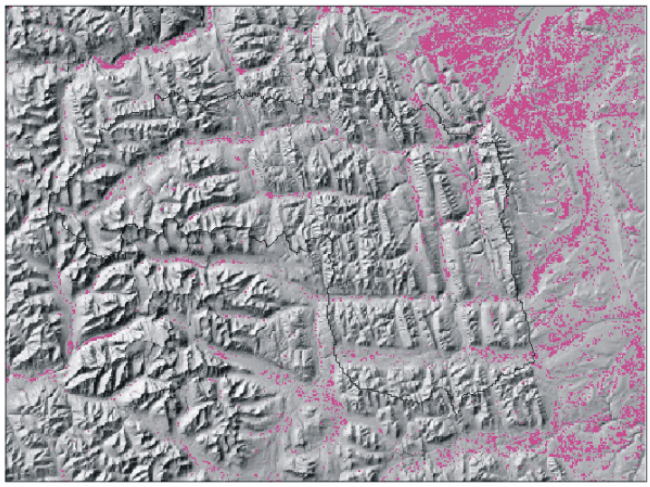

Figure C1. The Sedge Wetland class of the 15-class maximum likelihood classification developed for the Greater Besa-Prophet Area in northern British Columbia.

## DECIDUOUS SHRUB 2

**General Description:**

The Deciduous Shrub class represents areas dominated by willow (*Salix sp.*) and/or bog birch (*Betula glandulosa)* as well as those areas containing cinquefoil (*Potentilla fruticosa)* as a subordinate species. The dominance of the two species will alternate depending on micro-environmental features such as the drainage of the site. Cinquefoil appears in the driest sites - often at higher elevations, and other species such as soopolallie (*Sheperdia canadensis),* Labrador tea *(Ledum groenlandicum),* kinnikinnick *(Arctostaphylos uva-ursi),* lingonberry (*Vaccinium vitus-idae)* also occur but are rarely the dominant species.

**Distribution:**

This class is found throughout the study area: subalpine areas and high elevation valleys, river valleys with fair drainage, and wetlands (where it is often associated with the Sedge Wetland class). Distribution of species is not easily categorized by slope, aspect or elevation although bog birch and cinquefoil are more common at higher elevations.


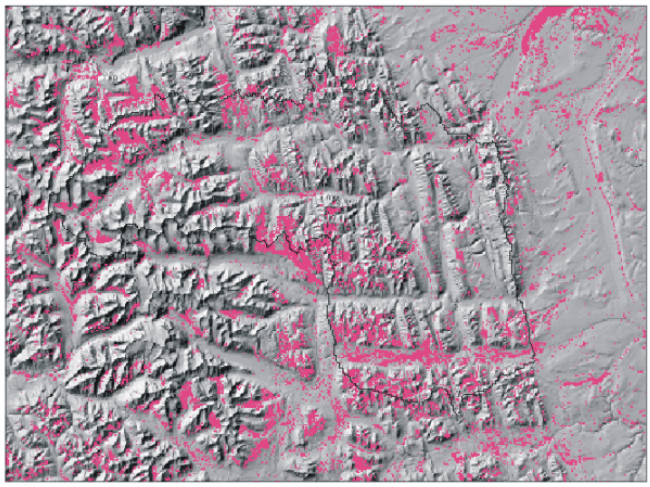

Figure C2. The Shrub class of the 15-class maximum likelihood classification developed for the Greater Besa-Prophet Area in northern British Columbia.

## LOW-PRODUCTIVITY SPRUCE 3

**General Description:**

Dominant species of the Low-productivity Spruce class is white spruce *(Picea glauca)*, although tree height, diameter and percent cover of trees are reduced compared to other coniferous classes. Vascular plants are infrequent in the understory; these are replaced by various moss species.

This class is also likely to represent spruce areas that have a limited understory (i.e., found on steep slopes where bare soil or rock replaces understory cover).

**Distribution:**

Low productivity Spruce is often found on northerly slopes along several river valleys in the study area, particularly the Muskwa Foothills.

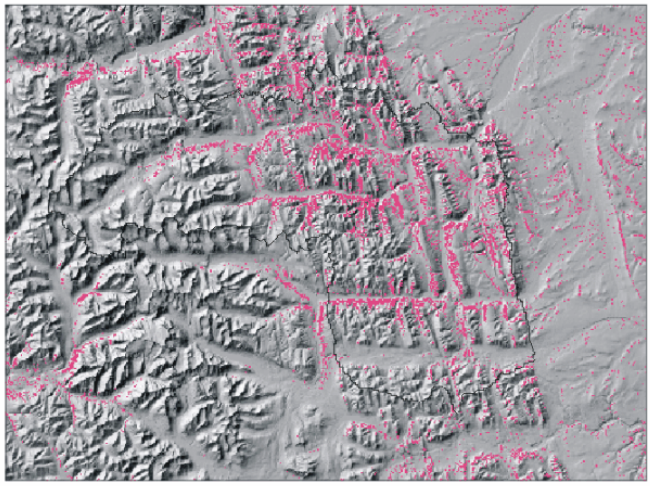

Figure C3. The Low-productivity Spruce of the 15-class maximum likelihood classification developed for the Greater Besa-Prophet Area in northern British Columbia.

## GRAVEL BAR 4

**General Description:**

Although generally non-vegetated, the Gravel Bar class may include Drummond's mountain avens *(Dryas drummondii)* or sparse willow.

**Distribution:**

Most gravel bars are found along rivers and streams, but the Gravel Bar class may also include dry stream beds. Many narrow areas of rivers have been classified as gravel bars; consequently, the gravel bar class is likely over represented in the classification. As water levels change throughout the season so will the actual ratio of water to gravel.

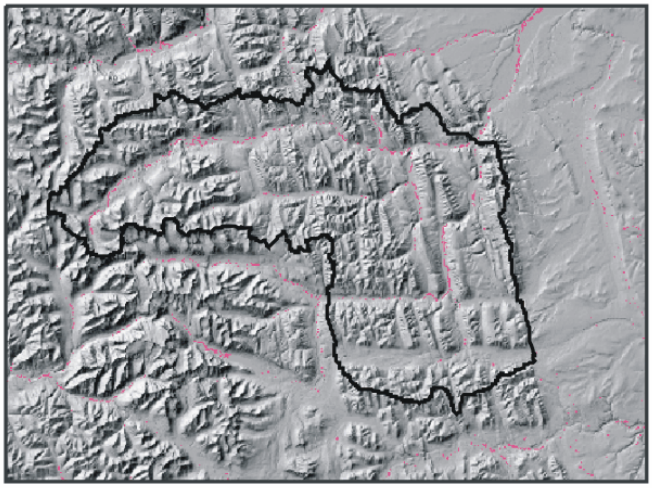

Figure C4. The Gravel Bar class of the 15-class maximum likelihood classification developed for the Greater Besa-Prophet Area in northern British Columbia.

## ROCK 5

**General Description:**

The Rock class includes areas of bedrock (such as those areas at elevations above vegetated alpine) as well as outcrops of talus. These areas have no significant lichen cover.

**Distribution:**

The bedrock type of this class can be found in the western portion of the study area - usually at elevations greater than 2000m. Talus slopes can be found frequently along slopes across the study area regardless of aspect or elevation.

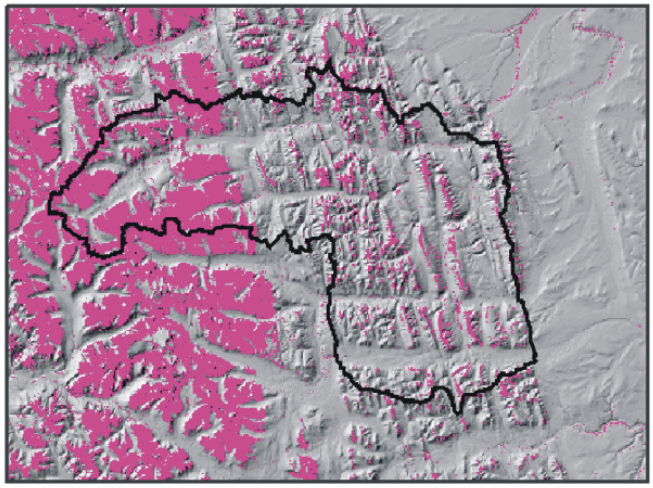

Figure C5. The Rock class of the 15-class maximum likelihood classification developed for the Greater Besa-Prophet Area in northern British Columbia.

## ROCK WITH CRUSTOSE LICHEN 6

**General Description:**

This class contains large broken boulders that have a significant cover of crustose lichens - particularly *Melanelia hepatizon* -often on steep slopes. Ridge tops and peaks that have these areas may alternate with the Moist Alpine class where soil cover is sufficient.

**Distribution:**

These areas are primarily found in the lower elevation slopes found between the high mountains and the eastern lowland area.

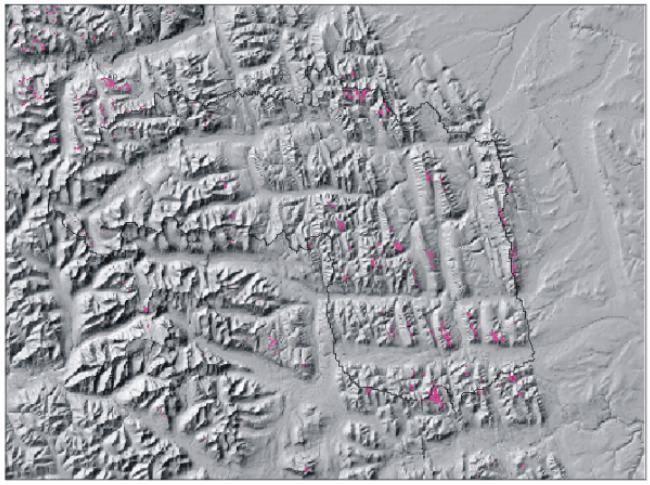

Figure C6. The Rock/Crustose Lichen class of the 15-class maximum likelihood classification developed for the Greater Besa-Prophet Area in northern British Columbia

**WATER** **7**

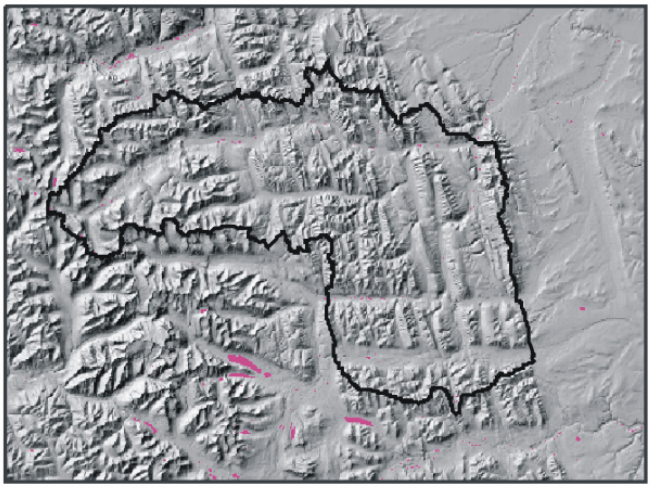

The water class includes rivers and lakes throughout the study area. Narrow rivers and creeks may be classified as gravel bars.

**SNOW** **8**

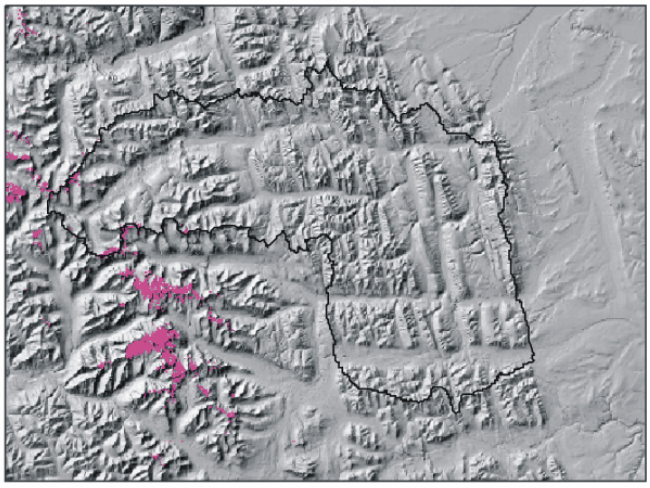

This class represents glaciers and snow present when the Landsat TM image was captured (August 2001). Percent cover of snow will change within and between years, but it is assumed that most temporary snow has melted by this date, leaving only permanent snow and ice.

Snow and glaciers are found above 2000m.

Figure C7. The Water and Snow classes of the 15-class maximum likelihood classification developed for the Greater Besa-Prophet Area in northern British Columbia.

## PINE 9

**General Description:**

The Pine class includes all areas of mature or growing *Pinus contorta.* Understory and percent cover vary. Three types of pine areas were encountered during field work:

1. Dry understory -significant amounts of lichen, some moss and scattered bog birch or willow shrubs. This type has limited percent cover of trees.
2. Shrub understory - understory is characterized by willow or soopolallie shrubs, often with high percent cover of fuzzy spiked wildrye.
3. Immature - understory is limited to moss species because of high stem density.

**Distribution:**

Pine is found throughout the study area. Slope, aspect (and consequently, the drainage of the site) and stand age are the primary determinants of understory type.




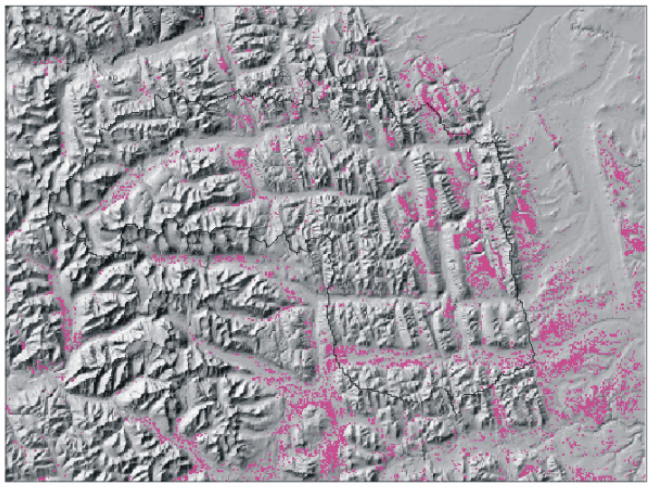

Figure C8. The Pine class of the 15-class maximum likelihood classification developed for the Greater Besa-Prophet Area in northern British Columbia

## SUB-ALPINE SPRUCE TRANSITION ZONE 10

**General Description:**

The Sub-alpine Spruce Transition Zone class represents the transition area between sub-alpine shrubs and forested areas at lower elevations. These areas are characterized by white spruce or fir (*Abies lasiocarpa)* trees with a percent cover that may be lower than that of the understory species (generally bog birch and/or willow.). Krummholz is often located in these areas and is included in this class.

**Distribution:**

This class is generally found in areas with elevations between 1400m and 1700m. This class represents a 'buffer' around the treeline, but is not uniformly distributed across the study area. In some areas, trees stop abruptly at areas of bare rock.

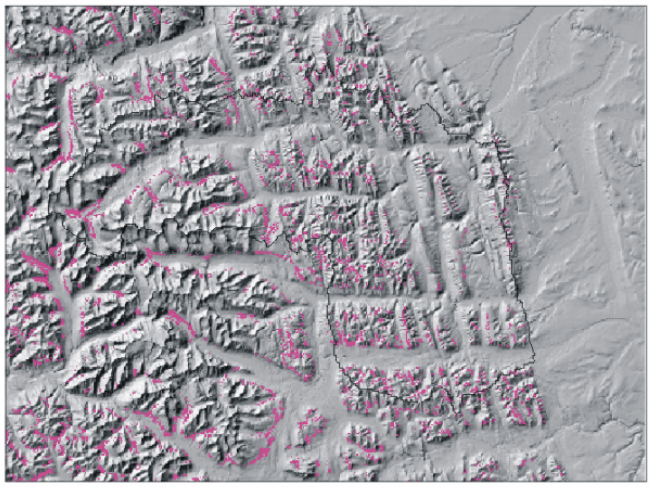

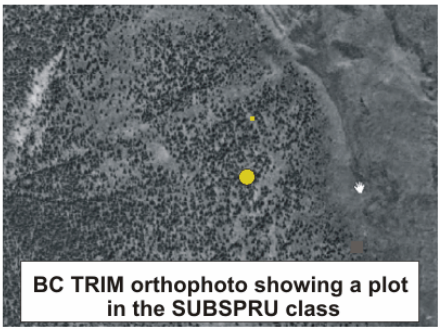


Figure C9. The Sub-alpine Spruce Transition Zone class of the 15-class maximum likelihood classification developed for the Greater Besa-Prophet Area in northern British Columbia.

## SPRUCE 11

**General Description:**

The Spruce class includes those areas dominated by mature white spruce or fir. Understory differences show gradients similar to that of the variations within the pine class, and will change with slope and aspect; however this class is generally dominated by shrubs (e.g., willow, bog birch, soopolallie, Labrador tea, kinnikinnick, and lingonberry) and grasses (e.g., fuzzy spiked wildrye).

**Distribution:**

This class is widespread in the study area, but does not include areas of riparian, sub-alpine or low-productivity spruce.

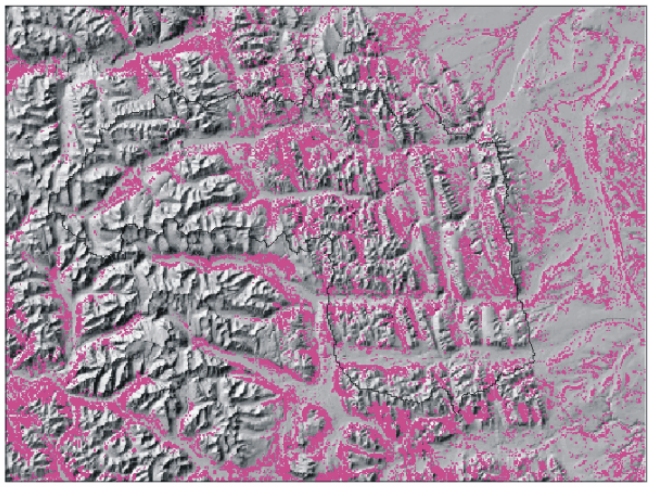

Figure C10. The Spruce class of the 15-class maximum likelihood classification developed for the Greater Besa-Prophet Area in northern British Columbia.

## RIPARIAN SPRUCE 12

**General Description:**

Riparian Spruce class is characterized by white spruce, but many trees are standing dead or are of limited height and diameter as compared to mature trees on better drained soils. These areas have a limited number of understory species, but may include willow shrubs or sedge, although dominant understory will vary by drainage and soil type. Percent cover of various moss species also appears to be dependent on frequency of flooding. This class may include black spruce *(P. Mariana)*, although white spruce is more common.

**Distribution:**

The Riparian Spruce class is most often associated with areas of predictable flooding or consistent standing water that have negligible slope or aspect. These areas are found along most rivers and creeks of the study area, including the wide floodplain areas to the west of Redfern Lake. This class also dominates the Eastern portion of the study area, where it alternates with the Sedge Wetland and Shrub classes.

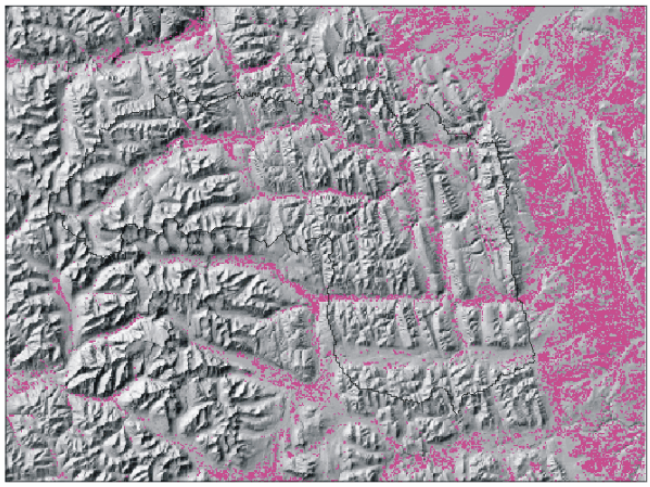

Figure C11. The Riparian Spruce class of the 15-class maximum likelihood classification developed for the Greater Besa-Prophet Area in northern British Columbia.

## DRYAS-DOMINATED ALPINE 13

**General Description:**

The dryas-dominated alpine class includes areas with a significant cover of mountain avens (*Dryas octopetala).* Fescue (*Festuca altaica)* and lupine (*Lupinus arcticus*) are generally found within this class, especially at lower elevations. Areas where fescue has a higher percent cover than mountain avens (i.e., alpine meadows) are included in this class. Lichen species are abundant and include (but are not limited to) the following: grey reindeer (*Clandina rangiferina),* rockworm (*Thamnolia vermicularis),* furled paperdoll (*Flavocetraria cucullata),* and baby finger *(Dactylina arctica).*

**Distribution:**

This class is generally located on southerly slopes at elevations above 1600-1700m, although it does occur at lower elevations on windswept slopes.

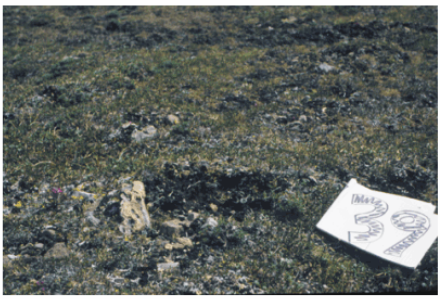

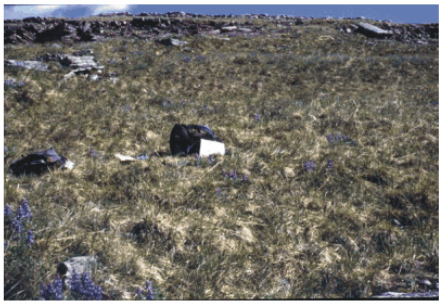

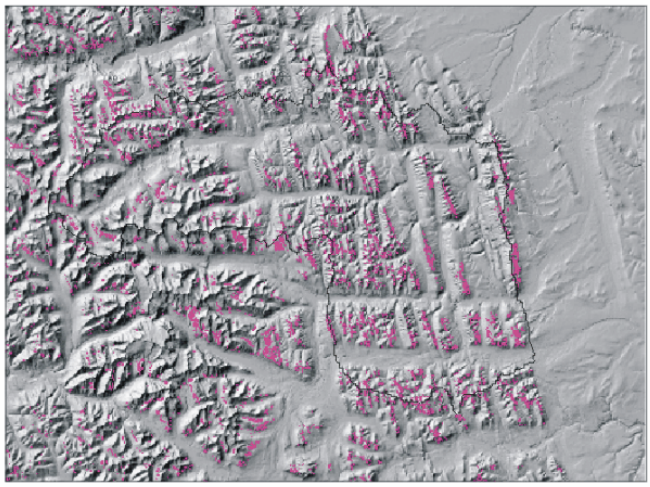

Figure C12. The *Dryas*-dominated Alpine class of the 15-class maximum likelihood classification developed for the Greater Besa-Prophet Area in northern British Columbia.

## MOIST ALPINE 14

**General Description:**

The moist alpine class is found on moist, cool slopes in the alpine of the study area. This class will usually be dominated by a variety of moss species such as step moss *(Mylocomium splendens)* and red-stemmed feathermoss *(Pleurozium schreberi),* and may also include *Cassiope tetragona and Carex sp.*

**Distribution:**

This class is found at similar elevations to the *Dryas*-domintated alpine class, however it generally occurs on more northerly aspects (360° - 45°) and in late snow melt areas.


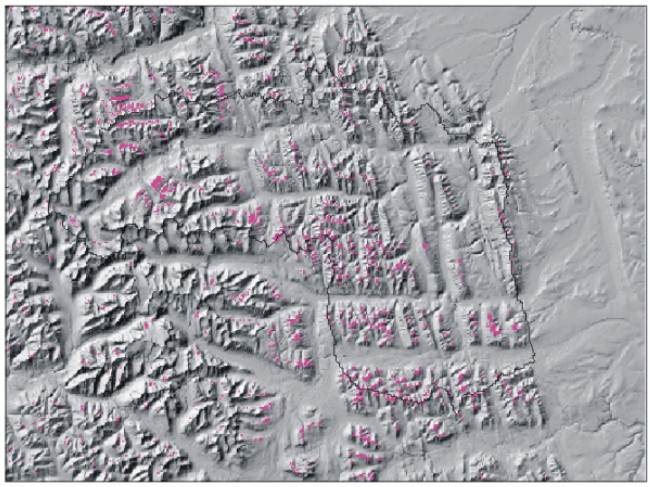

Figure C13. The Moist Alpine class of the 15-class maximum likelihood classification developed for the Greater Besa-Prophet Area in northern British Columbia.

## BURNED / DISTURBED 15

**General Description:**

This class includes burns, avalanche tracks and other disturbances that are at various stages of regrowth. These areas are generally dominated by *Elymus innovatus* and may have aspen (*Populus tremuloides)* or balsam poplar (*Populus balsamifera)* in the shrub (<2m) or tree (>2m) level, depending on the age of the disturbance. Some disturbed areas may be associated with the Pine class.

**Distribution:**

Most prescribed burning in the study area has occurred on south-facing slopes, consequently this class is primarily found on these slopes. This class covers a range of elevations and may reach sub-alpine and alpine areas.

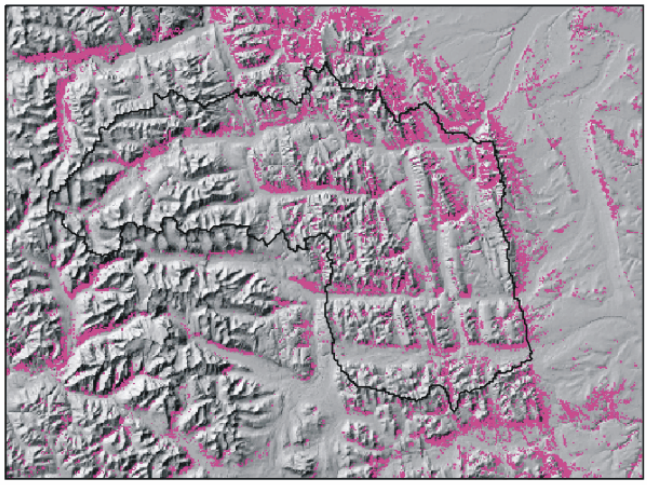

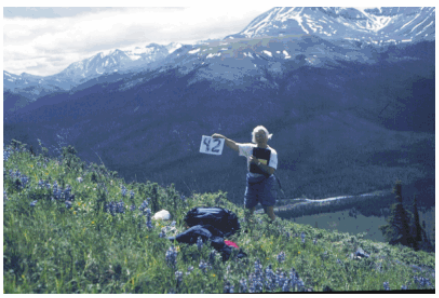

Figure C14. The Burned/Disturbed Area class of the 15-class maximum likelihood classification developed for the Greater Besa-Prophet Area in northern British Columbia.

**APPENDIX D: Confusion matrices and accuracy statistics of the maximum likelihood classifications developed for the Greater Besa-Prophet Area in northern British Columbia.**

Table D1. Confusion matrix of the 15-class maximum likelihood classification of the Greater Besa-Prophet Area in northern British Columbia. Inputs: TM bands 5, 4, 3, DEM, slope, angle of incidence. No filtration or modelling.

| | **REFERENCE** | | | | | | | | | | | | | | | |
|---|---|---|---|---|---|---|---|---|---|---|---|---|---|---|---|---|
| **CLASSIFIED** | **1** | **2** | **3** | **4** | **5** | **6** | **7** | **8** | **9** | **10** | **11** | **12** | **13** | **14** | **15** | **Total** |
| **1. Sedge Wetland** | 5 | 1 | 0 | 1 | 0 | 0 | 0 | 1 | 0 | 0 | 0 | 0 | 1 | 0 | 0 | 9 |
| **2. Shrub** | 2 | 7 | 0 | 0 | 0 | 0 | 0 | 0 | 0 | 2 | 0 | 0 | 0 | 1 | 2 | 14 |
| **3. Low-productivity Spruce** | 0 | 0 | 5 | 0 | 0 | 0 | 0 | 0 | 0 | 0 | 1 | 0 | 0 | 0 | 0 | 6 |
| **4. Gravel Bar** | 1 | 0 | 0 | 8 | 0 | 0 | 0 | 0 | 0 | 0 | 0 | 0 | 0 | 0 | 0 | 9 |
| **5. Rock** | 0 | 0 | 0 | 1 | 9 | 3 | 0 | 0 | 0 | 0 | 1 | 0 | 0 | 0 | 0 | 14 |
| **6. Rock / Crustose Lichen** | 0 | 0 | 0 | 0 | 0 | 7 | 0 | 0 | 0 | 0 | 0 | 0 | 1 | 0 | 0 | 8 |
| **7. Snow / Glacier** | 0 | 0 | 0 | 0 | 0 | 0 | 10 | 0 | 0 | 0 | 0 | 0 | 0 | 0 | 0 | 10 |
| **8. Water** | 0 | 0 | 0 | 0 | 0 | 0 | 0 | 9 | 0 | 0 | 0 | 0 | 0 | 0 | 0 | 9 |
| **9. Pine** | 1 | 0 | 1 | 0 | 0 | 0 | 0 | 0 | 5 | 0 | 1 | 1 | 0 | 0 | 0 | 9 |
| **10. Sub-alpine Spruce Transition** | 0 | 0 | 0 | 0 | 0 | 0 | 0 | 0 | 1 | 7 | 0 | 0 | 0 | 0 | 0 | 8 |
| **11. Spruce** | 0 | 0 | 1 | 0 | 0 | 0 | 0 | 0 | 4 | 0 | 5 | 0 | 0 | 0 | 0 | 10 |
| **12. Riparian Spruce** | 1 | 1 | 3 | 0 | 0 | 0 | 0 | 0 | 0 | 0 | 2 | 9 | 0 | 0 | 0 | 16 |
| **13. *Dryas*-dominated Alpine** | 0 | 1 | 0 | 0 | 1 | 0 | 0 | 0 | 0 | 0 | 0 | 0 | 7 | 5 | 0 | 14 |
| **14. Moist Alpine** | 0 | 0 | 0 | 0 | 0 | 0 | 0 | 0 | 0 | 0 | 0 | 0 | 1 | 4 | 0 | 5 |
| **15. Burned / Disturbed** | 0 | 0 | 0 | 0 | 0 | 0 | 0 | 0 | 0 | 1 | 0 | 0 | 0 | 0 | 8 | 9 |
| **Totals** | 10 | 10 | 10 | 10 | 10 | 10 | 10 | 10 | 10 | 10 | 10 | 10 | 10 | 10 | 10 | 150 |

Table D2. Accuracy Statistics of the 15-class maximum likelihood classification of the Greater Besa-Prophet Area in northern British Columbia. Inputs: TM bands 5, 4, 3, DEM, slope, angle of incidence. No filtration or modelling.

| | ***User's*** | ***Producer's*** | $\kappa$ |
|---|---|---|---|
| **Sedge Wetland** | 50.00% | 55.56% | 0.5238 |
| **Shrub** | 70.00% | 50.00% | 0.4643 |
| **Low-productivity Spruce** | 50.00% | 83.33% | 0.8214 |
| **Gravel Bar** | 80.00% | 88.89% | 0.881 |
| **Rock** | 90.00% | 64.29% | 0.6173 |
| **Rock / Crustose Lichen** | 70.00% | 87.50% | 0.8661 |
| **Snow / Glacier** | 100.00% | 100.00% | 1 |
| **Water** | 90.00% | 100.00% | 1 |
| **Pine** | 50.00% | 55.56% | 0.5238 |
| **Sub-alpine Spruce Transition** | 70.00% | 87.50% | 0.8661 |
| **Spruce** | 50.00% | 50.00% | 0.4643 |
| **Riparian Spruce** | 90.00% | 56.25% | 0.5312 |
| **Dryas-dominated Alpine** | 70.00% | 50.00% | 0.4643 |
| **Moist Alpine** | 40.00% | 80.00% | 0.7857 |
| **Burned / Disturbed** | 80.00% | 88.89% | 0.881 |
| | | | |
| **Overall Accuracy:** | | | **70.00%** |
| **Overall $\kappa$:** | | | **0.68** |

Table D3. Confusion matrix of the 15-class maximum likelihood classification of the Greater Besa-Prophet Area in northern British Columbia. Inputs: TM bands 5, 4, 3, DEM, slope, angle of incidence, and NDVI. No filtration or modelling.

| | **REFERENCE** | | | | | | | | | | | | | | | |
|---|---|---|---|---|---|---|---|---|---|---|---|---|---|---|---|---|
| **CLASSIFIED** | **1** | **2** | **3** | **4** | **5** | **6** | **7** | **8** | **9** | **10** | **11** | **12** | **13** | **14** | **15** | **Total** |
| **1. Sedge Wetland** | 5 | 1 | 0 | 1 | 0 | 0 | 0 | 0 | 0 | 0 | 0 | 1 | 1 | 0 | 0 | 9 |
| **2. Shrub** | 2 | 8 | 0 | 0 | 0 | 0 | 0 | 0 | 0 | 2 | 0 | 0 | 0 | 2 | 3 | 17 |
| **3. Low-productivity Spruce** | 0 | 0 | 6 | 0 | 0 | 0 | 0 | 0 | 0 | 0 | 2 | 0 | 0 | 0 | 0 | 8 |
| **4. Gravel Bar** | 1 | 0 | 0 | 8 | 0 | 0 | 0 | 0 | 0 | 0 | 0 | 0 | 0 | 0 | 0 | 9 |
| **5. Rock** | 0 | 0 | 0 | 1 | 10 | 4 | 0 | 0 | 0 | 0 | 0 | 0 | 0 | 0 | 0 | 15 |
| **6. Rock / Crustose Lichen** | 0 | 0 | 0 | 0 | 0 | 6 | 0 | 0 | 0 | 0 | 0 | 0 | 1 | 0 | 0 | 7 |
| **7. Snow / Glacier** | 0 | 0 | 0 | 0 | 0 | 0 | 10 | 0 | 0 | 0 | 0 | 0 | 0 | 0 | 0 | 10 |
| **8. Water** | 0 | 0 | 0 | 0 | 0 | 0 | 0 | 10 | 0 | 0 | 0 | 0 | 0 | 0 | 0 | 10 |
| **9. Pine** | 1 | 0 | 1 | 0 | 0 | 0 | 0 | 0 | 5 | 0 | 1 | 1 | 0 | 0 | 0 | 9 |
| **10. Sub-alpine Spruce Transition** | 0 | 0 | 0 | 0 | 0 | 0 | 0 | 0 | 0 | 7 | 0 | 0 | 0 | 0 | 0 | 7 |
| **11. Spruce** | 0 | 0 | 1 | 0 | 0 | 0 | 0 | 0 | 4 | 0 | 5 | 1 | 0 | 0 | 0 | 11 |
| **12. Riparian Spruce** | 1 | 0 | 2 | 0 | 0 | 0 | 0 | 0 | 1 | 0 | 2 | 7 | 0 | 0 | 0 | 13 |
| **13. *Dryas*-dominated Alpine** | 0 | 1 | 0 | 0 | 0 | 0 | 0 | 0 | 0 | 0 | 0 | 0 | 7 | 5 | 0 | 13 |
| **14. Moist Alpine** | 0 | 0 | 0 | 0 | 0 | 0 | 0 | 0 | 0 | 0 | 0 | 0 | 1 | 3 | 0 | 4 |
| **15. Burned / Disturbed** | 0 | 0 | 0 | 0 | 0 | 0 | 0 | 0 | 0 | 1 | 0 | 0 | 0 | 0 | 7 | 8 |
| **Totals** | 10 | 10 | 10 | 10 | 10 | 10 | 10 | 10 | 10 | 10 | 10 | 10 | 10 | 10 | 10 | 150 |

Table D4. Accuracy Statistics of the 15-class maximum likelihood classification of the Greater Besa-Prophet Area in northern British Columbia. Inputs: TM bands 5, 4, 3, DEM, slope, angle of incidence, and NDVI. No filtration or modelling

| | ***User's*** | ***Producer's*** | $\kappa$ |
|---|---|---|---|
| **Sedge Wetland** | 50.00% | 55.56% | 0.5238 |
| **Shrub** | 80.00% | 47.06% | 0.4328 |
| **Low-productivity Spruce** | 60.00% | 75.00% | 0.7321 |
| **Gravel Bar** | 80.00% | 88.89% | 0.881 |
| **Rock** | 100.00% | 66.67% | 0.6429 |
| **Rock / Crustose Lichen** | 60.00% | 85.71% | 0.8469 |
| **Snow / Glacier** | 100.00% | 100.00% | 1 |
| **Water** | 100.00% | 100.00% | 1 |
| **Pine** | 50.00% | 55.56% | 0.5238 |
| **Sub-alpine Spruce Transition** | 70.00% | 100.00% | 1 |
| **Spruce** | 50.00% | 45.46% | 0.4156 |
| **Riparian Spruce** | 70.00% | 53.85% | 0.5055 |
| **Dryas-dominated Alpine** | 70.00% | 53.85% | 0.5055 |
| **Moist Alpine** | 30.00% | 75.00% | 0.7321 |
| **Burned / Disturbed** | 70.00% | 87.50% | 0.8661 |
| | | | |
| **Overall Accuracy:** | | | **69.33%** |
| **Overall $\kappa$:** | | | **0.67** |

Table D5. Confusion matrix and of 15-class maximum likelihood classification of the Greater Besa-Prophet Area in northern British Columbia. Inputs: TM bands 5, 4, 3, DEM, slope, angle of incidence, and second principal component from the 6-band TM principal component analysis. No filtration or modelling.

| | **REFERENCE** | | | | | | | | | | | | | | | |
|---|---|---|---|---|---|---|---|---|---|---|---|---|---|---|---|---|
| **CLASSIFIED** | **1** | **2** | **3** | **4** | **5** | **6** | **7** | **8** | **9** | **10** | **11** | **12** | **13** | **14** | **15** | **Total** |
| **1. Sedge Wetland** | 4 | 0 | 0 | 1 | 0 | 0 | 0 | 1 | 0 | 0 | 0 | 0 | 1 | 0 | 0 | 7 |
| **2. Shrub** | 3 | 8 | 0 | 0 | 0 | 0 | 0 | 0 | 0 | 2 | 0 | 0 | 0 | 1 | 2 | 16 |
| **3. Low-productivity Spruce** | 0 | 0 | 5 | 0 | 0 | 0 | 0 | 0 | 0 | 0 | 1 | 0 | 0 | 0 | 0 | 6 |
| **4. Gravel Bar** | 1 | 0 | 0 | 8 | 0 | 0 | 0 | 0 | 0 | 0 | 0 | 0 | 0 | 0 | 0 | 9 |
| **5. Rock** | 0 | 0 | 0 | 1 | 9 | 3 | 0 | 0 | 0 | 0 | 1 | 0 | 0 | 0 | 0 | 14 |
| **6. Rock / Crustose Lichen** | 0 | 0 | 0 | 0 | 0 | 7 | 0 | 0 | 0 | 0 | 0 | 0 | 1 | 0 | 0 | 8 |
| **7. Snow / Glacier** | 0 | 0 | 0 | 0 | 0 | 0 | 10 | 0 | 0 | 0 | 0 | 0 | 0 | 0 | 0 | 10 |
| **8. Water** | 0 | 0 | 0 | 0 | 0 | 0 | 0 | 9 | 0 | 0 | 0 | 0 | 0 | 0 | 0 | 9 |
| **9. Pine** | 1 | 0 | 1 | 0 | 0 | 0 | 0 | 0 | 5 | 0 | 1 | 1 | 0 | 0 | 0 | 9 |
| **10. Sub-alpine Spruce Transition** | 0 | 0 | 0 | 0 | 0 | 0 | 0 | 0 | 1 | 6 | 0 | 0 | 0 | 0 | 0 | 7 |
| **11. Spruce** | 0 | 0 | 1 | 0 | 0 | 0 | 0 | 0 | 4 | 0 | 5 | 0 | 0 | 0 | 0 | 10 |
| **12. Riparian Spruce** | 1 | 1 | 3 | 0 | 0 | 0 | 0 | 0 | 0 | 0 | 2 | 9 | 0 | 0 | 0 | 16 |
| **13. *Dryas*-dominated Alpine** | 0 | 1 | 0 | 0 | 1 | 0 | 0 | 0 | 0 | 0 | 0 | 0 | 7 | 4 | 0 | 13 |
| **14. Moist Alpine** | 0 | 0 | 0 | 0 | 0 | 0 | 0 | 0 | 0 | 1 | 0 | 0 | 1 | 5 | 0 | 7 |
| **15. Burned / Disturbed** | 0 | 0 | 0 | 0 | 0 | 0 | 0 | 0 | 0 | 1 | 0 | 0 | 0 | 0 | 8 | 9 |
| **Totals** | 10 | 10 | 10 | 10 | 10 | 10 | 10 | 10 | 10 | 10 | 10 | 10 | 10 | 10 | 10 | 150 |

Table D6. Accuracy Statistics of the 15-class maximum likelihood classification of the Greater Besa-Prophet Area in northern British Columbia. Inputs: TM bands 5, 4, 3, DEM, slope, angle of incidence, and second principal component from the 6-band TM principal component analysis. No filtration or modelling.

| | ***User's*** | ***Producer's*** | $\kappa$ |
|---|---|---|---|
| **Sedge Wetland** | 40.00% | 57.14% | 0.5408 |
| **Shrub** | 80.00% | 50.00% | 0.4643 |
| **Low-productivity Spruce** | 50.00% | 83.33% | 0.8214 |
| **Gravel Bar** | 80.00% | 88.89% | 0.881 |
| **Rock** | 90.00% | 64.29% | 0.6173 |
| **Rock / Crustose Lichen** | 70.00% | 87.50% | 0.8661 |
| **Snow / Glacier** | 100.00% | 100.00% | 1 |
| **Water** | 90.00% | 100.00% | 1 |
| **Pine** | 50.00% | 55.56% | 0.5238 |
| **Sub-alpine Spruce Transition** | 60.00% | 85.71% | 0.8469 |
| **Spruce** | 50.00% | 50.00% | 0.4643 |
| **Riparian Spruce** | 90.00% | 56.25% | 0.5312 |
| **Dryas-dominated Alpine** | 70.00% | 53.85% | 0.5055 |
| **Moist Alpine** | 50.00% | 71.43% | 0.6939 |
| **Burned / Disturbed** | 80.00% | 88.89% | 0.881 |
| | | | |
| **Overall Accuracy:** | | | **70.00%** |
| **Overall $\kappa$:** | | | **0.68** |

Table D7. Confusion matrix and of 15-class maximum likelihood classification of the Greater Besa-Prophet Area in northern British Columbia. Inputs: TM bands 5, 4, 3, DEM, slope, angle of incidence, and third principal component from the 6-band TM principal component analysis. No filtration or modelling.

| | **REFERENCE** | | | | | | | | | | | | | | | |
|---|---|---|---|---|---|---|---|---|---|---|---|---|---|---|---|---|
| **CLASSIFIED** | **1** | **2** | **3** | **4** | **5** | **6** | **7** | **8** | **9** | **10** | **11** | **12** | **13** | **14** | **15** | **Total** |
| **1. Sedge Wetland** | 5 | 1 | 0 | 1 | 0 | 0 | 0 | 0 | 1 | 0 | 0 | 0 | 1 | 0 | 0 | 9 |
| **2. Shrub** | 2 | 7 | 0 | 0 | 0 | 0 | 0 | 0 | 0 | 2 | 0 | 0 | 0 | 1 | 1 | 13 |
| **3. Low-productivity Spruce** | 0 | 0 | 6 | 0 | 0 | 0 | 0 | 0 | 0 | 0 | 1 | 0 | 0 | 0 | 0 | 7 |
| **4. Gravel Bar** | 1 | 0 | 0 | 8 | 0 | 0 | 0 | 0 | 0 | 0 | 0 | 0 | 0 | 0 | 0 | 9 |
| **5. Rock** | 0 | 0 | 0 | 1 | 10 | 3 | 0 | 0 | 0 | 0 | 1 | 0 | 1 | 0 | 0 | 16 |
| **6. Rock / Crustose Lichen** | 0 | 0 | 0 | 0 | 0 | 7 | 0 | 0 | 0 | 0 | 0 | 0 | 1 | 0 | 0 | 8 |
| **7. Snow / Glacier** | 0 | 0 | 0 | 0 | 0 | 0 | 10 | 0 | 0 | 0 | 0 | 0 | 0 | 0 | 0 | 10 |
| **8. Water** | 0 | 0 | 0 | 0 | 0 | 0 | 0 | 10 | 0 | 0 | 0 | 0 | 0 | 0 | 0 | 10 |
| **9. Pine** | 1 | 0 | 1 | 0 | 0 | 0 | 0 | 0 | 4 | 0 | 2 | 2 | 0 | 0 | 0 | 10 |
| **10. Sub-alpine Spruce Transition** | 0 | 0 | 0 | 0 | 0 | 0 | 0 | 0 | 1 | 7 | 0 | 0 | 0 | 0 | 0 | 8 |
| **11. Spruce** | 0 | 0 | 1 | 0 | 0 | 0 | 0 | 0 | 4 | 0 | 5 | 0 | 0 | 0 | 0 | 10 |
| **12. Riparian Spruce** | 1 | 1 | 2 | 0 | 0 | 0 | 0 | 0 | 0 | 0 | 1 | 8 | 0 | 0 | 0 | 13 |
| **13. *Dryas*-dominated Alpine** | 0 | 1 | 0 | 0 | 0 | 0 | 0 | 0 | 0 | 0 | 0 | 0 | 7 | 4 | 0 | 12 |
| **14. Moist Alpine** | 0 | 0 | 0 | 0 | 0 | 0 | 0 | 0 | 0 | 0 | 0 | 0 | 0 | 5 | 0 | 5 |
| **15. Burned / Disturbed** | 0 | 0 | 0 | 0 | 0 | 0 | 0 | 0 | 0 | 1 | 0 | 0 | 0 | 0 | 9 | 10 |
| **Totals** | 10 | 10 | 10 | 10 | 10 | 10 | 10 | 10 | 10 | 10 | 10 | 10 | 10 | 10 | 10 | 150 |

Table D8. Accuracy Statistics of the 15-class maximum likelihood classification of the Greater Besa-Prophet Area in northern British Columbia. TM bands 5, 4, 3, DEM, slope, angle of incidence, and third principal component from the 6-band TM principal component analysis. No filtration or modelling.

| | ***User's*** | ***Producer's*** | $\kappa$ |
|---|---|---|---|
| **Sedge Wetland** | 50.00% | 55.56% | 0.5238 |
| **Shrub** | 70.00% | 53.85% | 0.5055 |
| **Low-productivity Spruce** | 60.00% | 85.71% | 0.8469 |
| **Gravel Bar** | 80.00% | 88.89% | 0.881 |
| **Rock** | 100.00% | 62.50% | 0.5982 |
| **Rock / Crustose Lichen** | 70.00% | 87.50% | 0.8661 |
| **Snow / Glacier** | 100.00% | 100.00% | 1 |
| **Water** | 100.00% | 100.00% | 1 |
| **Pine** | 40.00% | 40.00% | 0.3571 |
| **Sub-alpine Spruce Transition** | 70.00% | 87.50% | 0.8661 |
| **Spruce** | 50.00% | 50.00% | 0.4643 |
| **Riparian Spruce** | 80.00% | 61.54% | 0.5879 |
| **Dryas-dominated Alpine** | 70.00% | 58.33% | 0.5536 |
| **Moist Alpine** | 50.00% | 100.00% | 1 |
| **Burned / Disturbed** | 90.00% | 90.00% | 0.8929 |
| | | | |
| **Overall Accuracy:** | | | **72.00%** |
| **Overall $\kappa$:** | | | **0.70** |

Table D9. Confusion matrix of the 15-class maximum likelihood classification of the Greater Besa-Prophet Area in northern British Columbia. Inputs: TM bands 5, 4, 3, DEM, slope, angle of incidence, and Tasseled Cap 'greenness' component. No filtration or modelling.

| | **REFERENCE** | | | | | | | | | | | | | | | |
|---|---|---|---|---|---|---|---|---|---|---|---|---|---|---|---|---|
| **CLASSIFIED** | **1** | **2** | **3** | **4** | **5** | **6** | **7** | **8** | **9** | **10** | **11** | **12** | **13** | **14** | **15** | **Total** |
| **1. Sedge Wetland** | 5 | 0 | 0 | 1 | 0 | 0 | 0 | 0 | 1 | 0 | 0 | 0 | 1 | 0 | 0 | 8 |
| **2. Shrub** | 3 | 8 | 0 | 0 | 0 | 0 | 0 | 0 | 0 | 2 | 0 | 0 | 0 | 1 | 2 | 16 |
| **3. Low-productivity Spruce** | 0 | 0 | 7 | 0 | 0 | 0 | 0 | 0 | 0 | 0 | 1 | 0 | 0 | 0 | 0 | 8 |
| **4. Gravel Bar** | 1 | 0 | 0 | 8 | 0 | 0 | 0 | 0 | 0 | 0 | 0 | 0 | 0 | 0 | 0 | 9 |
| **5. Rock** | 0 | 0 | 0 | 1 | 10 | 3 | 0 | 0 | 0 | 0 | 1 | 0 | 1 | 0 | 0 | 16 |
| **6. Rock / Crustose Lichen** | 0 | 0 | 0 | 0 | 0 | 7 | 0 | 0 | 0 | 0 | 0 | 0 | 1 | 0 | 0 | 8 |
| **7. Snow / Glacier** | 0 | 0 | 0 | 0 | 0 | 0 | 10 | 0 | 0 | 0 | 0 | 0 | 0 | 0 | 0 | 10 |
| **8. Water** | 0 | 0 | 0 | 0 | 0 | 0 | 0 | 10 | 0 | 0 | 0 | 0 | 0 | 0 | 0 | 10 |
| **9. Pine** | 1 | 0 | 1 | 0 | 0 | 0 | 0 | 0 | 4 | 0 | 1 | 2 | 0 | 0 | 0 | 9 |
| **10. Sub-alpine Spruce Transition** | 0 | 0 | 0 | 0 | 0 | 0 | 0 | 0 | 1 | 7 | 0 | 0 | 0 | 0 | 0 | 8 |
| **11. Spruce** | 0 | 0 | 0 | 0 | 0 | 0 | 0 | 0 | 4 | 0 | 5 | 0 | 0 | 0 | 0 | 9 |
| **12. Riparian Spruce** | 0 | 1 | 2 | 0 | 0 | 0 | 0 | 0 | 0 | 0 | 2 | 8 | 0 | 0 | 0 | 13 |
| **13. *Dryas*-dominated Alpine** | 0 | 1 | 0 | 0 | 0 | 0 | 0 | 0 | 0 | 0 | 0 | 0 | 7 | 4 | 0 | 12 |
| **14. Moist Alpine** | 0 | 0 | 0 | 0 | 0 | 0 | 0 | 0 | 0 | 0 | 0 | 0 | 0 | 5 | 0 | 5 |
| **15. Burned / Disturbed** | 0 | 0 | 0 | 0 | 0 | 0 | 0 | 0 | 0 | 1 | 0 | 0 | 0 | 0 | 8 | 9 |
| **Totals** | 10 | 10 | 10 | 10 | 10 | 10 | 10 | 10 | 10 | 10 | 10 | 10 | 10 | 10 | 10 | 150 |

Table D10. Accuracy Statistics of the 15-class maximum likelihood classification of the Greater Besa-Prophet Area in northern British Columbia. TM bands 5, 4, 3, DEM, slope, angle of incidence, and Tasseled Cap 'greenness' component. No filtration or modelling.

| | ***User's*** | ***Producer's*** | $\kappa$ |
|---|---|---|---|
| **Sedge Wetland** | 50.00% | 62.50% | 0.5982 |
| **Shrub** | 80.00% | 50.00% | 0.4643 |
| **Low-productivity Spruce** | 70.00% | 87.50% | 0.8661 |
| **Gravel Bar** | 80.00% | 88.89% | 0.881 |
| **Rock** | 100.00% | 62.50% | 0.5982 |
| **Rock / Crustose Lichen** | 70.00% | 87.50% | 0.8661 |
| **Snow / Glacier** | 100.00% | 100.00% | 1 |
| **Water** | 100.00% | 100.00% | 1 |
| **Pine** | 40.00% | 44.44% | 0.4048 |
| **Sub-alpine Spruce Transition** | 70.00% | 87.50% | 0.8661 |
| **Spruce** | 50.00% | 55.56% | 0.5238 |
| **Riparian Spruce** | 80.00% | 61.54% | 0.5879 |
| **Dryas-dominated Alpine** | 70.00% | 58.33% | 0.5536 |
| **Moist Alpine** | 50.00% | 100.00% | 1 |
| **Burned / Disturbed** | 80.00% | 88.89% | 0.881 |
| | | | |
| **Overall Accuracy:** | | | **72.67%** |
| **Overall $\kappa$:** | | | **0.71** |

Table D11. Confusion matrix of the 15-class maximum likelihood classification of the Greater Besa-Prophet Area in northern British Columbia after post-classification modelling and filtration. Inputs: TM bands 5, 4, 3, DEM, slope, angle of incidence, and Tasseled Cap 'greenness' component.

| | **REFERENCE** | | | | | | | | | | | | | | | |
|---|---|---|---|---|---|---|---|---|---|---|---|---|---|---|---|---|
| **CLASSIFIED** | **1** | **2** | **3** | **4** | **5** | **6** | **7** | **8** | **9** | **10** | **11** | **12** | **13** | **14** | **15** | **Total** |
| **1. Sedge Wetland** | 7 | 1 | 0 | 0 | 0 | 0 | 0 | 0 | 0 | 0 | 0 | 0 | 1 | 0 | 0 | 9 |
| **2. Shrub** | 2 | 8 | 0 | 0 | 0 | 0 | 0 | 0 | 0 | 1 | 0 | 0 | 0 | 2 | 2 | 15 |
| **3. Low-productivity Spruce** | 0 | 0 | 7 | 0 | 0 | 0 | 0 | 0 | 0 | 0 | 1 | 0 | 0 | 0 | 0 | 8 |
| **4. Gravel Bar** | 1 | 0 | 0 | 9 | 0 | 0 | 0 | 0 | 0 | 0 | 0 | 0 | 0 | 0 | 0 | 10 |
| **5. Rock** | 0 | 0 | 0 | 1 | 10 | 3 | 0 | 1 | 0 | 0 | 0 | 0 | 1 | 0 | 0 | 16 |
| **6. Rock / Crustose Lichen** | 0 | 0 | 0 | 0 | 0 | 7 | 0 | 0 | 0 | 0 | 0 | 0 | 1 | 0 | 0 | 8 |
| **7. Snow / Glacier** | 0 | 0 | 0 | 0 | 0 | 0 | 10 | 0 | 0 | 0 | 0 | 0 | 0 | 0 | 0 | 10 |
| **8. Water** | 0 | 0 | 0 | 0 | 0 | 0 | 0 | 9 | 0 | 0 | 0 | 0 | 0 | 0 | 0 | 9 |
| **9. Pine** | 0 | 0 | 1 | 0 | 0 | 0 | 0 | 0 | 6 | 0 | 2 | 1 | 0 | 0 | 0 | 10 |
| **10. Sub-alpine Spruce Transition** | 0 | 0 | 0 | 0 | 0 | 0 | 0 | 0 | 0 | 8 | 0 | 0 | 0 | 0 | 0 | 8 |
| **11. Spruce** | 0 | 0 | 0 | 0 | 0 | 0 | 0 | 0 | 3 | 0 | 6 | 0 | 0 | 0 | 0 | 9 |
| **12. Riparian Spruce** | 0 | 0 | 2 | 0 | 0 | 0 | 0 | 0 | 1 | 0 | 1 | 9 | 0 | 0 | 0 | 13 |
| **13. *Dryas*-dominated Alpine** | 0 | 0 | 0 | 0 | 0 | 0 | 0 | 0 | 0 | 0 | 0 | 0 | 6 | 2 | 0 | 8 |
| **14. Moist Alpine** | 0 | 1 | 0 | 0 | 0 | 0 | 0 | 0 | 0 | 0 | 0 | 0 | 1 | 6 | 0 | 8 |
| **15. Burned / Disturbed** | 0 | 0 | 0 | 0 | 0 | 0 | 0 | 0 | 0 | 1 | 0 | 0 | 0 | 0 | 8 | 9 |
| **Totals** | 10 | 10 | 10 | 10 | 10 | 10 | 10 | 10 | 10 | 10 | 10 | 10 | 10 | 10 | 10 | 150 |

Table D12. Accuracy Statistics of the 15-class maximum likelihood classification of the Greater Besa-Prophet Area in northern British Columbia after post-classification modelling and filtration. Inputs: Inputs: TM bands 5, 4, 3, DEM, slope, angle of incidence, and Tasseled Cap 'greenness' component.

| | ***User's*** | ***Producer's*** | $\kappa$ |
|---|---|---|---|
| **Sedge Wetland** | 70.00% | 77.78% | 0.7619 |
| **Shrub** | 80.00% | 53.33% | 0.5 |
| **Low-productivity Spruce** | 70.00% | 87.50% | 0.8661 |
| **Gravel Bar** | 90.00% | 90.00% | 0.8929 |
| **Rock** | 100.00% | 62.50% | 0.5982 |
| **Rock / Crustose Lichen** | 70.00% | 87.50% | 0.8661 |
| **Snow / Glacier** | 100.00% | 100.00% | 1 |
| **Water** | 90.00% | 100.00% | 1 |
| **Pine** | 60.00% | 60.00% | 0.5714 |
| **Sub-alpine Spruce Transition** | 80.00% | 100.00% | 1 |
| **Spruce** | 60.00% | 66.67% | 0.6429 |
| **Riparian Spruce** | 90.00% | 69.23% | 0.6703 |
| **Dryas-dominated Alpine** | 60.00% | 75.00% | 0.7321 |
| **Moist Alpine** | 60.00% | 75.00% | 0.7321 |
| **Burned / Disturbed** | 80.00% | 88.89% | 0.881 |
| | | | |
| **Overall Accuracy:** | | | **77.33%** |
| **Overall $\kappa$:** | | | **0.76** |

**APPENDIX E: Original coefficients of models developed for all multiple linear regression models used to predict NDVI values in the Greater Besa-Prophet Area in northern British Columbia, 2001-2003.**

Table E1. Original $\beta$ coefficients and standard error ($\sigma$) for top five multiple linear regression models used to predict NDVI values for 04 Jun 2001 in the Greater Besa-Prophet Area in northern British Columbia. Models are listed by adjusted $r^2$.

| INPUTS | MODELS (by Adjusted $r^2$) | | | | | | | | | |
|---|---|---|---|---|---|---|---|---|---|---|
| | **0.606** | | **0.588** | | **0.565** | | **0.577** | | **0.535** | |
| | ***β*** | ***σ*** | ***β*** | ***σ*** | ***β*** | ***σ*** | ***β*** | ***σ*** | ***β*** | ***σ*** |
| **ANGLE OF INCIDENCE** | | | 0.157** | 0.015 | | | | | 0.136** | 0.016 |
| **SLOPE** | -0.002** | 0 | | | | | -0.003** | 0 | | |
| **ELEVATION (KM)** | -0.115** | 0.009 | -0.145** | 0.009 | -0.137** | 0.009 | | | | |
| **ASPECT**† | | | | | | | -0.039** | 0.005 | | |
| North | -0.038** | 0.005 | | | | | 0.018** | 0.004 | | |
| East | 0.022** | 0.004 | | | | | 0.023** | 0.005 | | |
| South | 0.029** | 0.005 | | | | | 0.004 | 0.005 | | |
| West | 0.004 | 0.004 | | | | | -0.039** | 0.005 | | |
| **VEGETATION TYPE**‡ | | | | | | | | | | |
| Sedge Wetland | 0.095** | 0.011 | 0.095** | 0.011 | 0.102** | 0.011 | 0.144** | 0.011 | 0.179** | 0.011 |
| Shrub | -0.015* | 0.007 | -0.009 | 0.007 | -0.002 | 0.007 | -0.015* | 0.007 | -0.009 | 0.008 |
| Low-productivity Spruce | 0.103** | 0.01 | 0.090** | 0.01 | 0.071** | 0.01 | 0.142** | 0.01 | 0.127** | 0.011 |
| Gravel Bar | -0.218** | 0.026 | -0.207** | 0.027 | -0.199** | 0.028 | -0.184** | 0.027 | -0.147** | 0.028 |
| Rock / Crustose Lichen | -0.076** | 0.029 | -0.066* | 0.029 | -0.068* | 0.03 | -0.130** | 0.03 | -0.138** | 0.031 |
| Water | 0.135** | 0.019 | 0.142** | 0.02 | 0.139** | 0.02 | 0.041* | 0.018 | 0.016 | 0.019 |
| Snow/Glacier | -0.305** | 0.035 | -0.294** | 0.035 | -0.291** | 0.036 | -0.316** | 0.037 | -0.273** | 0.037 |
| Pine | 0.114** | 0.012 | 0.126** | 0.012 | 0.132** | 0.012 | 0.131** | 0.012 | 0.156** | 0.012 |
| Sub-alpine Spruce Transition | 0.037** | 0.012 | 0.039** | 0.012 | 0.036** | 0.013 | 0.033** | 0.012 | 0.027* | 0.013 |
| Spruce | 0.103** | 0.007 | 0.096** | 0.007 | 0.094** | 0.007 | 0.128** | 0.007 | 0.123** | 0.007 |
| Riparian Spruce | 0.080** | 0.009 | 0.085** | 0.009 | 0.093** | 0.009 | 0.128** | 0.008 | 0.158** | 0.008 |
| Dryas-dominated Alpine | -0.023* | 0.011 | -0.015 | 0.011 | -0.016 | 0.011 | -0.046** | 0.011 | -0.059** | 0.011 |
| Moist Alpine | -0.046** | 0.017 | -0.069** | 0.017 | -0.082** | 0.018 | -0.075** | 0.018 | -0.114** | 0.018 |
| Burned / Disturbed | 0.051** | 0.008 | 0.030** | 0.008 | 0.046** | 0.008 | 0.086** | 0.008 | 0.061** | 0.008 |
| Intercept | 0.306** | 0.014 | 0.254** | 0.015 | 0.304** | 0.014 | 0.150** | 0.006 | 0.045** | 0.008 |

* $p < .05$

** $p < .01$

† Reference Category 'no aspect' is not listed.

‡ Reference Category 'rock' is not listed.

Table E2. Original $\beta$ coefficients and standard error ($\sigma$) for top five multiple linear regression models used to predict NDVI values for 22 Jul 2001 in the Greater Besa-Prophet Area in northern British Columbia.

| INPUTS | MODELS (by Adjusted $r^2$) | | | | | | | | | |
|---|---|---|---|---|---|---|---|---|---|---|
| | 0.646 | | 0.627 | | 0.649 | | 0.649 | | 0.647 | |
| | $\beta$ | $\sigma$ | $\beta$ | $\sigma$ | $\beta$ | $\sigma$ | $\beta$ | $\sigma$ | $\beta$ | $\sigma$ |
| **ANGLE OF INCIDENCE** | 0.015 | 0.017 | -0.005 | 0.017 | | | | | | |
| **SLOPE** | | | | | | | | | | |
| **ELEVATION (KM)** | -0.088** | 0.008 | | | | | -0.093** | 0.008 | -0.087** | 0.008 |
| **ASPECT**[†] | | | | | | | | | | |
| North | | | | | -0.002 | 0.004 | -0.001 | 0.004 | | |
| East | | | | | 0.005 | 0.004 | 0.010** | 0.003 | | |
| South | | | | | 0.004 | 0.004 | 0.008* | 0.004 | | |
| West | | | | | 0.003 | 0.004 | 0.003 | 0.004 | | |
| **VEGETATION TYPE**[‡] | | | | | | | | | | |
| Sedge Wetland | 0.121** | 0.008 | 0.163** | 0.007 | 0.164** | 0.007 | 0.123** | 0.008 | 0.122** | 0.008 |
| Shrub | 0.180** | 0.007 | 0.194** | 0.007 | 0.194** | 0.007 | 0.179** | 0.007 | 0.181** | 0.007 |
| Low-productivity Spruce | 0.068** | 0.008 | 0.085** | 0.008 | 0.086** | 0.008 | 0.065** | 0.008 | 0.066** | 0.008 |
| Gravel Bar | -0.162** | 0.018 | -0.128** | 0.019 | -0.125** | 0.019 | -0.157** | 0.018 | -0.162** | 0.018 |
| Rock / Crustose Lichen | -0.180** | 0.024 | -0.222** | 0.024 | -0.223** | 0.024 | -0.180** | 0.023 | -0.181** | 0.023 |
| Water | -0.219** | 0.024 | -0.300** | 0.023 | -0.301** | 0.023 | -0.216** | 0.024 | -0.219** | 0.024 |
| Snow/Glacier | -0.405** | 0.04 | -0.365** | 0.041 | -0.360** | 0.041 | -0.395** | 0.04 | -0.404** | 0.04 |
| Pine | 0.118** | 0.008 | 0.133** | 0.008 | 0.131** | 0.008 | 0.115** | 0.008 | 0.119** | 0.008 |
| Sub-alpine Spruce Transition | 0.174** | 0.012 | 0.158** | 0.012 | 0.157** | 0.012 | 0.173** | 0.012 | 0.174** | 0.012 |
| Spruce | 0.069** | 0.006 | 0.087** | 0.006 | 0.086** | 0.006 | 0.066** | 0.006 | 0.069** | 0.006 |
| Riparian Spruce | 0.055** | 0.007 | 0.091** | 0.006 | 0.091** | 0.006 | 0.053** | 0.007 | 0.056** | 0.007 |
| Dryas-dominated Alpine | 0.069** | 0.013 | 0.040** | 0.013 | 0.037** | 0.013 | 0.066** | 0.013 | 0.069** | 0.013 |
| Moist Alpine | 0.078** | 0.017 | 0.046** | 0.017 | 0.049** | 0.017 | 0.081** | 0.017 | 0.076** | 0.017 |
| Burned / Disturbed | 0.209** | 0.007 | 0.223** | 0.007 | 0.220** | 0.007 | 0.205** | 0.007 | 0.211** | 0.007 |
| Intercept | 0.385** | 0.013 | 0.270** | 0.008 | 0.267** | 0.005 | 0.395** | 0.012 | 0.389** | 0.012 |

* $p < .05$

** $p < .01$

[†] Reference Category 'no aspect' is not listed.

[‡] Reference Category 'rock' is not listed.

Table E3. Original $\beta$ coefficients and standard error ($\sigma$) for top five multiple linear regression models used to predict NDVI values for 14 Aug 2001 in the Greater Besa-Prophet Area in northern British Columbia.

| INPUTS | MODELS (by Adjusted $r^2$) | | | | | | | | | |
|---|---|---|---|---|---|---|---|---|---|---|
| | 0.815 | | 0.8 | | 0.821 | | 0.82 | | 0.8 | |
| | $\beta$ | $\sigma$ | $\beta$ | $\sigma$ | $\beta$ | $\sigma$ | $\beta$ | $\sigma$ | $\beta$ | $\sigma$ |
| **ANGLE OF INCIDENCE** | 0.047** | 0.014 | | | | | | | | |
| **SLOPE** | | | | | 0.001** | 0 | | | | |
| **ELEVATION (KM)** | -0.125** | 0.009 | | | -0.147** | 0.009 | -0.136** | 0.009 | -0.126** | 0.009 |
| **ASPECT**[†] | | | | | | | | | | |
| North | | | -0.01 | 0.005 | -0.010* | 0.005 | -0.008 | 0.005 | | |
| East | | | 0.015** | 0.005 | 0.018** | 0.005 | 0.019** | 0.005 | | |
| South | | | 0.019** | 0.005 | 0.026** | 0.005 | 0.027** | 0.005 | | |
| West | | | 0.014** | 0.005 | 0.020** | 0.005 | 0.020** | 0.005 | | |
| **VEGETATION TYPE**[‡] | | | | | | | | | | |
| Sedge Wetland | 0.060** | 0.012 | 0.138** | 0.011 | 0.076** | 0.012 | 0.070** | 0.012 | 0.060** | 0.012 |
| Shrub | 0.216** | 0.007 | 0.210** | 0.008 | 0.211** | 0.007 | 0.209** | 0.007 | 0.219** | 0.007 |
| Low-productivity Spruce | 0.056** | 0.01 | 0.081** | 0.01 | 0.033** | 0.01 | 0.043** | 0.01 | 0.050** | 0.01 |
| Gravel Bar | -0.150** | 0.03 | -0.078* | 0.032 | -0.103** | 0.031 | -0.110** | 0.031 | -0.149** | 0.03 |
| Rock / Crustose Lichen | -0.106** | 0.034 | -0.166** | 0.036 | -0.117** | 0.034 | -0.117** | 0.034 | -0.108** | 0.034 |
| Water | -0.270** | 0.019 | -0.380** | 0.018 | -0.258** | 0.019 | -0.265** | 0.019 | -0.270** | 0.019 |
| Snow/Glacier | -0.441** | 0.024 | -0.374** | 0.027 | -0.382** | 0.026 | -0.389** | 0.026 | -0.439** | 0.025 |
| Pine | 0.087** | 0.012 | 0.100** | 0.012 | 0.083** | 0.012 | 0.077** | 0.012 | 0.088** | 0.012 |
| Sub-alpine Spruce Transition | 0.200** | 0.011 | 0.184** | 0.011 | 0.186** | 0.011 | 0.188** | 0.011 | 0.200** | 0.011 |
| Spruce | 0.060** | 0.007 | 0.078** | 0.007 | 0.046** | 0.007 | 0.050** | 0.007 | 0.059** | 0.007 |
| Riparian Spruce | 0.032** | 0.01 | 0.088** | 0.01 | 0.030** | 0.01 | 0.027** | 0.01 | 0.033** | 0.01 |
| Dryas-dominated Alpine | 0.120** | 0.011 | 0.068** | 0.011 | 0.104** | 0.011 | 0.105** | 0.011 | 0.120** | 0.011 |
| Moist Alpine | 0.124** | 0.014 | 0.085** | 0.015 | 0.120** | 0.014 | 0.122** | 0.014 | 0.120** | 0.014 |
| Burned / Disturbed | 0.219** | 0.008 | 0.233** | 0.009 | 0.195** | 0.009 | 0.205** | 0.008 | 0.223** | 0.008 |
| Intercept | 0.409** | 0.015 | 0.235** | 0.005 | 0.439** | 0.014 | 0.437** | 0.014 | 0.426** | 0.014 |

* $p < .05$

** $p < .01$

[†] Reference Category 'no aspect' is not listed.

[‡] Reference Category 'rock' is not listed.

Table E4. Original $\beta$ coefficients and standard error ($\sigma$) for top five multiple linear regression models used to predict NDVI values for 15 Aug 2001 (Path 49 row 20) in the Greater Besa-Prophet Area in northern British Columbia.

| INPUTS | MODELS (by Adjusted $r^2$) | | | | | | | | | |
|---|---|---|---|---|---|---|---|---|---|---|
| | **0.851** | | **0.85** | | **0.855** | | **0.854** | | 0.842 | |
| | ***β*** | ***σ*** | ***β*** | ***σ*** | ***β*** | ***σ*** | ***β*** | ***σ*** | ***β*** | ***σ*** |
| **ANGLE OF INCIDENCE** | 0.065* | 0.029 | -0.083** | 0.007 | | | | | | |
| **SLOPE** | | | | | 0.001** | 0 | -0.090** | 0.007 | 0 | 0 |
| **ELEVATION (KM)** | -0.083** | 0.007 | | | -0.103** | 0.007 | | | | |
| **ASPECT**[†] | | | | | | | | | | |
| North | | | | | -0.014** | 0.004 | -0.012** | 0.004 | -0.013** | 0.004 |
| East | | | | | 0.011** | 0.003 | 0.012** | 0.003 | 0.008* | 0.003 |
| South | | | | | 0.019** | 0.003 | 0.018** | 0.003 | 0.013** | 0.004 |
| West | | | | | 0.007 | 0.004 | 0.007* | 0.004 | 0.005 | 0.004 |
| **VEGETATION TYPE**[‡] | | | | | | | | | | |
| Sedge Wetland | 0.121** | 0.008 | 0.122** | 0.008 | 0.132** | 0.008 | 0.128** | 0.008 | 0.171** | 0.008 |
| Shrub | 0.228** | 0.006 | 0.228** | 0.006 | 0.224** | 0.005 | 0.223** | 0.006 | 0.225** | 0.006 |
| Low-productivity Spruce | 0.068** | 0.008 | 0.067** | 0.008 | 0.056** | 0.008 | 0.067** | 0.008 | 0.088** | 0.008 |
| Gravel Bar | -0.185** | 0.025 | -0.186** | 0.025 | -0.184** | 0.025 | -0.189** | 0.025 | -0.144** | 0.026 |
| Rock / Crustose Lichen | -0.129** | 0.017 | -0.128** | 0.017 | -0.127** | 0.017 | -0.129** | 0.017 | -0.163** | 0.017 |
| Water | -0.348** | 0.016 | -0.347** | 0.016 | -0.335** | 0.016 | -0.342** | 0.016 | -0.417** | 0.016 |
| Snow/Glacier | -0.491** | 0.024 | -0.491** | 0.024 | -0.458** | 0.024 | -0.467** | 0.024 | -0.471** | 0.025 |
| Pine | 0.115** | 0.008 | 0.116** | 0.008 | 0.118** | 0.008 | 0.113** | 0.008 | 0.130** | 0.009 |
| Sub-alpine Spruce Transition | 0.205** | 0.009 | 0.205** | 0.009 | 0.198** | 0.009 | 0.200** | 0.009 | 0.194** | 0.009 |
| Spruce | 0.078** | 0.005 | 0.078** | 0.005 | 0.072** | 0.005 | 0.075** | 0.005 | 0.094** | 0.005 |
| Riparian Spruce | 0.066** | 0.007 | 0.067** | 0.007 | 0.071** | 0.007 | 0.066** | 0.007 | 0.104** | 0.006 |
| Dryas-dominated Alpine | 0.116** | 0.009 | 0.116** | 0.009 | 0.106** | 0.009 | 0.108** | 0.009 | 0.081** | 0.009 |
| Moist Alpine | 0.114** | 0.017 | 0.113** | 0.017 | 0.117** | 0.016 | 0.121** | 0.017 | 0.094** | 0.017 |
| Burned / Disturbed | 0.235** | 0.006 | 0.235** | 0.006 | 0.216** | 0.007 | 0.225** | 0.006 | 0.247** | 0.007 |
| Intercept | 0.319** | 0.016 | 0.346** | 0.011 | 0.359** | 0.011 | 0.354** | 0.011 | 0.223** | 0.005 |

* $p < .05$

** $p < .01$

[†] Reference Category 'no aspect' is not listed.

[‡] Reference Category 'rock' is not listed.

Table E5. Original $\beta$ coefficients and standard error ($\sigma$) for top five multiple linear regression models used to predict NDVI values for 16 Aug 2001 (Path 51 Row 20) in the Greater Besa-Prophet Area in northern British Columbia.

| INPUTS | MODELS (by Adjusted $r^2$) | | | | | | | | | |
|---|---|---|---|---|---|---|---|---|---|---|
| | **0.586** | | **0.579** | | **0.581** | | **0.581** | | **0.59** | |
| | ***β*** | ***σ*** | ***β*** | ***σ*** | ***β*** | ***σ*** | ***β*** | ***σ*** | ***β*** | ***σ*** |
| **ANGLE OF INCIDENCE** | 0.091** | 0.015 | | | | | | | | |
| **SLOPE** | | | | | | | 0 | 0 | 0 | 0 |
| **ELEVATION (KM)** | -0.047** | 0.007 | -0.043** | 0.007 | | | | | -0.056** | 0.008 |
| **ASPECT**[†] | | | | | -0.008** | 0.003 | -0.008** | 0.003 | -0.008** | 0.003 |
| North | | | | | 0.009** | 0.003 | 0.010** | 0.003 | 0.011** | 0.003 |
| East | | | | | 0.015** | 0.003 | 0.015** | 0.003 | 0.016** | 0.003 |
| South | | | | | 0.001 | 0.003 | 0.001 | 0.003 | 0 | 0.003 |
| West | | | | | -0.008** | 0.003 | -0.008** | 0.003 | -0.008** | 0.003 |
| **VEGETATION TYPE**[‡] | | | | | | | | | | |
| Sedge Wetland | 0.079** | 0.005 | 0.084** | 0.005 | 0.102** | 0.005 | 0.098** | 0.005 | 0.086** | 0.005 |
| Shrub | 0.126** | 0.005 | 0.132** | 0.005 | 0.134** | 0.005 | 0.132** | 0.005 | 0.129** | 0.005 |
| Low-productivity Spruce | 0.026** | 0.006 | 0.017** | 0.006 | 0.024** | 0.006 | 0.026** | 0.006 | 0.015* | 0.006 |
| Gravel Bar | -0.191** | 0.016 | -0.187** | 0.016 | -0.162** | 0.016 | -0.165** | 0.016 | -0.177** | 0.016 |
| Rock / Crustose Lichen | -0.215** | 0.015 | -0.217** | 0.015 | -0.238** | 0.015 | -0.237** | 0.015 | -0.212** | 0.015 |
| Water | 0.057** | 0.005 | 0.062** | 0.005 | 0.064** | 0.005 | 0.061** | 0.006 | 0.060** | 0.006 |
| Snow/Glacier | 0.112** | 0.011 | 0.105** | 0.011 | 0.095** | 0.01 | 0.097** | 0.01 | 0.106** | 0.01 |
| Pine | 0.021** | 0.004 | 0.024** | 0.004 | 0.030** | 0.004 | 0.029** | 0.004 | 0.021** | 0.004 |
| Sub-alpine Spruce Transition | 0.012** | 0.004 | 0.017** | 0.004 | 0.031** | 0.004 | 0.028** | 0.004 | 0.018** | 0.005 |
| Spruce | -0.017 | 0.009 | -0.012 | 0.009 | -0.036** | 0.009 | -0.034** | 0.009 | -0.019* | 0.009 |
| Riparian Spruce | -0.021 | 0.016 | -0.03 | 0.016 | -0.041** | 0.016 | -0.039* | 0.016 | -0.019 | 0.016 |
| Dryas-dominated Alpine | 0.147** | 0.005 | 0.158** | 0.005 | 0.155** | 0.005 | 0.156** | 0.005 | 0.147** | 0.005 |
| Moist Alpine | 0.342** | 0.011 | 0.370** | 0.01 | 0.312** | 0.003 | 0.316** | 0.004 | 0.381** | 0.01 |
| Burned / Disturbed | 0.079** | 0.005 | 0.084** | 0.005 | 0.102** | 0.005 | 0.098** | 0.005 | 0.086** | 0.005 |
| Intercept | 0.126** | 0.005 | 0.132** | 0.005 | 0.134** | 0.005 | 0.132** | 0.005 | 0.129** | 0.005 |

* $p < .05$

** $p < .01$

[†] Reference Category 'no aspect' is not listed.

[‡] Reference Category 'rock' is not listed.

Table E6. Original $\beta$ coefficients and standard error ($\sigma$) for top five multiple linear regression models used to predict NDVI values for 16-September-01 in the Greater Besa-Prophet Area in northern British Columbia.

| INPUTS | MODELS (by Adjusted $r^2$) | | | | | | | | | |
|---|---|---|---|---|---|---|---|---|---|---|
| | 0.772 | | 0.752 | | 0.754 | | 0.75 | | 0.769 | |
| | $\beta$ | $\sigma$ | $\beta$ | $\sigma$ | $\beta$ | $\sigma$ | $\beta$ | $\sigma$ | $\beta$ | $\sigma$ |
| **ANGLE OF INCIDENCE** | | | | | | | 0.125** | 0.012 | 0.135** | 0.011 |
| **SLOPE** | | | | | | | | | | |
| **ELEVATION (KM)** | -0.104** | 0.008 | | | -0.096** | 0.008 | | | -0.102** | 0.008 |
| **ASPECT**[†] | | | | | | | | | | |
| North | -0.031** | 0.004 | -0.029** | 0.004 | | | | | | |
| East | 0.019** | 0.003 | 0.016** | 0.004 | | | | | | |
| South | 0.029** | 0.004 | 0.026** | 0.004 | | | | | | |
| West | -0.003 | 0.004 | -0.003 | 0.004 | | | | | | |
| **VEGETATION TYPE**[‡] | | | | | | | | | | |
| Sedge Wetland | 0.066** | 0.01 | 0.107** | 0.01 | 0.068** | 0.01 | 0.105** | 0.009 | 0.064** | 0.01 |
| Shrub | 0.094** | 0.006 | 0.091** | 0.006 | 0.107** | 0.006 | 0.096** | 0.006 | 0.100** | 0.006 |
| Low-productivity Spruce | 0.021* | 0.009 | 0.046** | 0.009 | 0.011 | 0.009 | 0.051** | 0.009 | 0.027** | 0.009 |
| Gravel Bar | -0.121** | 0.021 | -0.079** | 0.022 | -0.117** | 0.022 | -0.078** | 0.022 | -0.120** | 0.021 |
| Rock / Crustose Lichen | -0.044 | 0.026 | -0.087** | 0.027 | -0.047 | 0.027 | -0.088** | 0.027 | -0.046 | 0.026 |
| Water | -0.205** | 0.016 | -0.293** | 0.015 | -0.219** | 0.017 | -0.299** | 0.015 | -0.214** | 0.016 |
| Snow/Glacier | -0.278** | 0.029 | -0.252** | 0.03 | -0.293** | 0.029 | -0.267** | 0.029 | -0.296** | 0.028 |
| Pine | 0.094** | 0.009 | 0.120** | 0.009 | 0.099** | 0.009 | 0.120** | 0.009 | 0.096** | 0.009 |
| Sub-alpine Spruce Transition | 0.141** | 0.009 | 0.137** | 0.009 | 0.147** | 0.009 | 0.143** | 0.009 | 0.148** | 0.009 |
| Spruce | 0.076** | 0.005 | 0.094** | 0.005 | 0.079** | 0.005 | 0.095** | 0.005 | 0.078** | 0.005 |
| Riparian Spruce | 0.065** | 0.007 | 0.105** | 0.007 | 0.066** | 0.007 | 0.101** | 0.007 | 0.061** | 0.007 |
| Dryas-dominated Alpine | 0.055** | 0.008 | 0.029** | 0.008 | 0.067** | 0.009 | 0.038** | 0.008 | 0.064** | 0.008 |
| Moist Alpine | 0.046** | 0.011 | 0.014 | 0.012 | 0.02 | 0.012 | 0.009 | 0.012 | 0.040** | 0.011 |
| Burned / Disturbed | 0.125** | 0.007 | 0.145** | 0.007 | 0.146** | 0.007 | 0.148** | 0.007 | 0.130** | 0.007 |
| Intercept | 0.277** | 0.012 | 0.119** | 0.004 | 0.263** | 0.013 | 0.091** | 0.005 | 0.242** | 0.012 |

* $p < .05$

** $p < .01$

[†] Reference Category 'no aspect' is not listed.

[‡] Reference Category 'rock' is not listed.

Table E7. Original $\beta$ coefficients and standard error ($\sigma$) for top five multiple linear regression models used to predict NDVI values for 01-October-01 in the Greater Besa-Prophet Area in northern British Columbia.

| INPUTS | MODELS (by Adjusted $r^2$) | | | | | | | | | |
|---|---|---|---|---|---|---|---|---|---|---|
| | 0.512 | | 0.505 | | 0.472 | | 0.494 | | 0.468 | |
| | $\beta$ | $\sigma$ | $\beta$ | $\sigma$ | $\beta$ | $\sigma$ | $\beta$ | $\sigma$ | $\beta$ | $\sigma$ |
| **ANGLE OF INCIDENCE** | -0.001** | 0 | | | | | | | 0.236** | 0.014 |
| **SLOPE** | -0.065** | 0.007 | | | | | -0.002** | 0 | | |
| **ELEVATION (KM)** | | | -0.080** | 0.007 | | | | | -0.080** | 0.007 |
| **ASPECT**† | | | | | | | | | | |
| North | -0.057** | 0.003 | -0.057** | 0.003 | -0.057** | 0.003 | -0.056** | 0.003 | | |
| East | 0.022** | 0.003 | 0.021** | 0.003 | 0.015** | 0.003 | 0.019** | 0.003 | | |
| South | 0.041** | 0.003 | 0.040** | 0.003 | 0.036** | 0.004 | 0.039** | 0.004 | | |
| West | 0.008* | 0.003 | 0.007* | 0.003 | 0.004 | 0.003 | 0.006* | 0.003 | | |
| **VEGETATION TYPE**‡ | | | | | | | | | | |
| Sedge Wetland | 0.076** | 0.007 | 0.081** | 0.007 | 0.114** | 0.007 | 0.094** | 0.007 | 0.073** | 0.008 |
| Shrub | 0.030** | 0.005 | 0.035** | 0.005 | 0.028** | 0.005 | 0.022** | 0.005 | 0.029** | 0.006 |
| Low-productivity Spruce | 0.012 | 0.006 | 0.003 | 0.006 | 0.013* | 0.006 | 0.025** | 0.006 | 0.009 | 0.006 |
| Gravel Bar | -0.057** | 0.015 | -0.051** | 0.015 | -0.024 | 0.016 | -0.043** | 0.015 | -0.071** | 0.016 |
| Rock / Crustose Lichen | -0.076** | 0.024 | -0.075** | 0.024 | -0.109** | 0.025 | -0.100** | 0.024 | -0.068** | 0.025 |
| Water | -0.219** | 0.036 | -0.211** | 0.036 | -0.189** | 0.037 | -0.210** | 0.037 | -0.201** | 0.037 |
| Snow/Glacier | 0.099** | 0.007 | 0.107** | 0.007 | 0.112** | 0.007 | 0.097** | 0.007 | 0.102** | 0.007 |
| Pine | 0.057** | 0.008 | 0.057** | 0.008 | 0.040** | 0.008 | 0.045** | 0.008 | 0.063** | 0.008 |
| Sub-alpine Spruce Transition | 0.060** | 0.005 | 0.059** | 0.005 | 0.063** | 0.005 | 0.064** | 0.005 | 0.055** | 0.005 |
| Spruce | 0.044** | 0.007 | 0.049** | 0.007 | 0.076** | 0.006 | 0.059** | 0.006 | 0.043** | 0.007 |
| Riparian Spruce | 0.015 | 0.008 | 0.012 | 0.008 | -0.018* | 0.008 | -0.003 | 0.008 | 0.023** | 0.009 |
| Dryas-dominated Alpine | -0.033** | 0.01 | -0.037** | 0.01 | -0.069** | 0.01 | -0.052** | 0.01 | -0.038** | 0.01 |
| Moist Alpine | 0.064** | 0.006 | 0.056** | 0.005 | 0.065** | 0.006 | 0.076** | 0.006 | 0.048** | 0.006 |
| Burned / Disturbed | 0.197** | 0.01 | 0.203** | 0.01 | 0.095** | 0.004 | 0.120** | 0.005 | 0.160** | 0.01 |
| Intercept | 0.076** | 0.007 | 0.081** | 0.007 | 0.114** | 0.007 | 0.094** | 0.007 | 0.073** | 0.008 |

* $p < .05$

** $p < .01$

† Reference Category 'no aspect' is not listed.

‡ Reference Category 'rock' is not listed.

Table E8. Original $\beta$ coefficients and standard error ($\sigma$) for top five multiple linear regression models used to predict NDVI values for 31 May 2002 in the Greater Besa-Prophet Area in northern British Columbia.

| INPUTS | MODELS (by Adjusted $r^2$) | | | | | | | | | |
|---|---|---|---|---|---|---|---|---|---|---|
| | 0.581 | | 0.582 | | 0.585 | | 0.584 | | 0.553 | |
| | $\beta$ | $\sigma$ | $\beta$ | $\sigma$ | $\beta$ | $\sigma$ | $\beta$ | $\sigma$ | $\beta$ | $\sigma$ |
| **ANGLE OF INCIDENCE** | -0.009 | 0.02 | | | | | -0.130** | 0.009 | | |
| **SLOPE** | | | | | -0.001* | 0 | | | -0.002** | 0 |
| **ELEVATION (KM)** | -0.127** | 0.008 | -0.127** | 0.008 | -0.120** | 0.009 | | | | |
| **ASPECT**[†] | | | | | | | | | | |
| North | | | | | -0.006 | 0.003 | -0.005 | 0.003 | -0.007* | 0.003 |
| East | | | | | 0.007* | 0.003 | 0.007* | 0.003 | 0.004 | 0.003 |
| South | | | | | -0.002 | 0.004 | -0.003 | 0.004 | -0.003 | 0.004 |
| West | | | | | 0.011** | 0.004 | 0.010** | 0.004 | 0.012** | 0.004 |
| **VEGETATION TYPE**[‡] | | | | | | | | | | |
| Sedge Wetland | 0.097** | 0.007 | 0.096** | 0.007 | 0.094** | 0.007 | 0.098** | 0.007 | 0.117** | 0.007 |
| Shrub | 0.005 | 0.007 | 0.005 | 0.007 | 0.002 | 0.007 | 0.005 | 0.007 | 0.009 | 0.007 |
| Low-productivity Spruce | 0.101** | 0.008 | 0.102** | 0.008 | 0.106** | 0.008 | 0.101** | 0.008 | 0.124** | 0.009 |
| Gravel Bar | -0.092** | 0.017 | -0.093** | 0.017 | -0.095** | 0.017 | -0.091** | 0.017 | -0.074** | 0.017 |
| Rock / Crustose Lichen | -0.137** | 0.024 | -0.137** | 0.024 | -0.135** | 0.024 | -0.135** | 0.024 | -0.182** | 0.025 |
| Water | -0.227** | 0.05 | -0.227** | 0.05 | -0.231** | 0.05 | -0.227** | 0.05 | -0.200** | 0.052 |
| Snow/Glacier | 0.168** | 0.008 | 0.167** | 0.008 | 0.162** | 0.008 | 0.167** | 0.008 | 0.158** | 0.008 |
| Pine | -0.001 | 0.017 | 0 | 0.017 | 0.002 | 0.017 | -0.001 | 0.017 | -0.019 | 0.017 |
| Sub-alpine Spruce Transition | 0.142** | 0.006 | 0.141** | 0.006 | 0.141** | 0.006 | 0.141** | 0.006 | 0.157** | 0.006 |
| Spruce | 0.144** | 0.006 | 0.144** | 0.006 | 0.140** | 0.007 | 0.144** | 0.006 | 0.156** | 0.007 |
| Riparian Spruce | -0.067** | 0.012 | -0.068** | 0.012 | -0.069** | 0.012 | -0.070** | 0.012 | -0.108** | 0.012 |
| Dryas-dominated Alpine | -0.105** | 0.017 | -0.104** | 0.017 | -0.100** | 0.017 | -0.100** | 0.017 | -0.142** | 0.018 |
| Moist Alpine | 0.048** | 0.007 | 0.048** | 0.007 | 0.051** | 0.007 | 0.047** | 0.007 | 0.065** | 0.007 |
| Burned / Disturbed | 0.251** | 0.015 | 0.247** | 0.012 | 0.245** | 0.012 | 0.249** | 0.012 | 0.115** | 0.006 |
| Intercept | 0.097** | 0.007 | 0.096** | 0.007 | 0.094** | 0.007 | 0.098** | 0.007 | 0.117** | 0.007 |

* $p < .05$

** $p < .01$

[†] Reference Category 'no aspect' is not listed.

[‡] Reference Category 'rock' is not listed.

Table E9. Original $\beta$ coefficients and standard error ($\sigma$) for top five multiple linear regression models used to predict NDVI values for 15 Jun 2002 in the Greater Besa-Prophet Area in northern British Columbia.

| INPUTS | MODELS (by Adjusted $r^2$) | | | | | | | | | |
|---|---|---|---|---|---|---|---|---|---|---|
| | 0.778 | | 0.785 | | 0.781 | | 0.777 | | 0.693 | |
| | $\beta$ | $\sigma$ | $\beta$ | $\sigma$ | $\beta$ | $\sigma$ | $\beta$ | $\sigma$ | $\beta$ | $\sigma$ |
| **ANGLE OF INCIDENCE** | 0.043** | 0.013 | | | | | | | | |
| **SLOPE** | | | 0.001** | 0 | | | | | | |
| **ELEVATION (KM)** | -0.212** | 0.008 | -0.235** | 0.008 | -0.218** | 0.008 | -0.213** | 0.008 | | |
| **ASPECT**[†] | | | | | | | | | | |
| North | | | -0.009* | 0.004 | -0.008* | 0.004 | | | | |
| East | | | 0.010** | 0.004 | 0.012** | 0.004 | | | | |
| South | | | 0.017** | 0.004 | 0.018** | 0.004 | | | | |
| West | | | 0.004 | 0.004 | 0.006 | 0.004 | | | | |
| **VEGETATION TYPE**[‡] | | | | | | | | | | |
| Sedge Wetland | 0.047** | 0.009 | 0.059** | 0.009 | 0.052** | 0.009 | 0.049** | 0.009 | 0.152** | 0.01 |
| Shrub | 0.049** | 0.007 | 0.047** | 0.007 | 0.046** | 0.007 | 0.051** | 0.007 | 0.056** | 0.008 |
| Low-productivity Spruce | 0.079** | 0.009 | 0.061** | 0.009 | 0.072** | 0.009 | 0.074** | 0.009 | 0.128** | 0.01 |
| Gravel Bar | -0.168** | 0.019 | -0.154** | 0.019 | -0.162** | 0.019 | -0.168** | 0.019 | -0.080** | 0.022 |
| Rock / Crustose Lichen | -0.055 | 0.03 | -0.047 | 0.029 | -0.054 | 0.03 | -0.055 | 0.03 | -0.143** | 0.035 |
| Water | -0.088** | 0.022 | -0.080** | 0.022 | -0.088** | 0.022 | -0.087** | 0.022 | -0.260** | 0.025 |
| Snow/Glacier | -0.285** | 0.028 | -0.254** | 0.028 | -0.267** | 0.028 | -0.284** | 0.028 | -0.249** | 0.033 |
| Pine | 0.120** | 0.009 | 0.127** | 0.009 | 0.118** | 0.009 | | | 0.165** | 0.011 |
| Sub-alpine Spruce Transition | 0.107** | 0.01 | 0.096** | 0.01 | 0.102** | 0.01 | 0.122** | 0.009 | 0.087** | 0.012 |
| Spruce | 0.088** | 0.006 | 0.080** | 0.006 | 0.085** | 0.006 | 0.106** | 0.01 | 0.134** | 0.007 |
| Riparian Spruce | 0.043** | 0.007 | 0.050** | 0.007 | 0.044** | 0.007 | 0.088** | 0.006 | 0.136** | 0.007 |
| Dryas-dominated Alpine | 0.001 | 0.011 | -0.01 | 0.011 | -0.006 | 0.011 | 0.045** | 0.007 | -0.070** | 0.012 |
| Moist Alpine | 0.027 | 0.016 | 0.027 | 0.016 | 0.03 | 0.016 | 0.001 | 0.011 | -0.040* | 0.018 |
| Burned / Disturbed | 0.141** | 0.007 | 0.122** | 0.007 | 0.135** | 0.007 | 0.021 | 0.016 | 0.184** | 0.008 |
| Intercept | 0.431** | 0.013 | 0.462** | 0.012 | 0.456** | 0.012 | 0.144** | 0.007 | 0.138** | 0.005 |

* $p < .05$

** $p < .01$

[†] Reference Category 'no aspect' is not listed.

[‡] Reference Category 'rock' is not listed.

Table E10. Original $\beta$ coefficients and standard error ($\sigma$) for top five multiple linear regression models used to predict NDVI values for 24 Jun 2002 in the Greater Besa-Prophet Area in northern British Columbia.

| INPUTS | MODELS (by Adjusted $r^2$) | | | | | | | | | |
|---|---|---|---|---|---|---|---|---|---|---|
| | 0.552 | | 0.538 | | 0.487 | | 0.539 | | 0.545 | |
| | $\beta$ | $\sigma$ | $\beta$ | $\sigma$ | $\beta$ | $\sigma$ | $\beta$ | $\sigma$ | $\beta$ | $\sigma$ |
| **ANGLE OF INCIDENCE** | | | | | | | -0.038* | 0.015 | | |
| **SLOPE** | 0.001** | 0 | | | | | | | | |
| **ELEVATION (KM)** | -0.130** | 0.008 | -0.109** | 0.007 | | | -0.038* | 0.015 | -0.114** | 0.007 |
| **ASPECT**† | | | | | | | | | | |
| North | 0.007** | 0.003 | | | 0.004 | 0.003 | | | 0.007** | 0.003 |
| East | -0.001 | 0.002 | | | -0.005* | 0.003 | | | 0 | 0.002 |
| South | 0.001 | 0.003 | | | 0.001 | 0.003 | | | 0.002 | 0.003 |
| West | 0.011** | 0.003 | | | 0.011** | 0.003 | | | 0.012** | 0.003 |
| **VEGETATION TYPE**‡ | | | | | | | | | | |
| Sedge Wetland | 0.074** | 0.006 | 0.062** | 0.005 | 0.098** | 0.005 | 0.063** | 0.005 | 0.066** | 0.005 |
| Shrub | 0.127** | 0.005 | 0.122** | 0.005 | 0.137** | 0.005 | 0.124** | 0.005 | 0.123** | 0.005 |
| Low-productivity Spruce | 0.035** | 0.007 | 0.053** | 0.007 | 0.056** | 0.007 | 0.048** | 0.007 | 0.047** | 0.007 |
| Gravel Bar | -0.186** | 0.012 | -0.199** | 0.013 | -0.155** | 0.013 | -0.197** | 0.013 | -0.193** | 0.013 |
| Rock / Crustose Lichen | -0.075** | 0.028 | -0.079** | 0.029 | -0.137** | 0.03 | -0.079** | 0.029 | -0.082** | 0.029 |
| Water | -0.281** | 0.025 | -0.305** | 0.026 | -0.271** | 0.027 | -0.303** | 0.026 | -0.292** | 0.026 |
| Snow/Glacier | 0.075** | 0.006 | 0.066** | 0.005 | 0.075** | 0.006 | 0.067** | 0.005 | 0.065** | 0.005 |
| Pine | 0.100** | 0.014 | 0.112** | 0.014 | 0.075** | 0.015 | 0.107** | 0.014 | 0.107** | 0.014 |
| Sub-alpine Spruce Transition | 0.043** | 0.005 | 0.048** | 0.005 | 0.058** | 0.005 | 0.049** | 0.005 | 0.044** | 0.005 |
| Spruce | 0.032** | 0.005 | 0.023** | 0.005 | 0.052** | 0.005 | 0.025** | 0.005 | 0.024** | 0.005 |
| Riparian Spruce | 0.033** | 0.01 | 0.040** | 0.01 | 0.001 | 0.01 | 0.041** | 0.01 | 0.041** | 0.01 |
| Dryas-dominated Alpine | 0.004 | 0.015 | 0.01 | 0.015 | -0.035* | 0.016 | 0.009 | 0.015 | 0.007 | 0.015 |
| Moist Alpine | 0.144** | 0.005 | 0.153** | 0.005 | 0.163** | 0.005 | 0.156** | 0.005 | 0.152** | 0.005 |
| Burned / Disturbed | 0.462** | 0.01 | 0.454** | 0.01 | 0.313** | 0.004 | 0.470** | 0.012 | 0.458** | 0.01 |
| Intercept | 0.074** | 0.006 | 0.062** | 0.005 | 0.098** | 0.005 | 0.063** | 0.005 | 0.066** | 0.005 |

* $p < .05$

** $p < .01$

† Reference Category 'no aspect' is not listed.

‡ Reference Category 'rock' is not listed.

Table E11. Original $\beta$ coefficients and standard error ($\sigma$) for top five multiple linear regression models used to predict NDVI values for 09 Aug 2002 in the Greater Besa-Prophet Area in northern British Columbia.

| INPUTS | MODELS (by Adjusted $r^2$) | | | | | | | | | |
|---|---|---|---|---|---|---|---|---|---|---|
| | 0.607 | | 0.618 | | 0.616 | | 0.608 | | 0.613 | |
| | $\beta$ | $\sigma$ | $\beta$ | $\sigma$ | $\beta$ | $\sigma$ | $\beta$ | $\sigma$ | $\beta$ | $\sigma$ |
| **ANGLE OF INCIDENCE** | | | | | | | | | | |
| **SLOPE** | | | 0.001** | 0 | | | | | | |
| **ELEVATION (KM)** | | | -0.059** | 0.008 | -0.049** | 0.007 | | | -0.044** | 0.007 |
| **ASPECT**† | | | | | | | | | | |
| North | | | -0.005 | 0.004 | -0.006 | 0.004 | -0.007 | 0.004 | | |
| East | | | 0.008* | 0.003 | 0.009** | 0.003 | 0.005 | 0.003 | | |
| South | | | 0.012** | 0.004 | 0.012** | 0.004 | 0.010** | 0.004 | | |
| West | | | -0.002 | 0.004 | -0.002 | 0.004 | -0.004 | 0.004 | | |
| **VEGETATION TYPE**‡ | | | | | | | | | | |
| Sedge Wetland | 0.108** | 0.007 | 0.093** | 0.008 | 0.089** | 0.008 | 0.109** | 0.007 | 0.087** | 0.007 |
| Shrub | 0.159** | 0.006 | 0.159** | 0.006 | 0.156** | 0.006 | 0.155** | 0.006 | 0.160** | 0.006 |
| Low-productivity Spruce | 0.027** | 0.007 | 0.016* | 0.007 | 0.022** | 0.007 | 0.030** | 0.007 | 0.021** | 0.007 |
| Gravel Bar | -0.204** | 0.018 | -0.220** | 0.018 | -0.224** | 0.018 | -0.203** | 0.018 | -0.224** | 0.018 |
| Rock / Crustose Lichen | -0.166** | 0.033 | -0.132** | 0.032 | -0.134** | 0.033 | -0.162** | 0.033 | -0.141** | 0.033 |
| Water | -0.299** | 0.028 | -0.290** | 0.028 | -0.297** | 0.028 | -0.297** | 0.028 | -0.306** | 0.027 |
| Snow/Glacier | 0.064** | 0.008 | 0.062** | 0.008 | 0.057** | 0.008 | 0.062** | 0.008 | 0.061** | 0.007 |
| Pine | 0.137** | 0.01 | 0.144** | 0.01 | 0.144** | 0.01 | 0.136** | 0.01 | 0.146** | 0.01 |
| Sub-alpine Spruce Transition | 0.040** | 0.005 | 0.034** | 0.005 | 0.035** | 0.005 | 0.040** | 0.005 | 0.037** | 0.005 |
| Spruce | 0.037** | 0.007 | 0.019* | 0.007 | 0.016* | 0.007 | 0.036** | 0.007 | 0.020** | 0.007 |
| Riparian Spruce | 0.052** | 0.009 | 0.064** | 0.009 | 0.066** | 0.009 | 0.049** | 0.009 | 0.069** | 0.009 |
| Dryas-dominated Alpine | 0.040** | 0.01 | 0.064** | 0.011 | 0.066** | 0.011 | 0.046** | 0.011 | 0.059** | 0.011 |
| Moist Alpine | 0.179** | 0.006 | 0.161** | 0.006 | 0.167** | 0.006 | 0.175** | 0.006 | 0.174** | 0.006 |
| Burned / Disturbed | 0.317** | 0.004 | 0.388** | 0.011 | 0.385** | 0.011 | 0.318** | 0.004 | 0.378** | 0.011 |
| Intercept | 0.108** | 0.007 | 0.093** | 0.008 | 0.089** | 0.008 | 0.109** | 0.007 | 0.087** | 0.007 |

* $p < .05$

** $p < .01$

† Reference Category 'no aspect' is not listed.

‡ Reference Category 'rock' is not listed.

Table E12. Original $\beta$ coefficients and standard error ($\sigma$) for top five multiple linear regression models used to predict NDVI values for 09 May 2003 in the Greater Besa-Prophet Area in northern British Columbia.

| INPUTS | MODELS (by Adjusted $r^2$) | | | | | | | | | |
|---|---|---|---|---|---|---|---|---|---|---|
| | 0.25 | | 0.249 | | 0.231 | | 0.199 | | 0.219 | |
| | $\beta$ | $\sigma$ | $\beta$ | $\sigma$ | $\beta$ | $\sigma$ | $\beta$ | $\sigma$ | $\beta$ | $\sigma$ |
| **ANGLE OF INCIDENCE** | | | | | 0.270** | 0.015 | | | 0.268** | 0.015 |
| **SLOPE** | -0.003** | 0 | -0.003** | 0 | | | | | | |
| **ELEVATION (KM)** | -0.019* | 0.009 | | | -0.051** | 0.009 | -0.055** | 0.009 | | |
| **ASPECT**† | | | | | | | | | | |
| North | -0.050** | 0.004 | -0.050** | 0.004 | | | -0.053** | 0.005 | | |
| East | 0.017** | 0.004 | 0.017** | 0.004 | | | 0.011** | 0.004 | | |
| South | 0.048** | 0.005 | 0.047** | 0.005 | | | 0.047** | 0.005 | | |
| West | -0.016** | 0.004 | -0.015** | 0.004 | | | -0.017** | 0.004 | | |
| **VEGETATION TYPE**‡ | | | | | | | | | | |
| Sedge Wetland | -0.002 | 0.01 | 0.005 | 0.01 | 0.013 | 0.01 | 0.015 | 0.011 | 0.039** | 0.009 |
| Shrub | -0.002 | 0.007 | -0.002 | 0.007 | -0.004 | 0.007 | 0.004 | 0.007 | -0.003 | 0.007 |
| Low-productivity Spruce | -0.001 | 0.01 | 0.004 | 0.009 | -0.011 | 0.009 | -0.027** | 0.01 | 0 | 0.009 |
| Gravel Bar | -0.124** | 0.028 | -0.119** | 0.028 | -0.097** | 0.028 | -0.103** | 0.029 | -0.077** | 0.028 |
| Rock / Crustose Lichen | 0.127** | 0.029 | 0.121** | 0.029 | 0.108** | 0.03 | 0.113** | 0.03 | 0.086** | 0.03 |
| Water | 0.104** | 0.019 | 0.090** | 0.018 | 0.112** | 0.02 | 0.125** | 0.02 | 0.072** | 0.018 |
| Snow/Glacier | -0.083** | 0.031 | -0.082** | 0.031 | -0.042 | 0.031 | -0.055 | 0.032 | -0.032 | 0.031 |
| Pine | -0.060** | 0.01 | -0.058** | 0.01 | -0.046** | 0.01 | -0.040** | 0.01 | -0.036** | 0.01 |
| Sub-alpine Spruce Transition | -0.054** | 0.011 | -0.055** | 0.011 | -0.052** | 0.011 | -0.059** | 0.011 | -0.057** | 0.011 |
| Spruce | 0 | 0.006 | 0.003 | 0.006 | -0.012 | 0.006 | -0.009 | 0.007 | -0.003 | 0.006 |
| Riparian Spruce | 0.020* | 0.009 | 0.027** | 0.008 | 0.024** | 0.009 | 0.035** | 0.009 | 0.047** | 0.008 |
| Dryas-dominated Alpine | 0.056** | 0.011 | 0.052** | 0.011 | 0.058** | 0.011 | 0.046** | 0.012 | 0.042** | 0.011 |
| Moist Alpine | 0.019 | 0.016 | 0.014 | 0.016 | 0.001 | 0.017 | 0.013 | 0.017 | -0.014 | 0.016 |
| Burned / Disturbed | -0.036** | 0.008 | -0.031** | 0.008 | -0.069** | 0.008 | -0.062** | 0.008 | -0.060** | 0.008 |
| Intercept | 0.073** | 0.014 | 0.048** | 0.006 | -0.036* | 0.015 | 0.084** | 0.014 | -0.110** | 0.007 |

* $p < .05$

** $p < .01$

† Reference Category 'no aspect' is not listed.

‡ Reference Category 'rock' is not listed.

Table E13. Original $\beta$ coefficients and standard error ($\sigma$) for top five multiple linear regression models used to predict NDVI values for 25 Jun 2003 in the Greater Besa-Prophet Area in northern British Columbia.

| INPUTS | MODELS (by Adjusted $r^2$) | | | | | | | | | |
|---|---|---|---|---|---|---|---|---|---|---|
| | 0.236 | | 0.193 | | 0.194 | | 0.216 | | 0.196 | |
| | $\beta$ | $\sigma$ | $\beta$ | $\sigma$ | $\beta$ | $\sigma$ | $\beta$ | $\sigma$ | $\beta$ | $\sigma$ |
| **ANGLE OF INCIDENCE** | | | | | -0.053 | 0.028 | | | | |
| **SLOPE** | 0.004** | 0 | | | | | | | | |
| **ELEVATION (KM)** | -0.121** | 0.016 | -0.053** | 0.015 | -0.052** | 0.015 | | | -0.054** | 0.015 |
| **ASPECT**† | | | | | | | | | | |
| North | 0.006 | 0.007 | | | | | 0.006 | 0.007 | 0.009 | 0.007 |
| East | 0.011 | 0.006 | | | | | 0.007 | 0.006 | 0.014* | 0.006 |
| South | -0.020** | 0.007 | | | | | -0.023** | 0.007 | -0.018* | 0.008 |
| West | -0.008 | 0.007 | | | | | -0.007 | 0.007 | -0.005 | 0.007 |
| **VEGETATION TYPE**‡ | | | | | | | | | | |
| Sedge Wetland | 0.055** | 0.014 | 0.029* | 0.014 | 0.032* | 0.014 | 0.088** | 0.014 | 0.029 | 0.015 |
| Shrub | 0.110** | 0.012 | 0.092** | 0.012 | 0.095** | 0.012 | 0.105** | 0.012 | 0.094** | 0.013 |
| Low-productivity Spruce | 0.033* | 0.014 | 0.068** | 0.014 | 0.063** | 0.014 | 0.060** | 0.014 | 0.069** | 0.014 |
| Gravel Bar | -0.083 | 0.046 | -0.107* | 0.047 | -0.105* | 0.047 | -0.054 | 0.047 | -0.109* | 0.048 |
| Rock / Crustose Lichen | -0.075 | 0.056 | -0.088 | 0.058 | -0.091 | 0.058 | -0.123* | 0.057 | -0.086 | 0.058 |
| Water | -0.161** | 0.062 | -0.205** | 0.063 | -0.203** | 0.063 | -0.165** | 0.063 | -0.203** | 0.064 |
| Snow/Glacier | 0.026 | 0.016 | 0.006 | 0.016 | 0.01 | 0.016 | 0.035* | 0.016 | 0.003 | 0.016 |
| Pine | 0.081** | 0.022 | 0.098** | 0.022 | 0.096** | 0.022 | 0.065** | 0.022 | 0.097** | 0.023 |
| Sub-alpine Spruce Transition | 0.026* | 0.011 | 0.041** | 0.011 | 0.041** | 0.011 | 0.045** | 0.011 | 0.038** | 0.011 |
| Spruce | -0.027* | 0.012 | -0.048** | 0.012 | -0.045** | 0.012 | 0.003 | 0.012 | -0.051** | 0.012 |
| Riparian Spruce | 0.064** | 0.019 | 0.075** | 0.019 | 0.074** | 0.019 | 0.03 | 0.019 | 0.076** | 0.02 |
| Dryas-dominated Alpine | 0.029 | 0.028 | 0.038 | 0.029 | 0.032 | 0.029 | -0.011 | 0.028 | 0.037 | 0.029 |
| Moist Alpine | 0.088** | 0.012 | 0.124** | 0.012 | 0.128** | 0.012 | 0.111** | 0.012 | 0.125** | 0.012 |
| Burned / Disturbed | 0.222** | 0.022 | 0.197** | 0.022 | 0.220** | 0.025 | 0.077** | 0.01 | 0.197** | 0.022 |
| Intercept | 0.055** | 0.014 | 0.029* | 0.014 | 0.032* | 0.014 | 0.088** | 0.014 | 0.029 | 0.015 |

* $p < .05$

** $p < .01$

† Reference Category 'no aspect' is not listed.

‡ Reference Category 'rock' is not listed.

Table E14. Original $\beta$ coefficients and standard error ($\sigma$) for top five multiple linear regression models used to predict NDVI values for 29 Jul 2003 in the Greater Besa-Prophet Area in northern British Columbia.

| INPUTS | MODELS (by Adjusted $r^2$) | | | | | | | | | |
|---|---|---|---|---|---|---|---|---|---|---|
| | 0.605 | | 0.604 | | 0.606 | | 0.612 | | 0.613 | |
| | $\beta$ | $\sigma$ | $\beta$ | $\sigma$ | $\beta$ | $\sigma$ | $\beta$ | $\sigma$ | $\beta$ | $\sigma$ |
| **ANGLE OF INCIDENCE** | 0.038** | 0.015 | | | | | | | | |
| **SLOPE** | | | | | | | | | 0 | 0 |
| **ELEVATION (KM)** | -0.035** | 0.007 | -0.034** | 0.007 | | | -0.038** | 0.007 | -0.043** | 0.007 |
| **ASPECT**[†] | | | | | | | | | | |
| North | | | | | -0.005 | 0.003 | -0.005 | 0.002 | -0.005 | 0.002 |
| East | | | | | -0.001 | 0.002 | 0.001 | 0.002 | 0.001 | 0.002 |
| South | | | | | 0.018** | 0.003 | 0.019** | 0.003 | 0.019** | 0.003 |
| West | | | | | -0.001 | 0.003 | -0.001 | 0.003 | -0.001 | 0.003 |
| **VEGETATION TYPE**[‡] | | | | | | | | | | |
| Sedge Wetland | 0.101** | 0.006 | 0.103** | 0.006 | 0.117** | 0.006 | 0.103** | 0.006 | 0.105** | 0.006 |
| Shrub | 0.151** | 0.006 | 0.153** | 0.006 | 0.156** | 0.006 | 0.149** | 0.006 | 0.150** | 0.006 |
| Low-productivity Spruce | 0.061** | 0.007 | 0.057** | 0.007 | 0.063** | 0.006 | 0.057** | 0.007 | 0.054** | 0.007 |
| Gravel Bar | -0.132** | 0.014 | -0.131** | 0.014 | -0.113** | 0.014 | -0.128** | 0.014 | -0.126** | 0.014 |
| Rock / Crustose Lichen | -0.196** | 0.015 | -0.198** | 0.015 | -0.218** | 0.015 | -0.198** | 0.015 | -0.198** | 0.015 |
| Water | -0.433** | 0.054 | -0.432** | 0.054 | -0.424** | 0.054 | -0.418** | 0.053 | -0.414** | 0.053 |
| Snow/Glacier | 0.090** | 0.007 | 0.092** | 0.007 | 0.094** | 0.007 | 0.090** | 0.007 | 0.092** | 0.007 |
| Pine | 0.157** | 0.011 | 0.154** | 0.011 | 0.146** | 0.011 | 0.156** | 0.011 | 0.154** | 0.011 |
| Sub-alpine Spruce Transition | 0.055** | 0.006 | 0.056** | 0.006 | 0.062** | 0.005 | 0.054** | 0.006 | 0.054** | 0.006 |
| Spruce | 0.042** | 0.006 | 0.043** | 0.006 | 0.054** | 0.005 | 0.042** | 0.006 | 0.043** | 0.006 |
| Riparian Spruce | 0.033** | 0.011 | 0.034** | 0.011 | 0.016 | 0.01 | 0.029** | 0.011 | 0.029** | 0.011 |
| Dryas-dominated Alpine | 0.054** | 0.015 | 0.051** | 0.015 | 0.041** | 0.015 | 0.057** | 0.015 | 0.055** | 0.015 |
| Moist Alpine | 0.175** | 0.006 | 0.178** | 0.006 | 0.175** | 0.006 | 0.171** | 0.006 | 0.169** | 0.006 |
| Burned / Disturbed | 0.307** | 0.011 | 0.321** | 0.01 | 0.276** | 0.005 | 0.327** | 0.01 | 0.329** | 0.01 |
| Intercept | 0.101** | 0.006 | 0.103** | 0.006 | 0.117** | 0.006 | 0.103** | 0.006 | 0.105** | 0.006 |

* $p < .05$

** $p < .01$

[†] Reference Category 'no aspect' is not listed.

[‡] Reference Category 'rock' is not listed.

**APPENDIX F: Coefficients of multiple linear regression models using 'transition zone' class to predict NDVI values in the Greater Besa-Prophet Area in northern British Columbia, 2001-2003**

Table F1. $\beta$ coefficients standard error ($\sigma$) for multiple linear regression models that included a transition zone class used to predict NDVI values for 04 Jun 2001 in the Greater Besa-Prophet Area in northern British Columbia.

| INPUTS | MODELS (by Adjusted $r^2$) | | | | | | | | | |
|---|---|---|---|---|---|---|---|---|---|---|
| | 0.606 | | 0.588 | | **0.656** | | **0.578** | | **0.537** | |
| | ***β*** | ***σ*** | ***β*** | ***σ*** | ***β*** | ***σ*** | ***β*** | ***σ*** | ***β*** | ***σ*** |
| **ANGLE OF INCIDENCE** | | | 0.157** | 0.015 | | | | | 0.137** | 0.016 |
| **SLOPE** | -0.002** | 0 | | | | | -0.003** | 0 | | |
| **ELEVATION (KM)** | -0.118** | 0.01 | -0.148** | 0.009 | -0.139** | 0.009 | | | | |
| **ASPECT**† | | | | | | | | | | |
| North | -0.038** | 0.005 | | | | | -0.038** | 0.005 | | |
| East | 0.023** | 0.004 | | | | | 0.018** | 0.004 | | |
| South | 0.030** | 0.005 | | | | | 0.023** | 0.005 | | |
| West | 0.004 | 0.004 | | | | | 0.004 | 0.005 | | |
| **VEGETATION TYPE**‡ | | | | | | | | | | |
| Sedge Wetland | 0.096** | 0.011 | 0.097** | 0.011 | 0.106** | 0.012 | 0.148** | 0.011 | 0.184** | 0.01 |
| Shrub | -0.012 | 0.007 | -0.005 | 0.007 | 0.002 | 0.007 | -0.012 | 0.007 | -0.003 | 0.008 |
| Low-productivity Spruce | 0.105** | 0.01 | 0.093** | 0.01 | 0.074** | 0.01 | 0.145** | 0.01 | 0.133** | 0.011 |
| Gravel Bar | -0.216** | 0.027 | -0.205** | 0.027 | -0.196** | 0.028 | -0.180** | 0.027 | -0.142** | 0.028 |
| Rock / Crustose Lichen | -0.077* | 0.032 | -0.071* | 0.033 | -0.072* | 0.034 | -0.129** | 0.033 | -0.140** | 0.035 |
| Water | 0.140** | 0.019 | 0.147** | 0.02 | 0.145** | 0.02 | 0.044* | 0.018 | 0.021 | 0.019 |
| Snow/Glacier | -0.302** | 0.036 | -0.291** | 0.035 | -0.287** | 0.036 | -0.312** | 0.037 | -0.268** | 0.037 |
| Pine | 0.116** | 0.012 | 0.129** | 0.012 | 0.136** | 0.012 | 0.135** | 0.012 | 0.161** | 0.012 |
| Sub-alpine Spruce Transition | 0.040** | 0.012 | 0.042** | 0.012 | 0.041** | 0.013 | 0.036** | 0.012 | 0.032* | 0.013 |
| Spruce | 0.105** | 0.007 | 0.099** | 0.007 | 0.098** | 0.007 | 0.132** | 0.007 | 0.129** | 0.007 |
| Riparian Spruce | 0.082** | 0.009 | 0.087** | 0.009 | 0.097** | 0.01 | 0.131** | 0.008 | 0.164** | 0.008 |
| Dryas-dominated Alpine | -0.019 | 0.011 | -0.011 | 0.011 | -0.011 | 0.011 | -0.043** | 0.011 | -0.053** | 0.011 |
| Moist Alpine | -0.042* | 0.017 | -0.064** | 0.018 | -0.077** | 0.018 | -0.072** | 0.018 | -0.108** | 0.018 |
| Burned / Disturbed | 0.053** | 0.008 | 0.033** | 0.008 | 0.050** | 0.008 | 0.089** | 0.008 | 0.066** | 0.008 |
| Transition Zone | -0.041** | 0.011 | -0.045** | 0.011 | -0.058** | 0.011 | -0.044** | 0.011 | -0.069** | 0.011 |
| Intercept | 0.307** | 0.014 | 0.254** | 0.015 | 0.303** | 0.015 | 0.146** | 0.006 | 0.039** | 0.008 |

* $p < .05$

** $p < .01$

† Reference Category 'no aspect' is not listed. ‡ Reference Category 'rock' is not listed

Table F2. $\beta$ coefficients and standard error ($\sigma$) for multiple linear regression models that included a transition zone class used to predict NDVI values for 22 Jul 2001 in the Greater Besa-Prophet Area in northern British Columbia.

| INPUTS | MODELS (by Adjusted $r^2$) | | | | | |
|---|---|---|---|---|---|---|
| | 0.677 | | 0.674 | | 0.65 | |
| | $\beta$ | $\sigma$ | $\beta$ | $\sigma$ | $\beta$ | $\sigma$ |
| **ANGLE OF INCIDENCE** | | | | | | |
| **SLOPE** | | | | | | |
| **ELEVATION (KM)** | -0.102** | 0.008 | -0.098** | 0.008 | | |
| **ASPECT**[†] | | | | | | |
| North | 2 1 | 0 | | | | |
| East | 3 2 | 0.008* | | | | |
| South | 4 3 | 0.015** | | | | |
| West | 5 4 | -0.003 | | | | |
| **VEGETATION TYPE**[‡] | | | | | | |
| Sedge Wetland | 0.107** | 0.008 | 0.104** | 0.008 | 0.150** | 0.007 |
| Shrub | 0.188** | 0.007 | 0.189** | 0.007 | 0.201** | 0.007 |
| Low-productivity Spruce | 0.062** | 0.008 | 0.061** | 0.008 | 0.082** | 0.008 |
| Gravel Bar | -0.171** | 0.018 | -0.177** | 0.018 | -0.131** | 0.018 |
| Rock / Crustose Lichen | -0.145** | 0.034 | -0.144** | 0.034 | -0.189** | 0.035 |
| Water | -0.174** | 0.025 | -0.176** | 0.025 | -0.271** | 0.025 |
| Snow/Glacier | -0.272** | 0.053 | -0.278** | 0.053 | -0.228** | 0.054 |
| Pine | 0.097** | 0.009 | 0.100** | 0.009 | 0.115** | 0.009 |
| Sub-alpine Spruce Transition | 0.182** | 0.014 | 0.183** | 0.014 | 0.168** | 0.014 |
| Spruce | 0.058** | 0.007 | 0.060** | 0.006 | 0.080** | 0.006 |
| Riparian Spruce | 0.048** | 0.007 | 0.050** | 0.007 | 0.090** | 0.006 |
| Dryas-dominated Alpine | 0.090** | 0.011 | 0.094** | 0.011 | 0.064** | 0.011 |
| Moist Alpine | 0.058** | 0.021 | 0.053** | 0.021 | 0.018 | 0.021 |
| Burned / Disturbed | 0.189** | 0.007 | 0.196** | 0.007 | 0.213** | 0.007 |
| Transition Zone | -0.103** | 0.012 | -0.102** | 0.012 | -0.113** | 0.013 |
| Intercept | 0.415** | 0.012 | 0.411** | 0.012 | 0.274** | 0.005 |

* $p < .05$

** $p < .01$

[†] Reference Category 'no aspect' is not listed. [‡] Reference Category 'rock' is not listed.

Table F3. $\beta$ coefficients and standard error ($\sigma$) for multiple linear regression models that included a transition zone class used to predict NDVI values for 15 Aug 2001 in the Greater Besa-Prophet Area in northern British Columbia.

| INPUTS | MODELS (by Adjusted $r^2$) | | | | | | | |
|---|---|---|---|---|---|---|---|---|
| | 0.868 | | 0.865 | | 0.864 | | 0.86 | |
| | $\beta$ | $\sigma$ | $\beta$ | $\sigma$ | $\beta$ | $\sigma$ | $\beta$ | $\sigma$ |
| **ANGLE OF INCIDENCE** | | | | | | | | |
| **SLOPE** | | | | | | | | |
| **ELEVATION (KM)** | -0.058** | 0.007 | -0.054** | 0.007 | | | | |
| **ASPECT**[†] | | | | | | | | |
| North | -0.013** | 0.003 | | | -0.013** | 0.003 | | |
| East | 0.010** | 0.003 | | | 0.008* | 0.003 | | |
| South | 0.021** | 0.003 | | | 0.019** | 0.003 | | |
| West | -0.003 | 0.003 | | | -0.005 | 0.003 | | |
| **VEGETATION TYPE**[‡] | | | | | | | | |
| Sedge Wetland | 0.134** | 0.008 | 0.134** | 0.008 | 0.165** | 0.007 | 0.164** | 0.007 |
| Shrub | 0.214** | 0.006 | 0.222** | 0.006 | 0.215** | 0.006 | 0.222** | 0.006 |
| Low-productivity Spruce | 0.065** | 0.007 | 0.061** | 0.007 | 0.082** | 0.007 | 0.077** | 0.007 |
| Gravel Bar | -0.114** | 0.02 | -0.117** | 0.02 | -0.088** | 0.02 | -0.091** | 0.021 |
| Rock / Crustose Lichen | -0.157** | 0.033 | -0.162** | 0.033 | -0.178** | 0.033 | -0.183** | 0.034 |
| Water | -0.353** | 0.014 | -0.354** | 0.015 | -0.401** | 0.013 | -0.400** | 0.014 |
| Snow/Glacier | -0.428** | 0.023 | -0.437** | 0.022 | -0.423** | 0.023 | -0.428** | 0.023 |
| Pine | 0.119** | 0.008 | 0.122** | 0.008 | 0.131** | 0.008 | 0.133** | 0.008 |
| Sub-alpine Spruce Transition | 0.194** | 0.007 | 0.196** | 0.007 | 0.190** | 0.007 | 0.192** | 0.007 |
| Spruce | 0.086** | 0.005 | 0.086** | 0.005 | 0.099** | 0.005 | 0.097** | 0.005 |
| Riparian Spruce | 0.068** | 0.006 | 0.071** | 0.007 | 0.096** | 0.006 | 0.097** | 0.006 |
| Dryas-dominated Alpine | 0.109** | 0.009 | 0.116** | 0.009 | 0.093** | 0.009 | 0.100** | 0.009 |
| Moist Alpine | 0.123** | 0.012 | 0.112** | 0.012 | 0.107** | 0.012 | 0.097** | 0.012 |
| Burned / Disturbed | 0.230** | 0.006 | 0.240** | 0.006 | 0.242** | 0.006 | 0.250** | 0.006 |
| Transition Zone | -0.049** | 0.008 | -0.047** | 0.008 | -0.060** | 0.008 | -0.058** | 0.008 |
| Intercept | 0.311** | 0.01 | 0.306** | 0.011 | 0.224** | 0.004 | 0.224** | 0.003 |

* $p < .05$

** $p < .01$

[†] Reference Category 'no aspect' is not listed. [‡]Reference Category 'rock' is not listed

Table F4. $\beta$ coefficients and standard error ($\sigma$) for multiple linear regression models that included a transition zone class used to predict NDVI values for 16-September-01 in the Greater Besa-Prophet Area in northern British Columbia.

| INPUTS | MODELS (by Adjusted $r^2$) | | | | | | | | | |
|---|---|---|---|---|---|---|---|---|---|---|
| | 0.815 | | 0.804 | | 0.787 | | 0.803 | | 0.792 | |
| | $\beta$ | $\sigma$ | $\beta$ | $\sigma$ | $\beta$ | $\sigma$ | $\beta$ | $\sigma$ | $\beta$ | $\sigma$ |
| **ANGLE OF INCIDENCE** | | | 0.145** | 0.011 | | | | | 0.133** | 0.011 |
| **SLOPE** | | | | | | | | | | |
| **ELEVATION (KM)** | -0.083** | 0.007 | -0.085** | 0.008 | -0.075** | 0.008 | | | | |
| **ASPECT**† | | | | | | | | | | |
| North | -0.038** | 0.003 | | | | | -0.038** | 0.003 | | |
| East | 0.017** | 0.003 | | | | | 0.014** | 0.003 | | |
| South | 0.036** | 0.003 | | | | | 0.035** | 0.003 | | |
| West | 0.007* | 0.003 | | | | | 0.006 | 0.003 | | |
| **VEGETATION TYPE**‡ | | | | | | | | | | |
| Sedge Wetland | 0.091** | 0.01 | 0.080** | 0.01 | 0.087** | 0.01 | 0.125** | 0.009 | 0.117** | 0.009 |
| Shrub | 0.105** | 0.006 | 0.108** | 0.006 | 0.116** | 0.006 | 0.104** | 0.006 | 0.106** | 0.006 |
| Low-productivity Spruce | 0.039** | 0.007 | 0.042** | 0.008 | 0.027** | 0.008 | 0.062** | 0.007 | 0.064** | 0.007 |
| Gravel Bar | -0.220** | 0.044 | -0.218** | 0.045 | -0.210** | 0.047 | -0.178** | 0.045 | -0.171** | 0.046 |
| Rock / Crustose Lichen | -0.090** | 0.019 | -0.079** | 0.02 | -0.080** | 0.021 | -0.121** | 0.02 | -0.112** | 0.02 |
| Water | -0.231** | 0.014 | -0.234** | 0.015 | -0.245** | 0.015 | -0.292** | 0.014 | -0.297** | 0.014 |
| Snow/Glacier | -0.241** | 0.021 | -0.268** | 0.02 | -0.266** | 0.021 | -0.246** | 0.022 | -0.268** | 0.021 |
| Pine | 0.125** | 0.008 | 0.124** | 0.008 | 0.130** | 0.008 | 0.146** | 0.008 | 0.145** | 0.008 |
| Sub-alpine Spruce Transition | 0.159** | 0.008 | 0.163** | 0.008 | 0.160** | 0.008 | 0.157** | 0.008 | 0.160** | 0.008 |
| Spruce | 0.095** | 0.005 | 0.096** | 0.005 | 0.095** | 0.005 | 0.110** | 0.005 | 0.111** | 0.005 |
| Riparian Spruce | 0.079** | 0.007 | 0.077** | 0.007 | 0.084** | 0.007 | 0.113** | 0.006 | 0.112** | 0.006 |
| Dryas-dominated Alpine | 0.067** | 0.008 | 0.081** | 0.008 | 0.083** | 0.008 | 0.046** | 0.008 | 0.058** | 0.008 |
| Moist Alpine | 0.078** | 0.011 | 0.066** | 0.011 | 0.048** | 0.012 | 0.055** | 0.011 | 0.042** | 0.011 |
| Burned / Disturbed | 0.137** | 0.007 | 0.140** | 0.007 | 0.158** | 0.007 | 0.152** | 0.007 | 0.155** | 0.007 |
| Transition Zone | -0.042** | 0.007 | -0.032** | 0.007 | -0.034** | 0.008 | -0.052** | 0.008 | -0.044** | 0.008 |
| Intercept | 0.226** | 0.012 | 0.198** | 0.012 | 0.216** | 0.013 | 0.099** | 0.004 | 0.070** | 0.005 |

* $p < .05$

** $p < .01$

† Reference Category 'no aspect' is not listed. ‡ Reference Category 'rock' is not listed.

Table F5. $\beta$ coefficients and standard error ($\sigma$) for multiple linear regression models that included a transition zone class used to predict NDVI values for 01 October 2001 in the Greater Besa-Prophet Area in northern British Columbia.

| INPUTS | MODELS (by Adjusted $r^2$) | | | | | | | | | |
|---|---|---|---|---|---|---|---|---|---|---|
| | 0.5 | | 0.489 | | 0.478 | | 0.449 | | 0.47 | |
| | $\beta$ | $\sigma$ | $\beta$ | $\sigma$ | $\beta$ | $\sigma$ | $\beta$ | $\sigma$ | $\beta$ | $\sigma$ |
| **ANGLE OF INCIDENCE** | | | | | | | | | 0.249** | 0.014 |
| **SLOPE** | -0.001** | 0 | | | -0.002** | 0 | | | | |
| **ELEVATION (KM)** | -0.069** | 0.007 | -0.086** | 0.007 | | | | | -0.083** | 0.007 |
| **ASPECT**[†] | | | | | | | | | | |
| North | -0.052** | 0.003 | -0.052** | 0.003 | -0.052** | 0.003 | -0.052** | 0.003 | | |
| East | 0.024** | 0.003 | 0.022** | 0.003 | 0.022** | 0.003 | 0.018** | 0.003 | | |
| South | 0.036** | 0.003 | 0.036** | 0.003 | 0.034** | 0.003 | 0.032** | 0.004 | | |
| West | 0.002 | 0.003 | 0 | 0.003 | 0 | 0.003 | -0.003 | 0.003 | | |
| **VEGETATION TYPE**[‡] | | | | | | | | | | |
| Sedge Wetland | 0.073** | 0.007 | 0.082** | 0.007 | 0.095** | 0.007 | 0.120** | 0.007 | 0.072** | 0.007 |
| Shrub | 0.039** | 0.005 | 0.045** | 0.005 | 0.035** | 0.005 | 0.043** | 0.005 | 0.040** | 0.005 |
| Low-productivity Spruce | 0.016* | 0.006 | 0.005 | 0.006 | 0.031** | 0.006 | 0.020** | 0.006 | 0.017** | 0.006 |
| Gravel Bar | -0.110** | 0.016 | -0.101** | 0.017 | -0.091** | 0.017 | -0.067** | 0.017 | -0.107** | 0.017 |
| Rock / Crustose Lichen | -0.093** | 0.019 | -0.093** | 0.019 | -0.117** | 0.019 | -0.128** | 0.019 | -0.088** | 0.019 |
| Water | -0.161** | 0.026 | -0.147** | 0.026 | -0.158** | 0.027 | -0.134** | 0.027 | -0.145** | 0.027 |
| Snow/Glacier | 0.095** | 0.006 | 0.106** | 0.006 | 0.095** | 0.007 | 0.114** | 0.006 | 0.099** | 0.006 |
| Pine | 0.065** | 0.008 | 0.065** | 0.008 | 0.055** | 0.008 | 0.050** | 0.009 | 0.073** | 0.008 |
| Sub-alpine Spruce Transition | 0.063** | 0.004 | 0.061** | 0.004 | 0.068** | 0.004 | 0.067** | 0.004 | 0.054** | 0.004 |
| Spruce | 0.050** | 0.006 | 0.058** | 0.006 | 0.066** | 0.006 | 0.087** | 0.006 | 0.056** | 0.006 |
| Riparian Spruce | 0.024** | 0.008 | 0.023** | 0.008 | 0.002 | 0.008 | -0.01 | 0.008 | 0.029** | 0.008 |
| Dryas-dominated Alpine | -0.029** | 0.01 | -0.032** | 0.01 | -0.051** | 0.01 | -0.066** | 0.01 | -0.038** | 0.01 |
| Moist Alpine | 0.072** | 0.005 | 0.062** | 0.005 | 0.085** | 0.005 | 0.074** | 0.005 | 0.052** | 0.005 |
| Burned / Disturbed | -0.031** | 0.009 | -0.046** | 0.009 | -0.035** | 0.009 | -0.063** | 0.009 | -0.036** | 0.009 |
| Transition Zone | 0.202** | 0.01 | 0.205** | 0.01 | 0.118** | 0.004 | 0.086** | 0.003 | 0.158** | 0.01 |
| Intercept | 0.073** | 0.007 | 0.082** | 0.007 | 0.095** | 0.007 | 0.120** | 0.007 | 0.072** | 0.007 |

* $p < .05$

** $p < .01$

[†] Reference Category 'no aspect' is not listed. [‡] Reference Category 'rock' is not listed.

**APPENDIX G: Per-class minimum (min), maximum (max), mean, standard deviation (s) and range for NDVI and NDVI derived from multiple linear regression (MNDVI) in the Greater Besa-Prophet Area in northern British Columbia, 2001.**

Table G1. Per-class minimum (min), maximum (max), mean, standard deviation (s) and range for NDVI and NDVI derived from multiple linear regression (MNDVI) analysis for June 2001 in the Greater Besa-Prophet Area in northern British Columbia.

| VEGETATION CLASS | NDVI MIN | MNDVI MIN | NDVI MAX | MNDVI MAX | NDVI MEAN | MNDVI MEAN | NDVI RANGE | MNDVI RANGE | NDVI s | MNDVI s |
|---|---|---|---|---|---|---|---|---|---|---|
| **Sedge Wetland** | -0.408 | -0.021 | 0.528 | 0.354 | 0.265 | 0.282 | 0.936 | 0.375 | 0.121 | 0.033 |
| **Shrub** | -0.321 | -0.155 | 0.577 | 0.350 | 0.106 | 0.112 | 0.898 | 0.505 | 0.122 | 0.063 |
| **Low-Productivity Spruce** | -0.240 | 0.070 | 0.476 | 0.355 | 0.213 | 0.214 | 0.717 | 0.285 | 0.068 | 0.046 |
| **Pine** | -0.216 | -0.008 | 0.472 | 0.347 | 0.248 | 0.260 | 0.688 | 0.355 | 0.080 | 0.031 |
| **Sub-alpine Spruce Transition** | -0.287 | -0.111 | 0.471 | 0.208 | 0.121 | 0.128 | 0.758 | 0.319 | 0.109 | 0.033 |
| **Spruce** | -0.344 | -0.081 | 0.499 | 0.356 | 0.222 | 0.224 | 0.843 | 0.437 | 0.088 | 0.048 |
| **Riparian Spruce** | -0.346 | -0.025 | 0.489 | 0.340 | 0.261 | 0.261 | 0.835 | 0.365 | 0.079 | 0.035 |
| **Dryas Alpine** | -0.244 | -0.132 | 0.401 | 0.137 | 0.049 | 0.050 | 0.645 | 0.269 | 0.089 | 0.024 |
| **Moist Alpine** | -0.266 | -0.206 | 0.331 | 0.094 | -0.009 | -0.014 | 0.597 | 0.300 | 0.099 | 0.028 |
| **Burned / Disturbed** | -0.332 | -0.014 | 0.541 | 0.296 | 0.168 | 0.177 | 0.873 | 0.309 | 0.092 | 0.038 |
| **Sedge Wetland** | -0.370 | -0.230 | 0.466 | 0.217 | 0.011 | 0.014 | 0.836 | 0.448 | 0.101 | 0.042 |

Table G2. Per-class minimum (min), maximum (max), mean, standard deviation (s) and range for NDVI and NDVI derived from multiple linear regression (MNDVI) analysis for July 2001 in the Greater Besa-Prophet Area in northern British Columbia.

| VEGETATION CLASS | NDVI MIN | MNDVI MIN | NDVI MAX | MNDVI MAX | NDVI MEAN | MNDVI MEAN | NDVI RANGE | MNDVI RANGE | NDVI s | MNDVI s |
|---|---|---|---|---|---|---|---|---|---|---|
| **Sedge Wetland** | -0.378 | 0.306 | 0.647 | 0.472 | 0.421 | 0.424 | 1.025 | 0.166 | 0.079 | 0.018 |
| **Shrub** | -0.448 | -0.003 | 0.716 | 0.554 | 0.460 | 0.466 | 1.164 | 0.557 | 0.088 | 0.049 |
| **Low-Productivity Spruce** | -0.247 | 0.298 | 0.627 | 0.426 | 0.360 | 0.357 | 0.874 | 0.128 | 0.063 | 0.021 |
| **Pine** | -0.030 | 0.322 | 0.634 | 0.452 | 0.399 | 0.391 | 0.664 | 0.130 | 0.052 | 0.015 |
| **Sub-alpine Spruce Transition** | -0.090 | 0.407 | 0.694 | 0.476 | 0.436 | 0.441 | 0.783 | 0.069 | 0.066 | 0.009 |
| **Spruce** | -0.281 | 0.279 | 0.652 | 0.423 | 0.355 | 0.356 | 0.933 | 0.143 | 0.064 | 0.023 |
| **Riparian Spruce** | -0.315 | 0.274 | 0.652 | 0.414 | 0.360 | 0.363 | 0.967 | 0.140 | 0.056 | 0.017 |
| **Dryas Alpine** | -0.231 | 0.276 | 0.645 | 0.384 | 0.319 | 0.336 | 0.876 | 0.108 | 0.109 | 0.014 |
| **Moist Alpine** | -0.184 | 0.243 | 0.579 | 0.326 | 0.321 | 0.293 | 0.763 | 0.084 | 0.099 | 0.010 |
| **Burned / Disturbed** | -0.173 | 0.413 | 0.719 | 0.554 | 0.487 | 0.486 | 0.892 | 0.140 | 0.071 | 0.021 |
| **Sedge Wetland** | -0.333 | 0.031 | 0.678 | 0.263 | 0.195 | 0.161 | 1.011 | 0.231 | 0.118 | 0.030 |

Table G3. Per-class minimum (min), maximum (max), mean, standard deviation (s) and range for NDVI and NDVI derived from multiple linear regression (MNDVI) analysis for August 2001 in the Greater Besa-Prophet Area in northern British Columbia.

| VEGETATION CLASS | NDVI MIN | MNDVI MIN | NDVI MAX | MNDVI MAX | NDVI MEAN | MNDVI MEAN | NDVI RANGE | MNDVI RANGE | NDVI s | MNDVI s |
|---|---|---|---|---|---|---|---|---|---|---|
| **Sedge Wetland** | -0.376 | 0.323 | 0.567 | 0.406 | 0.387 | 0.388 | 0.944 | 0.083 | 0.070 | 0.010 |
| **Shrub** | -0.305 | -0.195 | 0.738 | 0.509 | 0.444 | 0.442 | 1.043 | 0.704 | 0.074 | 0.034 |
| **Low-Productivity Spruce** | -0.158 | 0.273 | 0.532 | 0.333 | 0.312 | 0.301 | 0.690 | 0.060 | 0.054 | 0.010 |
| **Pine** | -0.183 | 0.328 | 0.565 | 0.389 | 0.360 | 0.359 | 0.748 | 0.061 | 0.054 | 0.007 |
| **Sub-alpine Spruce Transition** | 0.070 | 0.404 | 0.617 | 0.430 | 0.419 | 0.417 | 0.547 | 0.026 | 0.051 | 0.003 |
| **Spruce** | -0.138 | 0.289 | 0.560 | 0.358 | 0.318 | 0.322 | 0.698 | 0.069 | 0.059 | 0.012 |
| **Riparian Spruce** | -0.236 | 0.283 | 0.537 | 0.343 | 0.324 | 0.321 | 0.772 | 0.060 | 0.047 | 0.009 |
| **Dryas Alpine** | -0.102 | 0.299 | 0.613 | 0.350 | 0.319 | 0.325 | 0.715 | 0.051 | 0.088 | 0.007 |
| **Moist Alpine** | -0.050 | 0.300 | 0.546 | 0.340 | 0.299 | 0.322 | 0.597 | 0.041 | 0.083 | 0.005 |
| **Burned / Disturbed** | 0.058 | 0.440 | 0.715 | 0.512 | 0.472 | 0.475 | 0.657 | 0.072 | 0.066 | 0.012 |
| **Sedge Wetland** | -0.376 | 0.323 | 0.567 | 0.406 | 0.387 | 0.388 | 0.944 | 0.083 | 0.070 | 0.010 |

Table G4. Per-class minimum (min), maximum (max), mean, standard deviation (s) and range for NDVI and NDVI derived from multiple linear regression (MNDVI) analysis for September 2001 in the Greater Besa-Prophet Area in northern British Columbia.

| VEGETATION CLASS | NDVI MIN | MNDVI MIN | NDVI MAX | MNDVI MAX | NDVI MEAN | MNDVI MEAN | NDVI RANGE | MNDVI RANGE | NDVI s | MNDVI s |
|---|---|---|---|---|---|---|---|---|---|---|
| **Sedge Wetland** | -0.422 | 0.099 | 0.438 | 0.291 | 0.210 | 0.221 | 0.860 | 0.192 | 0.074 | 0.031 |
| **Shrub** | -0.398 | -0.139 | 0.567 | 0.324 | 0.221 | 0.217 | 0.965 | 0.463 | 0.065 | 0.030 |
| **Low-Productivity Spruce** | -0.202 | 0.086 | 0.450 | 0.239 | 0.153 | 0.154 | 0.652 | 0.153 | 0.085 | 0.030 |
| **Pine** | -0.422 | 0.099 | 0.438 | 0.291 | 0.210 | 0.221 | 0.860 | 0.192 | 0.074 | 0.031 |
| **Sub-alpine Spruce Transition** | -0.398 | -0.139 | 0.567 | 0.324 | 0.221 | 0.217 | 0.965 | 0.463 | 0.065 | 0.030 |
| **Spruce** | -0.202 | 0.086 | 0.450 | 0.239 | 0.153 | 0.154 | 0.652 | 0.153 | 0.085 | 0.030 |
| **Riparian Spruce** | -0.422 | 0.099 | 0.438 | 0.291 | 0.210 | 0.221 | 0.860 | 0.192 | 0.074 | 0.031 |
| **Dryas Alpine** | -0.398 | -0.139 | 0.567 | 0.324 | 0.221 | 0.217 | 0.965 | 0.463 | 0.065 | 0.030 |
| **Moist Alpine** | -0.202 | 0.086 | 0.450 | 0.239 | 0.153 | 0.154 | 0.652 | 0.153 | 0.085 | 0.030 |
| **Burned / Disturbed** | -0.422 | 0.099 | 0.438 | 0.291 | 0.210 | 0.221 | 0.860 | 0.192 | 0.074 | 0.031 |
| **Sedge Wetland** | -0.398 | -0.139 | 0.567 | 0.324 | 0.221 | 0.217 | 0.965 | 0.463 | 0.065 | 0.030 |

Table G5. Per-class minimum (min), maximum (max), mean, standard deviation (s) and range for NDVI and NDVI derived from multiple linear regression (MNDVI) analysis for October 2001 in the Greater Besa-Prophet Area in northern British Columbia.

| VEGETATION CLASS | NDVI MIN | MNDVI MIN | NDVI MAX | MNDVI MAX | NDVI MEAN | MNDVI MEAN | NDVI RANGE | MNDVI RANGE | NDVI s | MNDVI s |
|---|---|---|---|---|---|---|---|---|---|---|
| **Sedge Wetland** | -0.301 | -0.159 | 0.409 | 0.029 | 0.198 | -0.032 | 0.710 | 0.188 | 0.076 | 0.031 |
| **Shrub** | -0.174 | -0.126 | 0.413 | 0.264 | 0.136 | 0.173 | 0.587 | 0.390 | 0.063 | 0.041 |
| **Low-Productivity Spruce** | -0.162 | 0.022 | 0.415 | 0.225 | 0.094 | 0.119 | 0.577 | 0.203 | 0.097 | 0.039 |
| **Pine** | -0.171 | 0.105 | 0.443 | 0.269 | 0.202 | 0.201 | 0.614 | 0.165 | 0.076 | 0.035 |
| **Sub-alpine Spruce Transition** | -0.152 | 0.056 | 0.387 | 0.201 | 0.134 | 0.140 | 0.539 | 0.144 | 0.078 | 0.034 |
| **Spruce** | -0.162 | -0.002 | 0.456 | 0.251 | 0.149 | 0.155 | 0.618 | 0.253 | 0.087 | 0.040 |
| **Riparian Spruce** | -0.167 | 0.029 | 0.415 | 0.240 | 0.174 | 0.176 | 0.583 | 0.211 | 0.063 | 0.034 |
| **Dryas Alpine** | -0.186 | -0.005 | 0.317 | 0.161 | 0.087 | 0.101 | 0.503 | 0.166 | 0.062 | 0.019 |
| **Moist Alpine** | -0.190 | -0.098 | 0.231 | 0.086 | 0.003 | -0.009 | 0.421 | 0.184 | 0.064 | 0.028 |
| **Burned / Disturbed** | -0.155 | 0.054 | 0.455 | 0.254 | 0.174 | 0.180 | 0.610 | 0.200 | 0.070 | 0.027 |
| **Sedge Wetland** | -0.171 | 0.105 | 0.443 | 0.269 | 0.202 | 0.201 | 0.614 | 0.165 | 0.076 | 0.035 |

## APPENDIX H: Tables of loadings for standardized principal component analysis of the Greater Besa-Prophet Area in northern British Columbia, 2001

Table H1. Tables of loadings for all NDVI and MNDVI standardized principal component analysis of the Greater Besa-Prophet Area in northern British Columbia.

| | COMPONENTS | | | |
|---|---|---|---|---|
| | **1** | **2** | **3** | **4** |
| ***NDVI - with cloud masks*** | | | | |
| Total % variation | 99.65 | 0.28 | 0.06 | 0.02 |
| June | 0.996 | -0.086 | -0.013 | 0.003 |
| July | 0.999 | 0.042 | -0.023 | -0.016 |
| August | 0.999 | 0.044 | -0.003 | 0.020 |
| September | 0.999 | -0.001 | 0.039 | -0.007 |
| ***MNDVI -with NDVI cloud masks*** | | | | |
| **Total % variation** | **99.84** | **0.15** | **0.01** | **0** |
| June | 0.998 | -0.063 | -0.005 | 0.001 |
| July | 0.999 | 0.025 | -0.007 | -0.005 |
| August | 0.999 | 0.037 | -0.004 | 0.005 |
| September | 0.999 | 0.001 | 0.017 | -0.001 |
| ***MNDVI - Landscape*** | | | | |
| **Total % variation** | **99.44** | **0.52** | **0.03** | **0.01** |
| June | 0.993 | -0.118 | -0.01 | 0.002 |
| July | 0.999 | 0.047 | -0.014 | -0.01 |
| August | 0.998 | 0.069 | -0.008 | 0.01 |
| September | 0.999 | 0.001 | 0.032 | -0.001 |
| ***Muskwa Ranges*** | | | | |
| **Total % variation** | **99.82** | **0.17** | **0.01** | **0** |
| June | 0.998 | -0.067 | -0.006 | 0.001 |
| July | 1.000 | 0.029 | -0.006 | -0.006 |
| August | 0.999 | 0.038 | -0.006 | 0.006 |
| September | 1.000 | 0.000 | 0.017 | 0.000 |

Table H1. Continued.

| | COMPONENTS | | | |
|---|---|---|---|---|
| | **1** | **2** | **3** | **4** |
| ***Muskwa Foothills*** | | | | |
| **Total % variation** | **99.8** | **0.18** | **0.01** | **0** |
| June | 0.998 | -0.070 | -0.006 | 0.001 |
| July | 1.000 | 0.028 | -0.009 | -0.006 |
| August | 0.999 | 0.041 | -0.004 | 0.006 |
| September | 1.000 | 0.001 | 0.020 | -0.001 |
| ***Sikanni Chief Upland*** | | | | |
| **Total % variation** | **99.92** | **0.07** | **0.01** | **0** |
| June | 0.999 | -0.040 | -0.007 | 0.000 |
| July | 1.000 | 0.021 | -0.003 | -0.005 |
| August | 1.000 | 0.027 | -0.004 | 0.005 |
| September | 1.000 | -0.008 | 0.014 | 0.000 |